Studies on flexible electrode-based batch and continuous microbial fuel cell

Thesis submitted for partial fulfilment of Doctor of Philosophy

by

Miss Bhanupriya Das

Roll no: 176107011

Under the supervision of

Prof. Vimal Katiyar

Dept. of Chemical Engineering, IIT Guwahati

&

Dr. Anki Reddy Katha

Dept. of Chemical Engineering, IIT Tirupati

DEPARTMENT OF CHEMICAL ENGINEERING

INDIAN INSTITUTE OF TECHNOLOGY GUWAHATI

GUWAHATI– 781039, ASSAM, INDIA

April 2023

Dedicated to

My Beloved Parents and Teachers

for their unwavering faith,

Encouragement and Support to help me be

the best version of myself

Department of Chemical Engineering

Indian Institute of Technology Guwahati

CERTIFICATE

This is to certify that the research work in the thesis entitled **"Studies on flexible electrode-based batch and continuous microbial fuel cell"**, is carried out by me at Department of Chemical Engineering, Indian Institute of Technology Guwahati, under the supervision of Prof. Vimal Katiyar and Dr. Anki Reddy Katha. The results documented in this thesis are achieved by me and has not been submitted to any other University or Institute for the award of any degree or diploma.

Date:

_____

Bhanupriya Das

Roll No: 176107011

Department of Chemical Engineering

Indian Institute of Technology Guwahati

Guwahati - 781 039, India.

Department of Chemical Engineering
Indian Institute of Technology Guwahati

CERTIFICATE

This is to certify that the thesis entitled **"Studies on flexible electrode-based batch and continuous microbial fuel cell"**, being submitted by **Bhanupriya Das** for the award of Ph.D. Degree has been carried out by her at Department of Chemical Engineering, Indian Institute of Technology Guwahati, under our guidance and supervision. The work documented in this thesis has not been submitted to any other University or Institute for the award of any degree or diploma.

Date:

Prof. Vimal Katiyar
Professor
Department of Chemical Engineering
Indian Institute of Technology Guwahati
Guwahati - 781039, India.

Dr. Anki Reddy Katha
Associate Professor
Department of Chemical Engineering
Indian Institute of Technology Tirupati
Tirupati- 517619, India.

Acknowledgement

You should not give up and we should not allow the problem to defeat us. As rightly said by the Missile Man of India, and former President of India, Dr. APJ Abdul Kalam, my PhD journey at IIT Guwahati has been nothing short of an adventure with great learning lessons and support and love of numerous souls which have positively impacted my life and helped me evolve into a better version of myself ready to serve the world.

My deepest gratitude to my supervisor, Prof Vimal Katiyar, Professor at the Department of Chemical Engineering, Indian Institute of Technology Guwahati. From our very first encounter at CoE-Suspol five years ago, where he was looking for a passionate PhD student, entrusting me with the Indo-Taiwan Project to this day, as I pen down my thoughts, he has been a very supportive and positive influence on me. I am blessed to have received all the resources and opportunities to discover myself and full freedom to carry out my research. I am grateful to the Almighty for this opportunity to carry out my research under his supervision. I am forever grateful for his presence in this phase of my life.

I am fortunate to have Dr. Anki Reddy Katha, Associate Professor at the Department of Chemical Engineering, Indian Institute of Technology Tirupati, as my Co-supervisor. My sincere gratitude to hm for his constant guidance, mentoring and full support in all my endeavors even when he moved from IIT Guwahati. I am forever grateful for his presence and sincere efforts to help me in my simulation work.

I am also thankful to Prof C.T Wang, Distinguished Professor at Department of Mechanical and Electromechanical Engineering, National Ilan University, Taiwan and Professor, Dept of Chemical Engineering, IIT Guwahati for sharing his vast knowledge in microbial fuel

cells and providing me with all necessary research facilities to work in TFBE Lab in Taiwan. I sincerely appreciate his all-constant support and guidance, and, opportunities to attend various international conferences during my fruitful stay in Taiwan.

My sincere gratitude to my Doctoral Committee headed by Dr. Amit Kumar (Associate Professor, (Dept of Chemical Engineering, IIT Guwahati), Prof. Amaresh Dalal (Professor, Dept of Mechanical Engineering, IIT Guwahati), Prof. Chandan Mukherjee (Professor, Dept of, Chemistry, IIT Guwahati) for their time in serving on my committee, mentoring and guidance to complete my research work.

I also sincerely acknowledge the financial support provided by Ministry of Human Resource Development, Government of India in terms of fellowship during my PhD tenure.

I am deeply thankful to avail the research facilities at Department of Chemical Engineering, IIT Guwahati; Centre of Excellence for Sustainable Polymers, IIT Guwahati, funded by Department of Chemicals and Petrochemicals (GoI), Central Instruments Facility at IIT Guwahati, National Taipei University of Science and Technology, Taiwan and CSIR-North East Institute of Science & Technology, Jorhat and PARAM-ISHAN supercomputing facility at IIT Guwahati.

My sincere gratitude to the Head of Department, technical staff in the Dept of Chemical Engineering Mr. Harsaraj Biswanath, Mr. Debajit Borah, Mr. Ariful Hoque, Mr. Jayanta Kumar Mout; the office staff in the Dept of Chemical Engineering, Mr. Deep Jyoti Sinha,

Mr. Sailen, Mr. Bhagya Boro and staff in administrative position at IIT Guwahati for their kind cooperation to help me conduct my research work smoothly.

I would like to thank the researchers in Prof Wang's lab at NIU, Taiwan, Dr. Lan, Dr, Wu, Y Ting Li, Jui-Sen Lu, Kavya, Vicky, Ms Dai, Raymond, Dinh, Imee who have graciously helped me navigate the world of microbial fuel cells and supported me in all my endeavour. I would like to thank Ms. Chen and Prof Vincent Hsu, Department of Food Science and founder of Hai-Yun International FolkDance Club, National I-Lan University for their help and support to make me feel at home in a new country.

I am also fortunate to have carried out my research in two different laboratories amidst a diverse group of brilliant researchers at Centre of Excellence for Sustainable Polymers (CoE-SusPol) and Computational Material Science Lab (CMS lab) in IIT Guwahati. My sincere gratitude to my seniors: Dr. Surendra, Dr. Narendren, Dr. Kiran, Dr. Arvind, Dr. Shasanka, Dr. Gourhari, Dr. Monika, Dr. Tabli, Dr. Neha, Mr. Pankaj, Mr. Durlov, Mr. Sayan, Dr. Naba, Dr. Modu, Ms. Chetna, Mrs. Munmi, Dr. Purabi, Dr. Riddhi, Dr. Balendu, Dr, Sushil, Mr. Shivam, Dr. Bitang; my colleagues: Kona, Dr. Doli, Mrs. Deepshikha, Mr. Nagendra, Mr. Vasistha; my juniors Debleena, Arnob, Kshitij, Manoj, Mr.Amrit, Kuhelika, Parul, Mrs Mandavi, Aparajita, Anshuman, Mohini, Guddu, Anurag, Vikas and our staff members Moromi, Mr. Lakhya and Mr. Diganta. I am grateful for this huge family outside home whom I could reach out to for all kinds of help and moral support and truly made my stay in the labs memorable.

I am blessed and thankful to my lovely friends Debika and Punampriya for their friendship and for making my stay in Subansiri Girls Hostel cheerful and memorable. My friends and brothers and well-wishers in IITG campus whom I had the good fortune to get acquainted with during various co-curricular activities: Hrishikesh, Biswajyoti, Siddharth, Brijesh, Jeet, Araghni, and Gaurishankar. Dr. Minakshi Gohain and Neetish Raj Deka, my good old friends who are my biggest cheerleaders and have been very supportive during my troubled times.

I am forever in debt of my beloved mother Lt. Padma Das, the strongest person I ever knew, blessing me from the heavens above and my guiding light my biggest source of strength, my father Mr. Deben Chandra Das. The unconditional love and sacrifices of my parents have been my constant source of inspiration to forge ahead to achieve my goals. I am blessed to have the love and support and best wishes of my family, my brothers: Mr. Nayan Das, Mr. Moina Das, Mr. Laban Das, Mr Lab, Das, Mr. Monokrishna, Das, Mr. Kaustav moni Das, my sisters-in law: Mrs Minakshi Kakoti Das, Mrs Karabi Das, Mrs Anjana Das my adorable nephews: Bibhuranjan Das and Papumoni Das and cute nieces: Dubari Krishna Das and Jyotishna Das, my extended family of uncle, aunts and siblings whose blessings keep in good health and spirit. I would also like to sincerely acknowledge my long-distance partner, Mr. Mithilesh Paswan for his encouragement and wholehearted support to complete my research work. Lastly, I bow before the Almighty for showering upon me with his divine grace and guiding me to achieve my dreams.

Abstract

Microbial Fuel Cells (MFCs) are promising sustainable energy technology which integrate power generation with waste remediation. However, its practical application is mainly hindered by firstly, its low power density owing to poor bacterial adhesion and electron transfer efficiency between bacteria and anode. Secondly, the use of Nafion as proton exchange membrane in microbial fuel cells (MFCs) is expensive with operational issues like biofouling and fuel crossover. Therefore, the current work addresses three issues of MFCs namely, to improve its performance, reduce the cost of operation and expand its horizon to real field application. Besides, MFCs are a bio electrochemically complex system coupled with reactions and electron and proton transport in bulk media. The uniqueness of the work is the validation of the experimental study with comprehensive computational model complementing the experimental studies with new information about the system assembled with the indigenous membrane components The properties of the Nafion-alternative membranes, developed from environmentally benign polymers, poly (vinyl alcohol) (PVA) crosslinked with glutaraldehyde (GA) and Chitosan (CS)have been systematically studied and its performance evaluated against the commercial membrane in real wastewater fed MFCs. The membranes developed demonstrate potential as separator in future MFCs based on its enhanced performance and low cost of installation. Another important aspect hindering the practical application of MFCs which is low power density owing to poor bacterial adhesion and electron transfer efficiency between bacteria and anode. This issue is addressed by development of flexible electrodes using conducting polymer polyaniline (PANI) with sustainable polymer polylactic acid (PLA). An elaborate analysis of the performance of the bio-based flexible anode against commercial anode in

domestic wastewater fed MFCs asserts its excellent biocompatibility, outperforming the flat graphite anode in achieving maximum power density and COD removal efficiency. The knowledge gap in the area of energy harvesting using complex substrates like hospital wastewater has been addressed using the indigenous PVA membrane developed. Experimental study conducted by replacing the commercial membrane in the recirculation mode honeycomb pattern MFC displayed enhancement in power production. An attempt to delve deeper into the atomic level to investigate the proton transport mechanism across the developed PVA membrane using Classical Molecular Dynamics study is demonstrated. The proton transport mechanism forms a crucial step which is a difficult to observe experimentally. The findings of the study demonstrated presence of multi-hydrated protons observed from MD trajectories suggesting that the proton transfer in the PVA polymeric membrane system occurred via vehicular mechanism. Furthermore, an essential parameter for the MFCs operating in recirculation mode, is its operating flow rate. To this end, numerical modeling, is utilized with parallel experimental study to get deeper insight into its effect on the performance in real wastewater fed MFCs for its viability for future commercial applications. Simulation study is carried out using hospital wastewater for recirculation mode MFC to investigate the effect of flow rate and reaction kinetics on the current density. Thus, the present study is focussed on adding a new dimension to the design of sustainable anode material to enhance microbial binding and achieve high power output, besides, developing an in-depth understanding of proton transfer mechanism and flow dynamics and its effect on the performance of MFC and lastly, to indigenously develop low-cost membranes to demonstrate the enormous potential of scale-up of MFCs for wastewater treatment in the future.

Contents

List of Figures

List of Tables

List of Abbreviations

Abbreviation	Expanded form
BES	Bio-electrochemical systems
CHARMM	Chemistry at HARvard Macromolecular Mechanics
CV	cyclic voltammetry
CNC	Cellulose
CFD	Computational fluid dynamics
COD	Chemical oxygen demand
CNC	Cellulose Nanocrystals
CS	Chitosan
DMA	Dynamic mechanical analysis
DSC	Differential Scanning Calorimetry
EIS	Electrochemical impedance spectroscopy
EVB	Empirical Valence Bond
FEM	Fuller's earth-material
FFV	Fractional free volume
FESEM	Field Emission Scanning Electron Microscopy
FTIR	Fourier transform infrared spectroscopy
GA	Glutaraldehyde
HH	Hair Hydrolysate
HPLC	High-performance liquid chromatography
IEC	ion exchange capacity
MD	Molecular Dynamics
MFC	Microbial fuel cells
MSD	Mean square displacement
MWCNT	Multiwalled Carbon Nanotube
NAMD	Nanoscale Molecular Dynamics
OCV	Open Circuit Voltage
PANI	Polyaniline

PEM	Proton exchange membrane
PLA	Polylactic acid
PTFE	Polytetra-fluorethylene
PVA	Polyvinyl Alcohol
RDF	Radial Distribution function
SSA	Sulfosuccinic Acid
TRIS	Tris(hydroxymethyl) aminomethan
TGA	Thermo-Gravimetric Analysis
UTM	Universal Testing Machine
VOF	Volume of Fluid
VMD	Visual Molecular Dynamics
XRD	X-Ray diffraction
XPS	X-ray photoelectron spectroscopy
2D	Two-dimensional
3D	Three-dimensional

List of Symbols

Symbols	Indicates (Unit)
ρ	Density of water, (997 kgL^{-1})
μ	Viscosity (kg/m.s)
δ_D	Diffusion layer thickness(m)
E	Activation energy for the reaction (J/kmol)
F	Faraday's constant (C/mol)
H	Height of Channel(m)
Re	Reynolds number (-)
R	Universal gas constant (J/kmol-K).
Lys	Lysine(-)
His	Histidine(-)
T_g	Glass transition temperature (°C)
W	Width of Channel(m)

Chapter-1

Introduction and Literature Review

1.1 Background and motivation

One of the most important challenges of man's effort to combat climate change due to greenhouse gas emission is clean, efficient and reliable energy generation. Rapid depletion of fossil fuel resources because of increasingly higher energy demands, and increasing frequency of climate change phenomena such as extreme weather events because of global warming by green gas houses (GHGs) emitted from widespread use of fossil fuels, have raised the demand for new and clean sources of energy that do not pollute the earth and can be renewed by nature. Hence the search for alternate sources of energy generation that are cheap and ecofriendly have become a prime necessity(Logan et al., 2006). Furthermore, the demand for cost-effective and low-energy wastewater treatment has never been greater. Out of the 7.2 billion global population, currently, over two billion people lack adequate sanitation while another one billion do not have access to clean water(Verma et al., 2021). Besides, providing clean water for the ever-increasing urban global population at their doorstep is expensive. In addition, it is eating into our diminishing fossil-based energy reserves and thereby, contributing to GHGs in the atmosphere and climate change (S. T. Oh et al., 2010).Therefore, the necessity for cost-effective as well as low-energy wastewater treatment has never been greater. The immense possibility of employing microorganisms for recovering resource from waste and aiding in waste management has garnered a lot of interest in Microbial Fuel Cells (MFCs) Technology (**Fig 1.1**).

MFCs are a promising environmentally friendly and sustainable technology that can be an important tool in the transition from the traditional linear economy of "make, use and dispose" towards a more sustainable circular economy where waste is valued as a resource (Velenturf & Purnell, 2017). MFCs are electrochemical devices that convert the chemical energy of organic matter such as carbohydrate and organic acids into electricity directly using microorganisms. The use of MFC as an alternative source for power generation is considered as a reliable, clean, efficient process, which utilizes renewable methods and does not generate any toxic by-product. In recent years, MFCs have shown to be a potent technology for recovery and in-situ conversion of chemical energy into electricity. Unlike other electrochemical device, the microbial fuel cell is a highly efficient energy converting device that has attracted special attention of energy policy makers and researchers alike, because of its no moving part and flexibility in size.

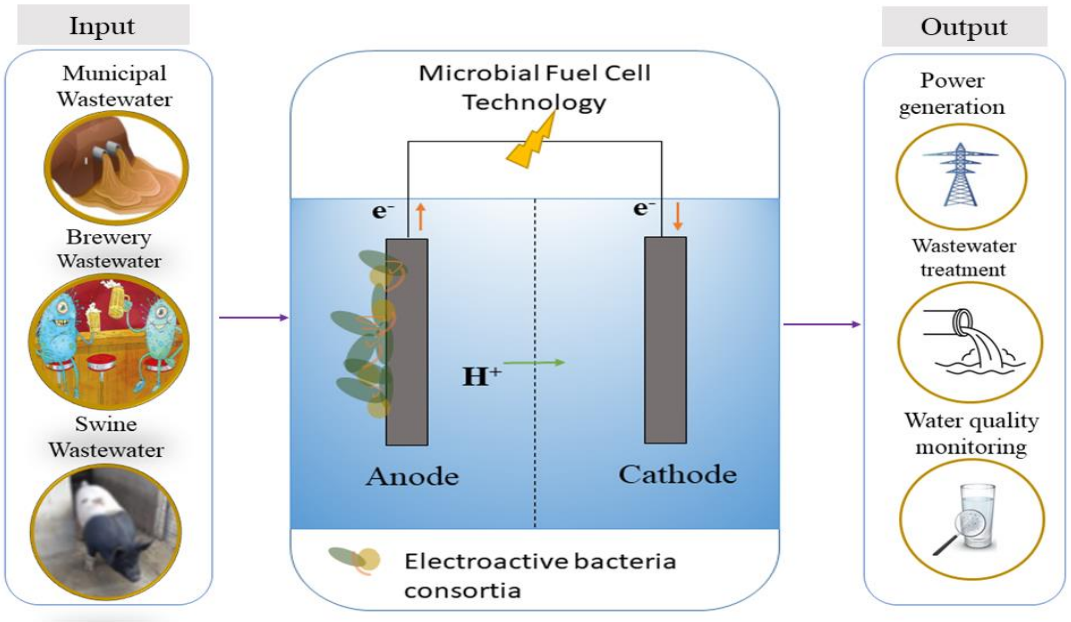

Figure 1.1 Schematic representation of the diverse feedstock and diverse application of Microbial Fuel Cell technology.

1.1.1 The mechanism of energy harvesting in MFC

The power generation principle behind MFCs is that bacteria gain metabolic energy by transferring electrons from an electron donor, such as glucose, to an electron acceptor, such as oxygen (**Fig 1.2**). The first mechanism of direct transfer of electrons between the electrode surface and microbes can occur via pili, electronically conductive protein filaments that are often referred to as 'nanowires' (Torres et al., 2010). The second mechanism of transport of electrons involves non-diffusible mediator excreted by the microbes which act as relays or electron shuttles between microbial biocatalytic system and the electrode surface. While the third mechanism can be indirect mode of transfer via mediators for those microbes that are unable to transfer the electrons to the anode. They take up the electrons from microbes and discharge them at the surface of the anode(Logan et al., 2006) The larger the potential difference between donor and acceptor, the larger the gain for the bacterium. In a microbial fuel cell (MFC), bacteria do not directly transfer their produced electrons to their characteristic terminal electron acceptor but these electrons are diverted towards an electrode (anode). The electrons are subsequently conducted over a resistance or power user towards a cathode and thus, bacterial energy is directly converted to electrical energy. To close the cycle, protons migrate through a proton exchange membrane from anode to cathode.

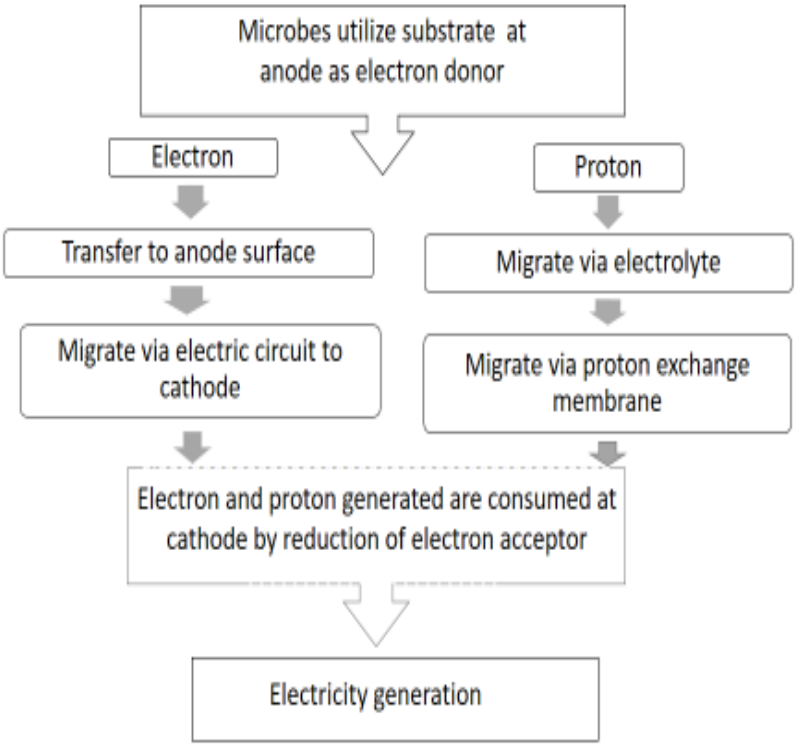

Figure 1.2 Schematic representation of energy harvesting mechanism of MFC.

1.2 Advantages of MFC as pollution control unit

If we consider MFC as an energy generation unit, its competitor in the market is the conventional PEM fuel cell. The power density for PEM Fuel Cell can easily reach 140 kW/m^3 or 10^5 W/m^2, whereas it stands at 100 W/m^2 for the MFC (Hu et al., 2018). However, when we question the suitability of the device for wastewater treatment, the MFC proves to have advantage over the PEM Fuel cell. A vital difference between PEM FC and MFC is the nature of electrode catalyst used. In the case of PEM Fuel Cell, noble metal catalysts are used which are substrate-specific and are easily poisoned by impurities. Besides, the substrate used is pure hydrogen and oxygen gas and it operates in engineered

environment at pressure of (3-5) atm and temperature range of (60-90) ^{0}C. Conversely, in case of MFC, microbes act as biocatalyst, the substrate at the anode chamber is organic matter dissolved in water with its optimal growth condition being room temperature and pressure. MFC is therefore capable of handling liquid medium and hence suitable for wastewater treatment.

1.3 Sustainable wastewater treatment using MFCs

Domestic wastewaters including sewage and gray waters are composed of higher amounts of organic loads and are currently treated using traditional aerobic treatment systems which are energy intensive and generate a large amount of sludge as a secondary pollutant MFCs-based domestic wastewater treatment system provide edge over the current wastewater treatment technologies as it is energy-yielding (YOU et al., 2006). It can convert chemical energy in waste directly into electrical energy by the catalytic activity of electroactive bacteria. The whole treatment process is amenable to real time control at low temperature as the bacteria donate electrons to an external circuit with a controllable resistance producing less amounts of excessive sludge which lead to reduction in the operating cost and sludge treatment or disposal cost. Integrating the MFC technology to wastewater treatment plant opens up another new avenue to meet emerging energy needs by utilizing metabolism of microorganisms especially by utilizing wastewater as substrates to generate energy and also accomplish wastewater treatment (**Fig 1.3**). However, the overall low performance of the MFC compared to other more established fuel cell technologies and the high cost of its components compared to the low value of the wastewater it treated, are the two major barriers to commercialization. The application of MFCs for wastewater

treatment or bioenergy production requires firstly the use of inexpensive electrode materials that are electrochemically and biologically stable, and that have a high specific surface area and electrical conductivity. Secondly, for the process to be economically feasible, it is necessary to cut cost by either eliminating the cationic membrane and reducing cost of membrane maintenance or using a cheaper membrane, running MFC in existing wastewater treatment plants.

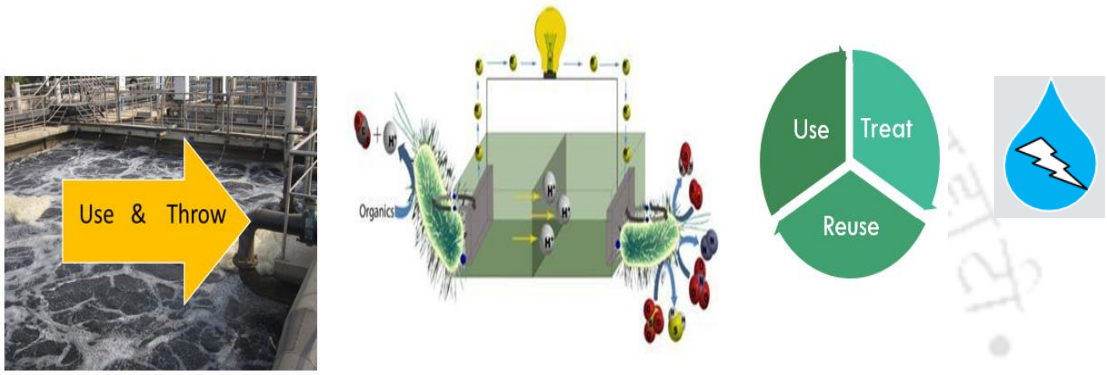

Figure 1.3 Waste to Wire: A paradigm shift from "use and throw – linear" to a "use, treat, and reuse – circular" approach to manage wastewater.

1.4 Challenges in practical application of MFC

Over the past decade, MFCs have evolved into a simple yet robust technology with researchers across the globe constantly working on various aspects namely material and architectural aspect of the electrodes, microbial inoculum, chemical substrate as the feed material as well as low cost proton exchange membrane, so as to enhance the performance of MFCs and also decrease its cost of operation. Although the power production is encouraging, however, the practical application of simultaneous energy harvesting and wastewater treatment process using MFCs is limited by the cost of the membrane material

and anode material, firstly, due to low electron transfer rate, and secondly, due to low affinity for bacterial cell attachment.

1.4.1 Membrane material in MFC

.

Proton Exchange Membranes are one of the most important components in MFCs. They physically separate the anode and cathode compartments while allowing protons to pass through to the cathode. For each electron that is produced, an equivalent proton must be transported to the cathode through the membrane to sustain the current. The most commonly used membrane is Nafion 117 membrane.

1.4.1.1 Nafion membrane and proton transport mechanism

The desirable qualities in a good proton exchange membrane (PEM) for MFC application include good hydrophilicity, low ohmic resistance, good proton conductivity, high chemical and mechanical stability, anti-biofouling property and low production cost to make the operation economically viable (Das et al., 2021).Conventionally, Nafion® (from DuPont) is, by far, the most preferred PEM used in fuel cell application primarily due to its high proton conductivity, high chemical and mechanical stability(Das et al., 2021) .Nafion, a sulfonated tetrafluorethylene copolymer, consists of fluorocarbon backbone (–CF_2–CF_2–) to which sulfonate groups (SO_3^-) are attached. The presence of negatively charged sulfonate groups in the membrane explains the high level of proton conductivity of Nafion, while also showing a significant undesirable affinity for other cations rather than protons. Such polymers naturally combine, in one macromolecule, the high hydrophobicity of the backbone with the high hydrophilicity of the sulfonic acid functional group, which results in a constrained hydrophobic/hydrophilic nanoseparation. The sulfonic acid

functional groups aggregate to form a hydrophilic domain that is hydrated upon absorption of water. It is within this continuous domain that ionic conductivity occurs: protons dissociate from their anionic counter ion ($-SO_3^-$) and become solvated and mobilized by the hydration water. However, it suffers from major disadvantages which include non-eco-friendliness, disposal issue, permeability to undesired cations like Na^+ and K^+ obstructing proton transfer, high fuel crossover and higher production cost ($ 600-1200 per m^2) which forms the main motivating factors behind looking for a cheaper alternative.

Proton conductivity of the membrane plays a crucial role in the performance of MFCs in terms of the operational fuel cell voltage and current output. The proton transferring property, however, is related to nanoscale structure of water and therefore the macroscopic method is not effective to analyse the phenomena. It is considered that protons transfer by two mechanisms in the PEM (Arntsen et al., 2016). One is called "Vehicle Mechanism" in which protons transfer as H_3O^+, and the other is called "Grotthus Mechanism" in which protons transfer by hopping along hydrogen bond network formed by water molecules. In a PEM, clusters are formed by water molecules and hydrophilic side chains and the nanoscale structure of water clusters largely depends on proton transfer by Grotthus mechanism. The Grotthuss mechanism also known as structure diffusion of protons in bulk water requires formation and cleavage of hydrogen bonds of water molecules in the second hydration shell of the hydrated proton therefore, any constraint to the dynamics of the water molecules will decrease the mobility of the protons. Thus, knowledge of the state or nature of the water in the membrane is critical to understanding the mechanisms of proton transfer and transport in PEMs

Classical MD simulations is an optimal choice to study proton transport mechanism in PEMs Considering the computational cost, as it can access relevant length and time scales and can handle systems consisting of thousands of particles over time periods of nanoseconds(Kreuer et al., 2004). Vishnyakov and Neimark studied the microphase segregation in the Nafion (DuPont trademark) perfluorinated membrane at different water contents using molecular dynamics simulations (Vishnyakov & Neimark, 2001). As the degree of solvation increased, they observed the formation of water clusters containing up to ca. 100 water molecules. In contrast to the conventional network models, the water clusters did not form a continuous hydrophilic subphase. Rather the cluster size distribution was wide and evolved in time due to formation and break-up of temporary bridges between the clusters. This dynamic behavior of the cluster system allows for the macroscopic transfer of water and counter ion. In Classical Molecular Dynamics, the Emprical Valence Bond Model describes the proton transfer between two water molecules by dynamic breaking and forming of O-H bonds. It was observed by that a proton bound to water molecule travel between two sulfonate group attached to Nafion side chain. Wu et al. studied the proton transfer mechanism in Nafion membrane by carrying out simulation based on EVB model for two different water contents at different temperatures(Y. Wu et al., 2006). The water content λ is the ratio of number of water molecules or hydronium ions to number of sulfonate group in the polymer. As observed from **Fig 1.4**, higher water content provided ease of proton transfer by forming large water clusters connected by narrow bridges. Whereas at low water content the water molecules form filamentous structure and not part of single structure which hampers the proton hopping between water molecules.

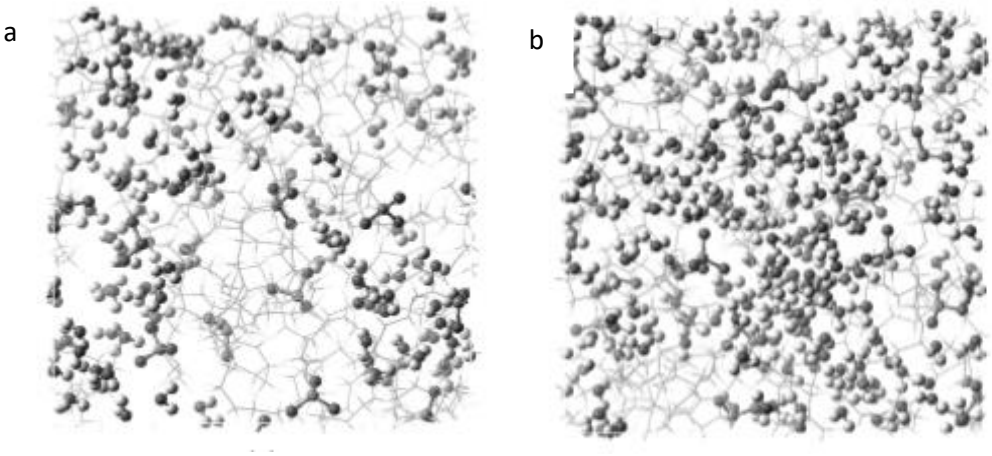

Figure 1.4 Snapshot of the simulation of interaction of Nafion polymer in aqueous phase for a) Low and b) High water content respectively.

1.4.1.2 Modified polyvinyl alcohol membrane based MFC and its proton transport mechanism

In the current scenario, to tackle the major challenge of bringing down the cost drastically of membrane material, a more suitable route is to fabricate low cost membrane to replace the Nafion, which accounts for 38% of the total capital cost. Recently PVA based polymer membranes have attracted a lot of attention owing to its broad applications in medical field, in fuel cells as proton exchange membrane and so on. PVA is a non-toxic, biodegradable and an inexpensive polymer. It is inherently hydrophilic which makes it favorable for wastewater treatment. It has good film forming property due to its ability to crosslink within available hydroxyl groups in presence of chemical crosslinker to retain the compact nature of the membrane under pressure. However, the low mechanical strength, thermal stability and poor proton conductivity of pure PVA discourage its use as a potential alternative for the commercial membranes in MFCs. To overcome this hurdle, various crosslinking agents have been explored so far in combination with PVA film such as sulfosuccinic acid, poly (styrene sulfonic acid-co-maleic acid) with glutaraldehyde (GA)

to name a few. The effect of crosslinking of PVA with GA under acidic condition on characteristics of the PVA membrane has been examined in single chambered MFCs. A straightforward technique is attempted in the current study to modify the membrane for the first-time utilizing crosslinking agent GA in neutral condition for MFC application. The use of water for membrane preparation instead of chemical solvent not only saves the preparation cost but also rules out the leaching of impregnated acid in long term that might restrict its application(Das et al., 2021) .

Although the effect of crosslinking agents with PVA in MFC have been experimentally studied but at a more fundamental atomistic level, it has been rarely focused upon how their interaction behavior would affect the performance in MFC environment.In a recent investigation, MD simulations carried out to study the T_g and mechanical properties of PVA/TRIS functionalized graphene oxide composite. The authors claimed that application of the modifier, Tris-GO, not only improved the mechanical properties of polymer composites, but also provided valuable insights for improving the thermal stability of the composite(Dong et al., 2021) .The current research work to investigate the proton transfer mechanism in crosslinked PVA membrane using Classical MD simulation is a significant step towards addressing the knowledge gap on switching to biopolymeric PVA membrane for the performance enhancement of the MFC reactors for simultaneous power generation and real wastewater treatment.

1.4.1.3 Modified chitosan membrane based MFC

Chitosan (CS) is an environmentally benign polymer and a potential candidate to prepare low-cost proton exchange membranes (PEMs) for Microbial Fuel Cell (MFC) applications.

It is another inexpensive, abundant biobased polymer derived from the deacetylation of chitin known for its biodegradability, nontoxicity, hydrophilic nature, good film forming properties and excellent thermal and mechanical strength. The major issue with CS when used as a membrane, is that in its pristine form, it demonstrates poor mechanical property due to high water uptake with lower proton conductivity and low ion exchange capacity (IEC) limiting its application as a potential Nafion-alternative membrane. One of the key solution to this problem however, is crosslinking. The backbone of chitosan consists of free amine and hydroxyl groups which are potential reactive sites and hence, can be easily associated with other crosslinking agents that allow improvement in performance by further modifications. Furthermore, CS can be blended with either hydrophilic or hydrophobic polymers (e.g. PVA) to enhance its mechanical and thermal stability Despite the rising number of researches on the application of various materials as PEM, but only a few studies address the usage of sustainable MFC components for real wastewater treatment(Das et al., 2023).

1.4.2 Anode materials used in MFC

Carbonaceous materials such as carbon cloth, carbon brush, carbon rod, carbon mesh, carbon veil, carbon paper, carbon felt, granular activated carbon, granular graphite, carbonized cardboard, graphite plate and reticulated vitreous carbon are used as commercially available anode electrode material. Among metal-based materials, stainless steel plate, stainless steel mesh stainless steel scrubber, silver sheet, nickel sheet, copper sheet gold and titanium plate were used as commercially available anode electrode material (Venkata Mohan et al., 2014). Although the power production is encouraging, but the simultaneous energy harvesting and wastewater treatment process using MFCs is limited

by the anode material due to low electron transfer rate and low affinity for bacterial cell attachment. The materials used as anode electrodes must possess several specific characteristics for improving interactions between the biofilm and the material surface. The most important characteristics are: a) electrical conductivity; b) resistance to corrosion; c) high mechanical strength; d) developed surface area; e) biocompatibility f) environmentally friendly and g) low cost. The limitations arising from the anode material can be overcome by introducing higher conductive materials, while the second drawback can be diminished by encapsulating the conducting polymer in a nanosized form-stable, a biocompatible supporting matrix in which the bacteria in the wastewater can thrive and grow. Recent reports suggest several approaches mostly focused on modifying the electrode to enhance conductivity with less emphasis on bacterial cell adhesion. One such effective approach for electrode modification that takes into consideration the above-mentioned solutions is bioaugmentation. It is considered a potential tool to boost the performance of MFCs by modifying electrodes with biopolymers(Das et al., 2022).

1.4.2.1 Polylactic acid polymer-based anode in MFC

Polylactic acid (PLA) is a thermoplastic and bio-based aliphatic polymer having chemical formula (C3H4O2)n. It is achieved by lactic acid condensation with loss of water (Pal & Katiyar, 2016). PLA is derived from renewable feedstock, namely starch, corn, sugarcane, etc. It is mechanically and thermally stable over synthetic polymers with good biocompatibility and is commercially available in large quantities. PLA has been widely electrospun in its neat form as well as composites by modifying its functionality depending on the application such as electrospun mats for drug delivery. PLA-based nanofibers are

being extensively used in various applications as functional composites, biosensors, tissue engineering, and advanced drug delivery systems. The recent success of the application of PLA-based nanofibers by electrospinning for cancer therapeutics, tissue engineering, immobilization of α-amylase etc, demonstrates its potential as a suitable platform for hosting microbes and promoting their growth, thereby mediating the electron transfer process. Electrospun PLA nanofibers are reported to be non-toxic, exhibiting high porosity and large surface area with improved biodegradability, which makes them suitable to make inroads in the field of MFC and other eco-friendly energy storage systems (Das et al., 2022).

1.4.3 Numerical Modeling of MFC

The research carried out in the MFC technology is mainly focused more on the biological experiment, while, the fundamental mechanisms of mass transport and electrochemical reactions are not much emphasized. Also, most of the studies lack experimental results to substantiate the mathematical modelling findings. It is observed that experiments on MFC take several weeks to months for the biofilm growth in the anode before stable power output is generated. Numerical modeling can be a powerful tool in providing deeper insight into the functionality of the MFC by validating the hypotheses and optimizing its design by running the simulation for a shorter period of time, which provides a strong motivation for pursuit of the current work.

1.4.3.1. Effect of flow parameters on performance of MFC

Majority of the numerical models are one-dimensional or two-dimensional(J. Kim et al.,

2014) . Examined the 2D flow in a MFC and found that the dead zones of the fluid flow influence the performance of the MFC. To our knowledge, very few of the models deals with simulations of 3D anode geometries, which are likely to be used in industrial environment (Farber et al., 2021). Simulated a 3D model of MFC based on the transient 2D model of (Merkey & Chopp, 2012) considering a mixed culture biofilm derived from wastewater on the textile carbon fibre anode. They found that the size of the biofilm influences its power output.

Shear rate is an essential parameter for an MFC in continuous mode of operation. Increase in the shear rate is reported to not only enable faster bacterial attachment on the electrode but also shorten the startup time of MFC(Pham et al., 2008). Higher shear rate enhances the mass transfer rate between the substrate and anode biofilm resulting in denser and thicker biofilm thereby, efficiently limiting the mass transfer losses of MFCs(Shen et al., 2013). Wang et al. found that high recirculation flow rate increased the mass transfer rate of MFC due to high shear stress(C.-T. Wang, Huang, Sangeetha, & Yan, 2018). Therefore, effect of shear stress on the power output of MFC is worthy for investigation.

Flow rate is another key parameter influencing the power production of MFCs in continuous mode MFCs. As the major component of anolyte in MFC is water therefore, the fluid dynamics will influence behavior of biofilm microbial consortia present in the wastewater thereby, its power performance(Oliveira et al., 2013). Reduced mass transfer rate of substrate from bulk of the liquid to the biofilm arising from low flow rate will lead to detachment of bacteria from the surface of the anode in search of favourable environment which will eventually lead to activation loss and mass transfer loss and a decline in the power output as well as COD removal (Ieropoulos et al., 2010; Logan, 2008; C.-T. Wang,

2014). Thus, the role of flow rate is significant in scale-up and industrial application of MFCs.

Dimensionless numbers such as Reynolds number, Péclet number, Schmidt number and Sherwood number are composed of combinations of basic fluid properties such as the flow velocity, density, viscosity, characteristic length of reactor etc. Therefore, they can give us a better understanding of the fluid flow effect on the power production of MFC. Reynolds number is commonly reported in the case of microfluidic MFCs(ElMekawy et al., 2013; Ren et al., 2014; Ye et al., 2013). A recent report by Kataky et al.,2020 on 3D MFC mimicking lab-scale MFC using lactate as substrate found variation of current density with change in Reynolds number (Re) (Kataky et al., 2020) .Similarly, Péclet number, Schmidt number and Sherwood number are good indicator of the transport phenomena in the MFCs (L. Zhao et al., 2016), but are rarely been focussed in lab-scale or large scale MFC as to how these dimensionless numbers impact the power performance (Ren et al., 2012).Hence, the effect of dimensionless numbers on MFCs performance is worth investigating.

1.4.4 Research objectives

Based on the current status of research in the field of practical application of MFC for wastewater treatment the following objectives have been formulated to analyse the feasibility of using bio based polymeric material as electrode and membrane replacement in batch and continuous mode MFC to generate power and simultaneous wastewater treatment.

1) Development of bio-polymer based ion conductive membranes and. investigation of the role of biobased membrane on the performance of MFC.
2) Development of bio-based flexible electrode developed by electrospinning and investigation on its role on the performance of MFC.
3) Investigation on effect of crosslinking of PVA membranes in MFC in real wastewater fed MFC.
4) Investigation on the proton transport mechanism using Molecular Dynamics Method and validation with experimental results.
5) Investigation of specific flow dimensionless parameter on enhancing the performance of the Continuous Microbial Fuel Cell and validation with experimental results

1.4.5 Significance of the work and Thesis outline

In the quest for new energy sources, MFC comes as a boon which makes waste treatment possible. Although the technology is promising, numerous hurdles need to be overcome to make it economically feasible. Therefore, the current study is of utmost importance to improve its performance, reduce the cost of operation and expand its horizon to real field application. Besides, MFCs are a bio electrochemically complex system coupled with reactions and

electron and proton transport in bulk media. Hence following methods have been adopted to have broad understanding of the MFCs that includes: a) experimental study involving real wastewater with electrochemical analysis in fed-batch and recirculation mode, b) biofilm growth process with mixed culture bacteria collected from wastewater, c) classical molecular dynamics to discover the proton transport mechanism across the membrane, d) numerical modeling to evaluate the flow dynamics in the complex MFC system. The uniqueness of the work is the validation of the experimental study with comprehensive computational model complementing the experimental studies with new information about the system assembled with the indigenous membrane components. The structure of the current work is presented in the form of eight chapters. The first chapter begins with an introduction to MFCs technology and its challenges, with an attempt to put into perspective the motivation behind the objectives of the current research work. The second chapter highlights the materials and methodology adopted to carry out the experimental study and the simulation studies.The third and fourth chapters address the need for developing alternate proton exchange polymeric membrane to reduce the cost of operation of MFCs. The properties of the Nafion-alternative membranes, developed from environmentally benign polymers, poly (vinyl alcohol) (PVA) crosslinked with glutaraldehyde (GA) and chitosan have been systematically studied and its performance evaluated against the commercial membrane in wastewater MFCs. The membranes developed demonstrate potential as fed separator in future MFCs based on its enhanced performance and low cost of installation. The fifth chapter looks into another important aspect hindering the practical application of MFCs which is low power density owing to poor bacterial adhesion and electron transfer efficiency between bacteria and anode. This issue is addressed by development of flexible electrodes using conducting polymer polyaniline (PANI) with sustainable polymer polylactic acid (PLA). An elaborate

analysis of the performance of the bio-based flexible anode against commercial anode in domestic wastewater fed MFCs asserts its excellent biocompatibility, outperforming the flat graphite anode in generating power and COD removal efficiency. In chapter six, the knowledge gap in the area of energy harvesting using complex substrates like hospital wastewater has been addressed using the indigenous PVA membrane developed. Chapter seven is an attempt to delve deeper into the atomic level to investigate the proton transport mechanism across the developed PVA membrane using Classical Molecular Dynamics study. The proton transport mechanism forms a crucial step which is a difficult to observe experimentally. The findings of the study demonstrated presence of multi-hydrated protons observed from MD trajectories suggesting that the proton transfer in the PVA polymeric membrane system occurred via Grotthuss and vehicle mechanisms. Furthermore, Chapter eight looks into an essential parameter for the MFCs operating in recirculation mode, which is its operating flow rate. To this end, numerical modeling, is utilized with parallel experimental study to get deeper insight into its effect on the performance in real wastewater fed MFCs for its viability for future commercial applications. Simulation results demonstrated enhancement in current density at higher flow rate which is experimentally validated by enhancement in the power performance compared to previous study using hospital wastewater for recirculation mode MFC. In the final chapter, we summarize our conclusions and impact of the research conducted and discuss the way forward for MFCs application in future. In addition to this, the last pages include references, research output in the form of papers published and conferences attended so far as part of the research journey.

Chapter-2
Materials and Methods

2.1 Materials for crosslinked PVA Membrane

2.1.1 Preparation of crosslinked PVA Membrane

For preparing the PVA Membrane, solution casting method was applied. To have a film thickness around 100 μm, 2 g (95 wt.%) of PVA was weighed and dissolved in 100 mL of deionized water at 85°C (the temperature at or above which PVA is easily soluble in water) under constant stirring at 650 rpm. 5 wt.% GA was added drop wise as a crosslinking agent to the PVA solution and is kept for stirring for another 15 min. 5 wt.% GA content was chosen based on the reduction in the % swelling. Further increase in GA concentration did not reduce % swelling of PVA membrane significantly. Pure PVA consist of hydroxyl groups attached to its backbone. Crosslinking with GA leads to formation of acetal linkage and aldehyde side chain. Mechanism of formation of crosslinking and branching by GA is shown in Fig. 3 and verified through FTIR analysis. The solution is then finally casted onto Teflon plates and left to dry in room temperature. The prepared membranes were further annealed at 120 °C for three hours to improve the crosslinking and here onwards the annealed sample is called as crosslinked PVA membrane.

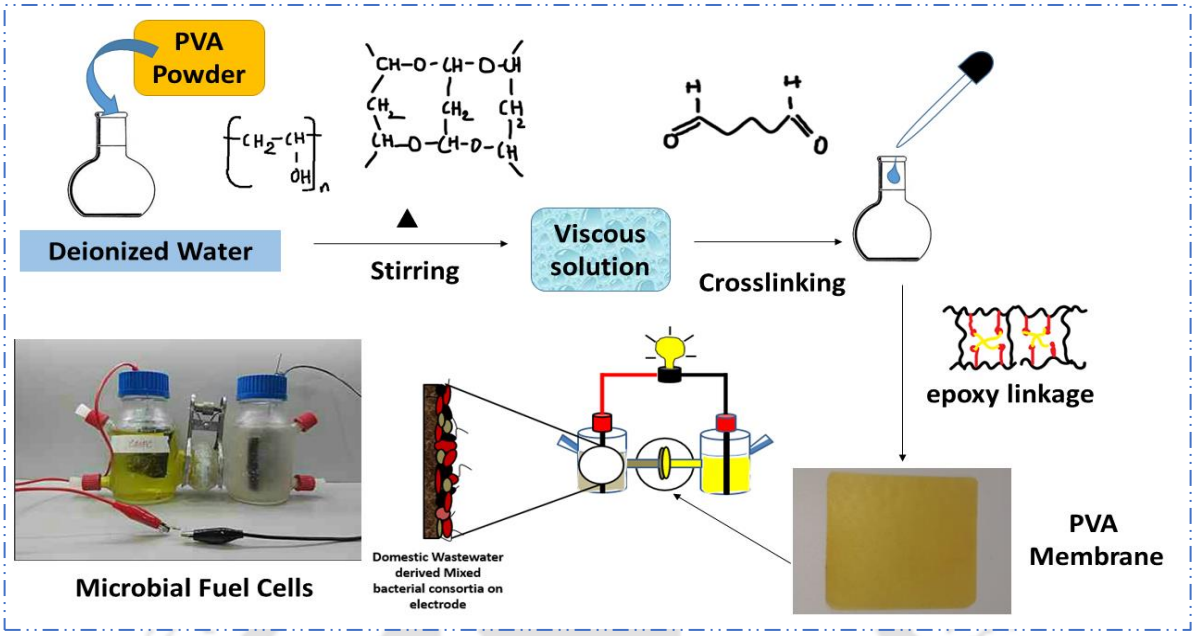

Figure.2.1 Schematic of PVA membrane preparation technique and its assembling into the Dual Chambered MFC.

2.1.2 Characterization of the crosslinked PVA Membrane

Crosslinked PVA membranes were characterized by Fourier transform infrared (FTIR) spectroscopy (in a PerkinElmer Frontier FTIR Spectrometer system) for its structural analysis, which was carried out in ATR mode. Crystalline nature of the crosslinked PVA membranes was evaluated through X-Ray diffraction (XRD) spectroscopy (a Rigaku TTRAX, Seifert XRD 3003 T/T model) in the range of 2θ = 3–60°, with 0.02° step size with Cu-Kα radiation (λ= 0.1541 nm) as X-ray source. Thermal stability of the crosslinked membrane was observed by thermo-gravimetric analysis (TGA) (in a PerkinElmer Thermo-Gravimetric Analyzer TGA 4000 system) in the temperature range 30 -700 °C, at heating rate of 10 °C/ min under N_2 atmosphere. While thermo-mechanical stability was checked by dynamic mechanical analysis (DMA) (a NETZSCH DMA 242 E model) in the

temperature range 25–200°C at 3°C/ min heating rate, 1 Hz frequency and 10 μm displacement amplitude. Water uptake and % swelling was measured for the annealed samples by taking three dried membrane pieces of sample of 5 cm×5 cm size. The samples were initially weighed and then dipped in the water for 24 hours. After that excess surface water was removed using soft tissue paper and the final weight as well as average change in the dimensions of the samples were measured to calculate the water uptake and % swelling using equation (2.1) and (2.2), respectively. The average of three samples is reported as results here.

$$Water\ uptake\ (\%) = \frac{W_{wet} - W_{dry}}{W_{dry}} \times 100\% \quad (2.1)$$

$$\%\ swelling\ = \frac{L_{wet} - L_{dry}}{L_{dry}} \times 100\% \quad (2.2)$$

Where W_{dry} is the dry membrane weight and W_{wet} is the weight of wet membrane and L_{dry} is the length of the sample in initially (5 cm) in dry state and L_{wet} is the length of the sample in the same direction after taking out from water.

Substrate crossover study was carried out for the crosslinked PVA membrane to rule out the leaching of acetate from anode to cathode chamber. A dual-chambered MFC filled with equal volume of deionized water in the two chambers separated by the PVA membrane was used for determination of acetate diffusion coefficient (Dcm, cm^2/sec). Acetate was added as substrate in the anode chamber and its diffusion coefficient was thereby calculated by measuring the change in concentration of acetate in the adjacent cathode chamber using Eq. (2.3). Acetate concentrations, were measured by a high-performance liquid chromatography HPLC (Agilent 1260, Agilent technologies, Palo) with Aminex column HPX-87H(Bio-rad). The mobile phase consisted of 0.005 M H_2SO_4 with the flow rate of

0.6 L/min; the injection volume sample of 20 µL, the column temperature of 38 ^{0}C; and the UV detector was set at 210 nm.

$$D_{cm} = \frac{-vLth}{2at} ln[\frac{Ca-2Cb}{Ca}] \quad (2.3)$$

Where, C_a represents the initial concentration of acetate in anode chamber and C_b represents the final concentration in cathode chamber after time t. v is the liquid volume, L_{th} is the average membrane thickness in cm, A is the projected surface area of PVA-GA membrane in cm^2, t is time in sec.

In order to test the antimicrobial activity of the crosslinked PVA membrane, 1 L of LB Media (10 g tryptone, 5 g yeast extract, 10 g NaCl) is prepared and sterilized for 30 min in autoclave. *Shewanella putrefaciens* bacterial species is then grown in two flat bottom flasks in the incubator shaker at temperature of 30°C at 150 rpm. Membrane samples were then kept in the bacterial media and observed after 72 h of incubation. The morphology of the microbes on the membrane surface were examined using FESEM (JSM-6500F). Samples were fixed in 2.5wt% of glutaraldehyde, washed three times in buffer, dehydrated stepwise in graded series of ethanol/ water solutions (30%, 50%, 70%, 80%, 90%,100%) for 30 min each. Samples were left to dry overnight. They were sputtered with Pt in vacuum prior to FESEM observation.

2.2 Materials for Hair Hydrolysate functionalized cellulose nanocrystal-based Chitosan membrane

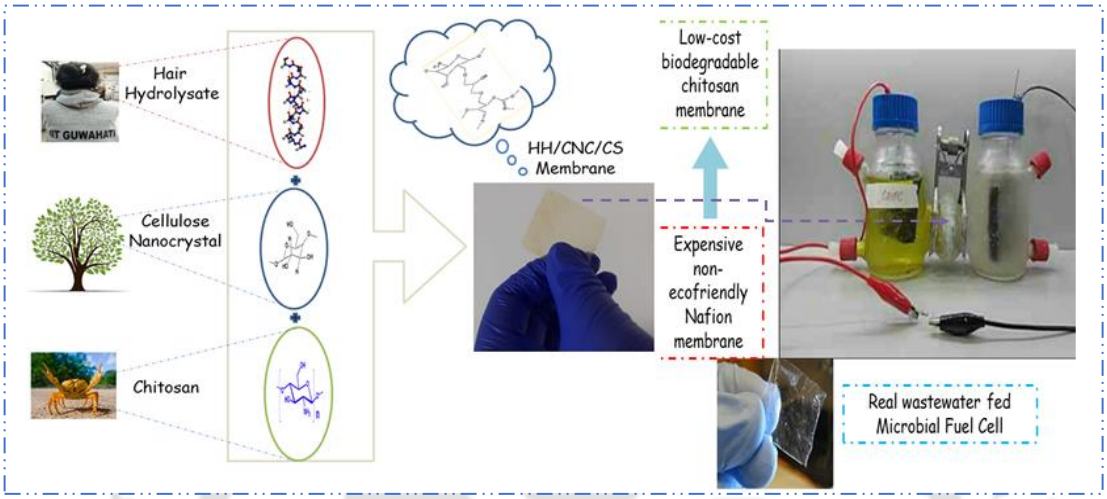

Figure.2.2 is a schematic representation of preparation of the modified chitosan membrane and its application as separator layer in the dual chambered MFC device.

Chitosan (CS) (medium molecular weight, degree of deacetylation >70%) was procured from Sigma-Aldrich India. Epichlorohydrin (ECH), and the rest of the solvents acetone, methanol and chloroform needed for analysis and washing purpose were purchased from HiMedia laboratories private limited, India.

2.2.1 Extraction of hair hydrolysate

Strands of human hair were collected from the barber's shop at IIT Guwahati. They were cleaned with soap solution, followed by acetone and then kept for drying at 60 °C overnight in hot air oven Thermal hydrolysis of the hair strands were carried out following the procedure described (Gaur et al., 2021) to extract amino acids out of the hair keratin.

2.2.2 Modification of CNCs by Hair Hydrolysate

The objective of this modification was to have functionalities on CNCs which can provide CNCs cation exchange sites which will help in the proton conductivity of the modified CS membrane. The hair hydrolysate obtained has lot of amine groups available and it can be used to modify the CNCs. At first, in order to create sites to bind the hair hydrolysate to CNCs, a very well-known technique: periodate oxidation of polysaccharide(Kristiansen et al., 2010), is used, which breaks the cellulosic ring from the part where two hydroxyl groups are on neighbouring carbon to form aldehyde. For the oxidation reaction, CNC and sodium periodate is used in 1:1 ratio. CNCs were dispersed in Millipore water by sonication followed by addition of sodium periodate. This mixture was kept for stirring for 3 h at around 70 °C in dark condition. After the oxidation reaction, the CNC dispersed solution was washed with water three times and centrifuged and subsequently freeze dried. Then the oxidized CNCs were modified by dispersing it in hair hydrolysate solution and stirring at 80 °C around 6 h. During this reaction, crosslinking occurs between the aldehydic group of oxidized CNCs with the amino group of hair hydrolysate (as shown in Fig.2.3). This was followed by centrifuging and washing stepwise several times with water acetone, methanol and chloroform to remove the unbound hair hydrolysate. Thus, the prepared material was freeze dried and used for further synthesizing the desired CS membrane.

2.2.3 Fabrication of functionalized CNCs based CS Membrane

To prepare modified CNCs based CS membrane, first functionalized CNCs (5 wt.% of total weight) were epoxidized by reacting it with epichlorohydrin (ECH) solution (5 ml ECH + 5ml water) at 80 °C for 6 hours to effectively preventing excessive swelling of the chitosan

membrane. As shown in Fig.2.3, epichlorohydrin was used as cross-linker between chitosan and modified CNCs. CS solution was prepared from CS powder by dissolving in water using 0.1 ml of 35 wt.% HCl solution. After epoxidization, CNCs mixture and the CS solution were mixed properly by stirring for another 30 minutes at 80 °C. The final solution obtained were then casted onto Teflon petri dishes and dried to prepare the modified CS membrane which is referred as HH/CNC/CS membrane for further discussion.

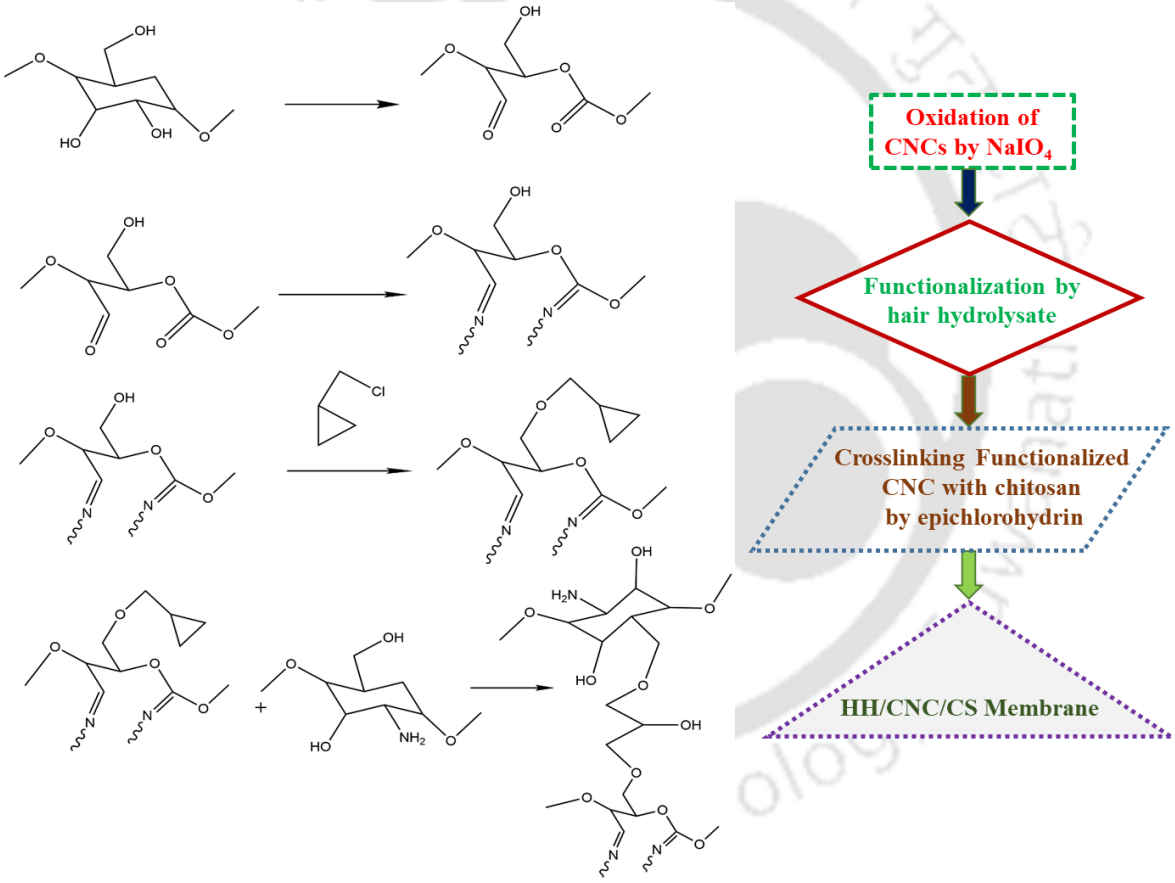

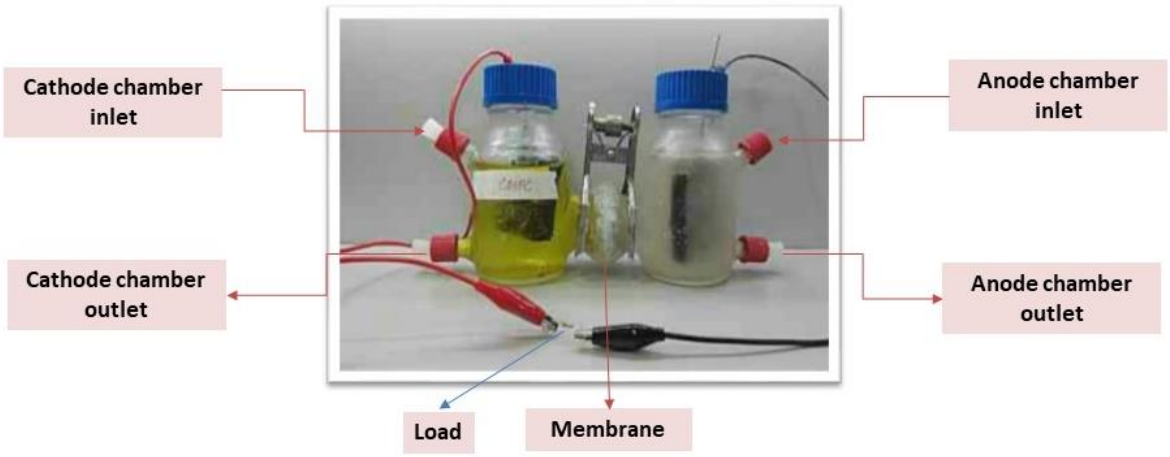

Figure.2.3 (a) Schematic representation of the reaction mechanism for preparation of modified chitosan membrane (b) The physical model of the microbial fuel cell equipped with the membrane.

2.2.4 Characterization of the HH/CNC/CS membrane.

To detect the presence of amine groups material in hair hydrolysate and functionalization of CNC by hair hydrolysate, X-ray photoelectron spectroscopy (XPS) was utilized. Surface Morphology of the membrane samples were analyzed by FESEM. Water uptake, % swelling of the membrane's proton conductivity analysis and antibacterial property of the membrane samples was tested following procedure as detailed in our previous report (Das et al., 2021c) The fabricated membrane samples are analyzed for mechanical stability in tensile mode using Electromechanical Universal Testing Machine (Zwick Roell: Z005TN). Each membrane was clamped between the grips of the tensile tester and 5 kN operating load was applied under automatic control with conditions of 5 cm gap length and 5 mm/min speed. The tensile strength and elongation were calculated as per recent study by (Srinophakun et al., 2017).

2.3 Preparation of the Dual Chambered MFCs Experimental Setup

A schematic representation of the membrane preparation and the physical model of the MFCs is illustrated in **Fig. 2.3(b).** Two identical dual chambered MFCs were constructed of two glass chambers of 250 mL joined by proton exchange membrane clamped in between the two chambers. Graphite felts electrodes of 5 cm× 5 cm in size were used as anode and cathode with fabricated membrane of size 5 cm in diameter as the experimental case. While graphite felt in both anode and cathode chamber with Nafion 117, Dupont Co., USA (with same size) was considered as the control case. The Nafion-117 was pre-treated before use with 5% H_2O_2 solution first and then with 0.5 M H_2SO_4 for 1 h each at 70 °C. It was then washed using deionized water repeatedly and treated membrane was then soaked in deionized water for use. The graphite felt electrodes were pre-treated with 10% H_2O_2 Solution for 3 hours at 90 °C after which it was left to dry in ambient conditions.

2.4 Operation of fabricated membrane assembled Dual Chambered MFC

Domestic wastewater, obtained from the Luodong Wastewater Treatment Plant situated at Luodong, Yilan County-260, Taiwan, was the source of mixed culture of bacteria. The inoculum in the anode chamber of the two MFCs modules was mixed 1:1 with wastewater containing mixed culture of bacteria and 50 mM phosphate buffer nutrient solution (PBS). The PBS consisted of 4.58 g/L of Na_2HPO_4, 2.45 g/L of $NaH_2PO_4.H_2O$, 0.31 g/L of NH_4Cl and 0.13 g/L of KCl. The cathode chambers were filled with 50 mM Potassium

Ferricyanide prepared in 50 mM PBS. The wastewater contained COD concentration in the range of 250 mg/L, BOD of 130 mg/L and SS of 100 mg/L and pH of 7.0 All experiments were carried out at temperature of 30 ^{0}C and the measurements were done in triplicate.

2.5 Electrochemical Measurements and Biofilm Analysis

The voltage was monitored in the interval of 1 min using a data logger (Jiehan 5020, Taiwan) with an external resistance of 1 kW resistor connected to the MFCs to substantially reduce the acclimation time. After acclimation process was over, both chambers of the MFC were replenished with fresh solution of the catholyte and anolyte. It was left in open circuit mode overnight to fully establish the open circuit voltage. The multichannel electrochemical analyzer, (Jiehan 5020, Taiwan) was used for obtaining the voltage and current. Power density generated was calculated based on the projected anode surface area (mW/m^2). And was obtained from the voltage and current recorded in open circuit conditions according to the formula,

$$P = \frac{VI}{A} \tag{2.4}$$

Where V represents voltage in Volts, I represents current in milliAmperes and A represents a working area of an anode in square centimeters. The experiments were carried out in duplicates and the results obtained were confirmed upon reproducibility in the output values.

Internal resistance of the MFCs was determined using electrochemical impedance spectroscopy (EIS) analysis which was recorded in multichannel electrochemical workstation (Jiehan, Taiwan) and the data were analyzed using EC-Lab software. A sine wave of amplitude 10 mV was used for EIS with frequency of the sine wave set at sweep

mode and frequency range was set from 100 kHz to 0.1 Hz. COD of the wastewater was determined using the potassium dichromate oxidation method. 2 ml of the samples were taken in vials (HR COD Vials K-7360S, Suntex) and digested for 2 h at 150℃ in a TR-1100 COD Thermoreactor (Suntex Instruments Co., Ltd., Taiwan) prior to analysis. The anolyte samples were collected at the start and end of each fed batch cycle which usually took 24 h. The COD vials were then inserted into the photometer (Multi-Analtye Photometer CHEMetrics V-2000, Taiwan).

To ensure microbial adhesion on the anode surface of the crosslinked PVA assembled MFCs, the anodes of both the modules were examined using FESEM. The biofilm developed on the electrodes were fixed in 2.5 wt% glutaraldehyde solution followed by washing three times in phosphate buffer solution and finally dehydrating stepwise for 30 min each in graded series of ethanol/ water solutions (30%, 50%, 70%, 80%, 90% and 100%, respectively). To ensure the presence of microbes, the surface morphology of the control electrodes (without microbes) were examined.

2.6 Materials for electrode preparation

Poly (lactic acid) beads of the grade 2003D (about 98.6% L-form) were obtained from Nature Works LLC. Chloroform HPLC Grade, Aniline (99.5%), Sodium persulphate (SPS; 98%), Hydrochloric Acid (HCl;37%), Cetyl Trimethyl Ammonium Bromide (CTAB;98%) and Propanol (99.9%) used were of analytical grade and obtained from Sigma Aldrich.

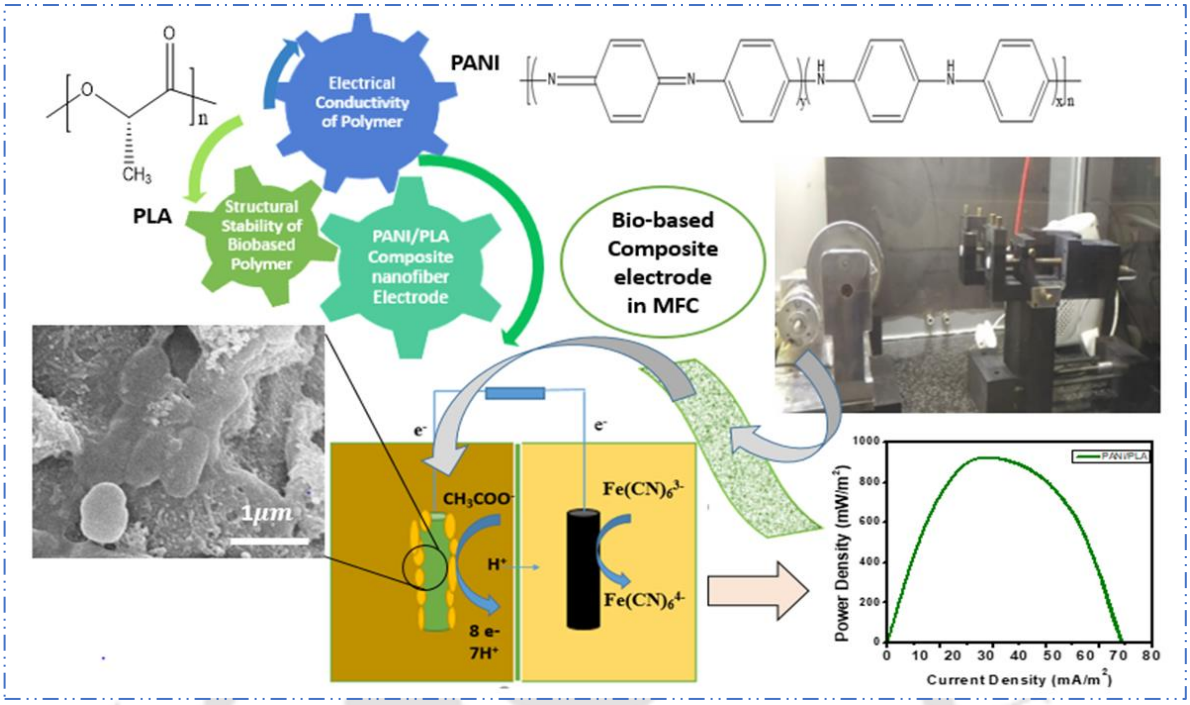

Figure.2.4 Schematic representation of flexible electrode preparation technique and its application as anode electrode in the dual chambered MFC device.

2.6.1 Synthesis of PANI/ PLA composite nanofiber electrode

The PANI/PLA electrode was fabricated by the electrospinning technique. In this procedure, the horizontal setup for electrospinning was used wherein the polymer jet discharged from a horizontal syringe pump which was maintained at a positive potential of 5.5 kV with the solution flow rate set at 0.8 mL/hr. PLA beads (11 wt%) were first dissolved in chloroform. 0.5ml of Aniline solution was added to 4.5g of the polymer solution. These solutions were then transferred to a syringe equipped with a blunt needle of 13.6 mm diameter attached to a pump for electrospinning. The charged polymer solution jet was collected onto the grounded drum collector also called the rotating mandrel set at 660 rpm. In the in-situ polymerization of aniline to polyaniline, the rotatory drum was intermittently dipped in initiator solution containing 0.1 M SPS in 1M HCl with 50 mg/L

CTAB. The procedure was continued until the polymer solution in the syringe was spent. After the electrospinning procedure was done, the nanofiber mats were washed with propanol and left to dry in a fume hood. It is left to dry for 2 h after which the fiber mats were ready to be used in the Microbial Fuel Cell as an anode electrode.

2.6.2 Assembling the Dual Chambered MFCs

The dual-chamber MFCs contained two glass chambers (250 ml each) with flanges of inner diameter 40 mm to which the membrane Nafion 117, 5 cm in diameter was clamped between the two chambers. The working volume of the MFC being 200 ml. The electrodes were $4cm \times 10cm$ in size. PANI/PLA composite nanofiber was used as anode and graphite felt as cathode while the control case was graphite felt in both anode and cathode chamber. The control graphite felt are pre-treated with 10 % (v/v) H_2O_2 Solution at 90 ^{0}C for 3 hours. The membrane was pre-treated with 5 % (v/v) H_2O_2 solution followed by 0.5 M H_2SO_4 solution for an hour at 70 ^{0}C after which it was washed repeatedly with deionized water.

2.6.3 Set-up of biobased electrode assembled Dual Chambered MFCs

The anolyte was prepared by mixing phosphate buffer nutrient solution (PBS) and domestic wastewater in the ratio of 1:1. The wastewater for the study was collected from Treatment Plant in Yilan County, Taiwan. The PBS (50 mM) solution had 4.58 g/L of Na_2HPO_4, 2.45 g/L $NaH_2PO_4.H_2O$, 0.31 g/L NH_4Cl and 0.13 g/L KCl. Sodium acetate (1g/L) was used as a substrate for the bacteria. The catholyte was Potassium Ferricyanide (50 mM) in 50 mM PBS. Total dissolved solids (TDS), pH, conductivity, Salinity, Turbidity, NH_4^+ and COD

of the wastewater was 2.0 ppt, 7.0 ± 0.03, 3.09 $mScm^{-1}$, 150 NTU, 825.71 ppm, and 340 ppm respectively. All MFC experiments were conducted at room temperature.

2.6.4 Characterization of anode material

The visualization of the surface of the nanofiber anode and control electrode was investigated using Field Emission Scanning Electron Microscopy (FE-SEM) (JSM-6500F) before and after application in the MFC. 2.5 % (w/v) glutaraldehyde (GA) to fix the samples and thenceforth washed thrice in PBS followed by dehydrating stepwise in ethanol solution from 30% (v/v), 50% (v/v), 70%(v/v), 80%(v/v), 90%(v/v) to 100% (v/v) respectively for 30 min each.

To observe the thermal stability of the fabricated anode, thermogravimetric analysis (TGA) was carried out in the temperature range of 30 to 700 ^{0}C under nitrogen atmosphere at a heating rate of 10 ^{0}C/min using TGA 4000 Thermogravimetric Analyzer (Perkin Elmer). Differential Scanning Calorimetry measurements were conducted under a nitrogen atmosphere from 25 to 180 ^{0}C for a heat-cool-heat cycle at a scanning rate of 10 ^{0}C using DSC 214 Palma (NETZSCH, Germany).

The structural analysis for the PANI/PLA composite sample was investigated using Fourier Transform Infrared Spectrophotometer from Shimadzu (Japan) using attenuated total reflectance mode (ATR) attachment under dry air. At first, the electrode samples were dried in an oven for 2 hours at 80 ^{0}C to remove any free moisture. FTIR spectra were obtained in the range 4000-300 cm^{-1} at a resolution of 2.0 cm^{-1} with 20 consecutive scans and the data obtained were analyzed using IR solution software.

The X-ray photoelectron spectroscopy was accomplished using Thermo Scientific Escalab Xi+ using X-ray source (Al(Kα) =1486.6 eV) at 10^{-10} mbar pressure. XPS resolution acquired for the Full Width at Half Maximum of Au (5f7/2) core level line was 1.2 eV. The binding energy (BE) of the core level C(1s) was set at 284.8 eV to recompense for any surface charge effects. The XPS peaks were devolved into their various components using Shirley Method and quantitative interpretation of the peaks was made after subtracting the background signal. Parameters namely, the full width at half maximum, binding energy, peak intensity, Gaussian\Lorentzian ratio, were fitted using the developed curve-fitting programs. Optimization of the parameters was done to best fit the experimental data. The quantitative analysis for O(1s), C(1s), and N(1s) was done based on integral intensity (peak area) of signals.

To measure the conductivity of the fabricated anode, the four-probe method was used. The contact angle of the sample with DI water was measured with a KRUSS DSA25 contact angle measurement system for a water/air system to observe the wetting properties of the nanofiber sample.

2.6.5 Electrochemical investigation

Electrical output generated by the MFCs was recorded every min with the help of a data acquisition system (Jiehan Technology Corporation 5020, Taiwan). A 1kW external resistance was connected for stable acclimation. After completion of the acclimation process, the chambers of the MFCs were replenished with fresh anolyte and catholyte solutions. The MFCs were left overnight in open circuit conditions for obtaining the stable Open Circuit Voltage. The polarisation curves were recorded at a scanning rate of 1mV/s

using EWare Software connected to the Multichannel Electrochemical Analyser, (Jiehan 5020, Taiwan). Power density based on the anode surface area (mW/m^2) was obtained from the voltage and is currently recorded in open circuit conditions according to the formula (2.4).

Where V represents voltage in Volts, I represents current in milliAmperes and A represents a working area of an anode in square centimeters. The experiments were carried out in duplicates and the results obtained were confirmed upon reproducibility in the output values.

To get a better understanding of the bioelectrochemical activity of the mixed culture, how the interaction between microbes and anode occurs during electron transfer, cyclic voltammetry analysis was carried out with Ag/AgCl as a reference electrode at scan rate of 10 mV/s in the in the potential range of -1 to +1 V.

The internal resistance of the MFCs was recorded in Zware software and analyzed using EC-Lab software by conducting Electrochemical Impedance Spectroscopy (EIS) analysis performed using a Multichannel Electrochemical Workstation (Jiehan, Taiwan) within 100 kHz-0.1 Hz. The DC Potential was set at 0.5 V and AC Amplitude was set at 10 mV. For determining COD of the wastewater, samples were digested at 150℃ in a digestor (Suntex, TR-1100) before analysis for 2 h and then measured using a photometer.

2.7 Construction and Operation of hospital wastewater fed MFC

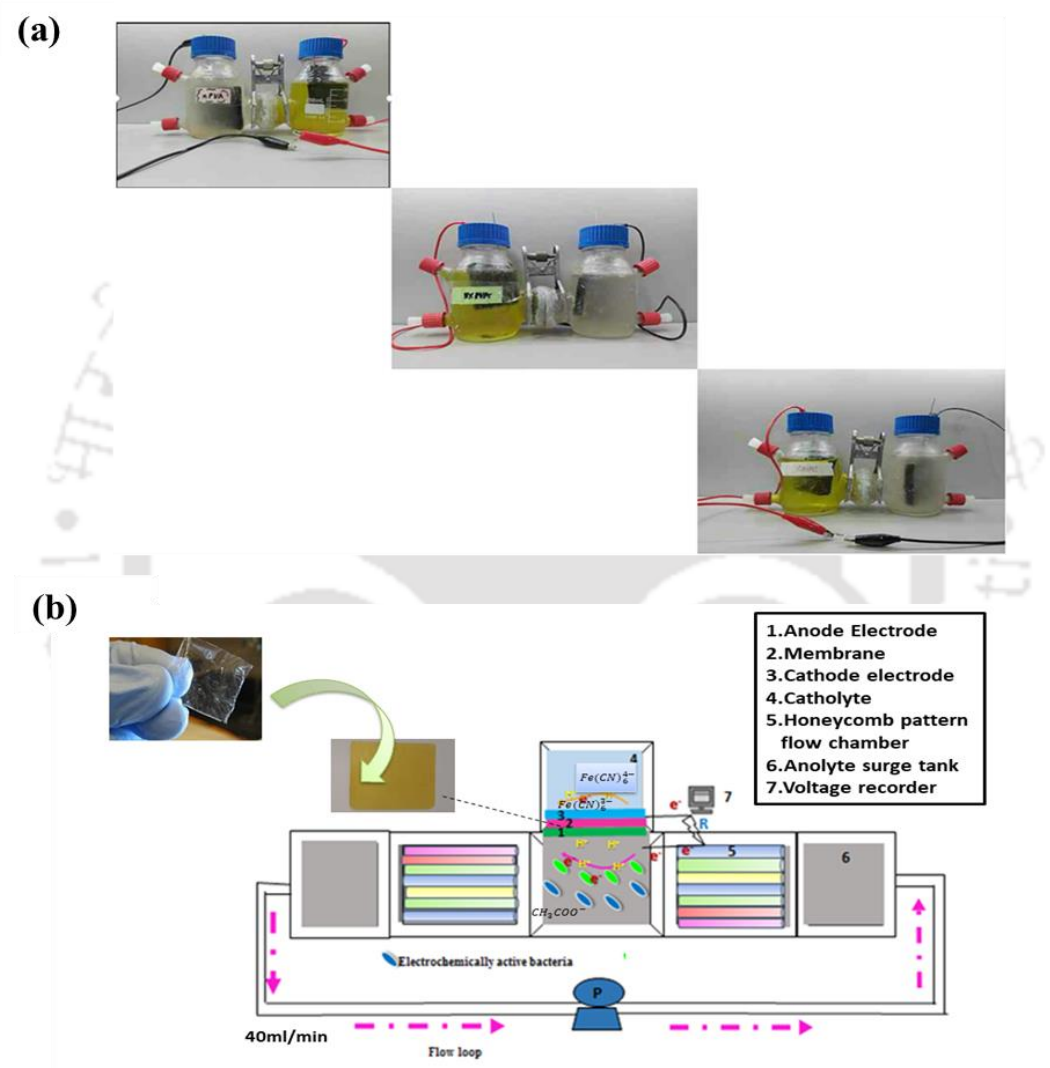

Figure.2.5 Physical models to study the performance of hospital wastewater fed (a) Dual chamber MFCs assembled with Nafion 117, neat PVA and crosslinked PVA membranes, (b) Honeycomb MFCs (HCMFCs)assembled with crosslinked PVA membranes.

A schematic representation of the membrane preparation and the physical model of the MFCs are illustrated in Fig. 2.5(a). Three identical H-MFCs were consisted of an anode chamber and a cathode chamber of reactor volume 250 mL separated by the membranes (5 cm× 5 cm) clamped in between the two chambers. PVA membranes are prepared as previously described (Das et al., 2021). Graphite felts (5 cm× 5 cm) were used as electrodes. Two identical HCMFCs were constructed using PMMA sheets. As illustrated in Fig 2.5 (b) each of the HCMFC setup consisted of an anode chamber of reactor volume of 1L and a cathode chamber of 150 mL separated by the PVA membranes (5 cm× 5 cm) clamped in between the two chambers. The graphite felt electrodes were pre-treated as previously described to enhance biofilm formation while the membranes required no such prior treatment(Das et al., 2021). Hospital wastewater, obtained from FEHM, Taiwan, was the source of mixed culture of bacteria. The wastewater contained initial concentrations of ammonium nitrate, TDS, DO, COD, 8000 ppm, 5.97 ppt, 14.6 ppm and 825 ppm respectively. The salinity and conductivity were 3.78 ppt and 6.32 mS respectively. All the wastewater parameters were analyzed according to the standard methods. The inoculum in the anode chamber of the two MFCs modules was mixed 1:1 with hospital wastewater and 50 mM phosphate buffer nutrient solution (PBS). The pH was adjusted to 7. The cathode chambers were filled with Potassium Ferricyanide (50 mM) prepared in 50 mM PBS. All experiments were carried out at temperature of 30 ^{0}C and the measurements were done in triplicate.

2.8 Classical Molecular Dynamics Simulation Details

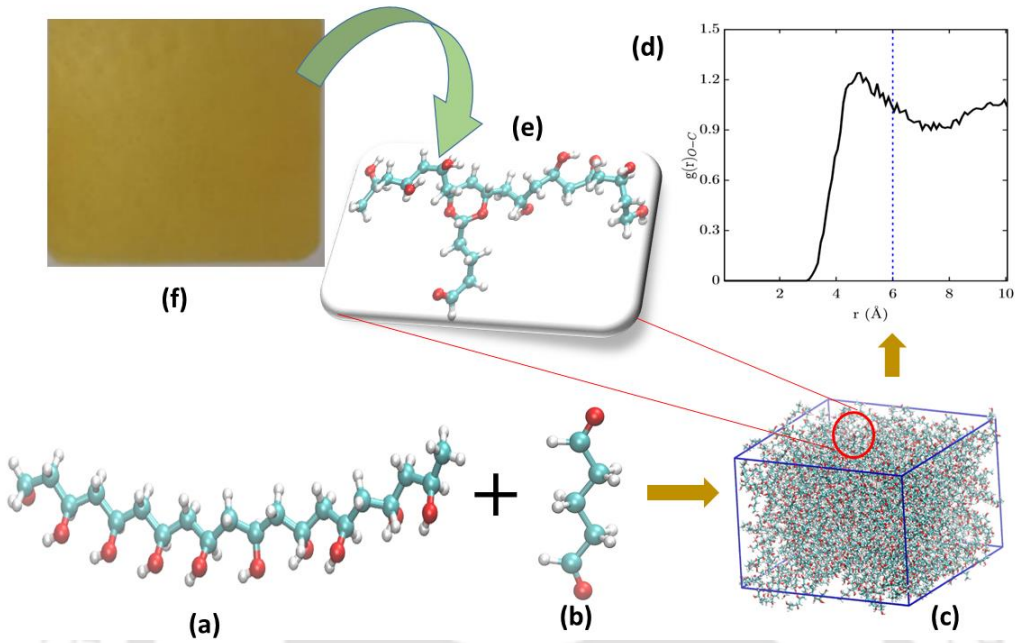

Figure 2.6 (a) Polyvinylalcohol model with 10 repeating units, (b) the glutaraldehyde model, (c)crosslinked PVA membrane model packed in the simulation box, (d) radial distribution function confirming the cut-off distance for bond formation after crosslinking reaction between PVA and GA, (e) inset picture shows the crosslinking reaction between PVA and GA, (f) experimentally synthesized crosslinked PVA polymeric membrane.

2.8.1 Construction of atomic models of the fabricated membranes

Classical molecular dynamics simulations were carried out for the crosslinked membrane using NAMD Molecular Dynamics Software Package(Phillips et al., 2020) and visualized using Visual Molecular Dynamics (VMD) (Humphrey et al., 1996).The crosslinked PVA membranes were modelled using CHARMM36 (‘Chemistry at HARvard Macromolecular Mechanics’) Force Field(Huang & MacKerell, 2013) native in the NAMD simulation

package. The first step encompasses the preparation of a system containing polymer chains constructed within the Avogadro 1.2.0 (Khalid et al., 2021) which were enclosed in a cubic cell using PACKMOL software (Martínez et al., 2009).Crosslinker concentration of 5 wt % used these simulations is similar to that obtained during experimental conditions. In order to avoid surface effects, 3-D periodic boundary conditions were used. A set of five different structures for possible crosslinking sites between PVA and GA was built at the same time, by means of Avogadro, for the molecular dynamics simulations. Water molecules were constructed using the TIP3P parameters. In order to understand the effect of crosslinking on the proton transport process, a control system is constructed of water and hydronium ions devoid of the membrane structure along with the neat polyvinyl alcohol membrane (nPVA). For the present study the membrane to be simulated is prepared by a heuristic approach where crosslinking between PVA and glutaraldehyde of the polymeric membrane is based on a distance criterion. The accuracy of the simulation is related to how realistic the polymer can be constructed with appropriate no. of repeating unit Specifically, 32 atactic chains of PVA with 10 repeating units and 9 GA monomers in the approximate stoichiometric ratio for the reactants, were packed volume in a box of 100 Å × 100 Å × 100 Å. Here, the number of PVA and GA repeat units are determined according to its relation with the density obtained after packing in Packmol without forceful packing which is similar to the experimental density of 1.26 gcm^{-3} for crosslinked PVA. Crosslinker concentration of 5 wt % used these simulations is similar to that obtained during experimental conditions. After the simulation system is constructed, the constructed cells are subjected to minimization for 10000 steps and the system is allowed to equilibrate for 2 ns in NPT ensemble at a temperature of 300 K and 1 atm pressure with 3-D periodic

boundary conditions in order to avoid surface effects. The modified Nose-Hoover (Martyna et al.,1992) thermostat and barostat with oscillation time and damping factor of 1 ps was applied for temperature and pressure control, respectively. Langevin Dynamics (Feller et al.,1995) is used for controlling the temperature with a damping factor of 1 ps. The integration time step was 1 fs. The variation in temperature and the total potential energy of the simulation systems is ascertained using the NAMD Plot in VMD. The absence of fluctuations ensures that the system has reached equilibrium. The final structures obtained from the energy minimization step further undergoes annealing equilibration method in order to avoid the system to be trapped on a local high energy minimum. The system is subjected to a three-step annealing process, where temperature is raised from 300 K to 1100 K at regular intervals and subsequent cooling to 300 K with a step of 50 K in an NVT ensemble. Then the simulation is continued by allowing new acetal bonds formation for every 10 ps of simulation time. The primary condition for the crosslinking reaction to occur is that the reaction sites should be adjacent. Initially bond formation reaction is allowed only when the distance between hydroxyl (OH) sites of PVA and aldehyde(-CHO) of GA (fig 6.1) is 3 A^0 forming the C-O-C linkage confirming the crosslinking of PVA and as the simulation progressed, this is relaxed to 3.5 A^0 with a step of 0.1 A^0 to speed up the crosslinking process. A code is written for the crosslinking reaction considering all possible combinations when a PVA chain comes in contact with GA molecule with the main goal to achieve charge neutrality unlike using PACKMOL which remains deficient in charge. Charges are assigned in such a way that when a new member arrives/attaches, the old ones remain in their position and new members are accommodated accordingly in the remaining sites. Energy minimization and equilibration is performed after each crosslinking step. The

crosslinking is followed by solvation of the membranes. For the crosslinked membrane, the solvation was 50 % while for the neat membrane the solvation was 100% as per the water content calculated from experimental findings. The resulting solvated polymer structure is minimized for 10000 steps and equilibrated for 2 ns in NPT ensemble. The final polymer structure after only equilibration is 64 A^0 thick and 87 A^0 x 87 A^0 in x and y direction. The structure after 50 ns of the virtual crosslinking simulations is shown in Fig 2.6 (d), where different colors represent different fragments, or chains, that are crosslinked. The resulting structure serves as an initial configuration for the subsequent studies of the dynamics of proton transfer.

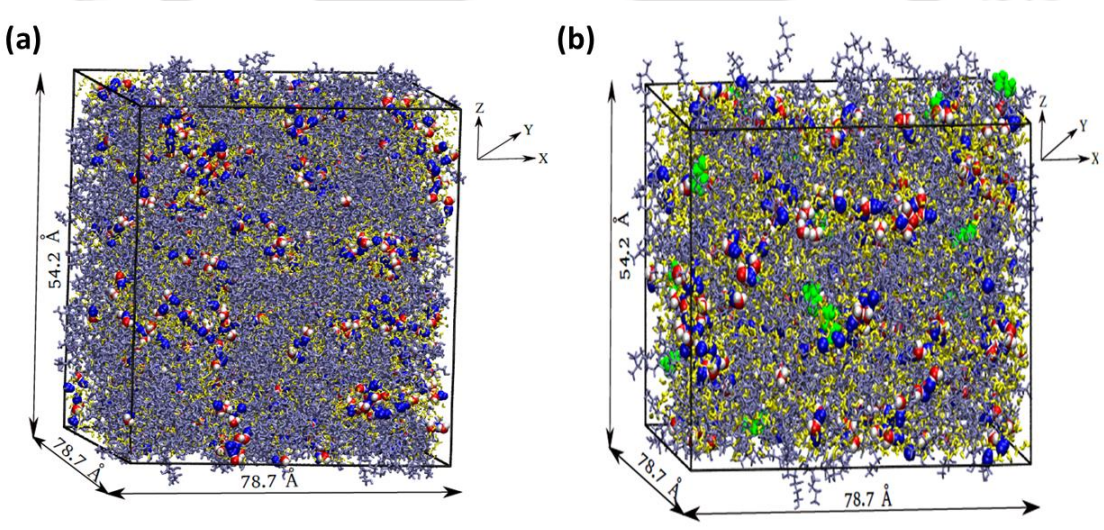

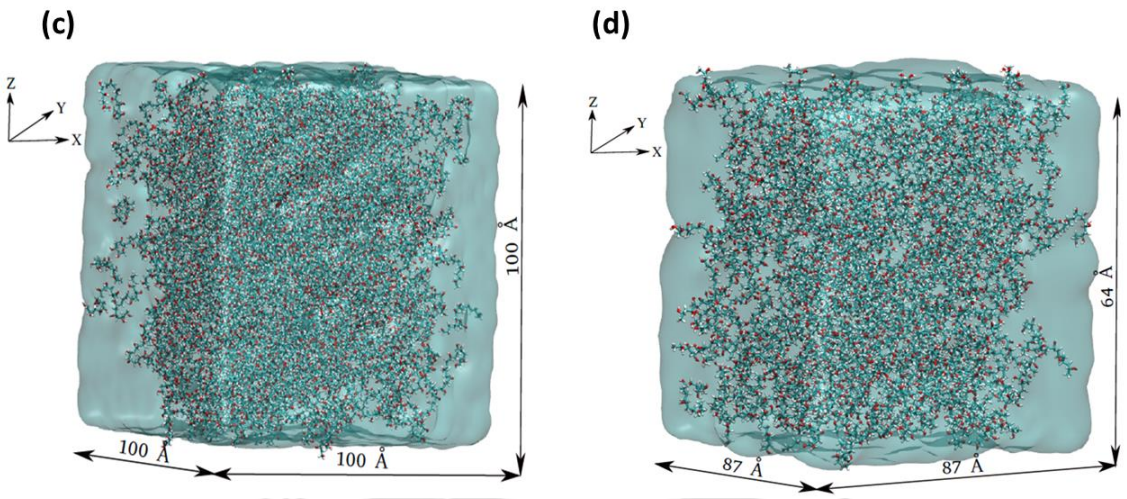

Figure 2.7 Simulation setup for (a)neat PVA system containing PVA, water molecules, and hydronium ions, where black lines denote the periodic boundaries of the unit cell;(b) Crosslinked PVA membrane (c) Solvated neat PVA membrane structure (d)solvated crosslinked membrane structure where white, red, blue, green colour corresponds to H, O, C atoms and crosslinker respectively.

2.9 Experimental and Numerical modelling on flow condition of hospital wastewater fed MFC

2.9.1 Description of the Numerical Model

The numerical simulation of MFC Model mimicking the experimental setup is based on the Finite Volume Method and analysis is carried out using ANSYS Fluent(Kataky et al., 2020). The multidimensional 2D model of Merkey & Chopp (Merkey & Chopp, 2012) serves as the base model for our study. The 3D structure of the MFC is projected to a big

rectangle which is composed of 6 zones in the order, anode chamber, biofilm, anode, proton exchange membrane, cathode and cathode chamber, as shown in Fig 2.8 with the cross-section 50 mm × 50 mm kept constant throughout the computational domain. The following subsections describe the model in more detail.

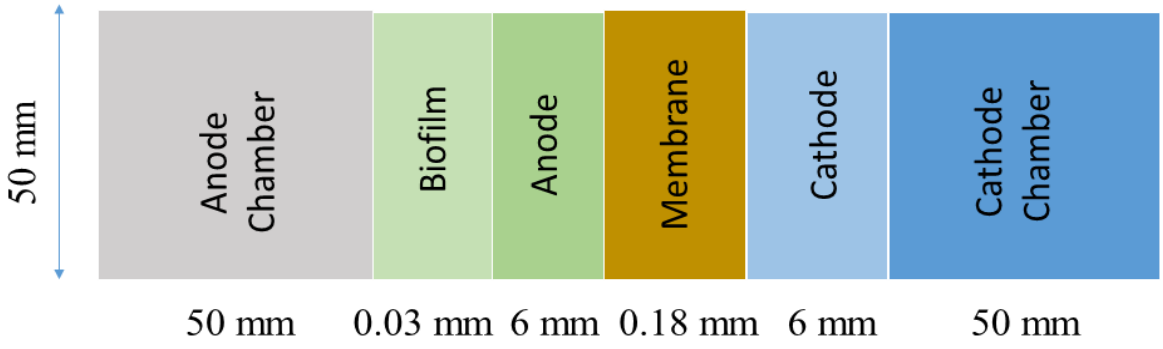

Figure.2.8 2D model representing the experimental setup under study.

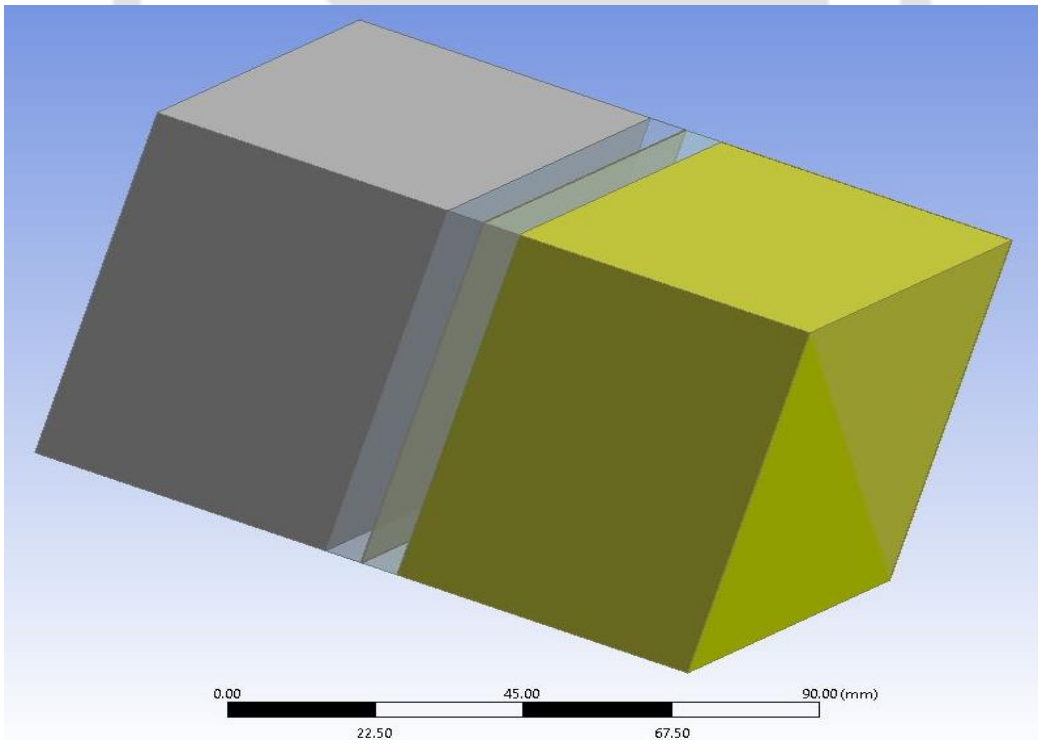

Figure.2.9 3D model representing the experimental setup under study.

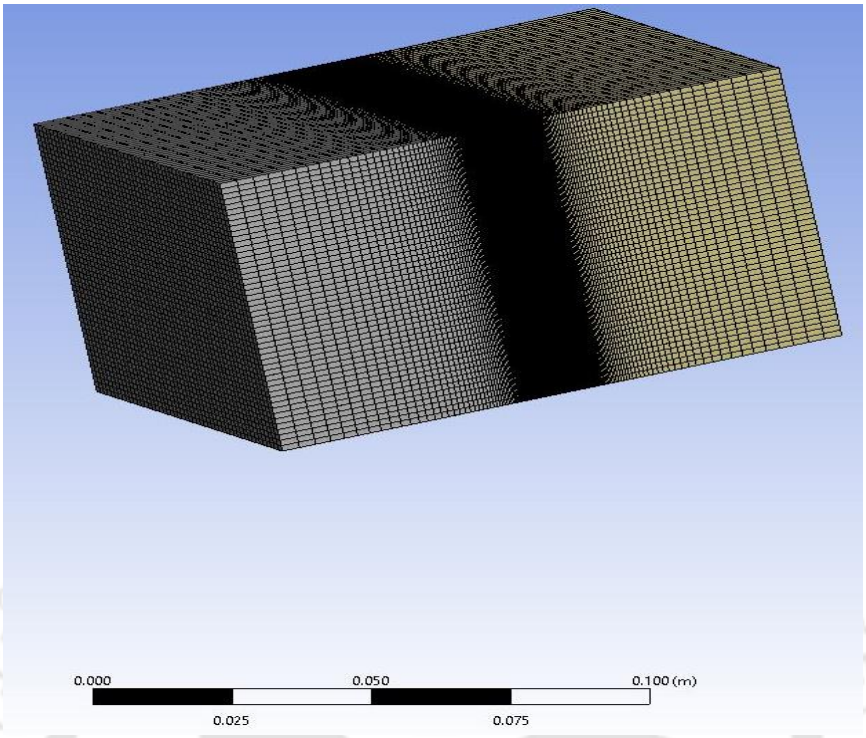

Figure.2.10 3D meshed structure of the MFC model.

2.9.2. Reaction Mechanisms in MFC

The mixed cultured bacterial consortia present in the domestic wastewater is a cocktail of both electroactive and non-electroactive species. However, after the acclimation period, the anodic biofilm developed is dominated up to 97% by electroactive species with Geobacter sulfurreducens being the predominantly found species in most anodes enriched with mixed culture bacteria. The flexibility to acclimatize to diverse electron acceptors along with the ability of forming thick and robust biofilms employing extracellular mode of electron transfer help the mixed culture bacteria biofilm in achieving higher power densities than its pure counterpart. Besides, G. Sulfurreducens possess the capability to aid as catalyst in conversion of acetate to electrons and carbon dioxide with an efficiency of 100% owing to its well characterized electrochemical behaviour and electron transfer mechanisms towards a solid electrode. Hence for our numerical model, the biofilm

developed on the surface of the graphite felt anode in the wastewater fed MFC is best represented by features of G. Sulfurreducens. Direct electron transfer from the biofilm to the anode is considered to occur via intracellular mediators as per experimental observation. Mixed culture bacteria in the wastewater is used to describe the biofilm at anode and current is calculated based on experimental data. The anodic reaction being the slowest step hence the effect of anode reaction kinetics on the current generation is studied. This model can be used as a convenient tool for performing detailed analysis of a range of parameters for assisting in process optimization.

Following are the assumptions considered to achieve a fast-numerical solution of the model:

- Steady state
- Incompressible flow
- Fluid properties were constant
- The carbon source acetate is well distributed in the anodic compartment, therefore ideal mixing is assumed and substrate gradient in the biofilm is neglected;
- Uniform distribution of microbial populations in the anodic compartment biofilm is assumed.
- Gas transport (e.g. oxygen, methane) through the porous cathode is neglected;
- Temperature and pH are considered fully controlled and kept constant.
- Steady state and no convection.

- In the anode compartment, only the liquid phase was considered, thus emitted carbon dioxide remained dissolved in solution.

The experimental batch mode condition of the MFC is realized by setting a constant acetate concentration in the anode chamber which diffuses to the biofilm on the anode for bacteria to consume, i.e. bacteria consume acetate in the biofilm and generate carbon dioxide, protons and electrons with the help of mediators (both reduced and oxidized); the protons and electrons from the anode side are then transferred to the cathode for oxidation. Anaerobic condition is maintained only in the anode chamber. Therefore, considering the presence of oxygen in cathode, electron reduction of oxygen at the cathode is also considered in the model.

The oxidation reaction happening at the anode is

$$CH_3COO^- + 2\,H_2O \xrightarrow{k_1} 2CO_2 + 7H^+ + 8e^- \quad (2.5)$$

The reduction reaction at the cathode is given as

$$4Fe\,(CN)_6^{-3} + 4e^- \xrightarrow{k_2} 4Fe\,(CN)_6^{-4} \quad (2.6)$$

$$O_2 + 4H^+ + 4e^- \xrightarrow{k3} 2H_2O \quad (2.7)$$

The anodic oxidation reaction producing electron that are consumed in cathodic reduction reactions are considered as volumetric reactions because of simple modeling theory. The Arrhenius expression for stating the forward rate of a non-reversible reaction in FLUENT is given by

$$k = AT^{\beta r}\, e_{RT}^{-E} \quad (2.8)$$

Where A is the pre-exponential factor,βr is the temperature exponent, E is the activation energy for the reaction (J/kmol) and R is the universal gas constant (J/kmol-K). Assuming that the MFC is not affected by change of temperature along with zero activation energy. Hence the equation simplifies to k=A which is therefore, used as the input variable and its range is varied to see for the variation occurring in the performance of the MFC. Considering the variation in concentration of the reacting species which also will lead to variation in the reaction rates throughout the MFC, the total reaction rate $R_{i,\ tot}$ of consumption/production of a species i in the MFC is obtained by taking integration over the whole reacting area is given by the finite rate model in FLUENT in kmol/m^3-s as

$$R_{i,\ tot} = \int_0^x R_i\ (x)dx \qquad (2.9)$$

Since the anodic reaction caused by bacteria is the rate limiting step, the performance of the MFC is therefore, best described by the linear relationship of rate of anodic reaction with current density which is calculated as follows:

$$i = ZxFr \qquad (2.10)$$

Where, Z=no. of electrons from the reaction in the anode electrode., x=anode thickness, F=Faraday's constant, r= average reaction rate in the anode electrode

2.9.3 Dimensionless parameters

Reynolds number (Re) is a ratio of inertia force to viscous forces used to investigate the fluid flow situation It is a dimensionless quantity used to investigate the different fluid flow situations in the MFC and is defined as follows:

$$Re=\rho V D_T/\mu \qquad (2.11)$$

Where ρ represents the density of water (997 kg/m^3); V indicate the inlet flow velocity (2.47×10^{-3} m/s, corresponding to the flow rate of 40 mL/min); μ is viscosity of water (8.9×10^{-4} kg/ms) and, D_T represents the hydraulic diameter (6.153 cm);

$$D_T = 2WH/W+H \quad (2.12)$$

Where W is the channel width of MFC anode chamber (5 cm) and H means channel height of MFC anode chamber (8 cm), the inlet Reynolds number of 1.7×10^2 corresponding to the flow rate of 40 ml/min) were applied to MFC by using a peristalsis pump.

Diffusion layer thickness (δ_D) (m) is defined as

$$\delta_D = D/K \quad (2.13)$$

2.9.4 Boundary layer thickness and shear rate

The hydrodynamic boundary layer formed by liquid flow through a flat plate due to the viscosity of liquid particle, and the thickness of flat plate boundary layer thickness, where x is the electrode position

$$\delta = 5\sqrt{\mu x/\rho V} \quad (2.14)$$

Where x is the electrode position of 5 cm (Corresponding to the hydrodynamic boundary layer thickness of 2 cm)

Shear rate G can influence the mass transfer and biofilm formation in MFC.Biofilm detachment from the anode surface depends on the value of shear rate and the shear rate is defined as shown below:

$$G = V/d \quad (2.15)$$

Where V is the flow velocity at hydrodynamic boundary layer (0.99 times less than inlet flow velocity) (m/s), and d represents the thickness of the hydrodynamic boundary layer (0.02 m).

2.9.5 Boundary conditions and balance equations

The rate of reactions and the boundary conditions are set so as to mimic an actual working MFC which results in oxidation reactions occurring at the surface of the anode and reduction reactions at the surface of the cathode. The mathematical model being stationary, the boundary region between anode chamber and biofilm is also stationary. Therefore, the biofilm thickness is constant. For our wastewater MFC model, the full-grown biofilm, 30 µm thick that developed on graphite anode surfaces in the wastewater fed MFC experimentally is represented. The boundary condition at the inlet of the MFC is a constant velocity vector $\vec{v}$ normal to the inlet surface while at the outlet, it is set to ambient pressure. The boundary condition on the top of the domain as well as between adjacent wall boundary is a no-slip wall boundary condition (velocity vector $\vec{v} = 0$). For the anode and anode-chamber interface, acetate(R1) is fixed to 1.174×10^{-3} (mass fraction) and no reflux for protons, and, product carbon dioxide (P1) is set to 0; While at the cathode and cathode-chamber, ferricyanide(R2) is set to 8.72×10^{-3} ,oxygen is set to 8.3×10^{-6} with no proton flux and the product ferrocyanide (P2), R1, P1 are all set to 0.

In FLUENT, after implementing the mesh, the next step is to add the reacting species. However, while doing so, the mixture material needs to be created in which various parameters such as density, mass fraction, mole fraction, molar concentrations of each of the individual reactant and product species are calculated. The calculation of mixture

density is done using volume weighted mixing law and the properties are implemented using the Volume of Fluid (VOF) model. The transfer of H^+ ions occurs through the membrane via diffusion and electrons through the circuit. The Navier Stokes equation comprehensively represents the calculation of 3D fluid flow in the MFC.

$$\partial\rho/\partial t + \nabla.(\rho \vec{V}) = 0 \quad (2.16)$$

$$\rho[\partial\vec{V}/\partial t + \vec{V}\cdot(\nabla\vec{V})] = -\nabla p + \mu\nabla^2(\vec{V}) + f \quad (2.17)$$

Where $\vec{V}$ is the flow velocity, ρ is the density, p is the pressure, μ is the viscosity and f are the body force.

The convection-diffusion conservation equation is given by,

$$\frac{\partial(\rho Y_i)}{\partial t} + \nabla.(\rho\vec{v}Y_i) = -\nabla.\vec{J_i} + R_i + S_i \quad (2.18)$$

$$\nabla.\vec{J_i} = R_i + S_i \quad (2.19)$$

Considering each species to have a specific diffusion coefficient, the mass diffusion flux for laminar flow is defined as

$$\vec{J_i} = -\rho D_{i,m}\nabla Y_i \quad (2.20)$$

$$Yi = (MW_i \times Ci)/\rho \quad (2.21)$$

Where, ρ is the density, D represents diffusivity coefficient, Y_i is the mass fraction of species

R_i represents the net rate of species produced by the chemical reaction, S represents the rate of creation due to various sources in the model, $\vec{J_i}$ is the diffusive flux due to concentration gradient.

Chapter-3

Crosslinked Poly (vinyl alcohol) Membrane as Separator for Domestic Wastewater Fed Dual Chambered Microbial Fuel Cells.

Motivation

Microbial fuel cell has proven to be an attractive technology to produce electricity from organic matter. As such it shows great potential as a tool for wastewater treatment. A key factor hindering its commercialization is the manufacturing cost which can be reduced by replacing the commercial membrane with low-cost biodegradable membrane. By switching to biodegradable material such as Polyvinylalcohol(PVA), microbial fuel cell can become an important cost-effective technology accessible in remotest part of the world for clean water as well as electricity generation in the future.

The work in this chapter is published as

Das, B., Gaur, S. S., Katha, A. R., Wang, C. T., & Katiyar, V. (2021). Crosslinked poly (vinyl alcohol) membrane as separator for domestic wastewater fed dual chambered microbial fuel cells. *International Journal of Hydrogen Energy*, *46*(10), 7073-7086. https://doi.org/10.1016/j.ijhydene.2020.11.213 (I.F 7.139)

Abstract

This chapter focusses on the development of low-cost biodegradable membrane utilizing Polyvinylalcohol (PVA) as an alternative to the costly, commercial membrane Nafion 117 for application as separator in Microbial Fuel Cells (MFCs). The use of Nafion as proton exchange membrane in microbial fuel cells (MFCs) is expensive with operational issues like biofouling and fuel crossover limiting the practical application of the device to harvest energy from wastewaters. In this connection, a facile route is adapted to fabricate a Nafion-alternative membrane using PVA crosslinked with glutaraldehyde (GA) as a relatively low-cost, effective membrane for MFCs. The crosslinking of the PVA membrane resulted in reduction in hydroxyl groups and formation of acetal ring and ether linkage demonstrated by controlled water uptake and swelling ratio with enhanced thermo-mechanical stability. The crosslinked membrane displayed higher power density than those typically reported for domestic wastewater fed MFCs, reaching a maximum of 158.28 mW/m^2 for the fabricated membrane. The PVA-GA membrane with antimicrobial activity, high power performance and negligible fuel crossover shows its potential as separator in future MFCs based on its performance and low cost of installation

Graphical Abstract

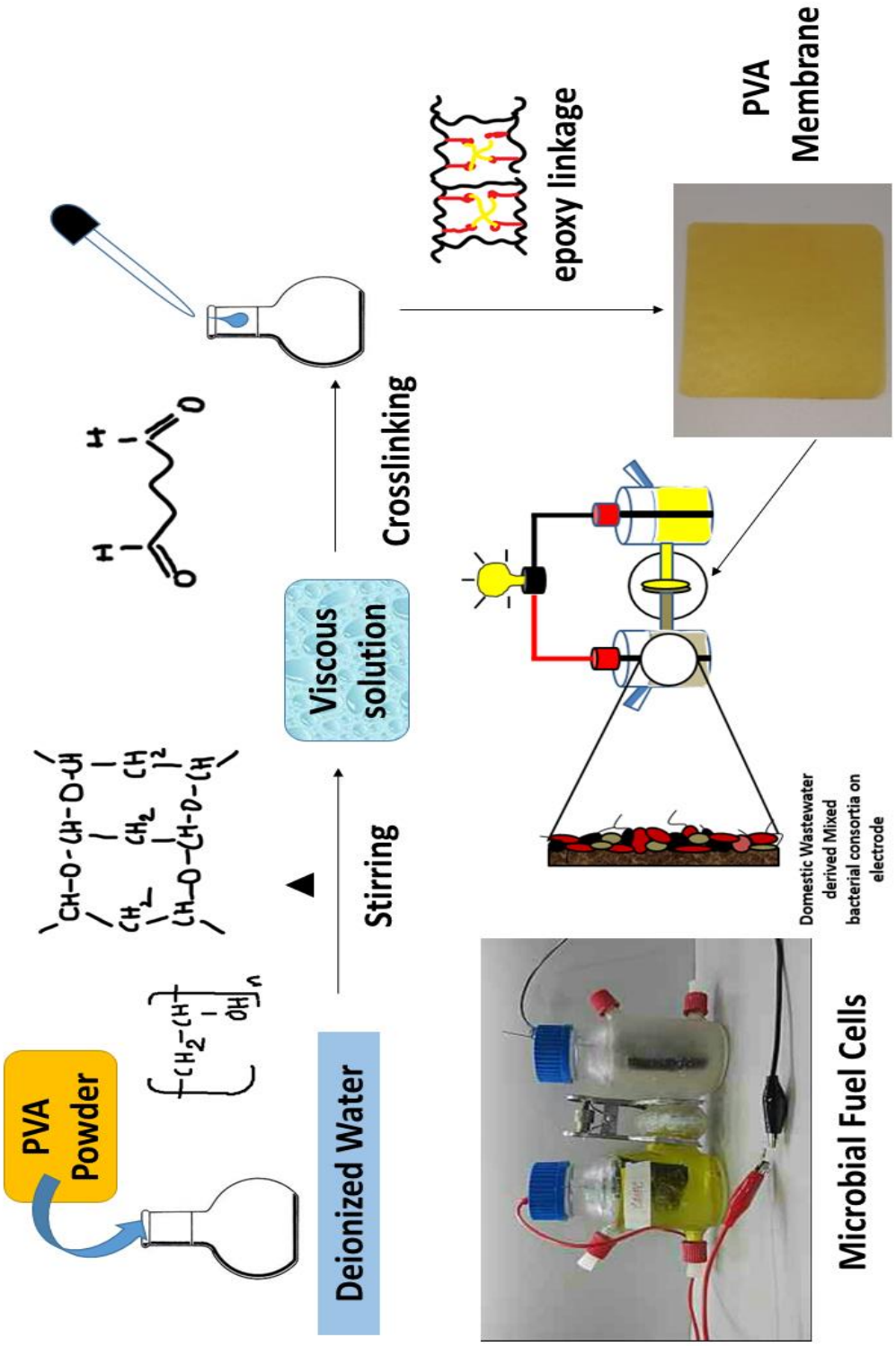

3.1 Introduction

Microbial fuel cells (MFCs) are bio-electrochemical devices which with the aid of bacteria convert organic matter to produce electricity. Over the past decade, MFCs have evolved into a simple yet robust technology with researchers across the globe constantly working on various aspects namely material and architectural aspect of the electrodes, microbial inoculum, chemical substrate as the feed material as well as low cost proton exchange membrane, so as to enhance the performance of MFCs and also decrease its cost of operation. A more suitable route to cut down the cost drastically is to fabricate low cost membrane to replace the Nafion, which accounts for 38% of the total capital cost (Ghasemi, Daud, et al., 2013). Although membrane-less MFCs can be promising at small scale because of its simple design, low cost and relatively high-power density however, the design is restricted to flat plate and tubular MFCs. Secondly, increase in diffusion of substrate and oxygen in absence of membrane makes the MFCs operation less efficient (Tiwari et al., 2016). Thirdly, closely packed electrode owing to limited spacing in such membrane-less MFCs adds to the risk of short circuit (Ayyaru et al., 2012; Fan et al., 2007). Fourthly, although the membrane-less configuration reduced the cost by eliminating the PEM membrane but it increased the internal resistance. For Air-cathode MFC configuration, fouling has led to decrease in power production and increase in the operational cost (Leong et al., 2015; Xu et al., 2012). Therefore, membranes as separators are a necessity to ensure efficient operation in dual chambered MFCs, to allow the passage of protons through the membrane to maintain electro-neutrality and to prevent unfavourable crossover across the membrane which will result in enhancement in OCV value. An ideal separator has to be hydrophilic for low resistance and high ion transport,

neutral to avoid pH change and ion-selectivity, mechanically stable to resist any deformation and possess anti-biofouling property to ensure stable power generation for long duration (G. Chen et al., 2012). However, to make the process of using membranes practical three aspects need to be considered namely, (a) the cost of membrane, (b) its internal resistance, (c) biofouling during operation (Choi et al., 2011; W.-W. Li et al., 2011).

Recently PVA based polymer membranes have attracted a lot of attention owing to its broad applications in medical field, in fuel cells as proton exchange membrane and so on (Binsu et al., 2005; Luo et al., 2011; C. Wu et al., 2010; Y. Wu et al., 2010; Q. G. Zhang, Liu, Jiang, et al., 2007). PVA is a non-toxic, biodegradable (Daries Bella et al., 2016)and an inexpensive polymer. It is inherently hydrophilic which makes it favorable for wastewater treatment(X. F. Chen et al., 2015). It has good film forming property due to its ability to crosslink within available hydroxyl groups in presence of chemical crosslinker to retain the compact nature of the membrane under pressure(Anis et al., 2008; Ghasemi, Wan Daud, et al., 2013; Q. G. Zhang, Liu, Chen, et al., 2007). Various crosslinking agents have been explored so far in combination with PVA film such as sulfosuccinic acid (Hou et al., 2014a), poly (styrene sulfonic acid-co-maleic acid) with glutaraldehyde (GA) (Kang et al., 2005) to name a few. Although, the effect of crosslinking of PVA with GA under acidic condition on characteristics of the PVA membrane has been examined in single chambered MFCs(Rudra et al., 2015). It has been rarely focused upon how the PVA membrane crosslinked with GA would behave under neutral condition when applied as a membrane in dual-chambered MFCs with domestic wastewater as substrate(Logan et al., 2006; Rynkowska et al., 2019).

Therefore, a more straightforward technique is addressed in thus chapter to develop PVA membrane which is free from catalyst, controller or quencher. A major advantage of this technique being the use of water for membrane preparation instead of chemical solvent which saves the preparation cost and also rules out the leaching of impregnated acid in long term that might restrict its application. In this study, a Nafion-alternative membrane using biodegradable PVA crosslinked with GA has been synthesized and its performance as a low cost separator in a dual-chambered MFCs (DC-MFCs) fed with domestic wastewater has been evaluated for practical application. Microbial consortia in the wastewater acts as the biocatalyst while wastewater is used as the substrate. A detailed analysis on the performance of the crosslinked membrane when employed in the MFC based on its composition, thermo-mechanical stability and antimicrobial properties has been subsequently discussed in the chapter.

3.2 Results and Discussion

The low mechanical strength, thermal stability and poor proton conductivity of pure PVA deter its use as a potential alternative for Nafion^{TM} membranes in MFCs. A straightforward solution casting method is applied to modify the PVA membrane for the first time utilizing crosslinking agent GA in neutral condition for MFC application. The resultant membrane developed successfully by crosslinking alters the undesirable properties with controlled water uptake, degree of swelling and enhanced thermal, chemical and mechanical stability which has been discussed in the chapter. Further, the suitability of the crosslinked membrane when employed as separator during actual MFC operation fed with domestic wastewater is analyzed in the later section of this chapter.

3.2.1 Structural analysis of the crosslinked membrane

Crosslinking of PVA by GA was verified from the FTIR spectra, shown in **Fig 3.1**. The spectra show all the characteristic peaks of PVA, which includes O-H stretching at 3248 cm^{-1} characteristic of hydrogen bonded hydroxyl group of PVA, C-H asymmetrical and symmetrical stretching at 2917 cm^{-1} and 2855 cm^{-1}, respectively assigned to C-H stretching modes of PVA backbone on crosslinking, C-H bending at 1416 cm^{-1}, C-H vibration at 1322 cm^{-1}, C-O stretch at 1086 cm^{-1} due to acetal linkage, O-H out of plane deformation at 915 cm^{-1} and C-C stretch at 828 cm^{-1} (Kharazmi et al., 2015; Sun et al., 2020) . Presence of C-O-C stretch peak at 1048 cm^{-1} confirms the crosslinking of PVA, while the C=O peak observed at 1744 cm^{-1} is due to branching of PVA by formation of aldehyde side chain by GA (Figueiredo et al., 2009; Gaur et al., 2017) . Formation of crosslinking and branching by GA is shown in **Fig. 3.2**. **Fig. 3.3** shows the XRD spectra depicting the crystalline nature of crosslinked PVA membrane. The sharp peak with high intensity around $2\theta = 19.8°$ corresponds to PVA (101) crystal plane, which is the dominating phase of crystalline PVA. While low intensity peaks with crystal planes (200) and (220) observed at $2\theta = 23°$ and 41° (determined based on the lattice values reported in the previous literature (JCPDS card No. 65–2870) (Menazea et al., 2020; Mostafa & Menazea, 2020), respectively are present in minute amount.

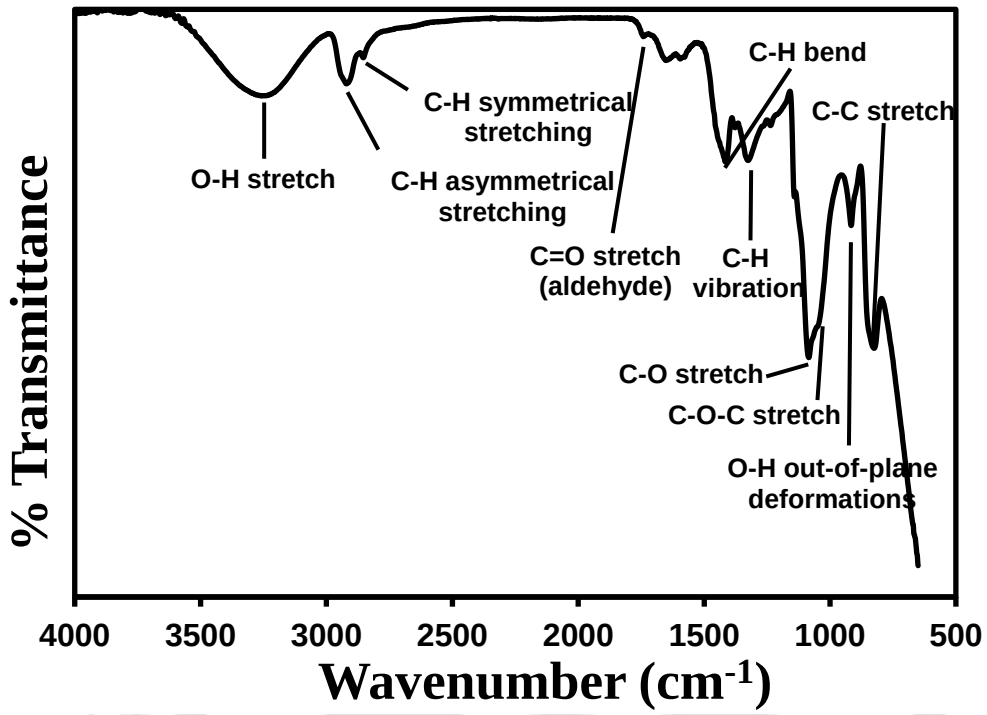

Figure 3.1 FTIR spectra of crosslinked PVA membrane.

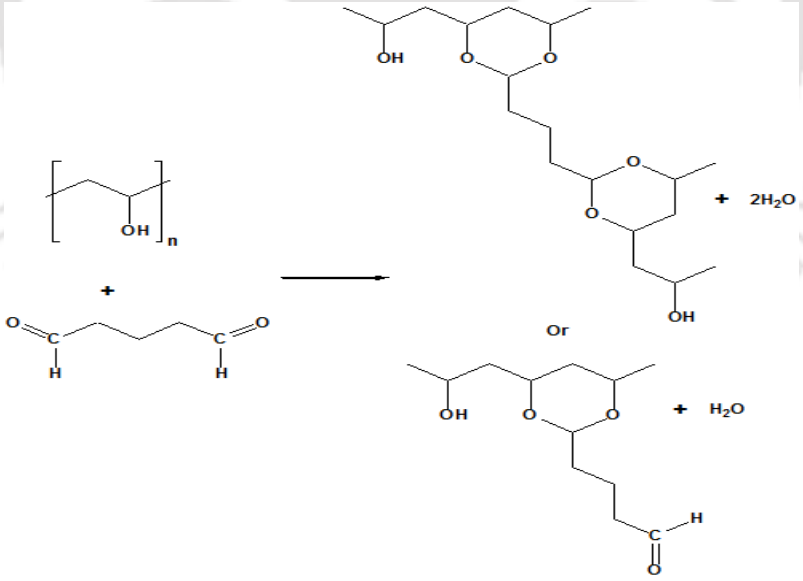

Figure 3.2 Crosslinking reaction of PVA with GA.

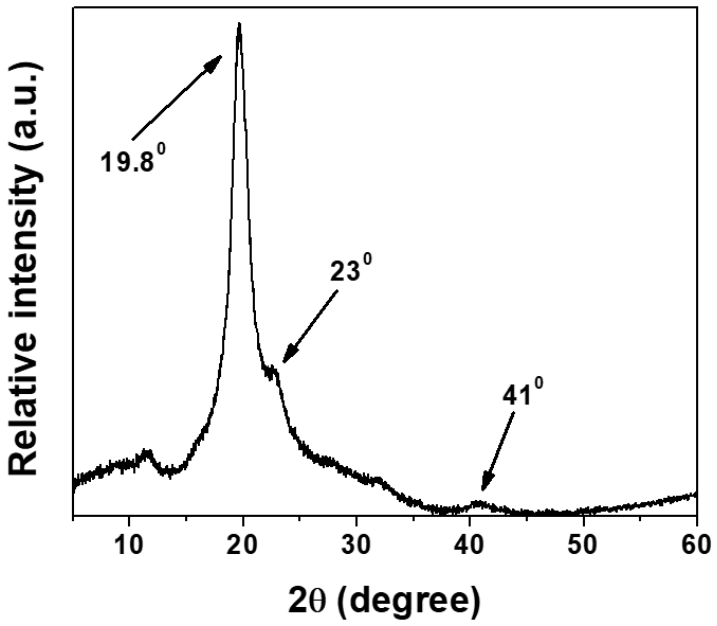

Figure 3.3 XRD micrograph of crosslinked PVA membrane.

3.2.2 Thermal and Thermomechanical stability analysis of crosslinked membrane

The intrinsic property of PVA being water soluble on one hand and the requirement to serve long operation hours on the other demands thermal and mechanical stability of the PEM for successful fuel cell application. Thermal stability of the crosslinked PVA membrane was observed through TGA analysis and by derivative curve of the TGA results, which is called as derivative thermogravimetry (DTG). From the TGA and DTG curves shown in the **Fig. 3.4**, four different regions and three major peaks of weight loss can be observed. The weight loss due to physically bound moisture was not observed in TGA as the sample was dried at 100°C prior to the TGA analysis. The first weight loss region was observed in the temperature range 230–330°C, shown by the first peak in DTG curve,

which shows the degradation of amorphous part of PVA. The second weight loss observed in the temperature range 330–430 °C was attributed to the degradation of crystalline chains of PVA. The third weight loss peak observed in the DTG curve was due to side chain and main chain degradation of PVA, which lies in the temperature range 430–550 °C. Final weight loss region beyond 550 °C is simple carbonation or conversion to CO_2 of the degraded PVA chains. DMA analysis was used to study the thermo-mechanical stability of the crosslinked PVA membrane. The results for DMA analysis (**Fig 3.5**) showed that annealing has significant positive effect on the thermo-mechanical stability of the membrane as storage modulus of the membrane sample was increased from 1250 MPa to 6000 MPa. Improved storage modulus showed the improvement in the rigidity of PVA membrane, which has plastic nature and mostly becomes fragile in presence of water. The storage modulus remains significantly high even at high temperatures, where before annealing the storage modulus dropped below 130 MPa after 75 °C, it remains at around 2200 MPa after annealing at the same temperature. This finding revealed that the crosslinked membrane has improved thermal stability and mechanical strength of PVA by restricting the mobility of the polymer chains (Rudra et al., 2015; Wong et al., 2020).

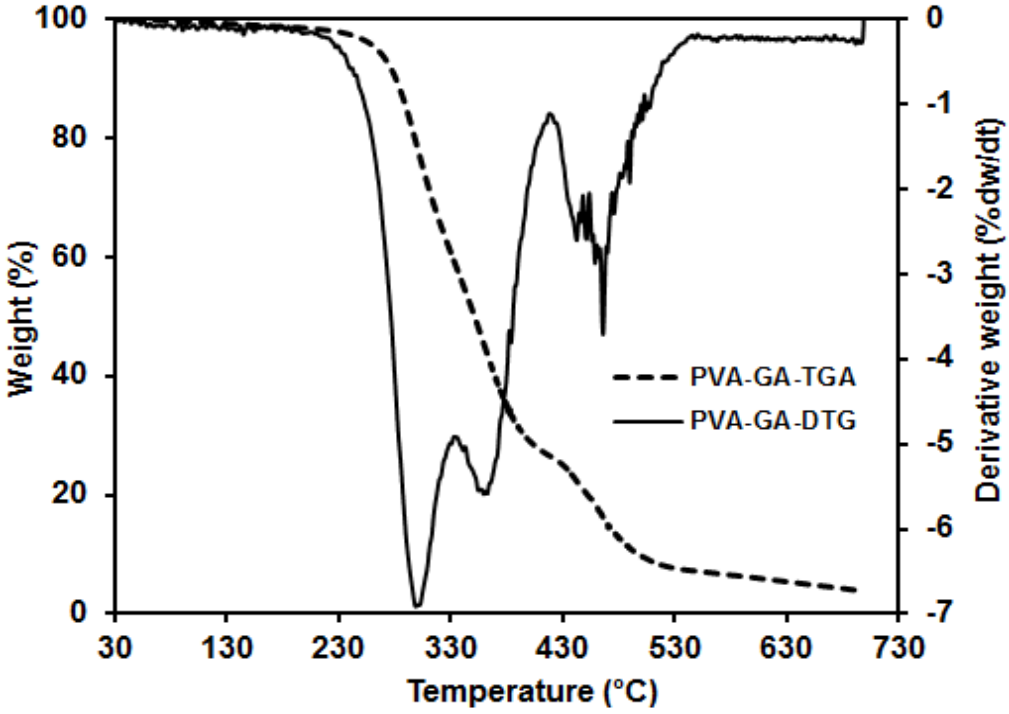

Figure 3.4 TGA and DTG curve of crosslinked membrane.

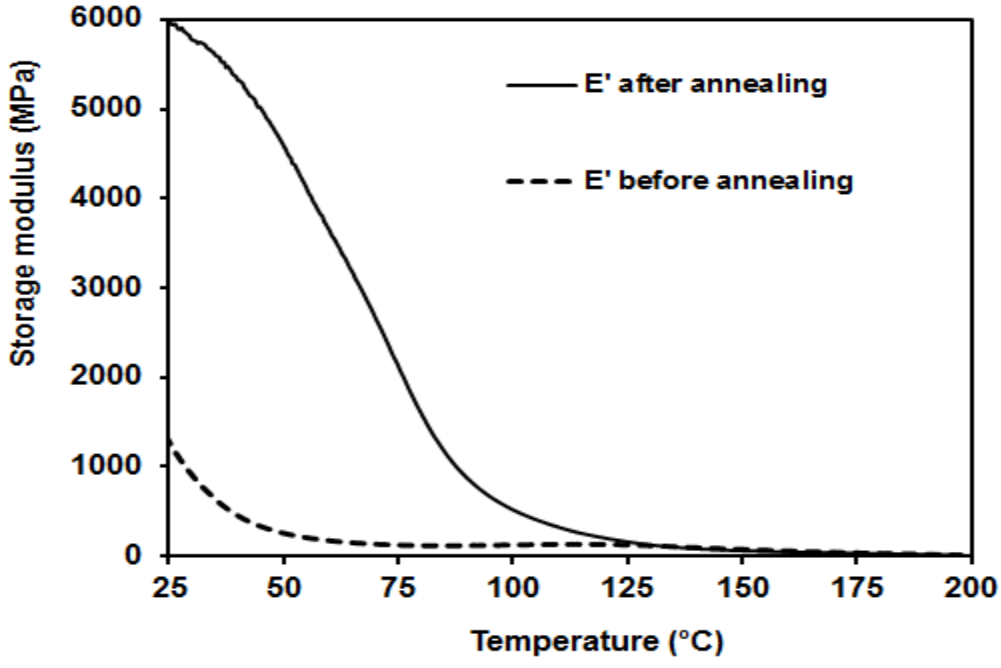

Figure 3.5 DMA curves for before annealed and after annealed PVA membrane.

3.2.3 Water Uptake, % Swelling

Water uptake capacity is a desirable property in proton transport across the membrane in MFC application. It is defined by the total water molecules present at the surface of the membrane and in its interstitial sites. Although, water uptake essentially helps in the transfer of protons across the membrane however, higher water content adversely affects its mechanical integrity (Wong et al., 2020). PVA in its native form is a straight chain polymer which enables it to form intermolecular and intramolecular hydrogen bonding with water. Crosslinking results in significant reduction in water uptake, as it was observed to be around 50%, as reported in our previous work (Gaur et al., 2017), while without crosslinking the water uptake was observed to be around 250% as shown in **Fig 3.6**. Although presence of water helps in proton conduction, 50% water uptake is more than enough for this purpose, at the same time reduced water uptake reduced the %swelling, which was observed to be around 20% for the crosslinked membrane as shown in **Fig 3.7**, while before crosslinking it was observed to be 50% (Gaur et al., 2017). Crosslinking with GA results in decrease in the available hydroxyl groups in PVA which results in lowering of water uptake and % swelling (Rudra et al., 2015).

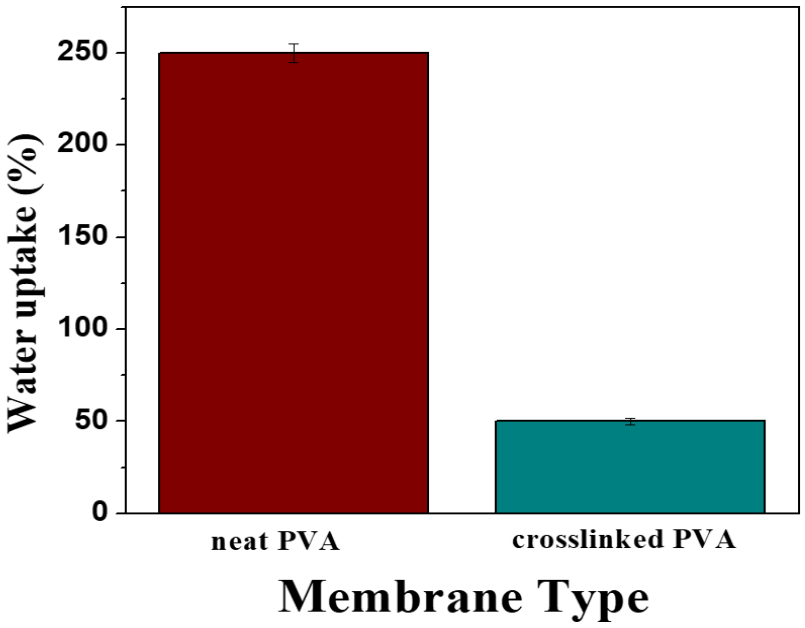

Figure 3.6 Water uptake of PVA membrane before and after crosslinking.

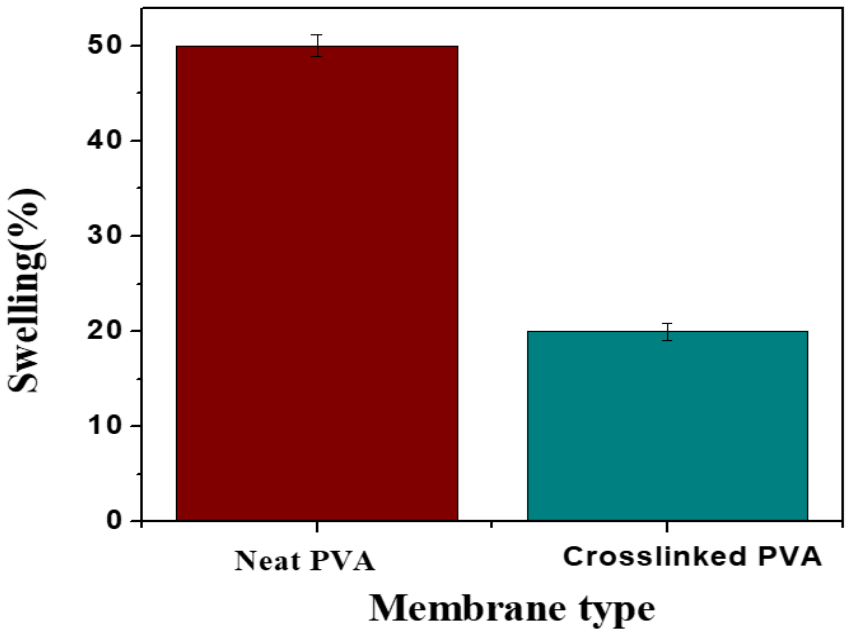

Figure 3.7 Swelling ratio of PVA membrane before and after crosslinking.

3.2.4 Substrate crossover study for crosslinked membrane

Fuel crossover from anode to cathode chamber through the membrane could severely affect performance of MFC (Neethu et al., 2019). Apart from the cost, substrate crossover in Nafion is one of the factors limiting its use in scaling up of MFCs(Bhowmick et al., 2018). Therefore, acetate diffusion was tested for the crosslinked membrane in its non-inoculated state of the MFCs by adding fixed amount of acetate in anodic chamber, and measuring its diffusivity to the cathode chamber as previously reported.(Ghadge & Ghangrekar, 2015). Compared to Nafion, as seen from **Table 3.1**, the acetate diffusion coefficient was found to be 8.57 times lower for the crosslinked membrane. This lower diffusion of acetate across the membrane can be attributed to its thickness and can be considered negligible under normal condition with inoculated MFCs as this value of substrate diffusion will be further reduced due to substrate degradation by the bacteria present in the anode chamber.

Table 3.1: Acetate diffusion coefficient in alternative membranes and conventional Nafion 117 membrane.

Separators	Thickness(mm)	Dcm (cm^2/sec) $\times 10^6$	Reference
Nafion	0.181	0.06 ± 0.003	(Ghadge & Ghangrekar, 2015)
Clay M-20	4	5.96 ± 0.28	(Ghadge & Ghangrekar, 2015)
ACCS/Clay	4.06	0.08	(Neethu et al., 2019)
CS	4	7.21	(Neethu et al., 2019)
PVA-GA	0.087± 0.10	0.007 ± 0.002	**This study**

3.2.5 Bioelectricity Production in the Dual Chambered MFC

Under the fed-batch mode of operation, the MFCs investigated, using Nafion-117, PVA−GA membranes, took a period of 2 weeks to reach stable conditions. A gradual increase in voltage under an external load of 1000 Ω was observed. No significant lag in the voltage generation was observed during start-up which is indication of the microbial cell to anode adhesion efficiency. In order to inoculate the graphite electrode with mixed culture of bacteria present in domestic wastewater, three successive acclimation cycles were carried out with acetate as the carbon source. The polarization curves for the Nafion based dual chambered MFC and PVA-GA based dual chambered MFC were obtained in open circuit mode after acclimation for 30 days, as shown in **Fig. 3.8 (a)** and **Fig. 3.8 (b).** Under no load condition, the average voltage of 753.5 $\pm$0.49 mV and 679.38 $\pm$ 0.30 mV was recorded for PVA-GA based MFC and Nafion based MFC respectively. The crosslinked PVA-GA membrane showed better OCV and current density over Nafion (as reported in **Table.3.2**), which is also higher compared to what have been achieved by using acid catalyzed PVA-GA membrane (Rudra et al., 2015a). The higher OCV for the PVA based MFCs clearly reflects the effectiveness of the designed membrane to selectively allow the passage of protons and suppressing unfavorable crossover across the membrane. The maximum current density of 835.17 mA/m^2 was observed for the PVA−GA membrane with the maximum power of 158.28 mW/m^2.Although the maximum power shoot to 181.60 mW/m^2 for the Nafion membrane with a maximum current density of 558.18 mA/m^2. However, a close observation of the shape of the two polarization curves reveal that the Nafion based dual chambered MFCs suffered from power overshoot which is identified by the doubling back of the power density curve (after the peak power) towards lower current

densities, rather than the expected higher current. The reason why this phenomenon occurs still remains unclear, although population of the anode community, insufficient anodic abiotic capacitance, bacterial substrate utilization and the maturity of the biofilm are among few investigations carried out on power overshoot(Aelterman, Rabaey, Pham, et al., 2006; Bhowmick et al., 2018; Hong et al., 2011; Ieropoulos et al., 2010b; J. R. Kim et al., 2010; S.-E. Oh & Logan, 2007; Peng et al., 2013; Winfield et al., 2011). Notably, it was possible to achieve larger power density in both the cases with and without using the conventional membrane than those reported for complex substrates, as shown in **Table.3.3** The % COD Removal depicted by **Fig. 3.8 (c)** was marginally higher for the conventional membrane in the 30-days operation with 91 ± 0.17 % for the PVA-GA membrane and 93 ± 0.10 % for the Nafion-117 membrane, which indicates that the PVA-GA membrane can be integrated as a low-cost alternative to the costly Nafion-117.Thus the PVA-GA based domestic wastewater MFCs was capable of simultaneously generating electricity along with organic matter removal.

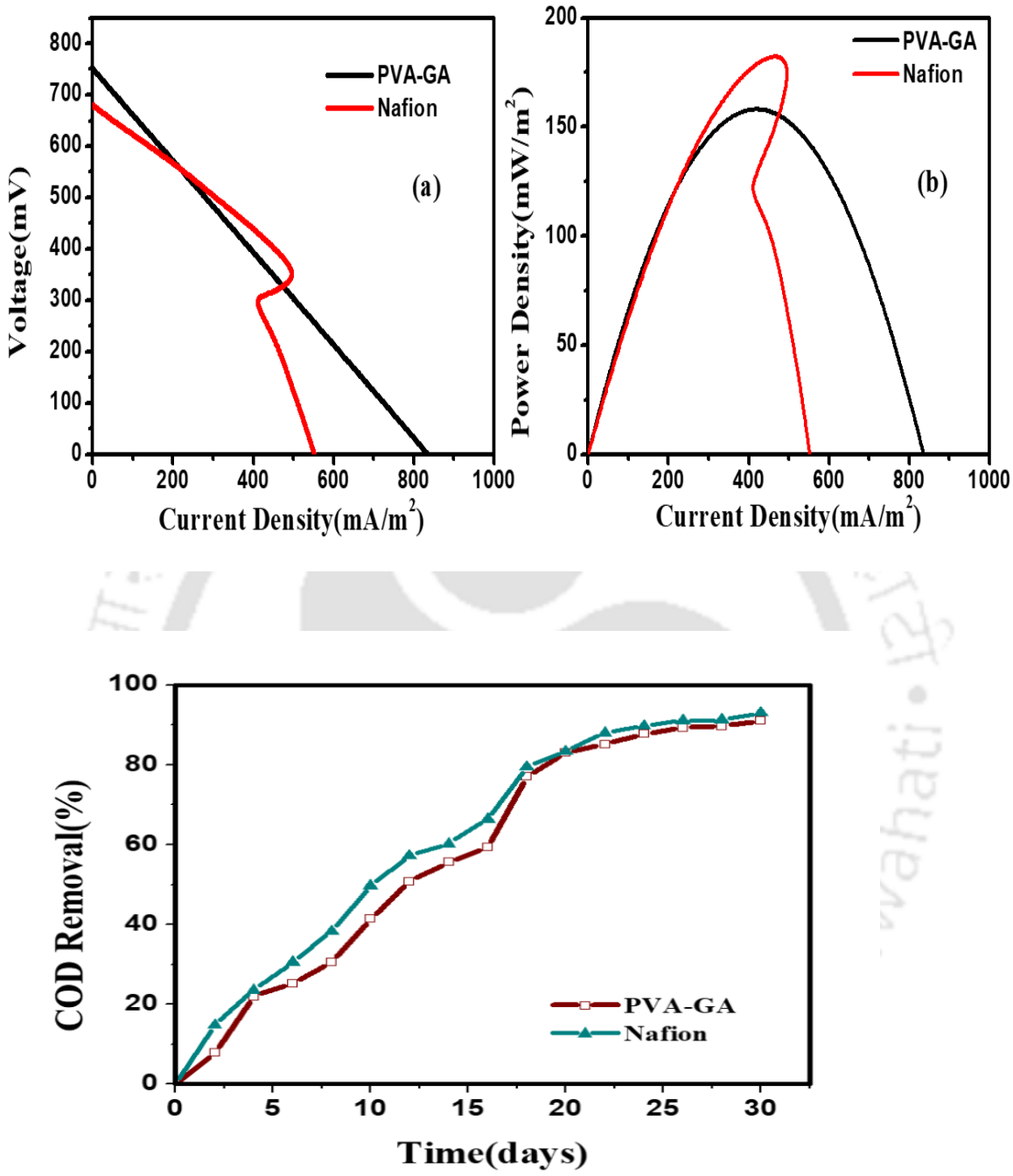

Figure 3.8 Polarization curves of MFCs equipped with commercial membrane and synthesized membrane (**a)** Open circuit voltage and (**b)** Power density generated by MFCs w.r.t the current density, **(c)** COD removal in 30-day operation for the PVA-GA and Nafion based MFCs fed with domestic wastewater**.**

Table 3.2: Properties of the MFCs with the fabricated membrane and commercial Nafion-117 membrane.

Membrane	**Nafion-117**	**PVA-GA**
Maximum Open Circuit Potential (mV)	679.51 ± 0.35	754.28 ± 0.58
Maximum Power Density (mW/m^2)	181.60 ± 0.03	158.28 ± 0.28
Maximum Current Density (mA/m^2)	558.18 ± 0.20	835.17 ± 0.63
R_{ohm} (Ω)	75.31 ± 0.35	157.9 ± 0.22
R_{ct} (Ω)	3.60 ± 0.40	2.47 ± 0.17
W (Ω)	123.5 ± 0.62	72.88 ±0.12

3.2.6 Internal resistance of the MFC with crosslinked membrane

The proton exchange membrane is one of the most critical components in the fuel cell configuration. It not only provides a separation between the two electrolytes, but also provides electroneutrality by facilitating transport of H^+ to compensate for transport of electrons. In order to assess the internal resistance of the MFCs equipped with the membranes, the EIS results were interpreted according to the Randles equivalent circuit shown in **Fig. 3.9 (b)**. R_1, R_2, C_2 and W_2 represent the ohmic resistance, charge transfer resistance, double layer capacitance, and Warburg impedance, respectively which are components of the internal resistances. The diameter of the semicircle in the low frequency side of the Nyquist plot as seen from **Fig. 3.9 (a)** represents the charge transfer resistance while the linear portion in low frequency side represents diffusion resistance. The difference between origin to the initial start of the semicircle gives the ohmic resistance (Neethu et al., 2019).Nafion exhibited lower ohmic resistance compared to the crosslinked membrane which is mainly due to the presence of sulphonic acid groups in its polymer chain (Wong et al., 2020). Although PVA is an insulating material with no polar groups (Rudra et al., 2015), yet the charge transfer resistance was found to be lower in case of the PVA-GA based MFCs and comparable to the charge transfer resistance observed in the Nafion based MFCs. This can be attributed to crosslinking with GA which resulted in low value of charge transfer indicating better charge transport through the crosslinked membrane due to optimum water content facilitating proton transfer through vehicular mechanism (Zinadini et al., 2017).

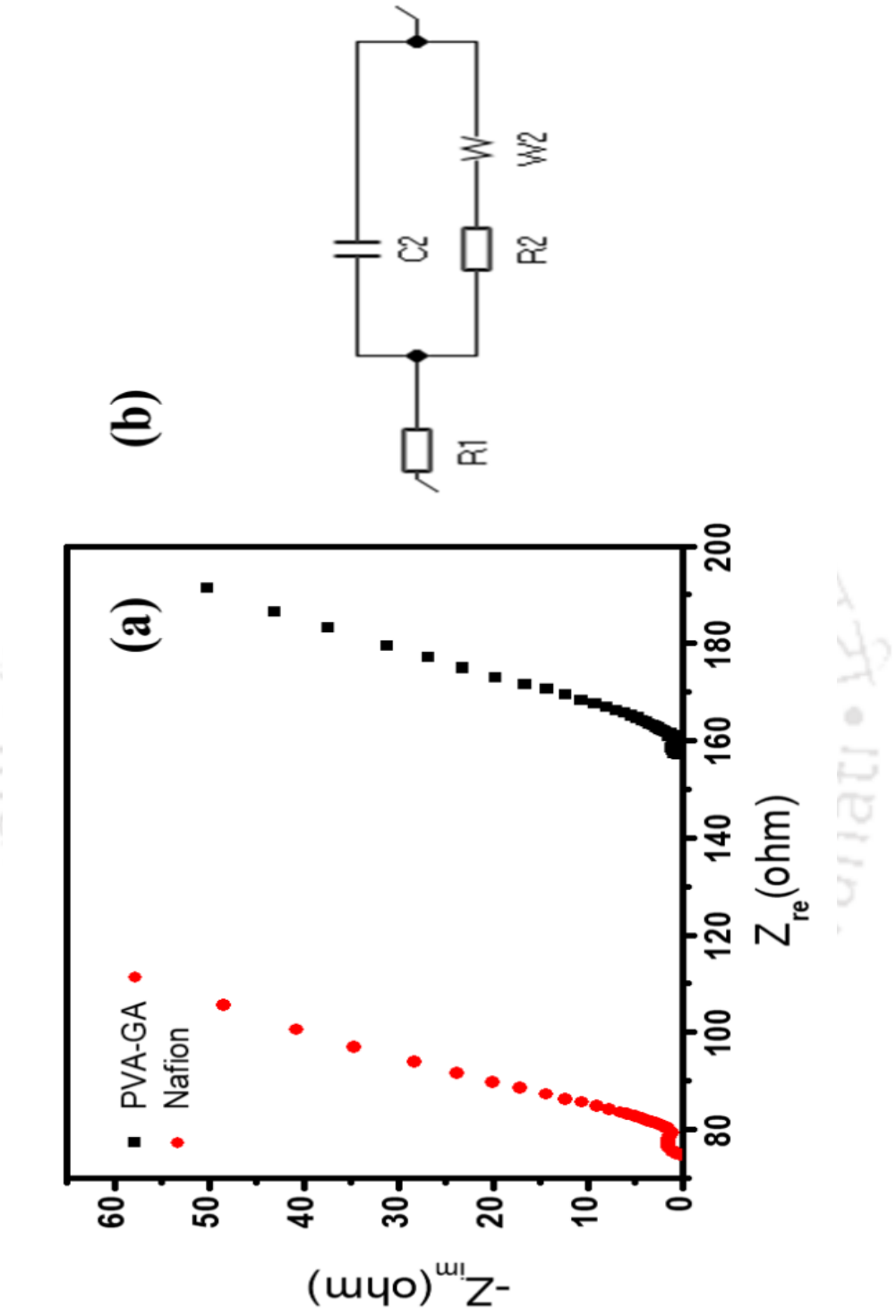

Figure 3.9. (a) Nyquist Impedance Plot of Nafion based MFCs and PVA-GA based MFCs, **b)** Equivalent Randles Circuit of the MFCs.

Table 3.3: Power density reported in literature versus those obtained in the present study.

Substrate	Power Density (mW/m^2)	Reference
Domestic wastewater	28	(H. Liu et al., 2004)
Anaerobic sediments	28	(Tender et al., 2002)
Starch Wastewater	20	(Gil et al., 2003)
Anaerobic sediments	16	(Reimers et al., 2001)
Domestic Wastewater-PEM	28	(H. Liu & Logan, 2004)
Domestic Wastewater-No PEM	146	(H. Liu & Logan, 2004)
Domestic Wastewater	158.28 ± 0.28	**This study**
Domestic Wastewater-PEM	181.60 ± 0.03	**This study**

3.2.7 Biofilm Analysis

Compared to the pure culture, a mixed consortium is preferred for performance enhancement in MFCs fed with wastewater. The reason is it exhibits the "nutrient cycle ecosystem" in which some species degrade the organic matter, while some species act against harmful pollutants present in wastewater. In previously reported works on MFC, acetate is mostly chosen as substrate, as it is simple form of carbon, non-fermentable and readily used by anodic bacteria (Hou et al., 2014; Tiwari et al., 2016). But, when we use real wastewater, which consist of complex macromolecules, fermentation of complex molecules like polysaccharide to simple carbon molecules takes place followed by electrogenesis. The electrogenic microbes utilize a part of the reduced carbon molecules to produce protons and electrons while the rest is used to support its metabolic activities. The process of biofilm formation undergoes three steps namely, adhesion on the electrode surface, maturation and then detachment. The conductivity of the biofilm formed by the electrogens plays a key role in the power generation**. Fig 3.10 (a) & (b)** show the FESEM images of the graphite felt electrode before and after biofilm is formed on the anode electrode with domestic wastewater as the substrate. As seen from **Fig.3.10 (c),** the mixed culture of bacteria has colonized the electrode by forming a biofilm. The bacterial cells are observed to have interlinked with each other through hair like extensions called pili which play a crucial role in developing a stable biofilm on the anode surface as well as conducting electrons from the microbes to the anode **Fig.3.10 (d)** (Borole et al., 2011; Philips et al., 2016) .The stable biofilm developed favored low resistance to the electrochemical reaction at the anode surface, as demonstrated by the low R_{ct} value in EIS analysis.

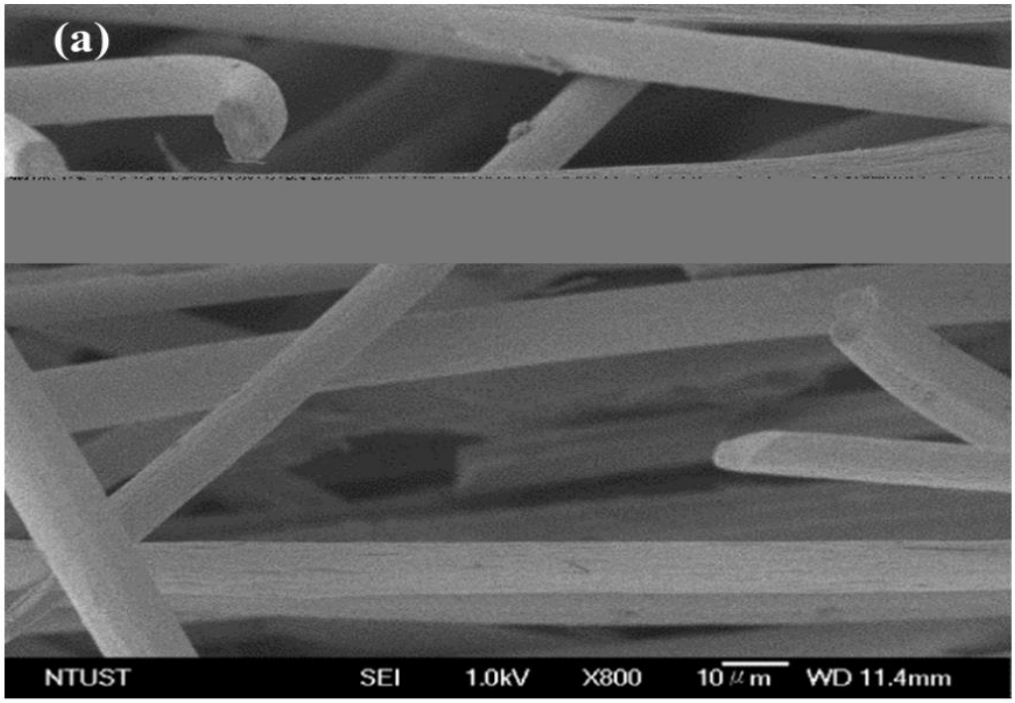

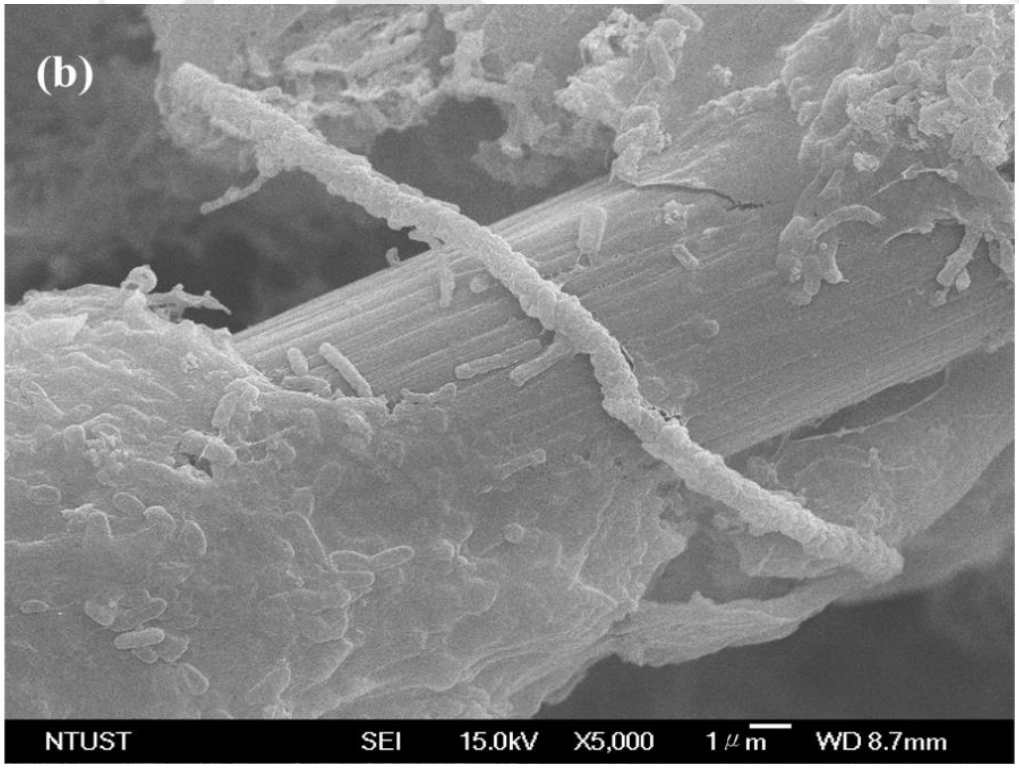

Figure 3.10. Surface Morphology of **(a)** Graphite felt electrode without biofilm, **(b)** Mixed consortia of bacterial biofilm layer encircling the graphite felt fibre electrode(**c)** Magnified image of the biofilm on the electrode, **(d**) Magnified image of the conductive pili used by the bacterial consortium as mode for electron transfer on the graphite felt surface.

3.2.8 Effect of Crosslinked Membrane on Antibacterial Activity

One of the main reasons why scaling-up of MFCs has not yet been successfully accomplished is biofouling. With long duration of operation, membranes on the anode side are prone to a surface phenomenon called biofouling, which is an extra biofilm created by the anodic bacteria (Choi et al., 2011; Daud et al., 2015). Nafion membranes are prone to biofouling because of the availability of both hydrophobic and hydrophilic sites associated

with $–CF_2 –CF_2–$ links and $–SO_3^-$ terminals, respectively (Wong et al., 2020). Membrane biofouling on long term operation is an inevitable process in a MFC system. Biofilm formation on the surface of membrane poses as a hindrance in the transport of ions from anode to cathode compartment, which affects the rate of ion migration causing internal resistance and hence lowering the power performance of the MFC. There are two techniques to minimize membrane biofouling, a) the anti-adhesive approach which prevents the attachment of bacteria on a membrane and b) the anti-microbial approach, kills bacteria already present on the membrane (Srinophakun et al., 2017). After incubation for 72 h, the damaging impact on the microbial cells is observed for the crosslinked membrane. The morphology of the S. Putrefaciens is rod shaped. As exhibited by the FESEM images in **Fig. 3.11 (b),** on contact with the surface of the membrane the bacterial cells have undergone morphological change. Comparison of the two membranes, crosslinked PVA and Nafion, before **(Fig.3.11 (a) & Fig.3.11 (c))** and after on the basis of antimicrobial activity reveals least bacterial cells adhering to the PVA membrane surface, which had ruptured cells shown by arrow marks **(Fig. 3.11 (b)).** Rupturing of the cells can be attributed to reduction in –OH functional group and formation of hydrophobic barrier by the acetal ring linkage as a result of crosslinking with GA [22]. This result is consistent with earlier report on reduced biofouling of PVA separators(G. Chen et al., 2012). Deformation of the bacteria cells implies low microbial activity on the membrane hence, reduction in internal resistance and enhancement in ion transfer. Nafion,on the otherhand, had aggregates of bacterial cells on its surface as shown in **Fig. 3.11 (d)** due to the presence of hydrophilic sites favouring more bacterial attachment(Choi et al., 2011; Daud et al., 2015) .The antibacterial test results indicate that another reason for increased proton

conductivity of the crosslinked PVA membrane is due to reduced biofilm formation on membrane. The excellent stability of the crosslinked PVA membrane against microbial degradation favors its application in particularly microbially aggressive environment such as sewage or sludge.

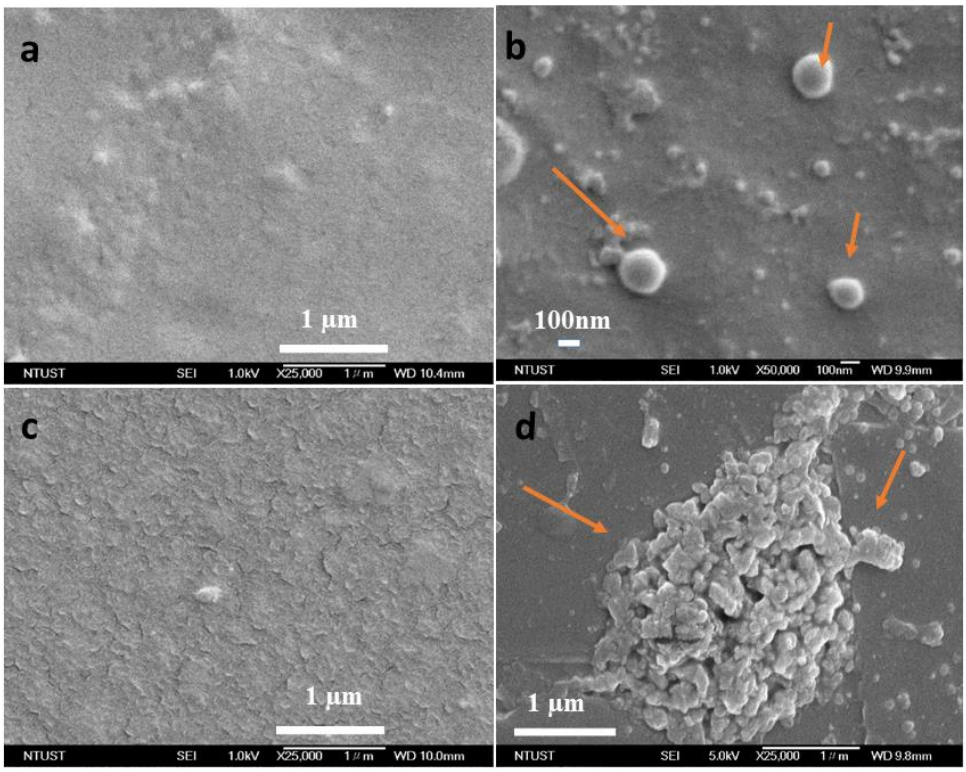

Figure 3.11 Surface Morphology of **(a)** PVA-GA membrane before antibacterial testing, **(b)** PVA-GA membrane with disrupted S. Putrafaciens bacteria cells on its surface (**c)**Nafion-117 membrane before antimicrobial testing **(d**)Aggregates of morphological change of S.Putrafaciens bacteria on Nafion membrane.

3.3 Conclusions

This chapter focusses on overcoming the drawbacks of the PVA membrane in its pristine form for its application as a low-cost alternative to Nafion 117 in real wastewater fed MFC.GA crosslinked PVA membrane is successfully prepared by solution casting which was further characterized and evaluated as a low-cost alternative for Nafion-117 in a dual chambered MFC fed with domestic wastewater. The combination of simple fabrication step, devoid of catalyst or other reinforcing agent and environmental friendliness is a big advantage for its practical application. Besides its ease of synthesis, the fabricated membrane is relatively cheap and shows excellent potential with 3-fold increase in power performance utilizing complex substrate with antibacterial property. The substrate loss was 8.57 times lower than Nafion which can be considered negligible in normal MFCs operation and hence this study provides a viable approach to prepare a potential alternative for the conventional membrane for bioelectricity generation and wastewater treatment in future MFCs.

Chapter-4

Hair Hydrolysate functionalized cellulose nanocrystal-based Chitosan membrane to harness power from real wastewater fed microbial fuel cells

Motivation

In the recent times, natural biopolymers such as chitosan and cellulose have received tremendous concern on their potentiality to replace the existing membranes which are costlier and non-environmentally friendly. Their potential as greener polymer electrolyte to enhance MFC properties and performance is an interesting topic. However, research on utilization of such natural biopolymers in MFCs to treat real wastewater and simultaneously harvest electricity is very limited. Also, utilization of human hair waste for PEM application is another exciting approach. Such interesting properties offered by the biopolymer namely, high economic value, sustainable, carbon–neutral and renewable production processes make an additional value for such green technology application.

The work in this chapter is published as:

Das, B., Gaur, S. S., Katha, A. R., Wang, C. T., & Katiyar, V. (2022). Hair hydrolysate functionalized cellulose nanocrystal-based chitosan membrane to harness power from wastewater fed MFCs. *International Journal of Hydrogen Energy*. https://doi.org/10.1016/j.ijhydene.2022.12.054 (I.F 7.139)

Abstract

This chapter focusses on the utilization of Chitosan (CS), an environmentally benign polymer increasingly utilized to prepare low-cost proton exchange membranes (PEMs) for Microbial Fuel Cell (MFC) applications. In this work, hair hydrolysate functionalized CNCs have been utilized with CS matrix followed by cross-linking with epichlorohydrin to enhance the properties of neat chitosan for its application as Nafion-alternative membrane to harvest electricity from domestic wastewater fed MFC device for the first time. Characterizations reveals the structural interaction between the hair hydrolysate functionalized CNC and chitosan matrix resulting in higher antibacterial property with a low percentage of water uptake (60%) and swelling (26%) and higher ion conductivity (1.04 mS/cm). Maximum power density of 142.57 mW/m^2 and maximum open circuit voltage of 769.58 mV is derived from real wastewater which is higher compared to previous literature. The results demonstrate the possibility of application of the new low-cost, sustainable PEM with enhanced properties for MFC and wastewater treatment in future.

Graphical Abstract

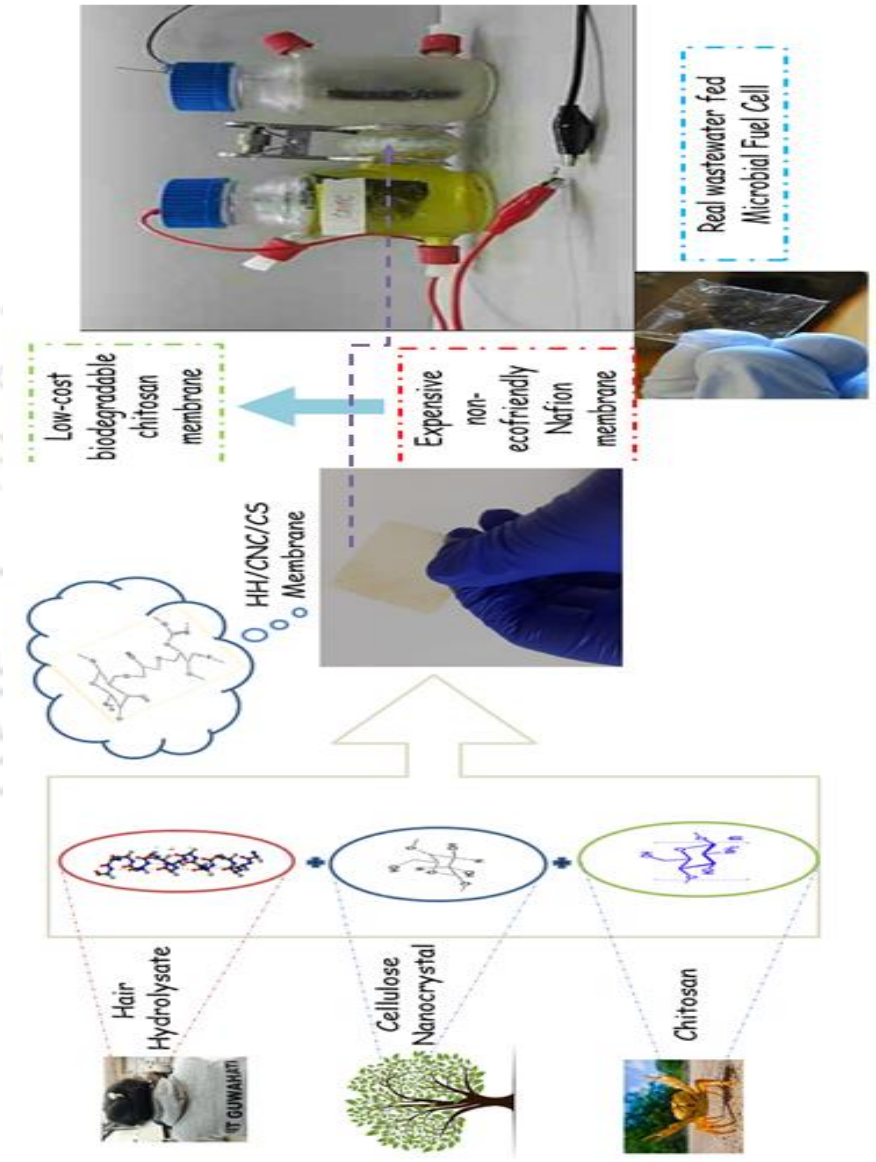

4.1 Introduction

The immense possibility of employing microorganisms for recovering resources from waste and aiding in waste management has garnered a lot of interest in Microbial Fuel Cells (MFCs) Technology(Albarracin-Arias et al., 2021; Din et al., 2021). MFCs utilize bacteria as catalyst to derive electricity from organic waste such as wastewater(Obileke et al., 2021; Peera et al., 2021). A key component of the device is the Proton Exchange Membrane which serves as a semipermeable barrier between the electrodes with the purpose of strictly permeating protons (Tabassum et al., 2021). The desirable qualities in a good proton exchange membrane (PEM) for MFC application include good hydrophilicity, low ohmic resistance, good proton conductivity, high chemical and mechanical stability, anti-biofouling property and low production cost to make the operation economically viable (Das et al., 2021a). Conventionally, Nafion® (from DuPont) is, by far, the most preferred PEM used in fuel cell application primarily due to its high proton conductivity, high chemical and mechanical stability(Ali et al., 2021). However, it suffers from major disadvantages which include non-eco-friendliness, disposal issue, permeability to undesired cations like Na^+ and K^+ obstructing proton transfer, high fuel crossover and higher production cost ($600-1200 per m^2) which forms the main motivating factors behind looking for a cheaper alternative(Das et al., 2021).

Chitosan (CS) is an inexpensive, abundant biobased polymer derived from the deacetylation of chitin known for its biodegradability, nontoxicity, hydrophilic nature, good film forming properties and excellent thermal and mechanical strength (Gupta et al., 2018; Pal & Katiyar, 2017; D. Zhao et al., 2018). The major issue with Chitosan when used as a membrane, is that in its pristine form, Chitosan demonstrates poor mechanical property

due to high water uptake with lower proton conductivity and low ion exchange capacity (IEC) limiting its application as a potential Nafion-alternative membrane. One of the key solution to this problem however, is crosslinking (Shaari & Kamarudin, 2015). The backbone of chitosan consists of free amine and hydroxyl groups which are potential reactive sites and hence, can be easily associated with other crosslinking agents that allow improvement in performance by further modifications (Patel et al., 2021). (Narayanaswamy Venkatesan & Dharmalingam, 2013) modified CS with multi-walled carbon nanotube as PEM for MFC. The maximum power density and OCV achieved for pure culture E. coli was 46.94 mW/m^2 and 0.75 V respectively. No data was reported on the losses incurred with the current PEM under study. Another recent work carried out by (Srinophakun et al., 2017), reported incorporating sulfosuccinic acid as crosslinker and Chloro-2-hydroxypropyl trimethylammonium chloride for quaternization to improve the antimicrobial activity and proton conductivity of Chitosan for application in MFC(Hanna Rosli et al., 2020). There was no information about the power output from the device. Although its proton carrier sites improved on modification, however, the mechanical stability of the membrane was compromised in the process due to significantly high-water uptake (160%). In another study by(Holder et al., 2016), reports modification of chitosan by phosphorylation for application in municipal wastewater fed MFC. The maximum voltage attained is 504 mV while the maximum power density achieved is 130.03 mW/m^2. The high internal resistance (464 Ω) is another reason leading to its loss in performance.

Despite the rising number of research on the application of various materials as PEM, but only a few studies address the usage of sustainable MFC components(ElMekawy et al., 2017). The goal of the present study is therefore to modify Chitosan utilizing cheap human

hair waste and cellulose nanocrystals. Human hair contains proteins and α-keratin which can be an excellent source of protein-based electrolyte. Keratin strands have a twisted coil structure with H-bonding and disulfide linkage (Menefee, 1977). This imparts higher mechanical and chemical stability making it insoluble in water. For the fabrication of electrolyte membrane, keratin strands have to be disintegrated by breaking the disulphide bonds. Hydrolysis is a preferred technique as it leads to formation of water-soluble amino acids, peptides and lower molecular weight keratin (Bertini et al., 2013; Villa et al., 2013) The other being enzymatic and thermo-chemical hydrolysis which also helps in disintegrating the keratin strands by breaking the disulfide bonds(M. Li et al., 2018). Likewise, incorporating material containing ion-conductive functional groups such as Cellulose Nanocrystals (CNCs) is advantageous as it not only helps in improving the ion conductivity of Chitosan but also provides dimensional stability to the neat Chitosan membrane (Lu et al., 2015). Addition of CNCs as bio-fillers to polyvinylalcohol/chitosan (PVA-CS) matrix have been reported to impart good conductivity in direct methanol fuel cells(Gaur et al., 2017). It is however, noteworthy that despite its favourable properties, evidence on fuel cell tests for assessment of the cell performance is missing from majority of the publications due to which the real potential of CNCs-based CS PEMs has not come to the fore. Based on the above discussion of research reports reviewed, a novel modified chitosan membrane by incorporating hair hydrolysate functionalized cellulose nanocrystals is being studied. Properties of the thus prepared environment-friendly PEM will be evaluated to act as a separator layer in MFC.

4.2. Results and Discussion

A novel attempt has been made to develop modified chitosan membrane by incorporating hair hydrolysate functionalized cellulose nanocrystals. Properties of the thus prepared environment-friendly PEM have been evaluated. To assess the suitability of the separator layer as membrane, fuel cell tests are carried out using real wastewater fed MFC with Nafion membrane as the control case which are discussed in the subsequent sections below.

4.2.1 Surface analysis of hair hydrolysate functionalized chitosan membrane

To confirm the functionalization of CNCs by hair hydrolysate, XPS analysis was carried out. **Fig.2.3(a)**, showed the possible reaction mechanism of CNC modification by hair hydrolysate. As shown in **Fig.4.1**, carbon 1s spectra of CNCs shows four peaks for C-C at 285 eV, C-O at 286.2 eV, C=O and O-C-O at 287.3 eV and O-C=O at 288 eV, while hair hydrolysate shows three peaks of C-C at 285 eV, C-O and C-N at 286.3 eV and O-C=O at 288.3 eV attributed to the presence of amino acids in hair hydrolysate(Gaur et al., 2021).The effect of modification of oxidized CNCs by hair hydrolysate is clearly visible from the carbon 1s spectra of modified CNCs. It has major peak of C-C due to attached keratinic protein/peptide chains of hair extract, while the high intensity of the second peak is a result of formation of C=N bond along with the presence C=O from non-crosslinked aldehyde groups. The modification of oxidized CNCs was further confirmed by the presence of nitrogen in nitrogen 1s spectra of modified CNCs. The spherical shape nanoparticle morphology of hair hydrolysate as shown in **Fig. 4.1(f)** matches with the morphology of keratin micro and nanoparticles reported in the literature (Ma et al., 2016; Sharma et al., 2017; J. Zhang et al., 2013).

In order to delve deeper into the mechanism of hair hydrolysate in enhancing the performance of the fabricated membrane the amino acid composition of the hair hydrolysate was investigated. As per previous report (Gaur et al., 2021), hair hydrolysate consists almost 70 wt.% keratin protein and around 26 wt.% part of charged amino acids such as arginine, histidine etc. Out of which 0.92 wt.% consists of Histidine (His) and another 3.27 wt% consists of Lysine (Lys) which are instrumental in enhancing the proton transport in the fabricated HH/CNC/CS membrane. Amino acids consist of charged and ionizable hydrogen donor and acceptor species aiding transfer of ions. Histidine is reported to be an active residue that participates in the proton transfer path(Kaur et al., 2021). It can accept as well as donate proton. Proton transport in membranes occur via Grotthuss or Vehicular mechanism. His analogs are reported to facilitate proton transfer via Grotthuss transfer mechanism (Odella et al., 2018, 2019). His facilitated proton transfer in the M2 proton channel (C. Wang et al., 1995) and in carbonic anhydrase(Tu et al., 1989). Lys and His are frequently found coupled to acidic residues in clusters. Hydronium ion trapped between several acidic residues is reported to be part of proton loading site clusters(Freier et al., 2011; Kovalevsky et al., 2011; Supekar et al., 2016).

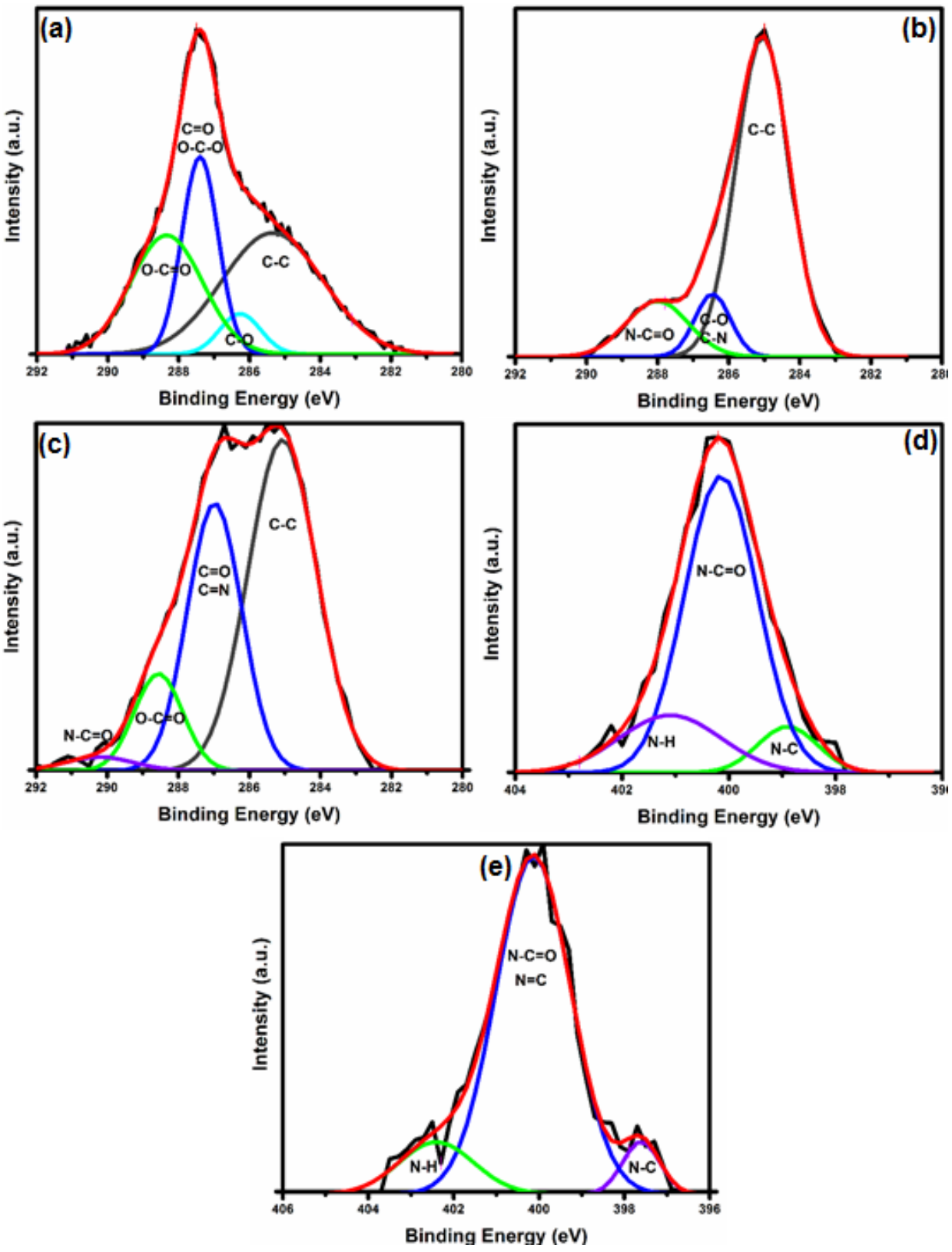

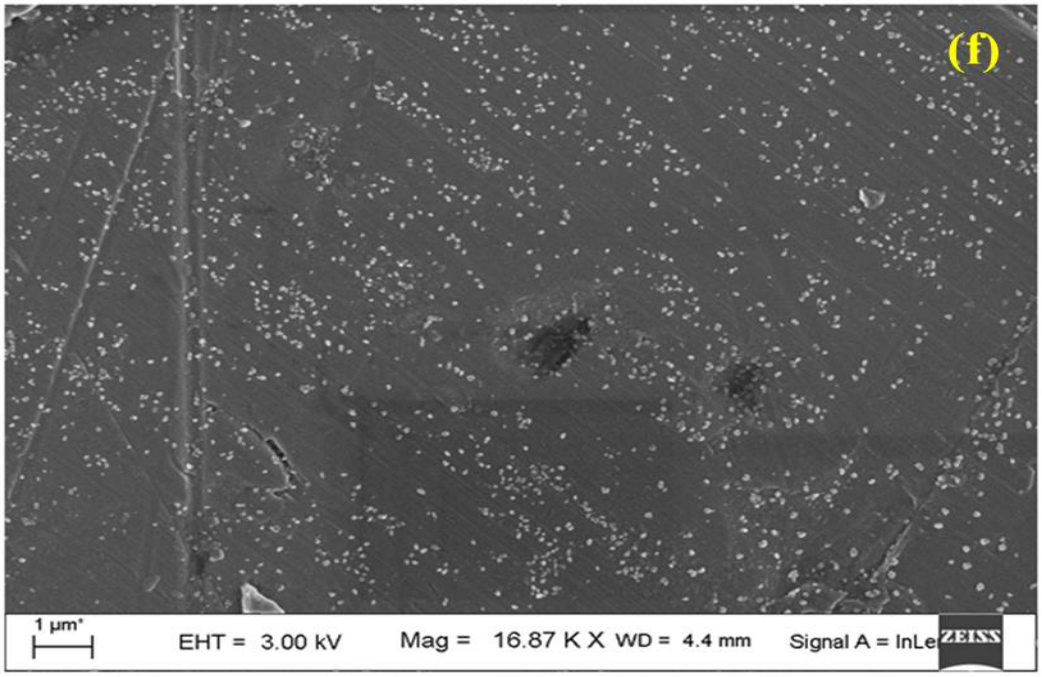

Fig.4.1. XPS spectra of carbon 1s (a) CNCs (b) Hair extract (c) Modified CNCs and nitrogen 1s spectra of (d) Hair extract (e) Modified CNCs, (f) Surface morphology of the HH/CNC/CS membrane.

4.2.2 Ionic Conductivity, Water Uptake and % Swelling

Water uptake and swelling degree are closely related to the proton transport in the polymeric membrane, which directly affect the proton conductivity and the overall MFC performance. An optimum level of water uptake and % swelling helps in the proton transport in the membrane while preserving its mechanical integrity. The ion conductivity of the HH/CNC/CS membrane at room temperature increased to 1.04±0.02 mS/cm from 0.25±0.02 mS/cm for pristine chitosan membrane. The lower value of ohmic resistance can be attributed to the improvement in ion conductivity of the modified membrane. Water uptake was increased slightly from 48±5% to 60±2% due to the hydrophilic network

formed by hair hydrolysate modified CNCs in CS mixed matrix. This network formation however enhanced the matrix to filler interaction holding the membrane tight together thereby resulting in the reduction of % swelling from 38±4% to 26±2%.

4.2.3 Effect of modified membrane on power generation and COD removal from wastewater

The performance of the MFCs assembled with the new membrane is evaluated in terms of voltage and power density with commercial Nafion-117 as the control case. The study reveals that the hair hydrolysate modified chitosan membrane has distinct influence on the voltage generation of the MFCs. It has outperformed the other modified chitosan membranes provided in the literature. The power output normalized to the anode surface for different modified chitosan membranes based MFCs fed with real wastewater is tabulated in **Table 4.1,** for comparison. Furthermore, the polarization curves depicted in **Fig. 4.2a-b**, indicates a voltage output of 769.58±0.13 mV and a corresponding power density of 142.5±0.21 mW/m^2 achieved by the MFCs operated using the new membrane for the first time. This indicates the efficiency of the new membrane fabricated for bioelectricity production using MFC. Moreover, the new membrane is suitable to sustainably harvest power from MFCs for longer batch cycles. This is demonstrated by the acclimation study in which the cells were monitored under external resistance of 1000 Ω for 30 days with domestic wastewater as feed and maximum voltage of 600±0.2 mV was achieved for 3 repeated cycles

The ohmic resistance is a sign for resistance to proton transfer in the PEM which ultimately determines the performance of the MFC device. As expected, in addition to the amino

groups in chitosan, an increase in the charged and ionizable hydrogen donor species in the hair hydrolysate functionalized chitosan membrane assisted in the proton conduction by providing pathway for proton transfer. This in turn resulted in lowering the internal resistance of the MFCs demonstrated by the low ohmic resistance (165.1Ω) in **Fig. 4.2c**. Modification of ceramic membrane using chitosan also reported notable decrease in internal resistance(Goy et al., 2009). The lower charge transfer resistance of 6.57Ω displayed also explains the bacterial activity and therefore the high performance of the device. To sum up, this biocompatible and non-fluorinated membrane played a vital role in enhancing the power performance of the real wastewater fed MFC device.

The cyclic voltammogram (CV) acquired for the anodes with biofilm grown from the domestic wastewater is shown in **Fig. 4.2d**. The CV attained for 10 cycles in the HH/CNC/CS membrane assembled MFC at scan rate (10 mV/s) displayed a complex form which is usually reported to be observed in real wastewater with redox peaks from – 0.5 V to 0.0 V (vs. Ag/AgCl) which could be an indication of presence of mediator produced by the mixed culture of bacteria. High current density in mA range suggests that the concentration of mediator is high and these mediators are presumably bound to the biofilm on the anode surface(X. Li et al., 2019; H. Liu et al., 2005).The voltammetry scans of Nafion based MFC did not display any detectable response. Thus, the observed redox peaks in the HH/CNC/CS membrane were more likely from self-induced bacterial mediators held in biofilm which formed the main mechanism of power production in the HH/CNC/CS membrane assembled MFC.

Biofilm adhesion on the anode in the modified chitosan based MFC was imaged using FESEM. **Fig.4.2e** shows the rod-shaped graphite felt fibers before biofilm formation. **Fig.**

4.2f shows the growth of biofilm on the electrode with the mixed consortia of bacteria in the wastewater encircling the felt which is 10 μm in diameter after 30 days of acclimation period. The inset picture displayed in **Fig.4.2g** shows the bacterial community which are mostly rod shaped of different sizes of less than 1 μm in diameter which helped in transporting electrons from the microbes to the anode. Such a stable biofilm offered less resistance to the electrochemical reaction at the anode surface, as revealed by the low charge transfer resistance (R_{ct}), which together with the low ohmic resistance offered by the membrane resulted in higher power generation by the MFC device. The modified membrane assembled MFC is also capable of simultaneous wastewater treatment. This is demonstrated by the contour plots presented in **Fig. 4.2i and 4.2j** for the COD percentage removal. The HH/CNC/CS membrane based MFC is effective for COD removal, with removal efficiencies exceeding 80%. The uptake of nutrients present in the wastewater by the mixed culture bacteria through degradation of the organic matter is the leading mechanism of COD removal. The removal efficiency is lowest on Day 1 when the bacteria is acclimatizing due to insufficient bacterial biofilm formation. As the experiments continued over a period of 30 days, growth of biofilm formation occurs leading to improved COD removal.

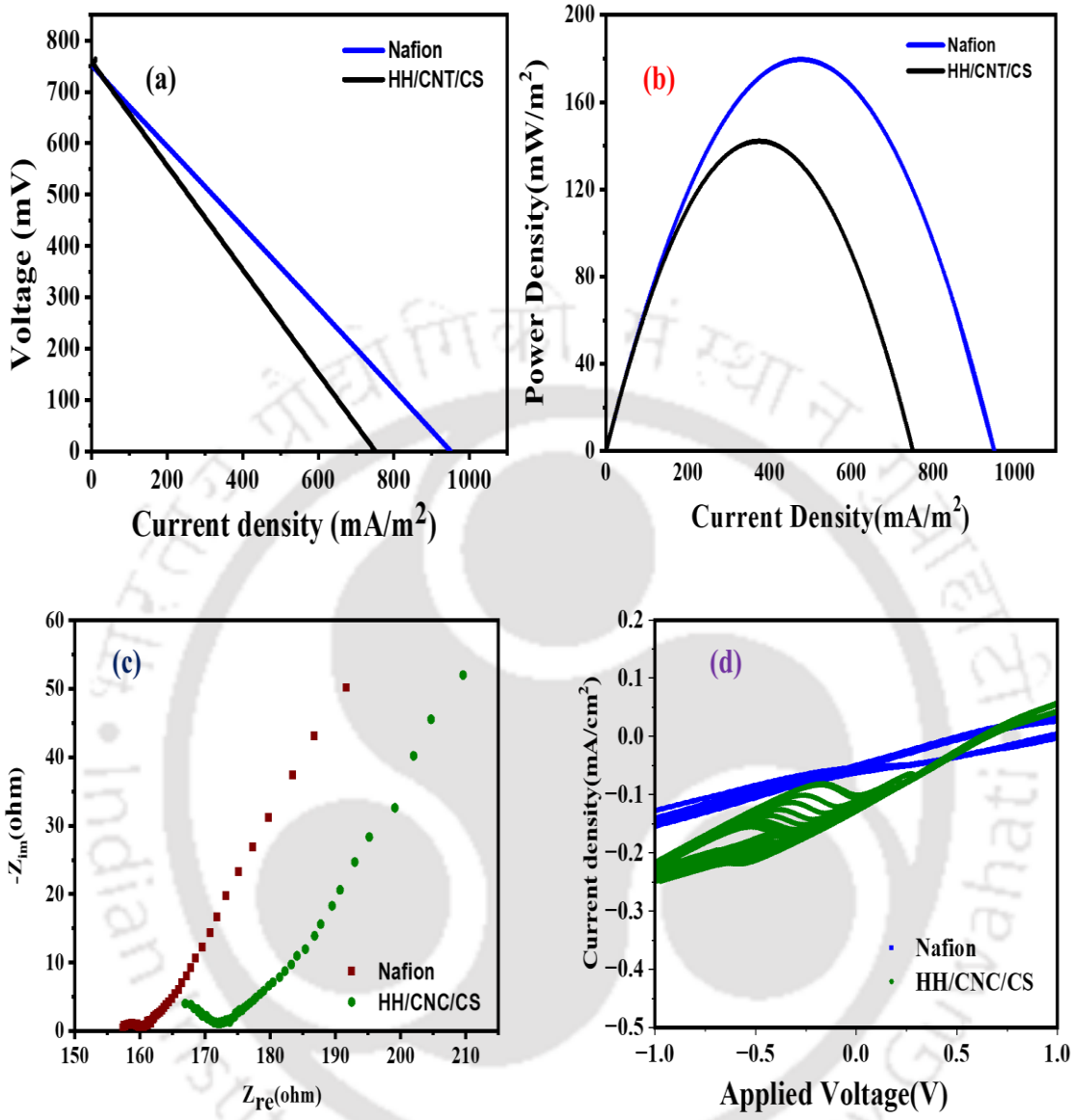

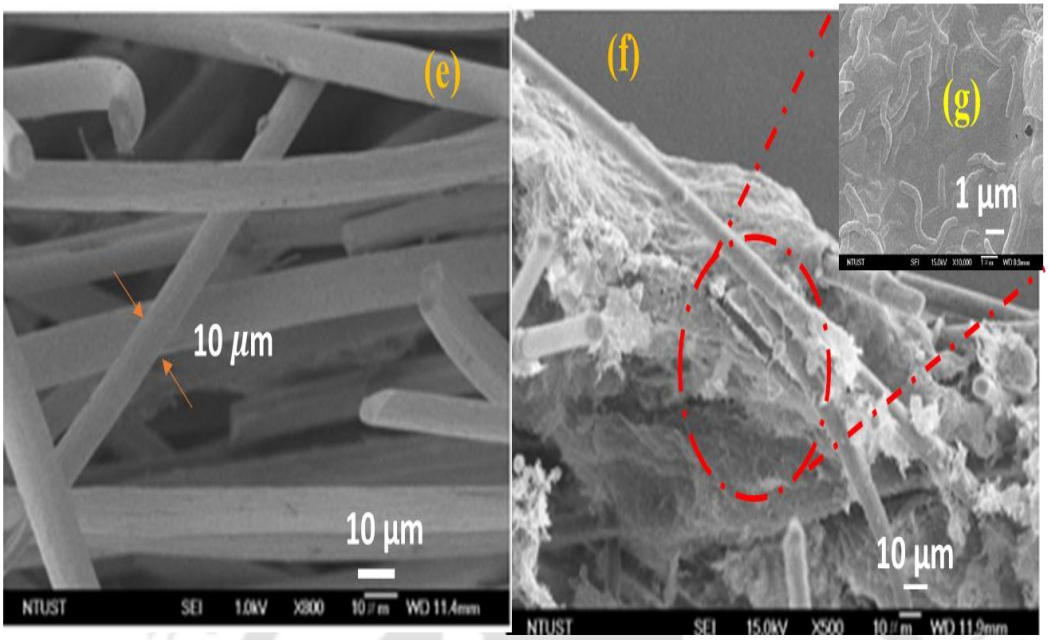

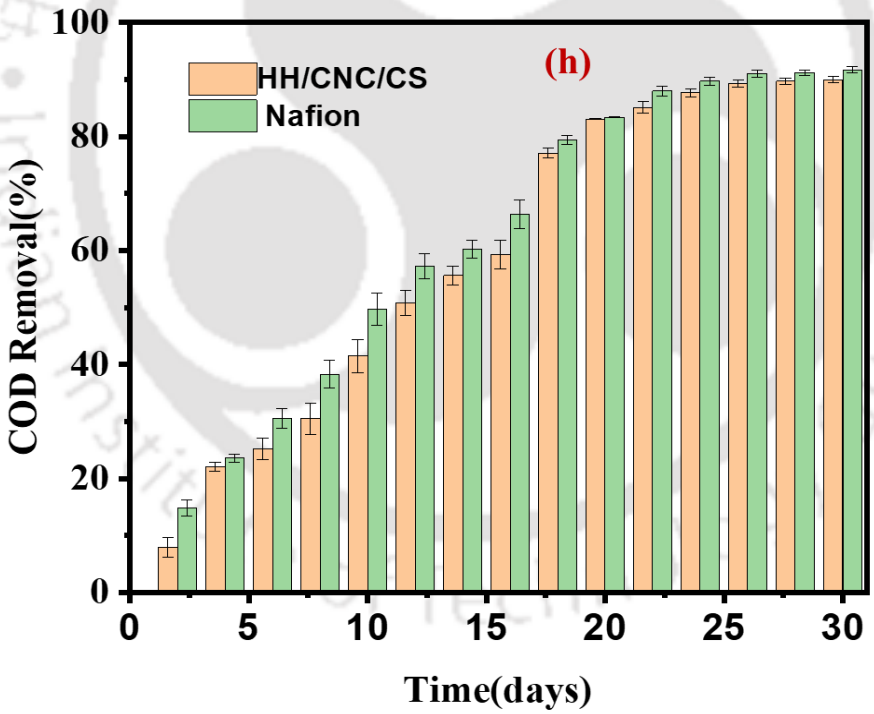

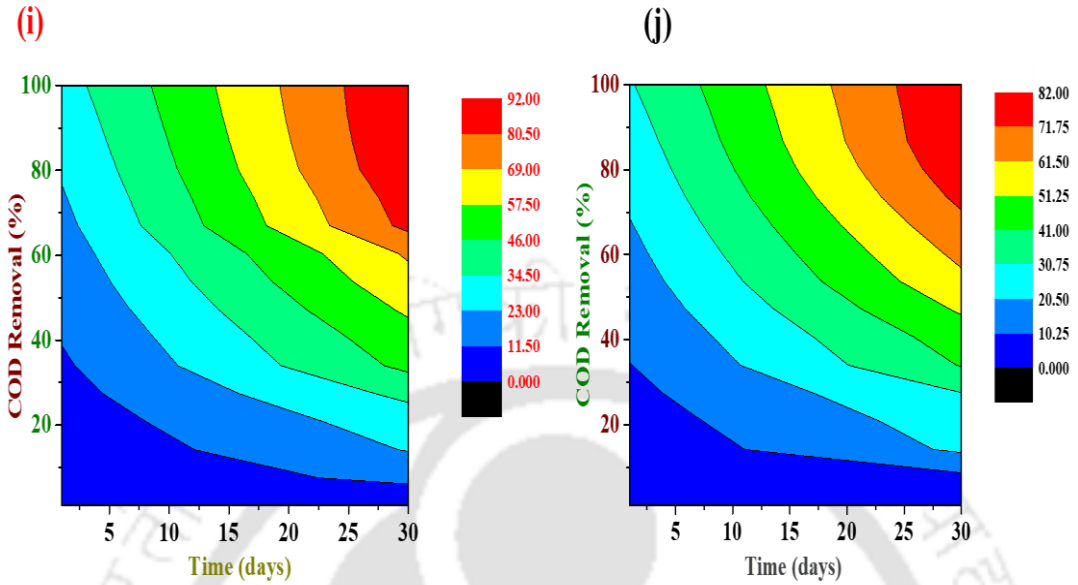

Fig.4.2. Polarization curves of MFCs equipped with commercial Nafion 117 and HH/CNC/CS membrane (a) voltage output and (b) Power density w.r.t current density, (c) Nyquist plot demonstrating the internal resistance to the performance of the MFCs fed with domestic wastewater, (d) Cyclic voltammetry study showing the bioelectrochemical activity of the mixed consortia based MFCs, (e) Surface Morphology of anode without biofilm, (f) bacterial biofilm layer domestic wastewater encircling the electrode, (g) inset picture shows the magnified image of the bacteria present on the electrode,(h) COD removal from the wastewater using the fabricated membrane and commercial membrane assembled MFC device, the optimum COD removal region isopleth diagram of (i) Nafion-117 and (j) HH/CNC/CS membrane.

Table 4.1: Comparison of performance of modified Chitosan based MFC device fed with real wastewater.

Membrane	Anolyte	Maximum voltage (mV)	Maximum Power Density (mW/m^2)	Internal Resistance (Ω)	% COD Removal	Ref
CS-P	Municipal wastewater	504	130.03	464	50	(Holder et al., 2016)
S-CS-P	Municipal wastewater	425	20.76	2984		(Holder et al., 2016)
MWCNT/CS	E.Coli	750	46.94	__		(Narayanaswamy Venkatesan & Dharmalingam, 2013)
SSA/CS	Anaerobic sludge in culture medium	790	__	156		(Srinophakun et al., 2017)
HH/CNC/CS	Domestic Wastewater	769.58	142.57	165.1	82	**This study**

Table 4.2: Comparison of performance of MFC devices equipped with low-cost separators.

Separator	Anolyte	Maximum voltage (mV)	Power Density (W/m^3)	MFC type	% COD Removal	Ref
FEM 15%	Synthetic wastewater	872 ± 10	7.87	Air-cathode	82 ± 3.78	(Gunaseelan et al., 2022)
EPS	Domestic wastewater	932	1.36	Air-cathode	80	(Mathuriya & Pant, 2019)
Zirfon	Acetate	623	1.29	Air-cathode	-	(Sevda et al., 2016)
HH/CNC/CS	Domestic Wastewater	769.58	1.78	Dual chamber	82	**This study**

4.2.4 Effect of the modified membrane on antibacterial property

Another desirable aspect of the modified membrane is its antibacterial property as it prevents microbe migration from anode chamber hence ruling out the occurrence of biofouling phenomenon which is critical for long duration operation in wastewater treatment using MFC. During long duration of operation, anodic bacteria create extra biofilm on the anode side of the membrane which is known as biofouling. Biofouling leads to lowering of power output from the device as it resists the migration of protons through the membrane. Membrane biofouling can be minimized by mainly two methods, namely, i) the anti-adhesive approach which inhibits bacterial attachment onto the membrane and ii) the anti-microbial approach which causes death of the bacterial cells present on the

membrane. As observed from the FESEM images in **Fig. 4.3a-b**, the modified membrane has least number of cells on its surface which symbolizes that it prevents the bacterial cells from attachment. This is a sign of good anti-adhesion property. In addition, it has ruptured the cells which were originally rod-shaped **Fig. 4.3c**. It is therefore, obvious from the shape of the damaged cells that the membrane possesses high antimicrobial property. The rupturing of the cells in the modified chitosan membrane is due to the presence of amino group(Yilmaz Atay, 2020).The glucosamine backbone of chitosan membrane consists of high density of amino group. As a result, electrostatic interaction between cationic $–NH_2$ structure of chitosan and anionic cell surface proteins and lipopolysaccharide of the microbes takes place. This interaction changes the permeability of the microbial cell membrane resulting in leakage of intercellular components hence rupturing the cells and causing cell death. This result is consistent with the earlier report by (Srinophakun et al., 2017), on reduced biofouling of chitosan membranes. A key reason behind the enhanced performance of the modified chitosan membrane assembled MFC is the high antibacterial property as it inhibits microbial growth and ensures reduced biofilm formation on the modified chitosan membrane.

On the contrary, clusters or aggregates of microbial cells were observed on the surface of the Nafion membrane which shows its low antimicrobial property as well as anti-adhesion property (**Fig. 4.3e**). This is attributed to the presence of $–CF_2$ $–CF_2–$ links and $–SO_3^-$ terminals, present in Nafion membrane. Nafion is therefore, more prone to biofouling in comparison to the fabricated chitosan membrane during long term operation of MFC with real wastewater or sewage sludge.

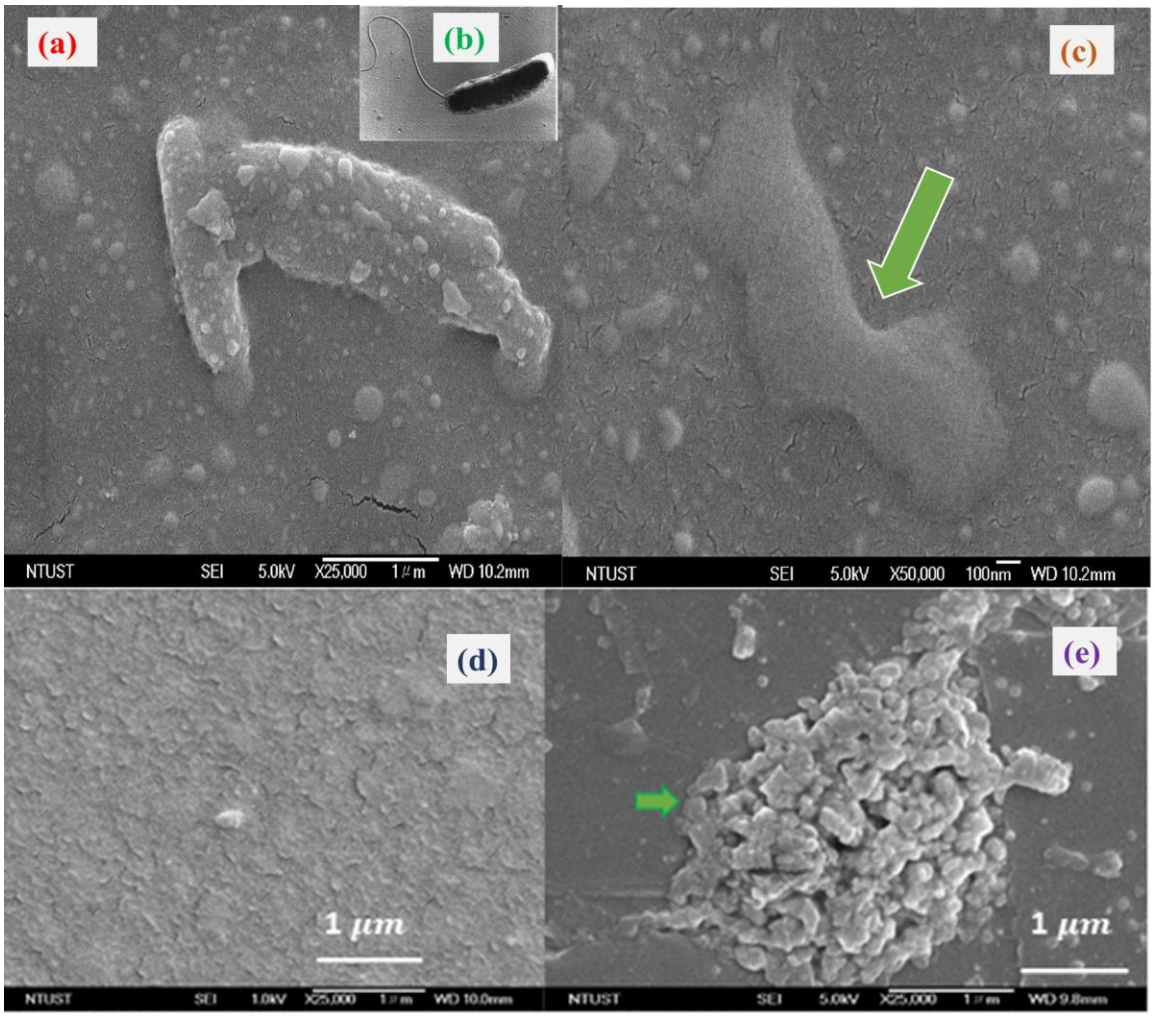

Fig. 4.3 (a) Surface morphology of the modified chitosan membrane with the damaged cells of S. P*utrefaciens* bacteria cells on the surface of modified Chitosan membrane, (b) Inset picture depicts the actual rod shape morphology of S. P*utrefaciens* before antibacterial testing, (c) Magnified image shows the damaging impact on the bacterial cell in contact with the modified chitosan membrane, (d) Surface morphology of Nafion-117 membrane before antibacterial testing, (e) Aggregates of microbial cell adhering to the surface of the Nafion-117 membrane.

4.2.5 Cost analysis of Nafion117 and HH/CNC/CS membranes

Although MFCs plays dual role providing wastewater treatment and simultaneous generation of green power, however the cost of manufacture associated with that of the PEM and electrodes is a major hurdle in its practical application. In this study, relatively cheap PEM is fabricated using Chitosan for application in MFCs. The total cost of synthesizing the HH/CNC/CS membrane was around 150 $/m^2, which is 10-fold lesser than Nafion 117 (1659 $/m^2). This difference in cost of the membrane can considerably lower the total production cost of MFCs. HH/CNC/CS membranes are cheaper in comparison to similar efforts to develop low cost separators from expanded polystyrene (ESP) (516.88 $/m^2) (Mathuriya & Pant, 2019).

4.3 Conclusions

Hair hydrolysate functionalized CNC based Chitosan membrane was successfully synthesized via method of solution casting. It was further characterized for application in MFC device fed with domestic wastewater as a low-cost substitute to commercial Nafion-117. The amalgamation of simple production step, utilization of human hair waste in the sustainable polymer is an innovative approach and novel attempt in this regard. Characterizations revealed the structural interaction between the hair hydrolysate functionalized CNC and chitosan matrix leading to 4-fold increase in ion conductivity, 46 % reduction in swelling than in it's pristine form. Besides, the membrane is relatively inexpensive and displays outstanding potential yielding increased power output of 142.57 mW/m^2 (1782.12 mW/m^3) utilizing wastewater as substrate. Compared to Nafion which is prone to biofouling, the fabricated membrane exhibits better antibacterial property and

hence can be a promising alternative for the costly membrane for harvesting electricity and wastewater treatment in future.

Chapter-5

Bioaugmented Polyaniline decorated Polylactic acid nanofiber flexible electrode by electrospinning technique for real wastewater fed MFC application

Motivation

In the recent times, natural biopolymers such as chitosan and cellulose have received tremendous concern on their potentiality to replace the existing membranes which are costlier and non-environmentally friendly. Their potential as greener polymer electrolyte to enhance MFC properties and performance is an interesting topic. However, research on utilization of such natural biopolymers in MFCs to treat real wastewater and simultaneously harvest electricity is very limited. Also, utilization of human hair waste for PEM application is another exciting approach. Such interesting properties offered by the biopolymer namely, high economic value, sustainable, carbon–neutral and renewable production processes make an additional value for such green technology application.

The work in this chapter is published as:

Das, B., Soundararajan, N., Kashyap, S. P., Jang, J. H., Wang, C. T., Katha, A. R., & Katiyar, V. (2022). Bioaugmented polyaniline decorated polylactic acid nanofiber electrode by electrospinning technique for real wastewater-fed MFC application. *International Journal of Energy Research*, *46*(3), 3588-3601. https://doi.org/10.1002/er.7407 (I.F 4.612)

Abstract

This chapter focusses on the utilization of sustainable polymer Polylactic Acid (PLA) for MFC application. PLA is a bio-based polymer and a biocompatible material used mostly in packaging application which makes it a suitable anode material for hosting microbes. But its potential as a supporting material/matrix for anode in domestic wastewater fed Microbial Fuel Cells (MFCs has not been explored as it does not possess electron transfer property. On the other hand, PANI is an intrinsically conductive polymer favoured for its electro catalytic activity. The bio-based flexible anode displayed excellent biocompatibility and outperformed the flat graphite anode with 8-fold increase in power density and COD removal efficiency of 91.7%. The cyclic voltammetry results rule out the presence of mediator in the electron transfer. Field Emission Scanning Electron Microscopy images indicated that the electrospun polymeric nanofibers played a good host with biofilm layer attached to the nanofibers. Therefore, the present study has successfully added a new dimension to the design of sustainable anode material to enhance microbial binding and achieve high power output revealing the enormous potential of scale-up of MFCs for wastewater treatment in the future

Graphical Abstract

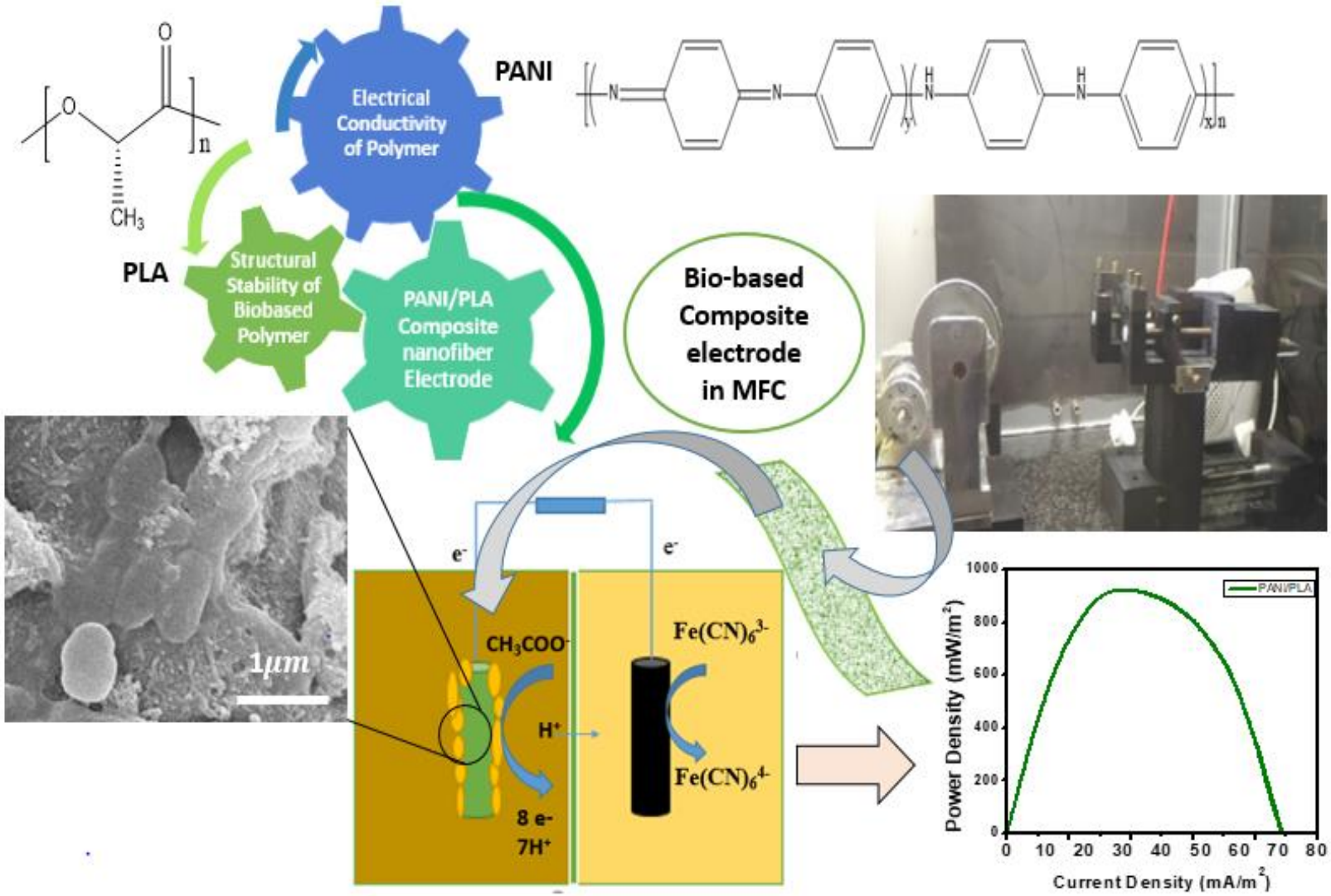

5.1 Introduction

Microbial Fuel Cells (MFCs) are an eco-friendly and sustainable technology that can be an important tool in switching from the conventional linear economy towards a more sustainable circular economy where waste is valued as a resource(Yaqoob, Ibrahim, Umar, et al., 2021). Domestic wastewaters which include sewage and gray waters contain large quantities of organic loads. They are usually treated employing aerobic treatment which has disadvantages of being energy-intensive and producing a large quantity of sludge as a contaminant (Yaqoob, Khatoon, et al., 2020). MFCs-based domestic wastewater treatment system provides an edge over the current wastewater treatment technologies as it is energy-yielding. It can convert waste directly into electricity via an electrogenic catalyst(Yaqoob, Ibrahim, Yaakop, et al., 2021). The entire treatment process is responsive to real-time control at low temperature as the electrons are donated by the bacteria to an external circuit producing fewer amounts of excessive sludge which leads to a reduction in the operating cost and sludge treatment or disposal cost(Fangzhou et al., 2011).

The common types of MFCs for generating electricity from different kinds of substrates are dual and single chamber MFCs (Yaqoob, Ibrahim, Umar, et al., 2021; Yaqoob, Mohamad Ibrahim, Rafatullah, et al., 2020). The oxidation and reduction reaction occurring at the anode and cathode respectively of a dual-chambered MFC is written below(Yaqoob, Ibrahim, & Guerrero-Barajas, 2021; Yaqoob, Mohamad Ibrahim, Rafatullah, et al., 2020):

$$\textbf{\textit{At anode}}: \ CH_3COO^- + 2H_2O \ \rightarrow 2CO_2 + 7H^+ + 8e^- \quad (5.1)$$

$$\textbf{\textit{At cathode}}: Fe(CN)_6^{3-} + e^- \ \rightarrow Fe(CN)_6^{4-} \quad (5.2)$$

Although the power production is encouraging, however, the practical application of simultaneous energy harvesting and wastewater treatment process using MFCs is limited by the anode material. Firstly, due to low electron transfer rate and secondly, due to low affinity for bacterial cell attachment(Yaqoob, Ibrahim, et al., 2020; Yaqoob, Mohamad Ibrahim, Rafatullah, et al., 2020). The first drawback can be solved by introducing higher conductive materials while the second drawback can be diminished by encapsulating the conducting polymer in a nanosized form-stable, biocompatible supporting matrix in which the bacteria in the wastewater can thrive and grow. Recent reports suggest several approaches mostly focused on modifying the electrode to enhance conductivity with less emphasis on bacterial cell adhesion (Lai et al., 2011). One such effective approach for electrode modification which takes into consideration the above-mentioned solutions is bioaugmentation. It is considered as a potential tool to boost the performance of microbial fuel cells (MFCs) by modifying electrodes with biopolymers (R et al., 2013). Therefore, in the present study, a bioaugmented anode is fabricated by introducing PLA with PANI in the form of electrospun nanocomposite for MFC application.

Polylactic acid (PLA) is a thermoplastic and bio-based aliphatic polymer having chemical formula $(C_3H_4O_2)_n$. It is achieved by lactic acid condensation with loss of water. PLA is derived from renewable feedstock namely starch, corn, sugarcane, etc(Katiyar et al., 2010) It is mechanically and thermally stable over synthetic polymers with good biocompatibility and is commercially available in large quantities(Mulchandani et al., 2022). PLA has been widely electrospun in its neat form as well as composites by modifying its functionality depending on the application such as electrospun mats for drug delivery. PLA-based nanofibers are being extensively used in various applications as functional composites,

biosensors, tissue engineering, and advanced drug delivery systems. The recent success of application of PLA based nanofibers by electrospinning for cancer therapeutics(Chi et al., 2020), tissue engineering(Magiera et al., 2017), immobilization of α-amylase(Gali et al., 2021)etc., demonstrates its potential as a suitable platform for hosting microbes and promoting their growth thereby mediating the electron transfer process. In fact, electrospun PLA nanofibers are reported to be non-toxic, exhibiting high porosity and large surface area with improved biodegradability which makes them suitable to make inroads in the field of MFC and other eco-friendly energy storage systems (Palmieri et al., 2020). The only reported application of PLA in MFC is 3D Printed Conductive PLA-based filament anode used as anode for Single Chamber MFC. The maximum power achieved being 43±1 μW attributed to the poor conductivity of the anode material(You et al., 2017). On the otherhand, polyaniline (PANI), has been frequently exploited for anode modification in MFCs because of its electrocatalytic activity, biocompatibility, mechanical flexibility, low charge transfers resistance, ease of synthesis, and low cost (Yaqoob, Mohamad Ibrahim, Umar, et al., 2020). However, its low processability as well as low solubility due to its rigid aromatic backbone and strong inter–intra chain interactions poses as a major limitation, making the fabrication process of pure PANI electrospun nanofibers quite challenging. Interestingly, composite electrospun nanofiber can be a better option by loading PANI onto PLA nanofiber. With reference to a very recent study, the morphology for the electrospun nanofibers (R. Liu et al., 2021) due to introduction of PLA biopolymer with PANI on electrospinning promoted cell adhesion and proliferation.

The bigger picture being that at the end of its service life, fabricated electrode from the amalgamation of PLA and PANI will degrade without environmental toxicity. Therefore,

the application of this sustainable polymer for MFC technology is new and worthy of investigation. To the best of our knowledge, PLA nanofiber decorated with in-situ polymerized PANI for application as anode in real wastewater fed MFCs has not been reported previously. Therefore, the work carried out in this chapter focusses on the development and application of electrospun PANI/PLA nanofiber as anode material using mixed culture of domestic wastewater borne bacteria as biocatalyst for real wastewater treatment. A thorough analysis of the structure, morphology and composition of the PANI/PLA nanofiber developed has been probed into to test its chemical stability and cell adhesion property. It is noteworthy to mention that the study did not involve the addition of a synthetic mediator or catalyst. For accessing its potential as an anode material, relative to commercial graphite felt a detailed electrochemical analysis of the flexible electrode in domestic wastewater-fed MFCs is carried out to comprehend the electron transfer ability and investigate its potential for attachment of microbial consortia present in real wastewater.

5.2 Results and Discussion

A one-step method is attempted to modify the PLA nanofiber as an electrode for MFCs for the first time employing PANI. The electrode developed by in-situ polymerization of aniline on PLA has been described below. Further, the suitableness of the flexible electrode being utilized as an anode electrode for MFC operation using domestic wastewater is investigated in the subsequent section of the chapter.

5.2.1 In-situ polymerization of PANI on electrospun PLA: Reaction mechanism, Thermal stability, and Surface Analysis studies

PANI/PLA flexible electrode has been fabricated by electrospinning technique. The proposed structure is depicted in **Fig. 5.1a** Polyaniline formed by in-situ polymerization of aniline functioned as the conductive element of the composite. Polyaniline by itself cannot be electrospun and thus, PLA assists as a carrier/support polymer in the electrospinning process. The combination of the two materials mitigated the structural disintegration of polyaniline in the solution phase. Doping the polyaniline with HCl acid, led to interaction of the cation in the acid with the imine N atoms characterized by solid green color. This resulted in the formation of polycation in the system which prompted the neighboring N atoms lone pair to uncouple which in turn led to the delocalization of electrons resulting in the high conductivity of PANI (80 Scm^{-1}) (Pinto et al., 2008).

The chemical structure of the PLA and PANI/PLA composite was studied using FTIR Spectroscopy as shown in **Figure 5.1(b)**. The spectrum of PANI/PLA composite has shown correlated spectral bands of neat PLA exhibiting characteristic peaks at 1748 cm^{-1} representing C=O stretching, peak at 1454 cm^{-1} and 1352 cm^{-1} representing -CH_3 bending, peak at 1382 cm^{-1} is attributed to -CH-bond deformation, peak at 1359 attributed to -CH_3 vibrations while peaks at 1182, 1130,1083, and 869 cm^{-1} corresponds to -C-O- bond stretching of -CH-O group, C-O-C asymmetric stretching, C-O vibrations, and C-C stretching vibrations, respectively(Pal & Katiyar, 2016).The in-situ polymerization of PANI is recognized by peaks at 1560 cm^{-1},1756 cm^{-1} 1482 cm^{-1},1293 cm^{-1} assigned to C=C bond in the quinoid ring, C=O stretching, C=C bond in the benzenoid ring, C-N stretching

respectively(GOLCZAK et al., 2008; R. Liu et al., 2021). The presence of intense broad peaks in the range 1084 cm^{-1} to 1182 cm^{-1} confirms the successful polymerization of PANI on the PLA matrix by(-$CONH_2$) amide-ester linkage(Mohan Bhasney et al., 2020).This amino-functionalized surface of the composite activated the cell attachment onto the bio-based anode.

To further analyze the chemical composition of the PANI-PLA composite electrode fabricated by in-situ polymerization the XPS analysis is shown in **Figure 5.1(c).** The presence of oxygen, O(1s) ~ 532 eV) has its origin in PLA while the elements carbon C(1s) at 285 eV along with nitrogen has its origin in the PANI backbone. A major peak positioned at around 285 eV is observed in the C(1s) core spectrum with a slight uneven broadening in the direction of high binding energies, typically reported for protonated PANI(GOLCZAK et al., 2008). N(1s) spectrum demonstrates the presence of peak observed at 399.8 eV for benzenoid amine component (–NH–). Thus the appearance of clear N 1s peak confirms the decoration of PANI on PLA nanofibers successfully. The relative concentrations in atomic weight % (C, O, N) obtained by calculating the peak areas are 23.62 for O 1s, 11.01 for N 1s, and 65.36 for C 1s.

The TGA curves of neat PANI, neat PLA, and PANI-PLA composite are depicted in **Figure 5.1(d)**. It is observed that the TGA curve for neat PLA and PANI/PLA composite displays one step degradation with its onset degradation temperature at around 334 ^{0}C and 348 ^{0}C(Mohan Bhasney et al., 2020). On the contrary, neat PANI demonstrates two distinct steps of degradation due to weight loss. The first step observed between 80 and 100 °C can be mainly attributed to the elimination of solvent molecules and other volatile impurities from the PANI backbone(Ismail et al., 2019). The second weight loss step, observed

between 300-400^{0}C might be due to the removal of the dopant (HCl) and low molecular weight oligomers from the backbone of the polymer. After which the curve demonstrates sharp decrease due to decomposition of the PANI backbone units. On comparing with the TGA curve of PANI/PLA it can be observed that the composite formed showed higher degradation temperature as compared to its neat counterpart. Hence, it can be concluded that on formation of nanocomposite, the degradation of PANI is inhibited and the thermal stability of the PANI-PLA electrode has enhanced compared to the neat polymers.

DSC study reveals glass transition behavior of the pristine polymer (PLA) and PANI/PLA electrospun fibers are presented in **Figure 5.1(e)**. In the first part of the PLA curve, the endothermic effect observed is related to the evaporation of a small amount of water, penetrating polymeric chain which originates from the high specific surface area of the electrospun fibers when compared to its granular form. The crystallization temperature shifts to a higher temperature with a broader crystallization peak for the nanocomposite. The incorporation of PANI within the PLA matrix requires higher energy for the growth of crystallites which could hinder the crystallization. The glass transition temperature and melting temperature for PLA are 67.04 ^{0}C and 151 ^{0}C respectively. However, on the incorporation of PANI, the endothermic peak shifted to a higher temperature. A higher glass transition temperature is observed (T_g) for the composite than the counterpart native state because the T_g of the polymer increases with the increasing of conductivity. Besides, the strong interaction between the PLA fiber and garland-like morphology of PANI encircling it leads to the limited mobility of polymer chain hence increasing the T_g.

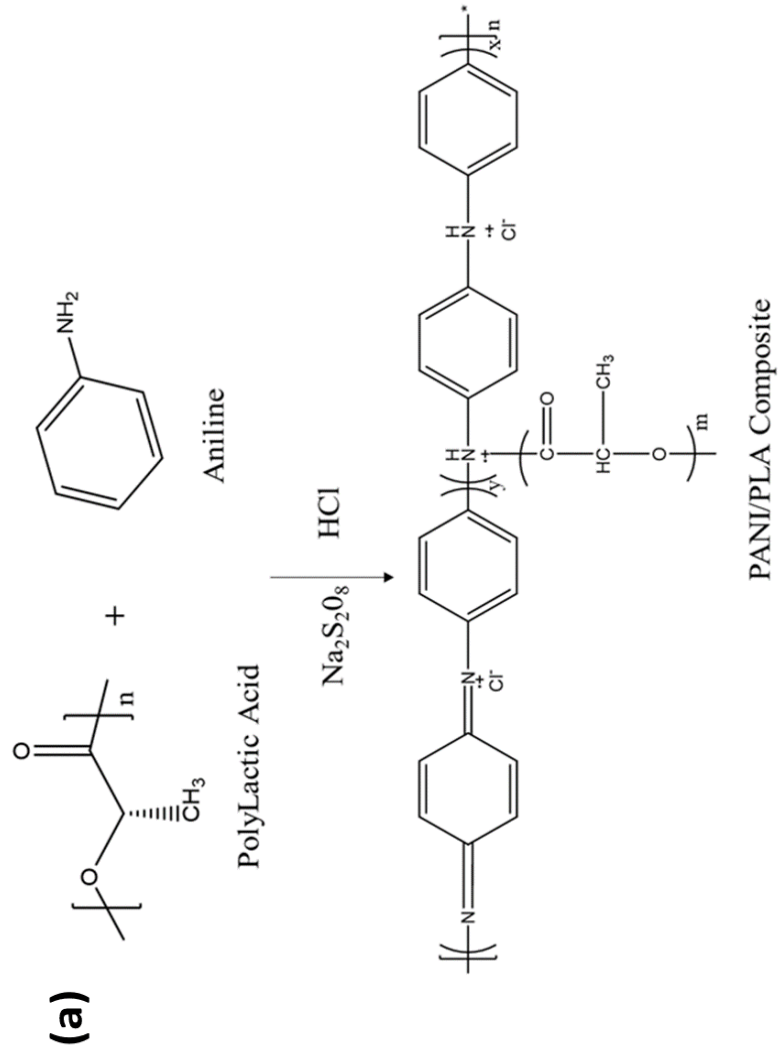

(b)

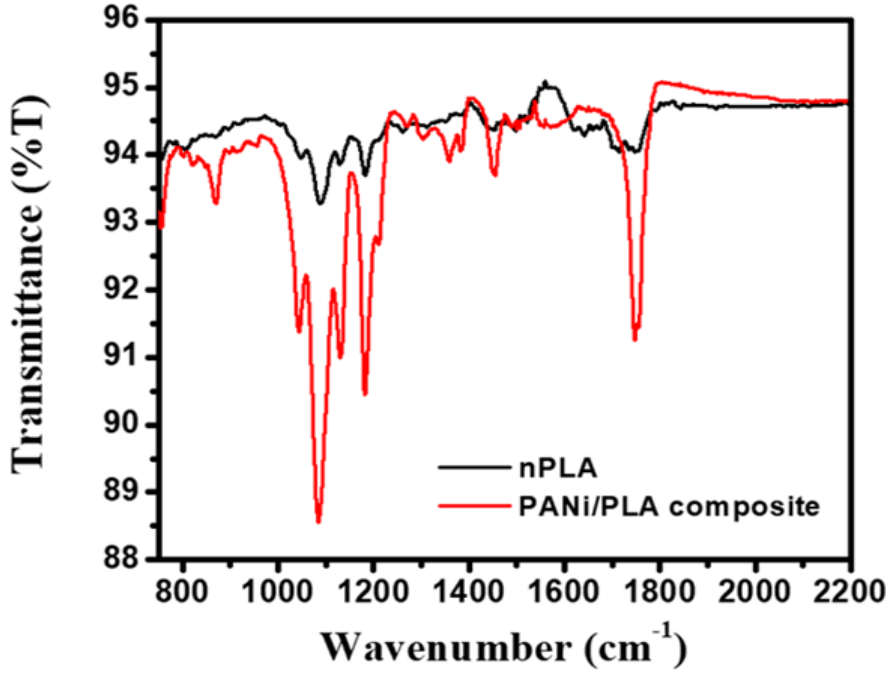

(c)

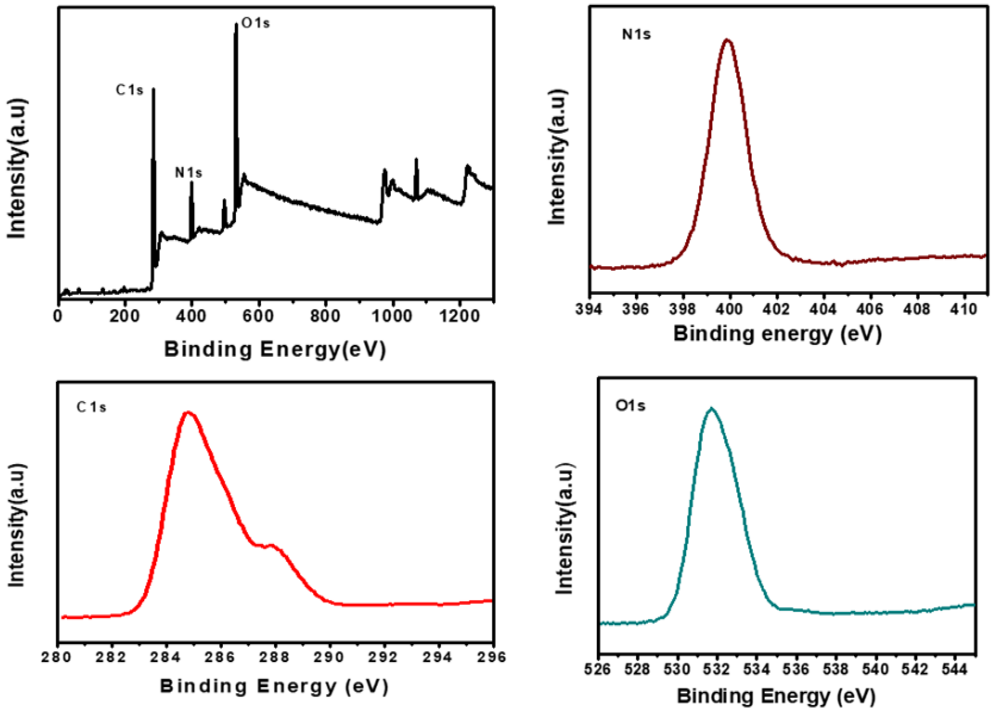

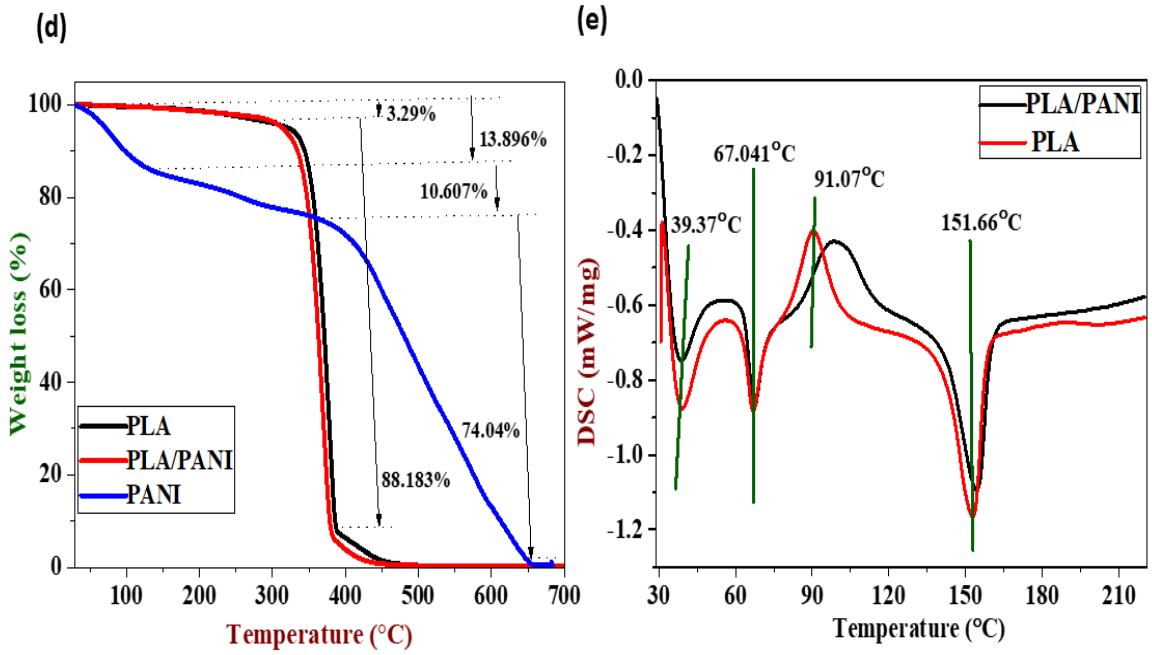

Figure 5.1: (a) Schematic of the proposed in-situ polymerization reaction of bio-based composite, **(b)** FTIR Spectra of the PANI/PLA composite electrode, (**c**) XPS spectra of PANI/PLA electrode **(d)** TGA curve of neat PLA, neat PANI, and the PANI/PLA composite, **(e)** DSC thermogram of neat PLA and PANI/PLA composite.

5.2.2 Biofilm analysis of the flexible electrode

The surface morphology of the graphite felt assembled as the control electrode is shown in **Fig 5.2(a)** and after biofilm formation is shown in **Fig 5.2(b)**. A close examination of the biofilm layer on graphite felt electrode as displayed in **Fig 5.2(d**) showed the presence of rod-shaped bacteria. Compared to the graphite felt, the biofilm formed on the PANI/PLA

flexible electrode had a uniform coverage of heterogeneous microbial culture while the graphite felt had patchy clusters holding onto the fibers (**Fig 5.2(c**). The surface morphology of the bare biobased PANI/PLA composite electrode (**Fig 5.2(e) and 5.2 (f)**) showed a uniform network of nanofibers with PLA nanofibers acting as the scaffold with PANI resembling a garland-like morphology. The flexible electrode constituted randomly arranged fibers with a smooth surface. These loosely arranged fibers offer space for the growth of the microbes. The large community of microbes varied from small to a large range of less than 1 micron and they were in both spherical and rod shape as observed from **Fig 5.2(h).** The experimental findings reveal that the nanofiber electrode promoted extracellular electron transfer kinetics during 30 days' operation which is evident from enhanced current density in the CV curve and lower resistance in EIS analysis. The obvious reason for such outstanding biocompatibility to house the exoelectrogens is a result of the high biocompatibility of polyaniline and PLA along with the presence of functional groups containing oxygen. The biocompatible nature of the composite nanofiber fabricated is consistent with the MTT method reported for PANI/PLA(R. Liu et al., 2021). The large exposed area of the nanofibers provides adequate sites for microbial attachment accounting for the enhanced performance of the PANI/PLA-based MFCs as demonstrated later. The bacterial cells were observed to be in direct contact with fibers of PANI/PLA confirming excellent biocompatibility of composite electrode **(Fig 5.2(g) and 5.2(h)**). The thickness of the biofilm reached 20 to 40 microns from the initial value of zero, within 30 days as observed in the cross-sectional image. This ready attachment displayed by the microbes and rapid growth of the biofilm can be ascribed to the combined advantage of the presence of functional groups (strong interaction of positively charged PANI with negatively

charged microbes) and biocompatibility of the composite electrode. On comparing the microbial community from the domestic wastewater adhering to the flexible PANI/PLA electrode with that on the flat graphite felt electrode, it is evident that there is limited colonization of bacteria on the surface of graphite fibers whereas, a host of mixed consortia of bacteria is observed on the PANI/PLA electrode. One can clearly observe that PANI/PLA outperforms graphite felt with its high conductivity, biocompatibility and 3D garland-like morphology allowing increased bacterial adherence resulting in enhanced biofilm-electrode interaction and better electron transfer between bacteria and electrode.

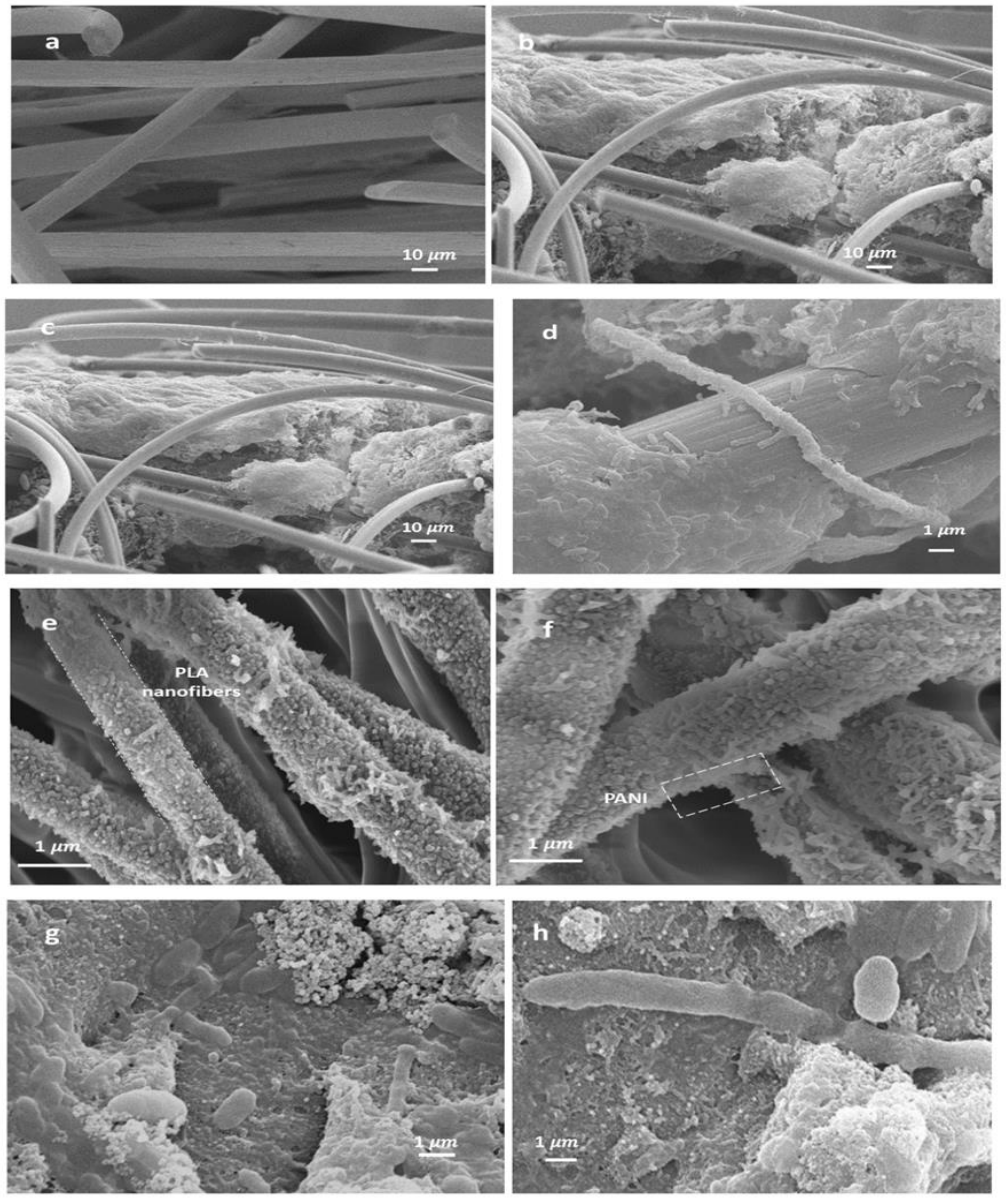

Figure 5.2. FESEM image of (a) control electrode devoid of biofilm, (b) microbial biofilm layer on the graphite felt (c), (d) enlarged images of graphite felt with biofilm, (e) PANI/PLA flexible electrode, without biofilm **(f)** magnified image of the composite electrode with PANI nanowhiskers on the PLA fibers, **(g)** growth of mixed consortia on the flexible anode**(h)** high-resolution image of mixed culture of bacteria on the surface of the flexible electrode.

5.2.3 Contact Angle Analysis and Electrochemical Analysis

An ideal anode material provides bacterial attachment onto its surface and also facilitates the process of electron transfer(Ismail et al., 2019; Sayed et al., 2020). Wettability is an essential property for cell attachment. Bacterial attachment is favored by the existence of functional groups such as carboxylic acid, alcohol, quinines, etc. Therefore, graphite felt electrodes were first pre-treated to make the surface hydrophilic thereby, conducive for bacterial attachment. However, its high thickness (6.9 mm) hinders the diffusion of the substrate to the inside of the felt minimizing the formation of microbial growth on the inside of the felt anode. Another study reported that commercial graphite felt electrodes possess minute pore size which hinders the accessibility of microbes to the innermost region of such flat electrodes(Yuan et al., 2013).This limitation of surface area for bacterial attachment often hinders its power generation. In contrast, the presence of nanofibers results from the insufficient surface area for the attachment of bacteria which is corroborated by the FESEM images. A study revealed that the wettability and cell attachment property of the electrode is essential for its potential application in Bioelectrochemical Systems. Contact Angle analysis revealed the wettability of the PANI/PLA electrode. A strong hydrophilic nature, indicated by the rapid uptake of water is displayed by the composite PANI/PLA (CA 65.3 ± 0.82^0) compared to neat PLA (CA 129.22 ± 0.56^0) which is hydrophobic as seen from the image (**Fig 5.3(a)**). The nanofibers provided a large surface area which resulted in rapid uptake of water. The presence of PANI (positively charged) enhanced the interaction with the cell wall of the microbial consortia (negatively charged) to colonize. As seen from the SEM images, the microbes

are in direct contact with the PANI nanofibers that in turn facilitated the electron transfer process from bacteria to anode surface.

To measure the internal resistance of the MFCs, Electrochemical Impedance Spectroscopy data were interpreted using Nyquist plot as shown in (**Fig 5.3(b)**)**.** The internal resistance in the MFC is interpreted in terms of the symbols in the Randles equivalent circuit (**Fig 5.3(c)**) are R_s for ohmic resistance, R_{ct} for charge transfer resistance, C_{dl} for double-layer capacitance, and W for Warburg impedance. From the Nyquist plot, it is observed that the utilization of the composite anode resulted in lowering the ohmic resistance to 74.82±0.02 Ω compared to the graphite felt anode which exhibited higher resistance value of 231.8±0.01 Ω.The higher degree of reduction in Rs value for the composite anode comes from the ease of charge transport with stable current generation through enhanced cell adherence of the microbial consortia on to the large surface of the biocompatible nanofiber electrode enabling better biofilm growth and resulting in higher power density compared to graphite felt. Further, the composite anode had the lowest Rct value of 4.45±0.17 Ω compared to graphite felt (58±0.12 Ω) which on one hand, indicates the lack of effective electron transfer within the graphite felt anode biofilm while on the other hand, explains the better performance for the composite anode as demonstrated in later section in the polarization test and CV test. The presence of amino groups explains the enhanced electron transfer. In addition, the lower R_{ct} is an indication of a faster rate of electron transfer due to adequate biofilm coverage displayed by the nanofiber composite material(Yellappa et al., 2021). This is in good agreement with the result obtained for NiO@PANi-CF(Zhong et al., 2018).Composite electrode developed by in-situ polymerization also showed super hydrophilicity and low charge transfer resistance.

Thus, the composite anode showed lower internal resistance effect compared to the graphite felt which indicates better electron transfer and consequently higher power performance in the MFCs.

The cyclic voltammetry (CV) response of the fabricated nanocomposite PANI/PLA anode and graphite felt are displayed in **Fig 5.3(d)**. For the same scan rate of 10 mV/s with Ag/AgCl as a reference electrode, the PANI/PLA electrode exhibited a couple of well-defined $[Fe(CN)_6]^{4-/3-}$ peaks at 460 mV and -460 mV while the graphite felt electrode donot exhibit such redox peaks. Further, non-quasi rectangular and symmetric shape CV profile is displayed by PANI/PLA electrode which suggests that the nanocomposite material has pseudocapacitive behavior. The specific capacitance of PANI/PLA electrode is found to be 381.38 F/g as calculated using the procedure reported(Yellappa et al., 2021).The presence of the characteristic redox peaks also indicates better interactions between the bacterial biofilm and PANI/PLA nanofiber network as well as enhanced EET efficiency due to the inherent conductivity of PANI. This also confirms the successful polymerization of PANI on PLA. The redox peaks in case of PANI/PLA electrode were much higher compared to the graphite felt electrode as observed in **Fig 5.3(e)**. This indicates that the fabricated electrode had higher faradaic charge capacity which is in turn proportional to the electrode surface area. For the same projected surface area of the electrodes, the surface area of PANI/PLA electrode is larger than the flat graphite felt electrode due to the flexible nanofiber structure. As a result, larger electrochemical active surface is available in case of the nanofibers resulting in the superior electron transfer rate between PANI/PLA nanofibers and microbial consortia which is observed from its lower charge transfer resistance.

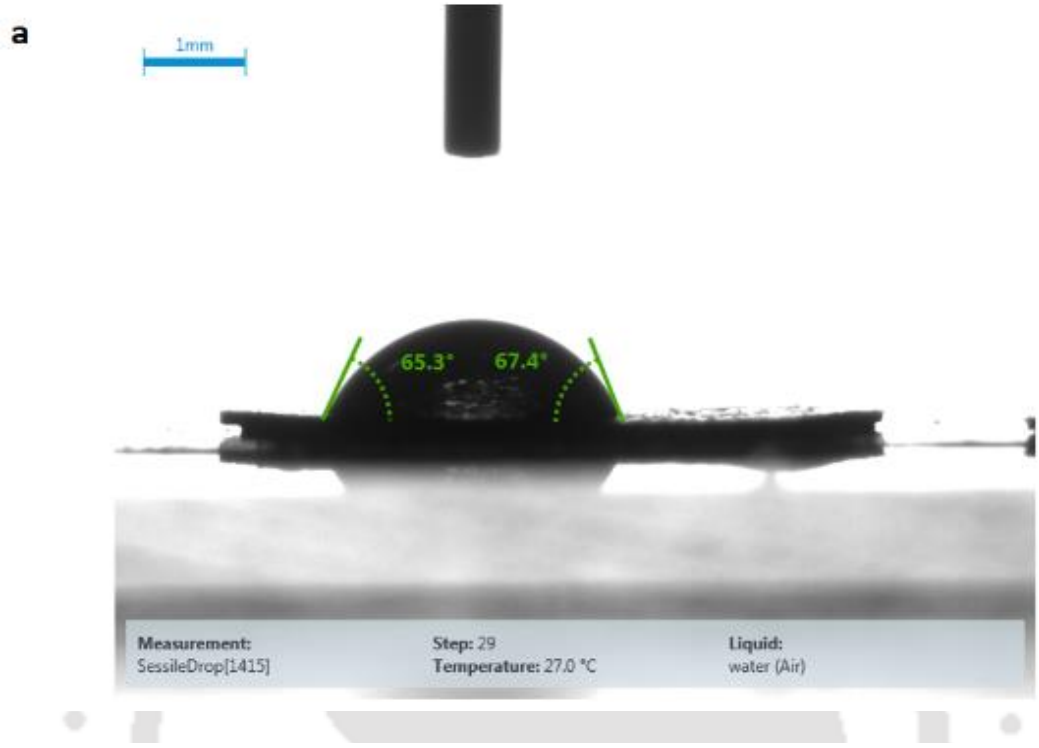

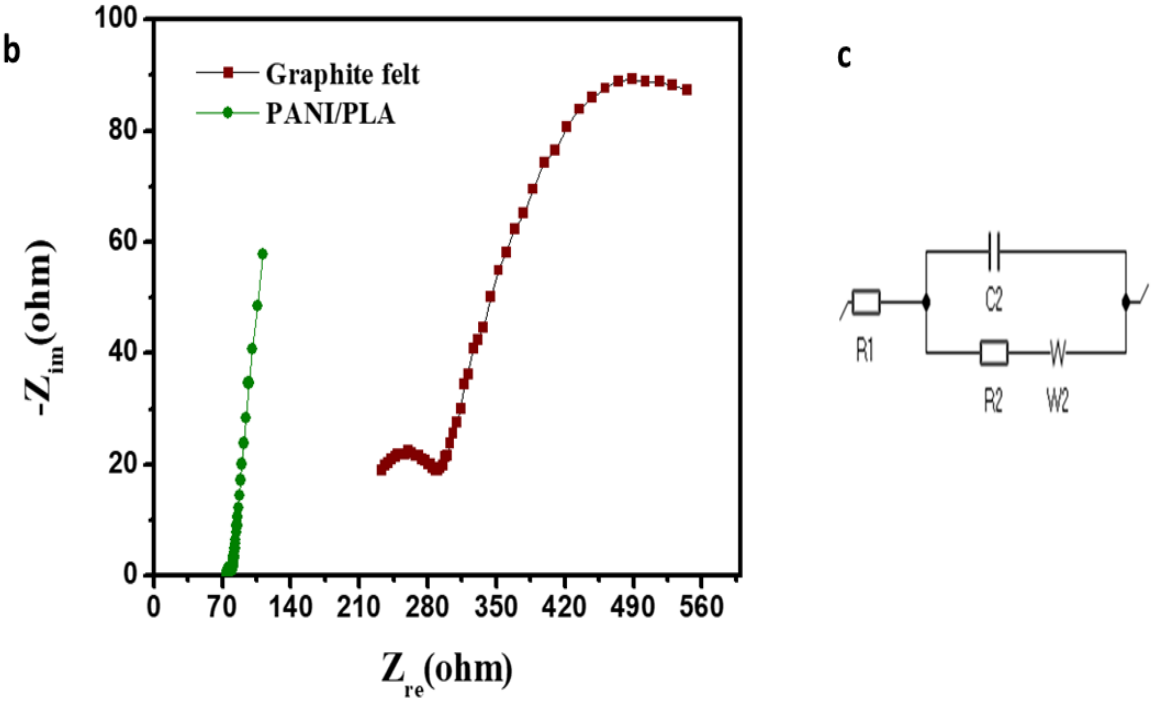

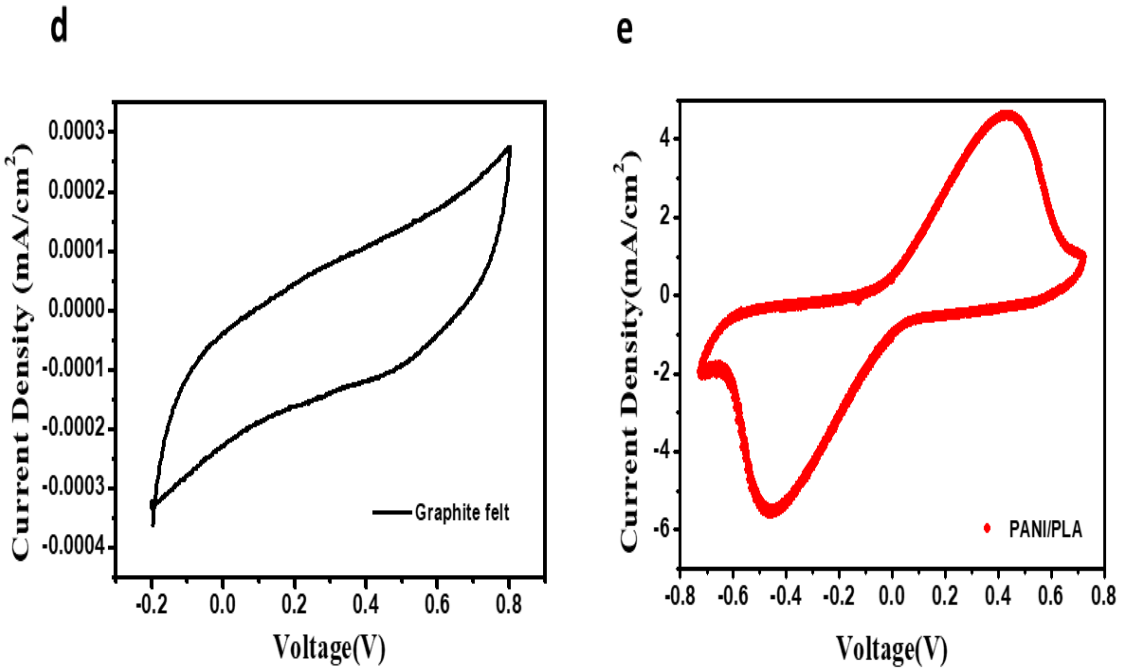

Figure 5.3. (a) Contact Angle Image of the PANi/PLA nanofiber, **(b)** Nyquist Plot for PANi/PLA and Graphite Felt **(c)** Equivalent Circuit for the MFCs, Bioelectrochemical behavior of **(d)**Graphite felt **(e)** PANI/PLA flexible electrode.

5.2.4 Acclimation Study of the domestic wastewater-fed MFCs

The dual-chamber MFCs were inoculated with domestic wastewater from the Loudong Wastewater Treatment Plant. The wastewater was collected once a week. Pre-acclimation step is carried out to ensure stable power supply. The voltage output for the two MFCs during the acclimation stage obtained is summarized in (**Fig 5.4)**. On assembling the systems, with an external resistance of 1000Ω, the voltage gradually increased for the PANI/PLA-based MFCs compared to the control system during the first 24 h to decline slightly in the next 24 h. The voltage increased from zero value, reached a peak value, and then dropped back to zero completing a cycle indicating biofilm growth on the surface of

the anode also known as the start-up period(YOU et al., 2006).This voltage variation during start-up indicated that the acclimatized microorganisms in the domestic wastewater-fed MFCs grew and proliferated(Logan BE., 2008).This is validated by the SEM images of the PANI/PLA electrode which suggest that the microbes have colonized the surface of the electrode which have been discussed later. The MFCs were replenished with wastewater when the voltage declined below 0.05 V. For the next two consecutive cycles of refilling domestic wastewater, the voltage remained stable at 0.25 V. Stable voltage generation for the graphite felt-based MFC was observed to take a longer time in comparison to the composite electrode-based MFCs. Thereafter, the voltage increased rapidly to remain stable at 0.59 V. It is to be noted that the pattern of voltage output was observed to be consistent without any precaution to hold anaerobic condition inside the anode chamber during refilling. This process was continued until the steady voltage of 0.59 V was obtained for another three consecutive cycles which indicated the successful completion of the acclimation step ensuring the stability of the biofilm(Adeniran et al., 2016).

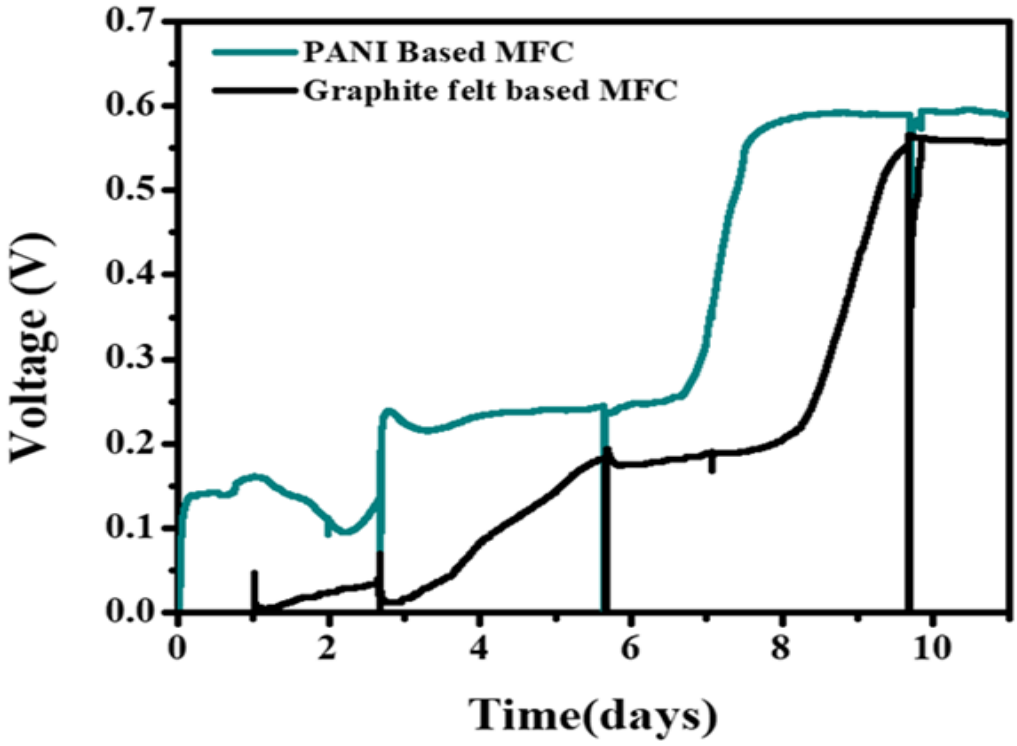

Figure 5.4. Voltage generated by the MFCs equipped with the different anodes during acclimation.

5.2.5 Enhanced Power Generation and COD Removal for the anode materials

The polarization curves, characterized by voltage vs current density is obtained by the potentiodynamic method for the PANI/PLA and graphite felt based MFCs are presented in (**Fig 5.5 (a) and 5.5(b))** and **Table 5.1** summarizes the performance of the PANI/PLA based MFCs in comparison to the graphite felt based MFCs**.** The highest value of OCV was obtained for the PANI/PLA-based MFCs (0.75 V vs 0.68 V of Graphite felt) which is higher compared to PANI deposited on commercial carbon felt reported in a previous study (R et al., 2013).The bio-based anode outperformed other inorganic acids doped PANI anode in terms of power output. Interestingly, the power output is higher than that obtained

using tartaric acid, an organic acid used as a dopant in PANI modified anode(Yaqoob, Mohamad Ibrahim, Umar, et al., 2020).

The typical polarization curve is split into three zones which signifies 3 losses namely, activation, ohmic, and concentration loss. The voltage output of PANI/PLA-based MFCs is higher than that of Graphite Felt-based MFCs exhibiting low activation potential at low current density. This relative superior performance can be attributed to the biocompatibility of the electrode making it conducive for microbial growth for stable biofilm, leading to improved power output(Sayed et al., 2020).Thus the biofilm developed on the anode is a major contributor to the power output.

As the current density increased, a significant difference in the polarization curve for the PANI/PLA-based MFCs and Graphite felt-based MFCs is observed. The dominant factor being ohmic loss and charge transfer loss in the case of the graphite felt-based MFCs which is confirmed from the EIS analysis. Interestingly, a sharp decrement in voltage is observed for the graphite felt at around 273 mA/m^2 in the polarization curve. As a consequence, after reaching the maximum power density of 113 mW/m^2 power overshoot is witnessed in the power density curve. Power overshoot, a phenomenon witnessed in the power density curve is characterized by its reverting back towards lower current density, after reaching the peak power. It has been observed that another reason for power overshoot to occur is the lack of ability of biofilm to generate high current density, or its inability to respond to elevated anode potentials. This leads to an increase in the internal resistance of the MFCs at higher current density. Thus, bacterial biofilm has been listed as one of the important factors for the occurrence of power overshoot. Although few investigations carried out on power overshoot trace its origin to the anode biofilm community, its maturity, and substrate

utilization yet the phenomena remain still unclear. **Table 5.2**, list the relative articles for comparison based on the type of MFCs, a substrate for bacteria, source of inoculum, power density, and percentage of COD removal. It depicts that the present study exhibited a higher power density of 921± 0.30 mW/m^2 among these diverse investigations. This higher value achieved can be attributed to the composite biobased flexible electrode with the mixed bacterial consortia forming a stable biofilm on the anode as opposed to pure cultures in various studies. A correlation can be drawn between the voltage generated and removal of COD for the acclimation period of 30 days as shown in (**Fig 5.6)**. It is evident that the COD consumption in the MFCs operated under external resistance occurred immediately without substantial enhancement in the voltage output in the first 60 h. This suggests firstly, that a sizeable portion of the substrate oxidized at the anode harboring the electrogens is utilized in the growth of the electro-active microorganisms with little being used for the generation of voltage. Secondly, because of the biocompatible property of the composite anode, the microbial consortia adhere to the surface quickly thereby accelerating the COD removal rate of wastewater. Following the growth period, COD removal as well as the energy generation increases in a sustained manner, as a combined effect of different mechanisms adopted by different anodic microbial consortia accelerating the substrate utilization hence the wastewater treatment. The presence of high external resistance can be another reason as it alters the metabolic activities of the bacterial community to drive the process of substrate utilization(Yuan et al., 2013).Thus in comparison, the two MFCs showed good variations in terms of COD removal efficiency. PANI/PLA-based MFCs demonstrated the highest COD Removal efficiency with 91.7±0.58 % as compared to Graphite felt-based MFCs with 90 ±0.65 %. This indicates that the microbial biofilm on

the composite electrode-based MFC effectively metabolized the organic compounds present in the domestic wastewater thereby, successfully treating the wastewater along with generating electricity.

Table 5.1: Parameters of domestic wastewater-fed MFCs using the bio-based anode and graphite felt anode.

Anode	**OCV(V)**	**Maximum Power Density (mW/m^2)**	**R_{ohm}**	**R_{ct} (Ω)**
PANI/PLA	0.749±0.49	921.30±0.02	74.82±0.02	4.45±0.17
Graphite felt	0.679±0.30	113.78±0.29	231.8±0.01	58±0.12

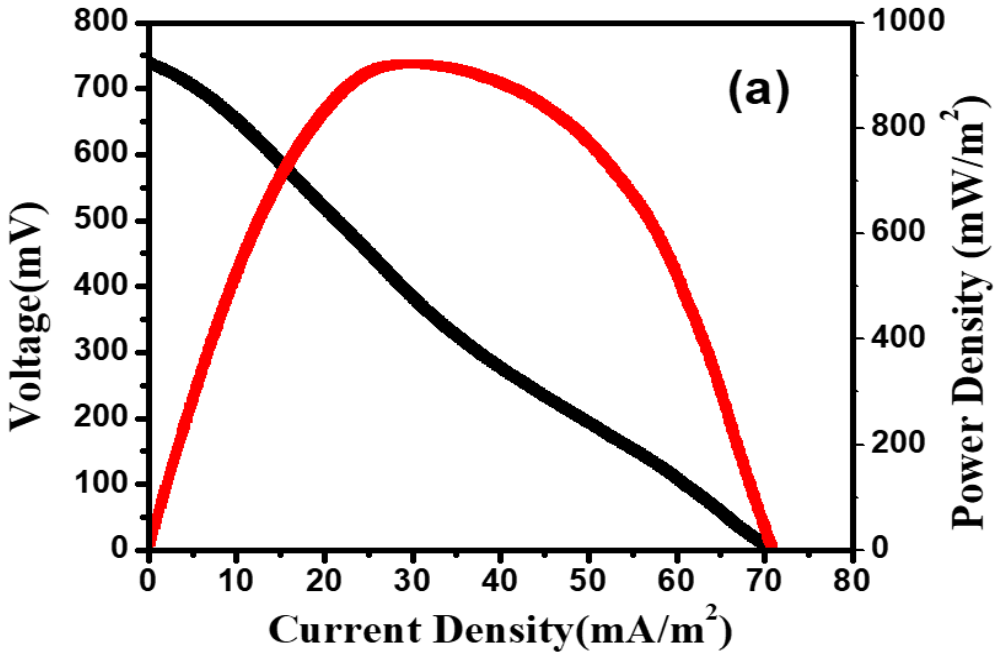

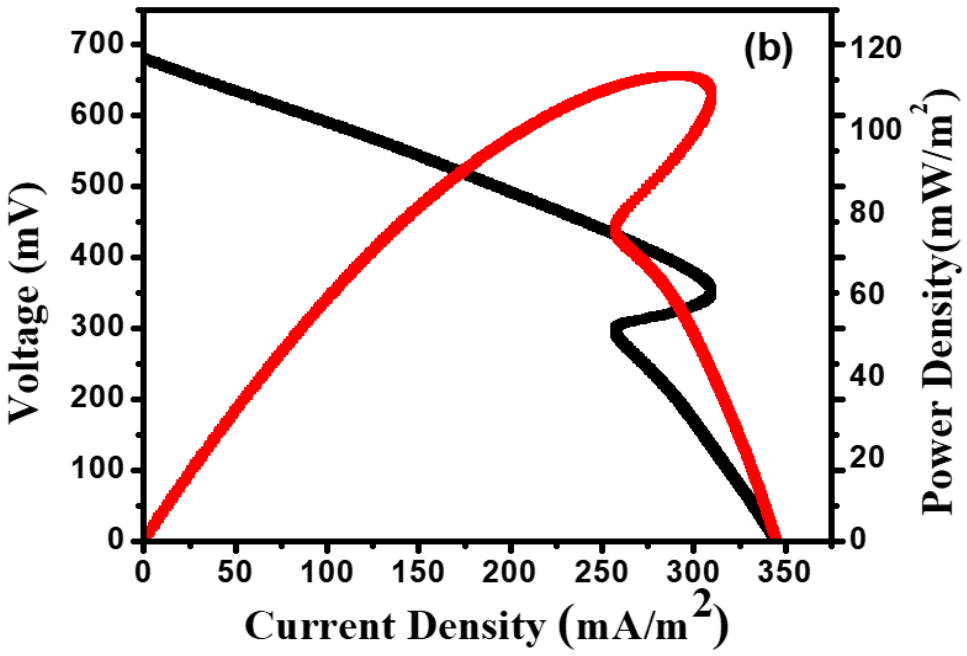

Figure 5.5. The voltage output from MFCs equipped with a) Fabricated anode and b) Control.

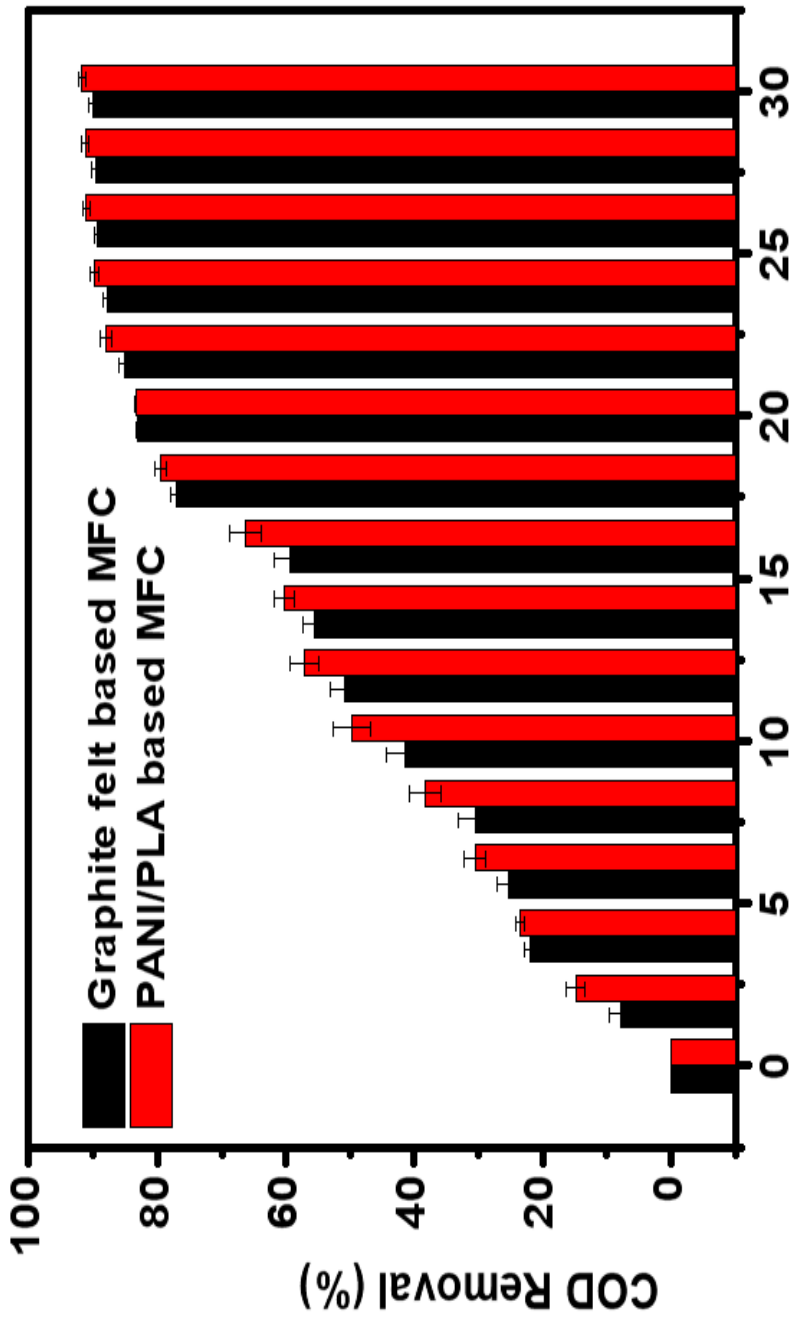

Figure 5.6: *COD Removal from domestic wastewater using MFCs.*

Table 5.2: Comparison of performance of PANI modified anodes in MFCs.

Reactor	Anode Material	Substrate	Preparation	Source of Inoculation	Power density (mW/m^2)	COD Removal Efficiency (%)	Ref.
Dual-chamber	SSM-PANI/CNT	Glucose	In situ oxidative chemical polymerization method	Anaerobic suspended growth reactor	48	80	[24]
Plate MFC	NiO@PANi	Biodegrade dye wastewate	In-situ polymerization	Proteobacteria i	1078.80	64.24	[32]
Dual-chamber	PANi nanoflower modified carbon cloth	Sodium Lactate	In-situ polymerization	S.oneidensis MR-1	388.60		[36]
Single-chamber	Conductive PLA filament	Acetate	3D Printing	Sewage Sludge	0.05		[17]
Dual-chamber	C-PANI	Glucose	Layer by layer technique deposition	S. cerevisiae	460		[29]
Dual-chamber	PPy/CNT/MnO_2	Sewage water	Electropolymerization	Mixed sewage culture	1125.40		[11]
H-shaped dual chamber	CP/GNRs/PANi	Culture medium	Electro-depositing	S. oneidensis,	856		[37]
H-shaped Dual chamber	CP/PANi	Culture medium	Electro-depositing	S. oneidensis,	312		[37]
Dual-chamber	Graphite felt	Synthetic wastewater (SWW)	In situ polymerization	Desmodesmus sp	64.20		[38]
Dual-chamber	NPANi/GC	Glucose	Electrochemical polymerisation	E. coli	820		[34]
Single-chamber	PANi modified Loofah sponge	PBS+Acetate	In situ polymerization +carbonization	Effluent of MFC	1090		[30]
Dual-chamber	Tartaric acid doped PANi/CC	Mineral medium	In situ polymerization	S. oneidensis	490		[39]
Dual-chamber	PANi decorated PLA	Acetate	In-situ polymerization +Electrospinning	Domestic Wastewater	921	91.7±0.58	This study

5.3 Conclusion

PANI/PLA composite nanofiber electrode was successfully prepared through electrospinning employing a novel single-step polymerization technique. Surface Analysis revealed a synergistic effect between the two polymers with successful loading of PANI onto PLA forming an interconnected nanofiber structure with garland-like morphology. The surface morphology study revealed that the flexible PANI/PLA electrode is a better host than graphite felt for housing the microbial consortia and also improving the electron transfer rate for harvesting electricity using the microbial consortia in the domestic wastewater. The flexible nanofiber electrode demonstrated better thermal stability and less hydrophobicity compared to its pristine form. Compared to the conventional graphite felt electrode, the biopolymer-based nanocomposite electrode displayed an 8-fold increase in the power density. Also, the pseudocapacitive nature of the anode can be explored in the future for the MFC to function as a bio capacitor. Thus, this new recipe of developing electrodes via bioaugmentation would broaden the scope of introducing versatile designs of the polymer composite for an array of applications from wearable energy storage devices to biosensors.

Chapter-6

Experimental study on the effect of crosslinking in PVA separator for hospital wastewater fed microbial fuel cells.

Motivation

Wastewater management is one of the many challenges in modern-day society due to the escalating energy demands on one hand and energy intensive treatment procedures on the other. Therefore, every possible cost and energy cutting measure for wastewater treatment needs be explored. Microbial fuel cell shows great potential as a tool for addressing the issue of wastewater treatment. Treatment of high strength wastewater utilizing low-cost PVA membranes as alternative to the costly commercial membrane definitely aids as a feasibility test for the scale-up of MFC technology.

Abstract

Crosslinked polyvinyl alcohol membranes have experimentally demonstrated a great potential for simultaneous achieving wastewater treatment and power generation over conventional Nafion membranes, making them promising candidates for fuel cell applications. However, there is no comprehensive report to understand how the membrane will perform for high strength wastewater. In this work, we employ PVA membranes crosslinked with 5% glutaraldehyde to harvest power from hospital wastewater fed mediatorless, dual chamber MFC and compare its performance with Nafion and PVA in its pristine form. The results demonstrate that crosslinked membrane played a crucial role for efficient power generation and wastewater treatment. The highest power density of 220 mW/m^2 was achieved for the crosslinked membrane at 0.3 g COD/L-d organic loading rate, achieving 65 % COD removal. The current work therefore, serves as a feasibility study for the scale-up of PVA based MFC. The experimental findings demonstrate the potential for its expansion to other industries generating wastewater with high organic content.

6.1. Introduction

In the wake of pandemic situation, hospitals have an important role in the health of humans. Their activities require large amounts of water and generate large amounts of wastewater. In general, the characteristics of wastewater from hospitals (WWH) are similar to those of domestic wastewater, but a part of WWH including drugs, organic substances, toxic metals, radioactive tracer. They also carry microorganisms such as viruses, bacteria, fungi, protozoa and helminths. Wastewaters are a source of large amount of potential energy in the form of pollutants (Logan & Rabaey, 2012). In the current scenario, the most promising application of MFC is the energy-efficient treatment of WWH with simultaneously generating power(Kumari et al., 2020).Conventional wastewater treatment is an energy intensive process, with aeration accounting for 50% of the operating cost for removal of organic compounds(Rabaey & Verstraete, 2005). Besides, anaerobic treatment of wastewater although produces biogas but the energy recovery is discouraging(Rozendal et al., 2008). With ever-increasing energy demands, the need for low-energy wastewater treatment has never been greater (McCarty et al., 2011; S. T. Oh et al., 2010).

Major challenges in the realization of MFC for practical application are in terms of material costs and energy recovery efficiency. The commonly used Nafion membrane accounts for 38% of the total capital cost. Hence, to make the process of using membranes practical three aspects need to be considered namely, (a) the cost of membrane, (b) its internal resistance, (c) biofouling during operation. Several studies have explored the use of alternative membranes in MFCs, such as cation or anion exchangers, fiberglass, osmotic or kinetic membranes; In addition, earthenware, salt bridges and other materials or equipment

have been used to improve the performance of MFCs in some way and reduce their costs (Min et al., 2005).

PVA being a non-toxic, biodegradable and an inexpensive polymer, inherently hydrophilic makes it favorable for wastewater treatment (Das et al., 2021). Previous published studies have dwelt mostly on acetate or synthetic based wastewater with few considering the case of real high strength wastewater to fuel MFC. The effectiveness of treating refinery wastewater was tested using air-cathode MFC by Zhang et al., 2014. They demonstrated the poor biodegradability of the refinery wastewater with lower power generation (255±2 mW/m^2) compared to domestic wastewater (280±6 mW/m^2) (F. Zhang et al., 2009). Following our previous report on crosslinked PVA membrane with GA as separator in domestic wastewater fed MFCs which exhibited high power density and COD removal with antibacterial property, thermo-mechanical stability and negligible fuel crossover. In this study, GA-linked biodegradable PVA was used as a low-cost dynamic honeycomb MFC separator fed hospital wastewater that was evaluated for practical application. The microbiota in wastewater acts as a biological catalyst while wastewater is used as a substrate. The motivation of the present study is therefore, to evaluate the power generation in GA-crosslinked biodegradable PVA membrane in MFC using real-field hospital wastewater as anolyte against its pristine form and the commercial Nafion 117. The microbiota in wastewater acts as a biological catalyst while wastewater is used as a substrate. A detailed analysis on the performance of the membranes in terms of power performance of the MFCs were studied in terms of biofilm growth, polarization studies, cyclic voltammetry and internal resistance.

6.2. Results and Discussion

6.2.1 Acclimation Study for the MFCs

All the three MFC Set-up were operated under similar conditions. The temperature was maintained at 27^0C to establish a favorable environment for the mixed culture bacteria to grow. **Fig.6.1** shows the development of voltage in the MFCs for 20 days with acclimated electrodes under external resistance of 1000Ω. The drops in voltage observed at the end of each batch cycle represent times when substrate was replaced with fresh media. In the case of 5PVA-MFC and NPVA-MFC, the voltage generation began to noticeably increase from day 1 of the anode enrichment, reaching $630 \pm 0.12\ mV$ and $330 \pm 0.2\ mV$ on day 7 of the first fed-batch operation. While the 5PVA-MFC demonstrated stable voltage generation of 630 mV till day 18 after which it was replenished, the voltage continued increasing to $600 \pm 0.14 mV$ for the NPVA-MFC. On the other hand, the control system, Nafion117-MFC, showed gradual increase in the open circuit voltage from zero voltage and the maximum voltage obtained after acclimation period of 25 days was $590 \pm 0.18 mV$.

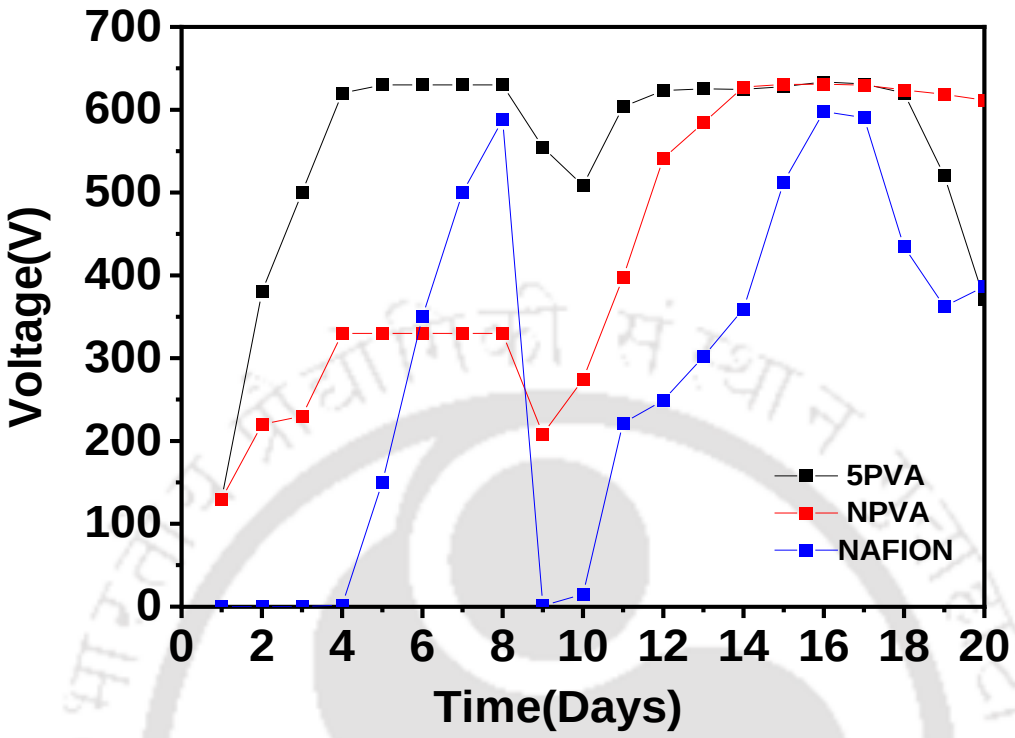

Figure.6.1. Voltage generated by the MFCs from dialysis hospital wastewater equipped with commercial Nafion membrane and synthesized 5PVA and NPVA membranes during acclimation period under load condition.

6.2.2 Bioelectricity harvest from hospital wastewater using MFCs

The polarization curves for the 5PVA-MFC, NPVA- MFC and Nafion-MFC were obtained in open circuit mode after acclimation for 25 days, as shown in **Fig.6.2 (a), (b) and (c).** Under no load condition, the average voltage of $745 \pm 0.3mV, 650. \pm 0.2mV$ and $550. \pm 0.41mV$ was recorded for 5PVA-MFC, Nafion-MFC and NPVA-MFC respectively. The 5PVA-MFC showed better OCV over its pristine counterpart and Nafion (as reported in Table.), which is also higher compared to what have been achieved by using acid catalyzed PVA-GA membrane (Rudra et al., 2015). The higher

OCV for the 5PVA-MFCs clearly reflects the effectiveness of the designed membrane to selectively allow the passage of protons and suppressing unfavorable crossover across the membrane (Das et al., 2021). The maximum current density of 1800 mA/m^2 was observed for the 5PVA membrane with the maximum power of 320 mW/m^2.While the power density was 220 mW/m^2 for the Nafion membrane with a maximum current density of 2600 mA/m^2. Notably, it was possible to achieve larger power density in the case of hospital wastewater fed MFCs compared to domestic wastewater and those reported for complex substrates, as shown in **Table.6.1**. Thus, the 5PVA-MFC fed with hospital wastewater was capable of simultaneously generating electricity along with organic matter removal.

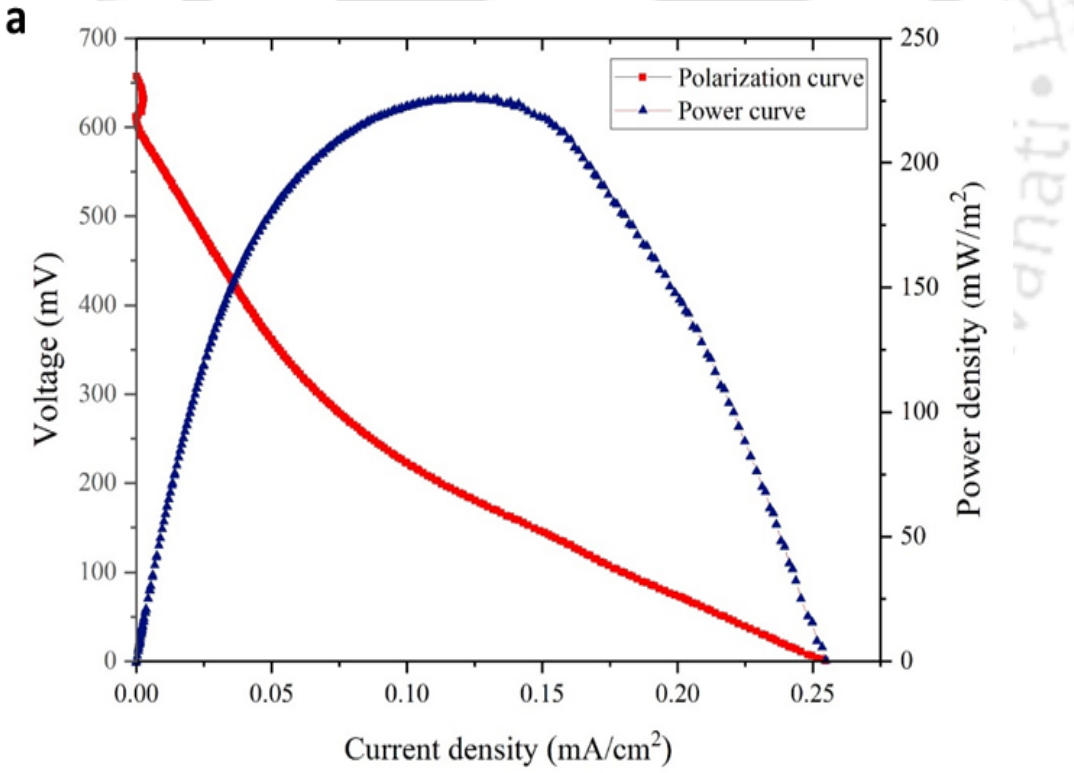

b

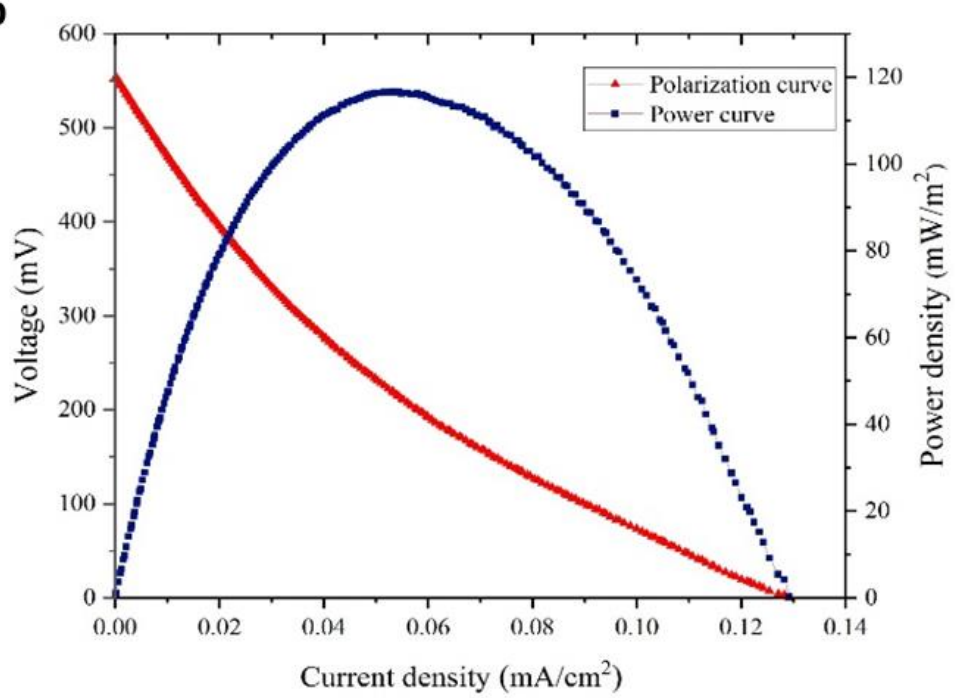

c

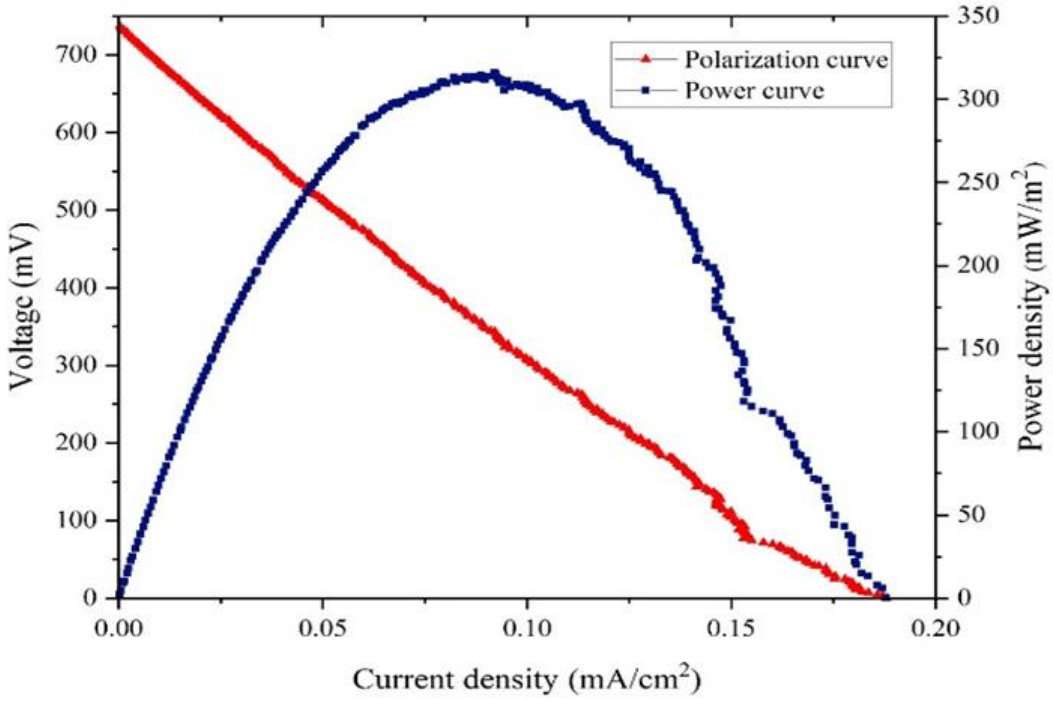

d

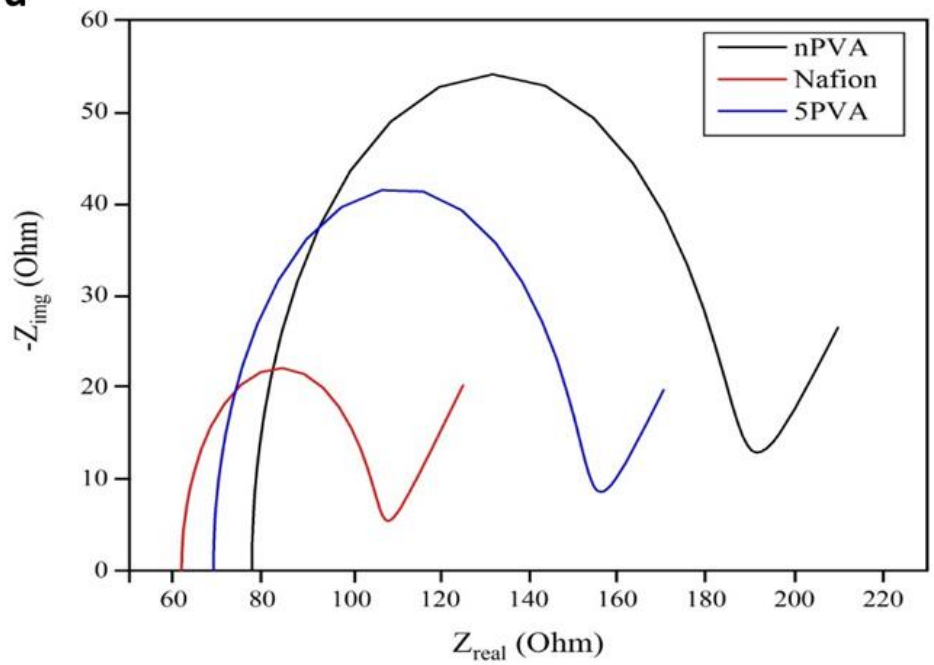

e

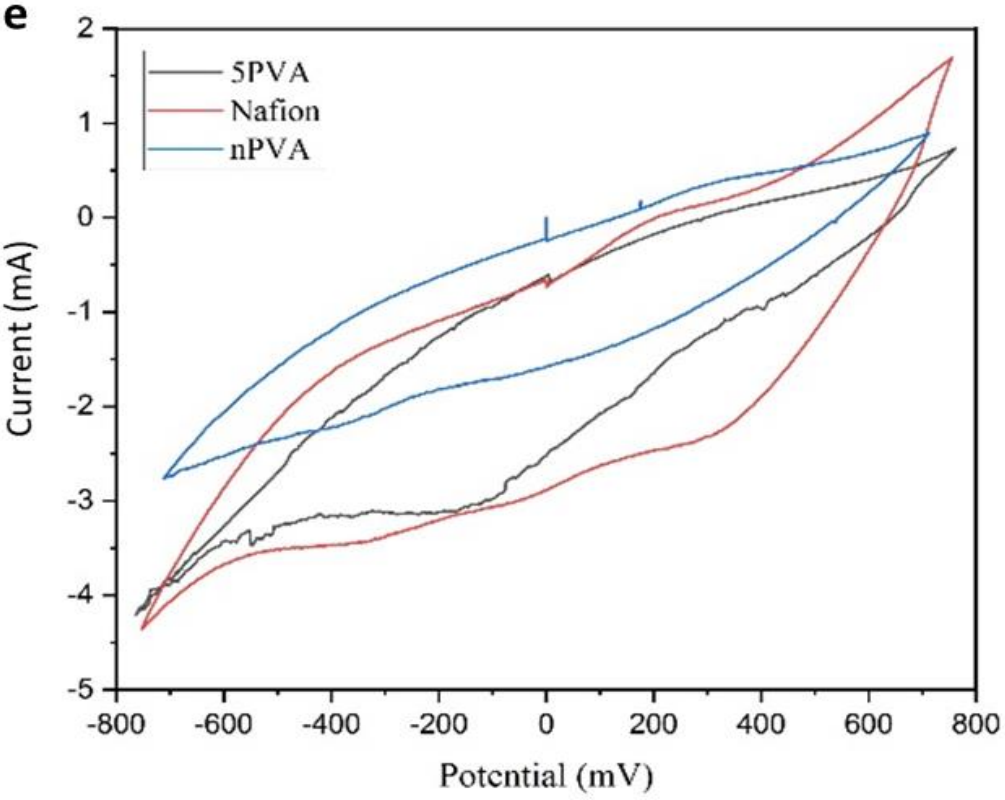

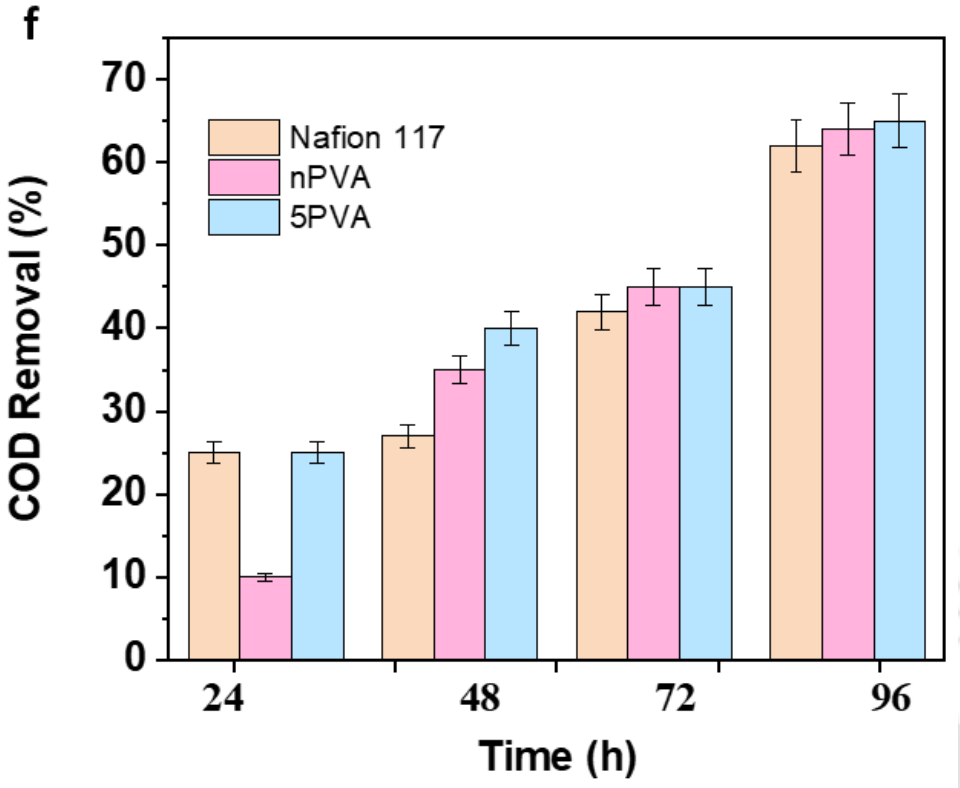

Figure 6.2. Polarization curves of MFCs equipped with commercial membrane and synthesized membrane demonstrating open circuit voltage and Power density generated by MFCs from dialysis hospital wastewater w.r.t the current density, **(a)** Nafion-MFC, **(b)** NPVA-MFC **(c)** 5PVA-MFC**, (d)** Nyquist Impedance Plot of Nafion -MFCs,5PVA- MFCs and NPVA-MFC, **(e)** Cyclic voltammogram of hospital wastewater-inoculum-based mixed culture microbial biofilm electrode. **(f)** COD removal in 30-day operation for the PVA-GA and Nafion based MFCs fed with domestic wastewater.

Table 6.1: Power density reported in literature versus those obtained in the present study.

Substrate	Power Density (mW/m^2)	Reference
Domestic wastewater	28	(H. Liu et al., 2004)
Domestic Wastewater-PEM	28	(Tender et al., 2002)
Domestic Wastewater-No PEM	146	(H. Liu & Logan, 2004)
Domestic Wastewater	158.28 ± 0.28	(Das et al., 2021)
Domestic Wastewater-PEM	181.60 ± 0.03	(Das et al., 2021)
Hospital Wastewater	320 ± 0.02	**This study**

6.2.3 Internal resistance of the MFC with crosslinked membrane

A critical component of these MFCs under study influencing their power output are the proton exchange membranes. Their function is to act as separator layer between the anode and cathode and to facilitate transport of proton across the membrane to the cathode chamber. The resistance to the transport of ions is obtained from the EIS results. The internal resistance of the MFCs equipped with the membranes is represented as sum of the components namely, ohmic resistance(R_1), charge transfer resistance (R_2), double layer capacitance(C_2), and Warburg impedance(W_2). The ohmic resistance is obtained from the difference between origin to the initial start of the semicircle of the Nyquist plot. While charge transfer resistance is obtained from the diameter of the semicircle in the low frequency side of the Nyquist plot. Diffusion resistance is represented by the linear portion in low frequency side. As observed from **Fig 6.2d,** Nafion exhibited lowest ohmic

resistance of 61.78 Ω. The crosslinked membrane demonstrated lower ohmic resistance of 68.97 Ω than its neat counterpart (77.65 Ω). Nafion exhibited the lowest ohmic resistance due to the presence of sulphonic acid groups in its polymer chain. While the charge transfer resistance was also found to follow the order Nafion>5PVA>NPVA. The low internal resistance exhibited by 5PVA can be attributed to crosslinking with GA which resulted in low value of ohmic as well as charge transfer indicating better charge transport through the crosslinked membrane due to optimum water content facilitating proton transfer through vehicular mechanism. On the contrary, the neat PVA being an insulating material with no polar groups hence, its ohmic as well as charge transfer resistance was found to be higher than 5PVA.

6.2.4 Bioelectrochemical behavior of the hospital wastewater fed MFCs

The voltammetric behavior of mixed culture biofilms developed from real wastewater or anaerobic sludge are reported to vary depending on various factors such as the nature of feedstock or substrate, inoculum used for biofilm growth which influences its electron transfer property(Katuri & Scott, 2010) . Besides, in the case of mediator-less MFCs fed with wastewater, extracellular electron transfer is reported to be caused either with the aid of membrane-bound proteins, mediators, or via electron shuttles, which are generated by the bacteria consortia (H. Liu et al., 2005). Cyclic voltammetry analysis carried out for the anode enriched with biofilm at the end of the batch electricity generation cycle for the hospital wastewater fed MFCs (**Fig 6.2e)** shows no detectable redox couple response. This reveals that the mechanism of electron transfer for harvesting power is more likely via direct electron transfer rather than self-induced mediators produced by the mixed culture

biofilm (Katuri & Scott, 2010). Bioelectrochemistry of wastewater produced biofilms are reported to be complex in nature and further study is in progress in this direction.

6.2.5 COD removal from hospital wastewater using the fabricated membranes

Comparing 5PVA-MFC's capacity to treat hospital wastewaters with results from nPVA and standard Nafion-MFC, revealed that COD removal efficiencies from 5PVA based MFC were higher compared to that from nPVA and Nafion 117 based MFC. In a study carried out by Opoku et al,(Opoku et al., 2022) using Nafion membrane based MFC, COD removal efficiencies of 29% was reported for hospital wastewater as compared to 47.2% for slaughterhouse wastewater and 45.6% for sewage wastewater. The maximum COD removal efficiency from synthetic wastewater was reported to be 62.7% using the commercial membrane.While highest removal efficiencies of 71.4% is observed in our case for the Nafion alternative membranes thus, demonstrating the 5PVA-MFC's and nPVA -MFCs capacity to treat real wastewaters with the added benefit of electricity production.

Table 6.2. Comparison of power generation and wastewater treatment from real wastewaters in MFCs in literature with this study.

Wastewater	Inoculum Source	MFC Type	Membrane	Anodic Volume (mL)	COD Rem. (%)	Pd_{max} (mW/m^2)	Ref.
Piggery Wastewater	Anaerobic sludge	Two-chambered loop MFC	CMI-7000	1000	NA	1415.6	(Ryu et al., 2013)
Human Feces Wastewater	Anaerobic sludge	Two-chambered MFC	Nafion 117	1000	71	70.8	(Fangzhou et al., 2011)
Dairy Wastewater	Anaerobic sludge	Two-chambered MFC	Nafion 117	2000	90.46	621.13	(Mansoorian et al., 2013)
Dairy, Potato & Paper Wastewater	Raw dairy, potato & paper wastewater	Multiple anode chamber MFC	Nafion 117	1000 × 3	89	356	(Mathuriya, 2016)
Slaughterhouse, Sewage & Hospital Wastewater	Anaerobic sludge	Multiple anode/share cathode MFC	Nafion 117	1500	48.8	2599	(Opoku et al., 2022)
Domestic Wastewater	Domestic Wastewater	Two-chambered MFC	Cross linked PVA	250	91	158.28	Das et al.,2021)
Dialysis Hospital Wastewater	Raw hospital wastewater	Two-chambered MFC	crossl inked PVA	250	70.41	320	This study
Dialysis Hospital Wastewater	Raw hospital wastewater	Two-chambered MFC	PVA	250	61.23	118	This study
Dialysis Hospital Wastewater	Raw hospital wastewater	Two-chambered MFC	Nafion 117	250	64.86	220 mW/m^2	This study

6.3. Conclusion

This study aimed to investigate the performance of the low-cost PVA membranes nPVA and 5PVA utilized as separators compared with the standard Nafion117 membrane and the simultaneous treatment of real wastewater. This is the first study to quantify (bio-electrochemically) the treatment of hospital wastewaters in PVA based MFC unit. The results indicated that the 5PVA based MFC showed superior performance in terms of power generation over neat PVA as well as Nafion 117. Although the use of real wastewaters reduced the power density, COD removal efficiency, compared to synthetic wastewater, stable electricity was generated despite the complex wastewater compositions and high COD concentrations. The 5PVA-MFC achieved over % COD removal .The power density produced in the 5PVA-MFC is higher than most studies in literature, demonstrating the potential of the PVA membrane for the exploitation of different high strength wastewater as feedstock. As an initial investigation into the simultaneous treatment of real wastewaters, this study provides a first step for the integration of wastewater treatment and energy recovery in one MFC unit, especially for remote locations or situations where treatment of different wastewaters is necessary. Further, to operate the MFC in a continuous flow mode to explore its long-term efficiency, improvement in COD removal is required. Altogether, the findings successfully demonstrated the capacity of the crosslinked membrane based microbial fuel cell (5PVA-MFC) to produce electricity from real wastewaters, with simultaneous wastewater treatment.

Chapter-7

Molecular Dynamics simulation study to investigate proton transport mechanism in PVA separator for application in MFCs

Motivation

Although the effect of crosslinking agents with PVA in MFC have been experimentally studied but at a more fundamental atomistic level, it has been rarely focused upon how their interaction behaviour would affect the performance in MFC environment. Understanding proton transport in the fabricated membranes can lead to new designs with better durability and conductivity. However, determining the molecular details of how the fabricated membranes operate is not easy with current experimental techniques. In this regard, Classical Molecular Dynamics computer simulations come as a boon as it can probe atomic length scales. Equilibrium MD (EMD) and Non-Equilibrium MD (NEMD) have been used to study transport through membranes. In EMD, no bias force is introduced, and transport properties are obtained from mean square displacements or from integrals of correlation functions based on the linear response theory. On the other hand, in NEMD, non-equilibrium conditions such as a pressure difference or concentration difference across the membrane can be introduced so that transport phenomena can be directly observed at the Ångström scale. EMD has been used to examine transport behaviors of water molecules through carbon nanotubes while NEMD has been used to demonstrate the potential use of a zeolitic metal-organic framework (MOF) for water desalination, gas permeation through membranes. Molecular dynamics (MD) simulations offer a powerful computational method to bridge the gap between the experimental observations and macroscopic theories for understanding the transport mechanisms.

Abstract

Polyvinylalcohol (PVA) membranes are a growing class of Nafion alternative low-cost polymeric material with potential for proton exchange in microbial fuel cell applications. The vital feature of the membranes being the presence of functional groups which in the presence of water facilitates the transport of proton across the membranes. At present, little is known about the organization of these membrane on the molecular level, reaction mechanism on crosslinking, transport of ion. The nature of transport mechanism as well as the factors influencing its behavior remains unclear. Despite numerous favourable experimental observations regarding the performance of the crosslinked PVA membrane in proton exchange in the field of microbial fuel cells application, very little is known about the actual transport mechanism or their structure on the molecular level. In the description of proton transport in PEM systems, a schematic representation is often invoked describing the proton hopping or channelling its way from one side of the membrane to the other; however, there is no direct evidence for such process in case of crosslinked PVA membranes. A lack of understanding of the actual processes in its atomistic level, presents a major challenge in the development of such materials for the purpose of PEM application. Proton transport involves mainly two key mechanisms, namely, Grotthuss or hopping mechanism and vehicular mechanism. The former is caused by the rearrangement of chemical bonds. A natural choice to study proton transport would be Ab initio calculations. Here, electrons are explicitly considered, but the length and time scales are too short to capture the relevant features of proton exchange membranes. On the contrary, classical molecular dynamics simulations have access to larger length and time scales making it the most suitable molecular dynamics simulations that can aid in portraying a detailed picture

of the transport phenomena in the PVA membrane. The objective of this study is to elucidate the structural organization of the PVA membrane in its pristine and crosslinked form and explore their properties with the aim to shed light on the nature of transport phenomena of the proton when these materials are used to facilitate proton exchange in MFC application. The radial distribution function, and movement trajectories of hydronium ions as indicated by the MD simulations were analyzed. The presence of multi-hydrated protons was observed from MD trajectories suggesting that the proton transfer in the PVA polymer system is via vehicular mechanisms.

7.1 Introduction

The proton exchange membrane (PEM) is a vital component of the MFC system that separates the anolyte from the catholyte and selectively transfers protons from the anode chamber to the cathode chamber (Peighambardoust et al., 2010) . The transport of proton when viewed at the molecular level, in case of a hydrated polymeric model takes place via proton hopping or Grotthus mechanism or vehicular mechanism (Tai et al., 2017). The study of large system sizes (>10 000 atoms) is critical in order to comprehend the internal water-phase structure in PEM materials which is possible using Classical Molecular Dynamics. Molecular simulations have been extensively applied to develop a better understanding of chemical structure of the polymeric membrane and molecular level interactions (Bahlakeh et al., 2012; Jansen et al., 2009) in the context of conventional PEM fuel cell(Sengupta & Lyulin, 2019).(Tai et al., 2017) Tai et al 2017 used molecular dynamics (MD) simulations to investigate proton transfer in Nafion 117 (Dupont) membrane. They concluded that protons could easily be coordinated with their neighboring water molecule forming multi-hydrated protons as observed from MD trajectories via Grotthuss and vehicle mechanisms. In another study carried out by (L. Chen et al., 2015) for Nafion 117 membrane found that thermal conductivity and diffusion of hydronium ion is affected by water content and temperature of PEM. In recent years, the interest in the research and development of new low-cost separators have been growing more rapidly than its costly counterpart, Nafion for MFC applications. PVA has demonstrated potential as separator layer in in domestic wastewater fed MFCs(Das et al., 2021) and direct methanol fuel cells(Gaur et al., 2017), The low-cost of fabrication is critical aspect for practical application of MFC which can lead to a dramatic reduction in the cost per kilowatt of power

in the device Although the effect of crosslinking agents with PVA in MFC have been experimentally studied but at a more fundamental atomistic level, it has been rarely focused upon how their interaction behavior would affect the performance in MFC environment. In a recent investigation, MD simulations were carried out to study the T_g and mechanical properties of PVA/TRIS functionalized graphene oxide composite. The authors claimed that application of the modifier, Tris-GO, not only improved the mechanical properties of polymer composites, but also provided valuable insights for improving the thermal stability of the composite (Dong et al., 2021). There have been no reports of MD simulation protocol suitable to model crosslinked PVA membrane with optimum water content and temperature similar to MFC applications. The current research work is a significant step towards addressing the knowledge gap on switching to biopolymeric PVA membrane for the performance enhancement of the MFC reactors for simultaneous power generation and real wastewater treatment. The motivation of the present study is therefore, to exploit the current computing capabilities of CHARMM force field to investigate the the proton transport mechanism in the indigenously developed PVA membrane via Classical MD simulation approach in the perspective to use this information for explaining and validating the performance of the membrane in the MFC device obtained experimentally.

7.2 Results and Discussion

The moisture sensitivity and high-water absorption rate of pristine PVA, reduces its mechanical stability and hence limits its applicability. Nevertheless, the abundance of hydroxyl groups pave route for chemical modification thereby allowing insertion of other functional groups or polymers in the PVA chain to broaden its horizon of application. Such modification was mainly achieved by crosslinking of the polymer with glutaraldehyde

which altered the undesirable properties with controlled water uptake, degree of swelling and enhanced thermal, chemical and mechanical stability. Equilibrium Molecular Dynamics is performed to derive the radial distribution function, pore size distribution, mean square displacement (MSD), movement trajectories which are analyzed to better understand the proton transport mechanism in the following section.

7.2.1 Calculation of density of the crosslinked membrane

In order to verify the accuracy of the CHARMM force field and simulation parameters, the density values of the PVA membrane were calculated. After optimization, the average densities of the neat PVA membrane in dry and hydrated state were found to be 1.06 g cm^{-3} and 1.068 g cm^{-3} respectively (Ni et al.,2017). The average density for dry crosslinked PVA membrane was calculated to be 0.86 g cm^{-3}, on the otherhand, the density of hydrated crosslinked PVA membrane was found to be of 1.067 g cm^{-3}. The average density values for the membrane obtained from simulation are in close range of the experimental values (1.26–1.29 g cm^{-3}) (Liu et al.,2022).

7.2.2 Radial Distribution function

Radial Distribution function (RDF) is an important property to understand the structural changes in the crosslinked membrane. The basic idea is to analyses how the interactions among different atoms such as the polyvinyl alcohol chain, glutaraldehyde group and water molecules occur in the crosslinked membrane systems. It indicates the probability density of finding atom A and B at a distance r, averaged over the equilibrium trajectory. To this end, we begin by exploring (RDFs) using Eq.7.1;

$$g_{AB(r)} = \frac{Vn_B}{N_B 4\pi r^2 dr} \quad (7.1)$$

Where, N_B is the no. of B atoms situated at distance r in a shell of thickness dr from particle A, N_B is the total number of B atoms and V is the total volume of the system. (Ohkubo et al.,2010).

The radial distribution curve between hydroxyl group O atom of PVA chain and O atom of water molecule denoted by O_W-O_{PVA} (black line) displays the crosslinked PVA membrane structuring effect on the surrounding water (**Fig,7.1**) The first hydration peak of the $g_{OPVA\text{-}OW}(r)$, is observed at 2.6 A^0, indicating the thickness of the first PVA hydration shell. This sharp peak is a clear indication of formation of hydrogen bonds between hydroxyl group of PVA and O of water molecule.(Bermejo & Ugarte 2008).The shorter distance is also an indication that the absorbed water molecules are more likely to be located in the vicinity of OH groups than on C atoms of the polymer network.(Bermejo & Ugarte 2008).It is noteworthy that the water ordering around PVA hydroxyl groups is lower in the case of backbone C than in the C adjacent to functional group. The reason being the backbone C atoms due to the chain connectivity have lesser mobility as compared to H.

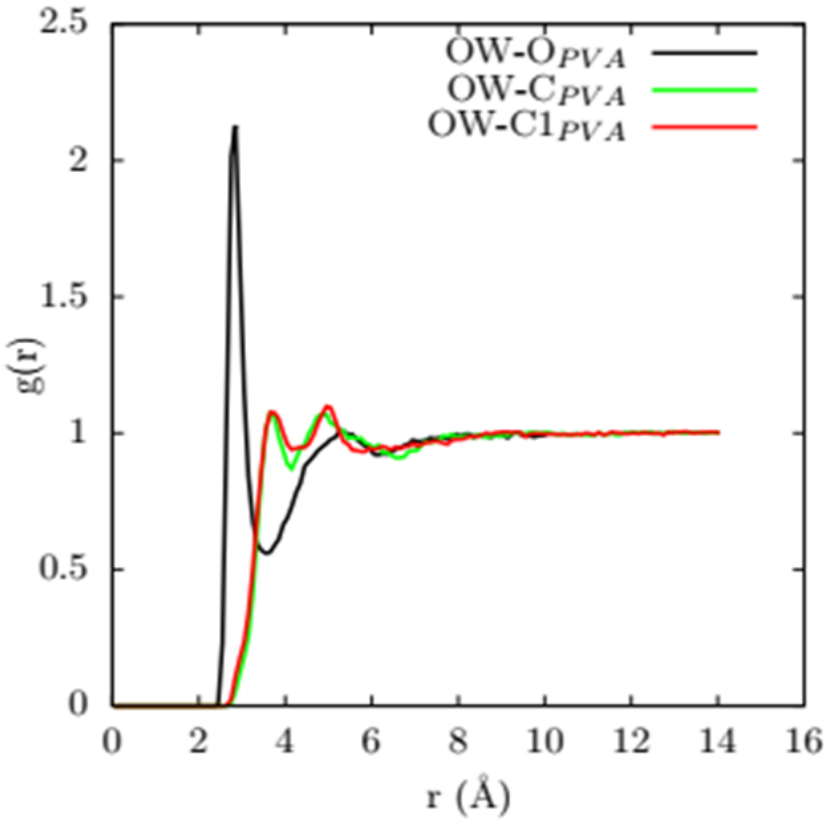

Figure 7.1. Radial distribution function profile between oxygen atoms of water molecule and oxygen atom (black line), backbone carbon (green line) and crosslinked carbon (red line) of crosslinked PVA membrane.

Fig.7.2 shows RDF between hydronium ions and oxygen atom of water molecule. The first peak appears with intense peak value at 2.05 Å. While, the first peak in the RDF plot between hydronium and oxygen atom of hydroxyl molecule of crosslinked membrane is observed at 2.22 Å. This represents the most probable distance between hydronium ion and hydroxyl oxygen of crosslinked PVA **(Fig 7.3).** Similar behavior is also noticed by Tai et

al.,2017 in case of Nafion membrane where, the proton was strongly bonded to the oxygen of water molecule as compared to oxygen at sulfonate group demonstrating vehicular mechanism of proton transport. Since 2.22 Å falls within the range of hydrogen-bonding distance, therefore this indicates that strong coordination of hydronium ion to water oxygen due to hydrogen bonding (Tai et al.,2017) and the proton transport in this system thus, corresponds to the reported vehicular mechanism.

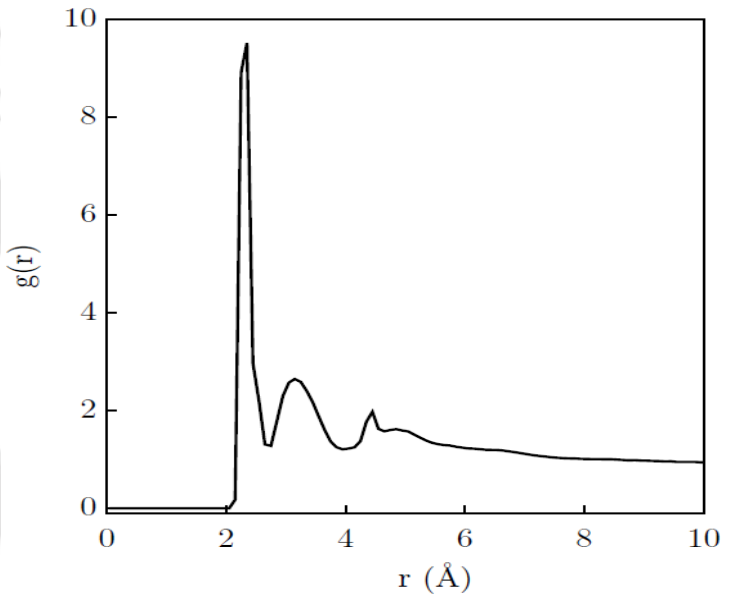

Figure 7.2 RDF between hydronium ion and oxygen atom of water molecule in the crosslinked membrane.

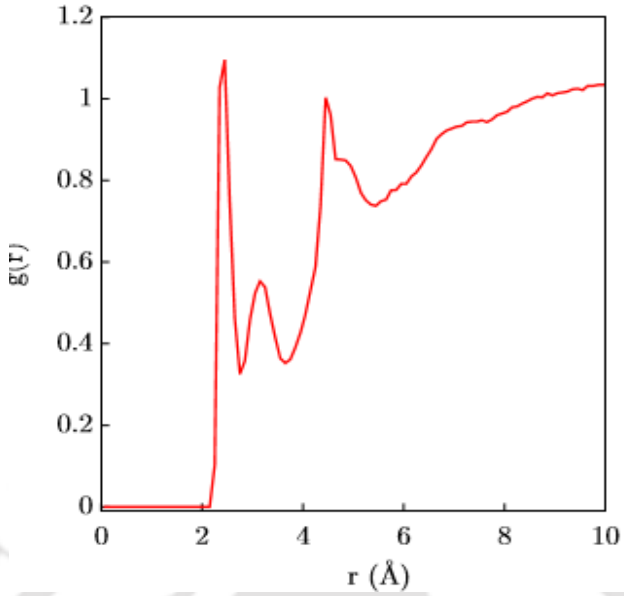

Figure 7.3 RDF between hydronium ion and oxygen atom of hydroxyl molecule in the crosslinked membrane.

7.2.3 Mean square displacement and diffusion coefficient

To study the movement characteristics of polymer chains in the simulation systems, the Mean square displacement (MSD) curves can be utilized to prove the influence of GA on the mobility of the backbone of PVA. MSD is represented by Eq 7.2

$$\text{MSD} = \langle | ri\ (\text{t}) - \ ri\ (0)|^2 \rangle \qquad (7.2)$$

Where r_i (0) represents the initial position coordinate of atom i and r_i (t) represents the position of atom i at the time t.

As well known, the slope of the MSD curve represents the flexibility of the PVA chains. Greater the slope of the curve, more is the flexibility of the PVA chains. Generally, the more flexible polymer chains are, the lower is the Tg value of polymer chains. The slope of the MSD curve of the crosslinked PVA is lower than that reported for pure PVA (Tai et al., 2017)which suggests the interaction between PVA molecular chains and PVA molecular

chains is the strongest. This is validated from our experimental findings of crosslinked membrane demonstrating improved thermal stability and mechanical strength of PVA by restricting the mobility of the polymer chains (Das et al., 2021). Moreover, the existence of the GA chains causes a stronger mechanical interlocking between the PVA and the GA, which needs more energy to break the freezing state of the PVA chains in the PVA/GA membrane and hence explains the rigidity and the higher Tg value experimentally obtained for the crosslinked membrane.

To characterize the mobility of proton in the membrane model system, the diffusion coefficient, *D* of atoms (or molecules) can be calculated from the slope of MSD, according to the Einstein relation as in Eg.7.3:

$$D = \frac{1}{6} \lim_{n\to\infty} (d/dt < | ri\ (t) - ri\ (0)|)^2 \quad (7.3)$$

Th diffusion coefficients of hydronium ion for the crosslinked PVA membrane was calculated to be $0.68 \pm 0.001x\ 10^{-6}\ cm^2\ s^{-1}$ as compared to $0.28 \pm 0.089\ x\ 10^{-6}\ cm^2\ s^{-1}$ for the neat PVA membrane. Compared with the neat PVA membrane, the crosslinked membrane demonstrated higher proton diffusion ability. The introduction of acetal bonds on crosslinking opened up new channels filled by water molecules and acting as bridge hence, contributing for proton to transport. The controlled water uptake ability exhibited by crosslinked PVA leads to moderate swelling characteristics and offers a continuous space for proton transport through the membrane (Kulasekaran et al.,2020).The formation of crosslinking had a significant role on the proton diffusion and ion conductivity. On the contrary, diffusion constant calculated by Tai et al., for Nafion membrane was $1.64x\ 10^{-6}\ cm^2\ s^{-1}$ (Tai et al., 2017).The presence of charged sulfonate groups explains its higher diffusion rate as well as its higher proton conductivity. The diffusion coefficient

D is also correlated with having an exponential relation to 1/FFV, which agrees well with the commonly employed free volume theory. Fractional free volume (FFV) is then defined as:

$$FFV = \frac{Vf}{Vt} x100\% \quad (7.4)$$

Where V_f is the free volume, and V_t is the total volume of the system. The FFV and chain mobility become poorer on addition of crosslinking agent, which also explains the higher diffusion coefficient for the crosslinked membrane.

7.2.4 Pore size distribution

The free volume can be seen as a space formed by pores of different sizes and characterized by the pore size distribution (PSD). It is the porous space available within the polymer structure and plays a central role in diffusion in polymer materials. In this study, the probe particle employed is water modelled by sphere with radius of 1.3 Å. Similar PSD is observed in **Fig 7.4** for the membranes indicating that the PVA membrane system consists of small network pores. Typically, such network pores are small spaces within aggregates, about (4.2-4.8) Å in diameter formed by polymeric segments, unlike aggregate pores which are (7-9) Å in diameter and are large open spaces between polymer aggregates (S. H. Kim et al., 2005), The prominent pores in crosslinked membrane is observed in the range of (2-6)Å in diameter whereas in case of the neat membrane it is observed to in the range of (4-8) Å in diameter respectively. The intermolecular cross-linking of the PVA chains through GA results in a three-dimensional network structure which is mainly responsible for formation of pore size in crosslinked PVA membrane. The interaction of both reactive ends of GA with the same polymeric chain results in a loop-type structure, chemically crosslinked by the aldehyde group had modified the original PVA network structure, and

thus significantly reducing the pore size distribution. This was also confirmed in the % swelling assessment (Das et al., 2021), The less dense formation of interconnected pores, in crosslinked membrane, allowed the membrane to absorb less water than its neat counterpart resulting in lesser swelling ability(Das et al., 2021).

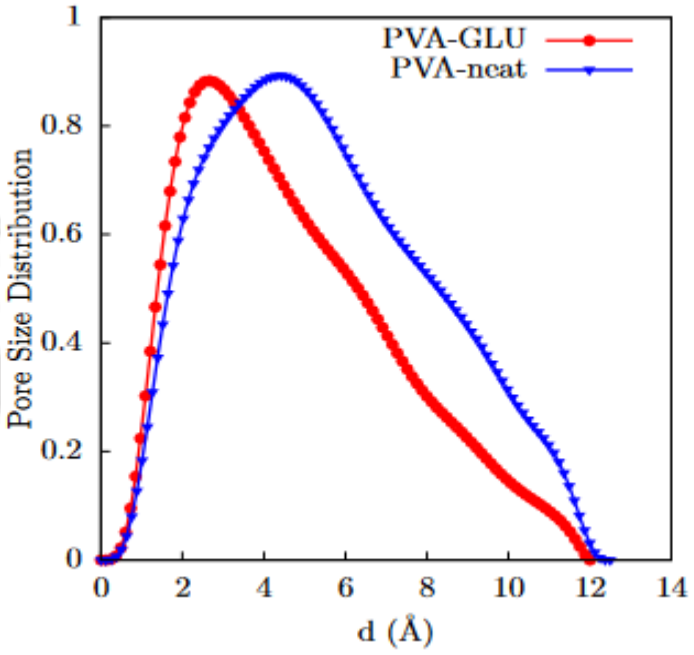

Figure 7.4 Pore size distribution curve of the crosslinked membrane (PVA-GLU) and neat PVA membrane (PVA-neat) at 300 K.

7.2.5 Assessment of molecular trajectories of hydronium ion

The pathway of five randomly selected hydronium ions traversing through the hydrated crosslinked PVA membrane is illustrated in **Fig.7.5 a-c** to track the hydronium ions as they traverse the thickness of the crosslinked PVA membrane which gives us a physical sense of the transport at the molecular level. Considering the 2D X-Z plane, the hydronium ion (marked by magenta) traverses up to 20 Å along the x-direction and 10 Å in the z-direction. While, in the Y-Z plane, the hydronium ion (marked by magenta) traverses up to 10 Å

along the y-direction and up to 20 Å in the z-direction. Furthermore, the analysis of two randomly selected neighboring water molecule surrounding the selected hydronium ion elucidates the interaction mechanism. The hydronium ion traverses up to 35 Å along x-direction over the simulated time of 50 ns (**Fig 7.5 d)**. The distance between O of neighboring water molecule and H_3O^+ being less than 3 Å. Along y-direction, (**Fig 7.5 e)** the hydronium ion traverses up to 25 Å while along z-direction(**Fig 7.5 f)**, the hydronium ion traverses up to 45 Å Initially, the hydronium ion (marked by magenta) is moving in close proximity between two water molecules (marked by blue and black). As time passed, the hydronium ion moved away from black colored water oxygen and moved closer to the blue colored water oxygen. This indicates that the proton was solvated by the water molecules and moved in between two oxygen confirming the vehicular mechanism of proton transport. Thus, the trajectories of the hydronium ion in x, y and z direction, clearly shows that hydronium ion was not confined in a small region in the PVA environment but travelled considerable large distance in all three directions. This indicates high mobility of proton as it moves in between a so-called "cluster-network" of PVA membrane. To further understand the hydronium ion transport, we compare the trajectories of a selected hydronium ion (magenta color) that traverse through membrane. Snapshots of the equilibrating configurations of the crosslinked membrane are displayed using Visual Molecular Dynamics (VMD) in parts **g-j** of **Fig. 7.5.** The representative snapshots images demonstrated illustrates the point that the hydronium ion easily got associated with more than a single water molecule as it transported across the membrane forming poly-hydronium complex. The hydrated H_3O^+ ion moves dynamically with water molecules with probable combination being associated with one water molecule forming $H_5O_2^+$ (**Fig 7.5**

g), (Tuckerman et al., 1994) or in association with two water molecules [H_3O^+ .$2H_2O$](**Fig 7.5 h**), or with three water molecules forming $H_9O_4^+$(**Fig 7.5 i**), or in association with four water molecules $H_{11}O_5^+$ (**Fig 7.5 h**), up to five water molecules forming $H_{13}O_6^+$((**Fig 7.5 j**), similar to the phenomena observed in Nafion membrane by Tai et al.,2017 which emphasizes the possibility of vehicular mechanism.

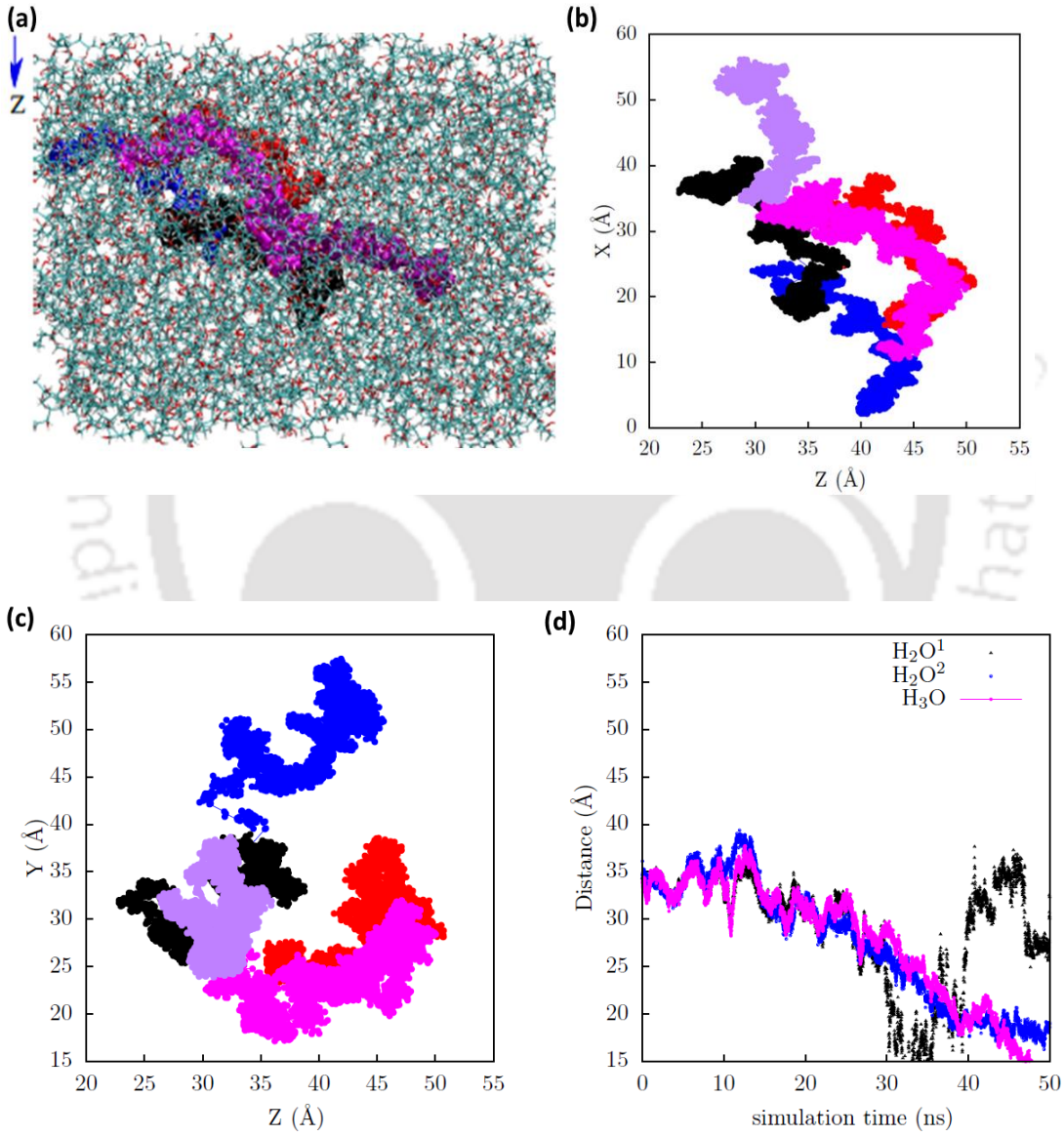

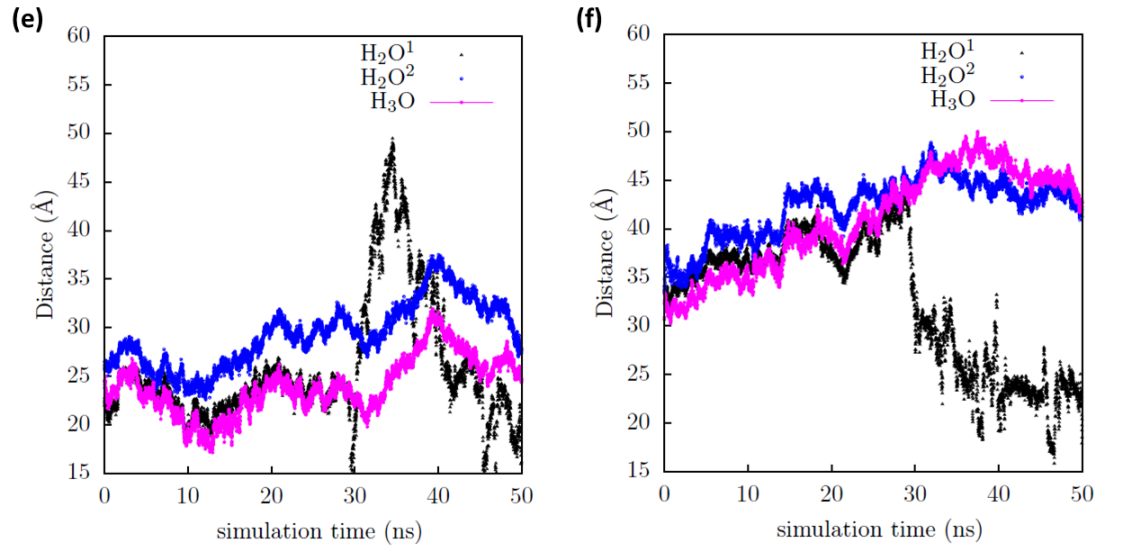

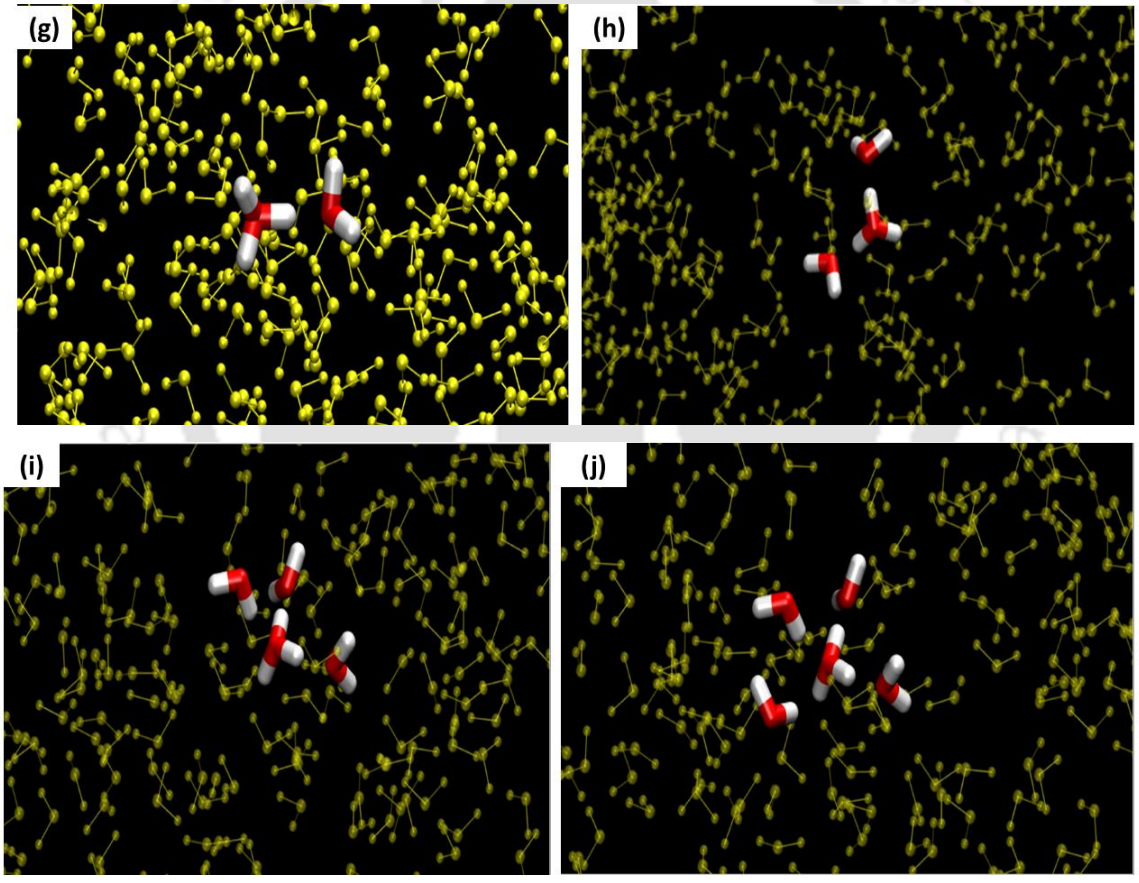

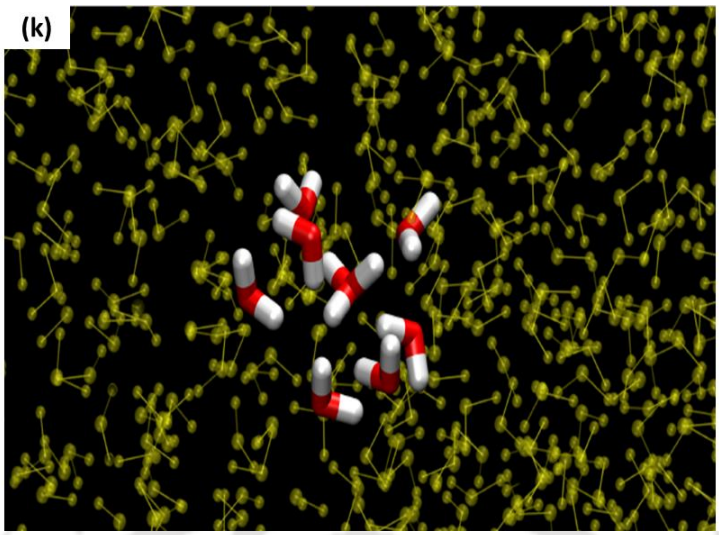

Figure 7.5 (a) The pathway of hydronium ions in hydrated crosslinked PVA environment; trajectories of hydronium ions (b) in X-Z plane; **(c)** in Y-Z plane, distance travelled by selected hydronium ion moving in hydrated crosslinked PVA polymeric membrane along (d) x-direction, (e) along y-direction, (f) along z-direction; (g-j) representative snapshots of selected hydronium ion forming poly hydronium complex with neighbouring water molecules as it traverses across the thickness of the membrane. Red and white spheres represent O and H atoms respectively while yellow spheres represent crosslinked PVA polymer.

7.3 Conclusion

Proton transport mechanism in crosslinked PVA membrane has been investigated using Classical Molecular Dynamics simulation, employing CHARMM force field. The simulated parameters such as diffusion coefficient validated the enhanced performance of the modified membrane found from the experimental findings over its pristine form. The analysis of radial distribution function, pore size distribution and molecular trajectories

clearly shows that hydronium ion was not confined in a small region in the PVA environment but travelled considerable large distance in all three directions, moving in cluster in association with the neighbouring water molecules forming polyhydronium complex Proton transport in the crosslinked PVA membrane thus belongs to proposed vehicular mechanism.

Chapter-8

Experimental investigation and numerical modelling on flow dimensionless parameters for enhancing the performance of recirculation mode HoneyComb MFC

Motivation

Wastewater treatment plants are either continuous ore recirculation flow mode systems. MFC can treat diverse host of wastewater while simultaneously harvesting electricity. So, the effect of fluid flow parameters in MFC device cannot be ignored. Also,to make the treatment of wastewater feasible using MFC, indigenously developed PVA membranes have been utilized as separator layer to bring down the cost of the MFC. Avoiding the Nafion membrane and employment of recirculation mode to treat high strength wastewater is therefore, worthy of investigation.

Abstract

This study presents a steady state, 3D mathematical model of microbial fuel cells (MFCs) developed by linking mass, charge and energy balance with the bioelectrochemical reactions. The model parameters are estimated and validated using experimental results obtained from MFCs operated at different flowrate in recirculation mode. The model allows the computation of local current density and reaction rates in the biofilm, helping to correctly capture the interdependence of system variables and predict the rise in power density at higher flowrate. The influence of the organic flow rate on bioelectricity generation in a recirculation, two-chamber microbial fuel cell for the treatment of hospital wastewater, with acetate as the only carbon source, was examined. Two sets of experiments with flow mode and batch mode combinations with hydraulic retention time of 1 day and influent chemical oxygen demand concentration were performed to verify the impact of flow rate on the voltage generation capacity of a dual-chamber microbial fuel cell working in continuous mode. Experimental results showed that the ohmic resistance decreased by 40-fold while the power density enhanced by 14-fold on switching to flow mode. The maximal current density obtained in the dynamic state, 2143.75 mA/m^2 is higher compared to literature data. Computational results imply that variation of current density occurs with increase in Reynolds number (Re) and anodic rate of reaction (k). The results demonstrate the possibility of application of the new low-cost, sustainable PEM for continuous operation of MFC for power generation and wastewater treatment in future.

8.1 Introduction

Honey comb MFC configurations (HCMFCs), are a relatively new MFC device implemented for long-term recirculation-based operation as it maintains homogeneous laminar fluid flow inside a reactor, which positively affects the mass transfer of protons and substrates (Y.-M. Chen et al., 2018; C.-T. Wang, Huang, Sangeetha, & Yan, 2018; C.-T. Wang, Huang, Sangeetha, Chen, et al., 2018) . However, a crucial aspect hindering its practical application is the search for a sustainable, low-cost, Nafion-alternative membrane. PVA being a non-toxic, biodegradable and an inexpensive polymer, inherently hydrophilic makes it favorable for wastewater treatment (Das et al., 2021). Following our previous report on glutaraldehyde (GA)crosslinked polyvinylalcohol (PVA) membrane as separator in domestic wastewater fed MFCs which exhibited high power density and COD removal with antibacterial property, thermo-mechanical stability and negligible fuel crossover it is worth experimenting how the membrane would behave when exposed to high strength wastewater.

Hydrodynamic effect plays a significant role in wastewater fed MFC. With a major portion of anolyte being water, fluid dynamics inside the anode chamber impacts the biofilm developed from microbial consortia present in the wastewater (Oliveira et al., 2013). Recirculation rate is a vital parameter as wastewater treatments plants are mostly operated in continuous or recirculation mode. It is reported to facilitate proton transfer thereby aiding in higher power output. It is considered more flexible compared to batch /continuous mode operations (Jafary et al., 2017). Increase in recirculation rate is reported to increase the shear rate and biofilm thickness (Pham et al., 2008). Furthermore, shear stress is another vital parameter as it enables microbial attachment on the anode surface at faster rate thus,

shortening the acclimation or startup time of MFC and efficiently limiting mass transfer loss (Celmer et al., 2008).

Wang et al.2018 reported that high shear stress improved the mass transfer rate of MFC (C.-T. Wang, Huang, Sangeetha, & Yan, 2018). However, the role of reaction rate and Reynolds No on the power density was not attempted. and hence it is worthy for investigation along with the shear stress effect.(Kataky et al., 2020) carried out another 3D modeling study mimicking lab-scale MFC using lactate as substrate. They reported that variation in Reynolds No impacts the reaction rate. However, the biofilm on anode was neglected and the power output was also not mentioned in this study. The numerical simulation of recirculation mode HCMFC with biofilm and avoiding the Nafion membrane is important in this study. As per our knowledge, PVA has not been integrated into HCMFC and therefore, the current work is strongly considered to be a big step towards addressing the knowledge gap on switching to biopolymeric PVA membrane for the performance enhancement of these novel HCMFC reactors for scale-up applications.

8.2 Results and Discussion

The Nafion alternative, low-cost crosslinked PVA Membrane synthesized is applied as a separator in a Recirculation batch mode Honeycomb Microbial Fuel Cell (RMFC) and a comparative analysis of the performance is done of two systems. System 1 is operated at flow rate of 40 ml/min called as dynamic mode and System 2 is at 0 ml/min called as static mode.

8.2.1 Power performance and COD Removal efficiency of the reactors with respect to the flow dynamics

It is obvious from the polarization curves shown in **Fig 8.1** that the MFC with wastewater flowing at 40 ml/min produced maximum power density whereas the MFC with 0 ml/min produced low power density. The reason for a better power generation might be due to the laminar flow of substrate which might have induced uniform distribution of substrates and ions inside the reactor. High power at laminar velocities is due to proper substrate availability for anodic biofilm, resulting in higher substrate conversion efficiency and electrochemical activity. This might have eventually resulted in a mature and strong biofilm with maximum power performance. However, at very high flow velocities, washout of electro active microbes occurs, resulting in rapid fall in current generation (Wang, et al., 2018). The peak power density production of this current study has been compared with that of some previous studies as shown in Table 8.1, Wang et al had produced a maximum power density of 32 mW//m^2 in sediment MFCs using domestic wastewater as the fuel source, which was almost 14-fold lesser than the production in the

current study (714.21 mW/m^2). Chen et al., employed domestic wastewater in HCMFCs which had a better power density production of 210 mW/m^2 (Y.-M. Chen et al., 2018). However, Wang et al., could only produce power density values of 58 mW//m^2 and 41 mW//m^2 respectively in their photosynthetic MFCs with domestic wastewater substrate(C.-T. Wang et al., 2017). Sediment MFCs designed and operated by Wang et al, could only produce 32 mW/m^2 of power density with domestic wastewater fuel(C.-T. Wang et al., 2019). Therefore, these abovementioned comparisons of peak power density productions have proved that HCMFCs utilized in this present study possess enhanced power performance. The capacity of the crosslinked membrane based HCMFC to treat hospital wastewaters is also higher revealed from the COD removal efficiencies of 58.17% in dynamic mode and 61.43% in static mode. In a study carried out by Opoku et al,using Nafion membrane based MFC, COD removal efficiencies of only 29% was reported for hospital wastewater (Opoku et al., 2022). On comparing the energy harvested from hospital wastewater with previous literature as tabulated in Table **8.3,** the power density harvested utilizing the low-cost crosslinked PVA membrane equipped MFC in recirculation flow mode is encouraging which shows its potential to treat high strength wastewater along with simultaneous power generation.

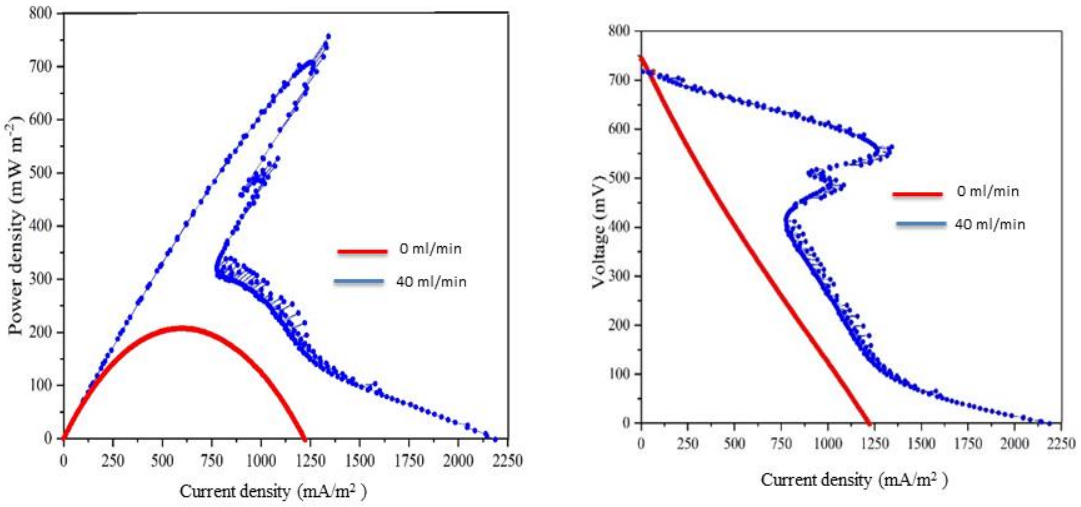

Figure 8.1: Polarization curves for the PVA Based Honeycomb MFC in static condition and dynamic mode.

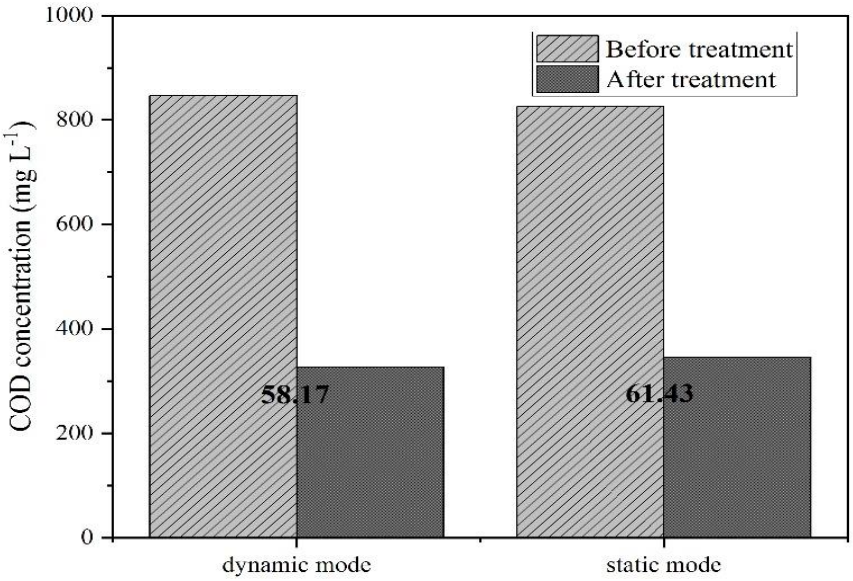

Figure 8.2: COD Removal efficiency of the reactors when operated in dynamic and static mode.

Table 8.1 Comparative analysis of performance of HCMFCs operated with different membranes.

Membrane	Maximum Open Circuit Potential (mV)	Maximum Power Density (mW/m^2)	Maximum Current Density (mA/m^2)	Reference
Nafion 117	570	5.71	50.19	(Wang, et al., 2018).
Nafion 117	770	4.5	32.94	(Wang, et al., 2018).
Nafion 117	430	4.06	46.34	(Wang, et al., 2018).
PVA	750	714.21	2258.02	This study

8.2.2 Impact of flow dynamics on internal resistance of the MFCs

The Nyquist plot for the HCMFCs has been depicted in **Fig 8.3** The individual resistance components in the reactors employed in this study have been listed in **Table.8.2** The loss in the HCMFC reactor in dynamic mode was lesser compared to the control reactor in static mode and this may be due to the fact that homogenous mass and ionic transfer rendered by the flow straighteners might have brought about a great reduction in ohmic and concentration losses (Cui et al., 2020).But further in depth research has to be performed for detailed understanding of the losses inside the reactors and mechanisms to reduce them. Internal resistance in MFCs encompasses 3 important losses as ohmic, charge transfer losses and concentration losses. R1 represents the ohmic losses present in the HCMFCs and it is their assessment is usually associated with the conductivities of anolyte and the electrodes. R2, signifies the account of anode biofilm activity that is calculated as anode charge transfer losses. Capacitance C designates the phenomenon of electrical double layer

occurrence in the titanium wire and graphite felt sheet of the anode and cathode chambers. This usually occurs in the boundary between the electrode and electrolyte. Along with that, the Wd1 (Warburg resistance) characterizes the concentration losses in the MFCs, and it could designate the diffusions of substrate, gases and other reactants. A correlation between substrate flow velocity and the MFC internal resistance has been evaluated in the previous research studies. Wang et al., had operated photosynthetic honey comb MFCs under various flow rates (0-240 ml/min) and estimated their influence on the electrochemical performance of the reactors(Wang et al., 2018). The charge transfers and Warburg resistances were observed to decrease as the flow rate increased from 0 to 40 ml/min, but when the flow rate was too high at 240 ml/min, the resistances shot up. This was linked to the formation and washout of anodic biofilm and also the trend of mass transfer under various flow rates.

The ohmic resistance for the same flow rate of 40 ml/min recorded lowest in our study compared to static mode and other previous studies with Nafion membrane. This can be attributed to the low resistance provided by the PVA membrane as well as due to the flow regime which contributed to the higher power output. Eradication of power overshoot in power density curves and reduction in internal resistance were observed in flow straightener MFCs by (Wang et al., 2018) .The internal resistance reduced from 69 Ω to 17 Ω when the flow velocity increased from 0.0004 m/s to 0.004 m/s, but the velocity further increased to 0.04 m/s, the resistance value increased to 30 Ω. This eventually altered the overall power performance of the MFC. They also concluded that the electrochemical parameters and performance dynamics of a MFC are totally dependent on flow constraints. Thus, the above-mentioned results and justifications were in complete accordance with the

outcomes of the present study that flow parameters of the substrate through honey comb channels with low resistance of the membrane, have had definite and prominent effects on the reduction of losses inside a reactor which thereby might have resulted in reduced overall internal resistance of the reactor. This also emphasized the fact that design of MFC reactor can definitely influence the electrochemical parameters of it.

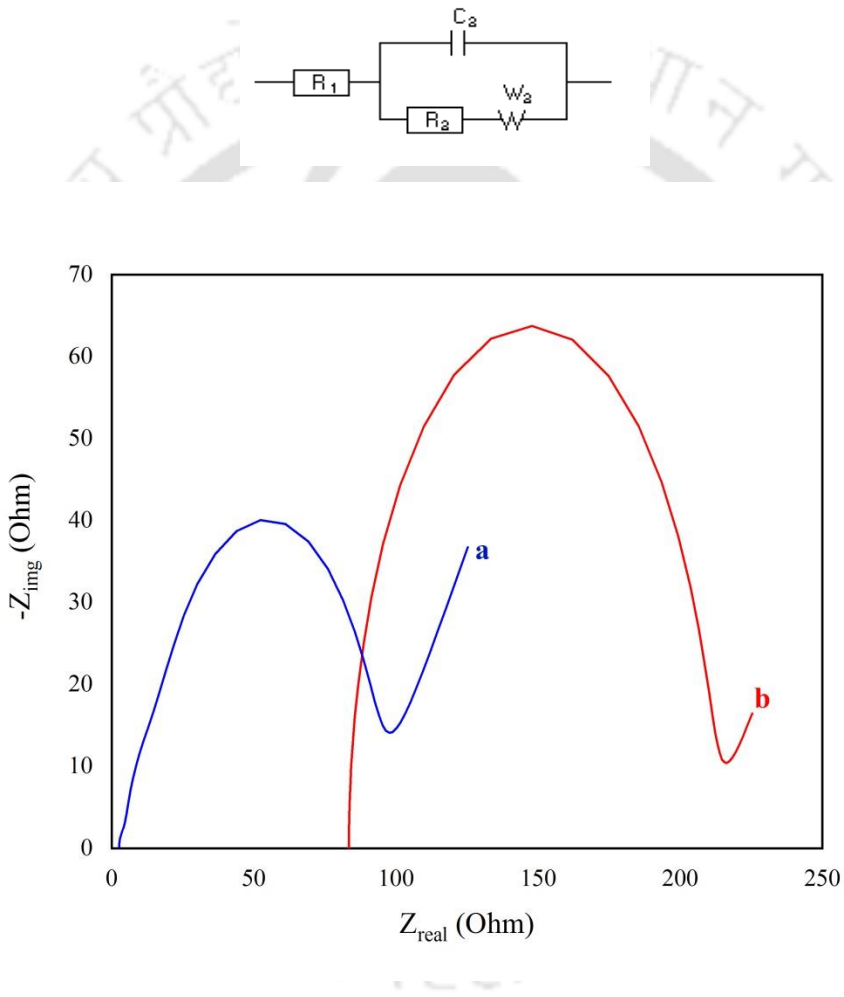

Figure 8.3. Nyquist plot for the HCMFC operated at flow rate a) 40ml/min, b) 0 ml/min with the equivalent circuit showing the various resistances during operation.

Table 8.2 Comparative analysis of present study with literature on internal losses incurred by the HCMFCs.

Componentsof Internal Resistance/flow rate	**Ohmic losses (R_1)**	**Charge Transfer loss (R_2)**	**Warburg resistance (Wd)**	**Ref**
0 ml/min	12.24	411.59	7670	Wang et al.,2018
	83.47	126.4	12.46	This study
40 ml/min	18.58	21.96	611.8	Wang et al.,2018
	2.4	97.18	-	This study

Table 8.3. Power outputs in laboratory-scale MFC during hospital wastewater treatment.

Anode materials	**Anode volume (mL)**	**Exchange membrane**	**MFC devices**	**Power density (W/m^{-3})**	**Ref.**
Graphite granules	390	UltrexeCMI7000, Membranes International Inc., USA)	Recirculation at flow rate of 6 L h^{-1}	8 ± 5	(Rabaey et al., 2005)
Graphite granules	60	UltrexeCMI7000, Membranes International Inc., USA)	Recirculation at flow rate of 106 mL h^{-1}	14 ± 1	(Aelterman, Rabaey, Clauwaert, et al., 2006)
Aluminium	2,000	Gar-salt bridge	Static	~0.25	(Shakunthala & Manoj, 2018)
Graphite felts	1,000	PVA	Recirculation at flow rate of 2.4 L h^{-1}	1.78	This work

8.2.3. Effect of flow dimensionless number on performance of MFC

In this study, the dimensionless parameters Reynolds number (Re), was used to investigate the performance of recirculation mode MFC equipped with the crosslinked PVA membrane. A flowchart containing the steps involved in the CFD Work is shown in **Fig 8.4(a).** By varying primarily Re and kinetic rate of anode reaction k_1, the current density is calculated in each case. With the increase in Re, the power performance of MFC improved due to enhanced mass transfer of substrate. Maximum power density of 714.21 mW/m^2 and limit current density of 2258.02 mA/m^2 were obtained by MFC at Re=170 which were 3.57 times and 1.80 times higher than MFC at Re=0.The simulation results follow similar trend and match with the experimental findings. Variation in Re leads to increase in current density proved by experimental data. As observed in **Fig 8.4 b & c**, the current density increases with increase in the anodic rate of reaction When the kinetic rate of reaction is kept constant, with increase in Reynolds number there is increase in the current density. For Re=170, corresponding to the current density value achieved experimentally, the kinetic rate of reaction computationally calculated was k=0.3 as compared to k =0.01 for Re=0.This indicates significant rise in reaction rate and current density with increase in Reynolds number. The mathematical model provided a new perspective in understanding the reaction kinetics. Variation of species concentration for the reactant acetate in anode chamber, oxygen in cathode chamber, proton transfer across the membrane and product carbon dioxide at anode are plotted along x-direction as shown in **Fig 8.5**. The concentration of reactants decreases in the electrodes and closer to the membrane it is totally consumed. The concentration of protons decreases closer to the cathode chamber as

it crosses the membrane. The concentration of the product increases from the anode electrode and peaks as it flows to the anode chamber

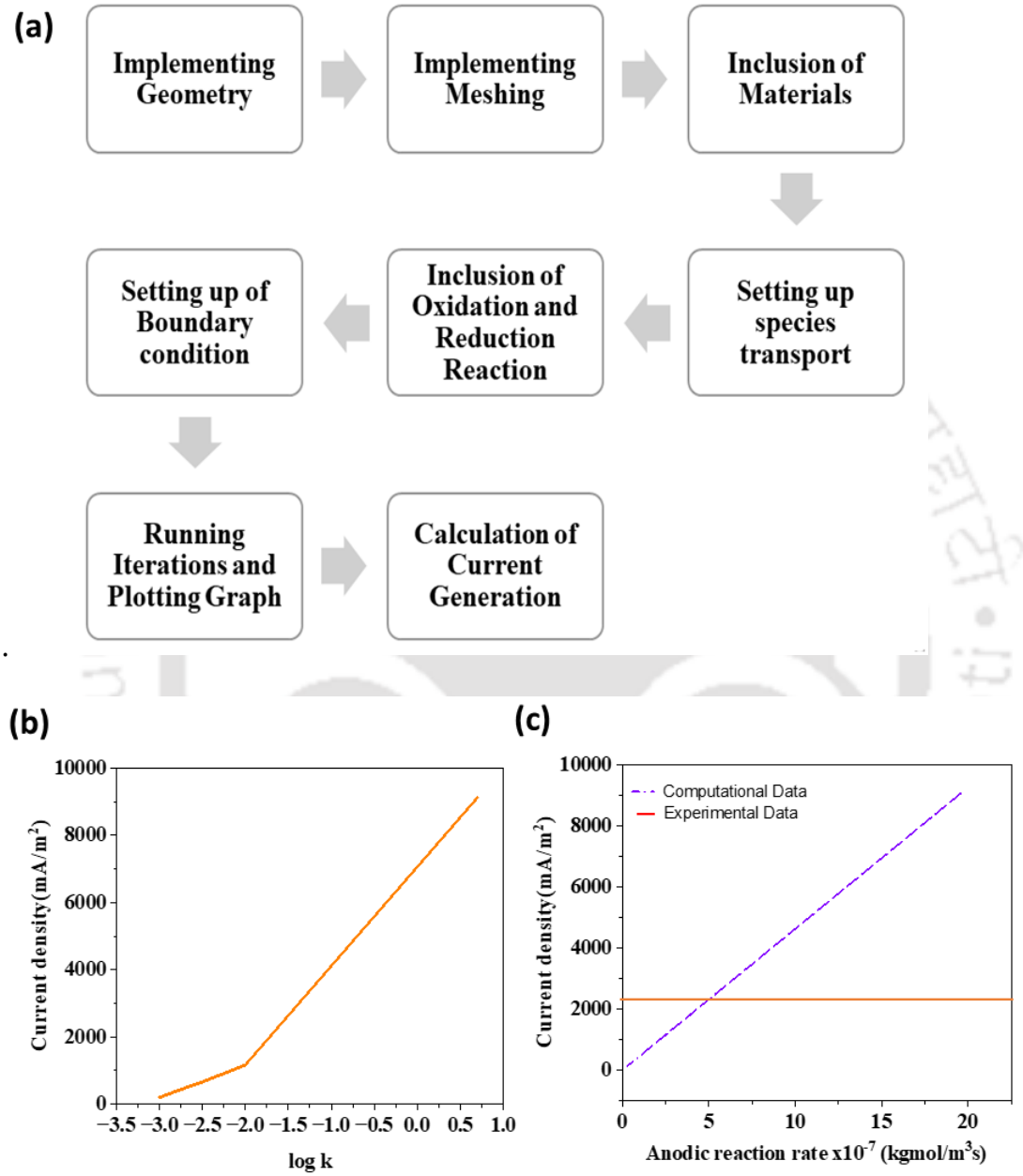

Figure 8.4 (a) Flowchart depicting the steps involved in the CFD work to generate current density (b)Variation of current density with anodic reaction rate, (c) Variation of current density with log k.

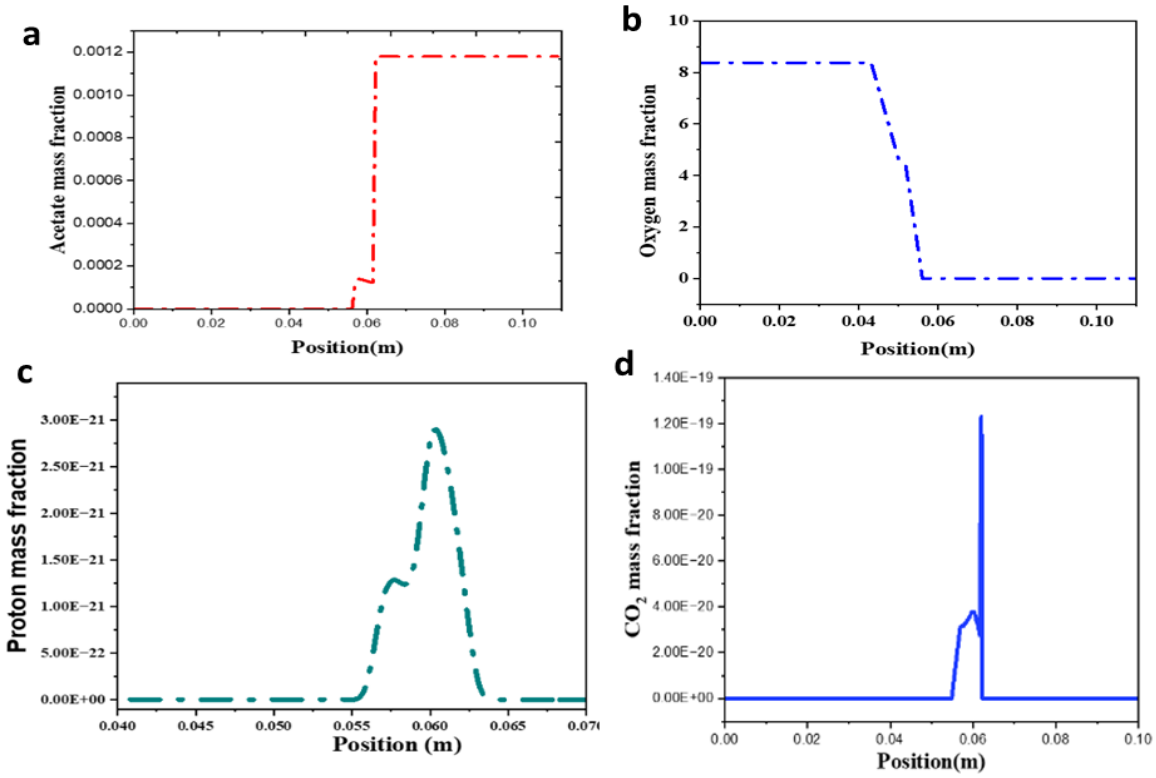

Figure 8.5. Variation of the reactant, product and intermediate species along the length of the MFC.

8.3 Conclusion

Hospital wastewater is successfully employed as a cheap substrate for electricity production in crosslinked PVA equipped HCMFC. Highest power density of 714.21 mW/m^2 and maximum current density of 2258.02 mA/m^2 was observed for the crosslinked PVA based MFCs in dynamic state. This can be attributed to the low drastic reduction in ohmic loss along with enhanced contact time between the substrates and the

microorganisms which in turn helped in performing better metabolism leading to the reduction of COD concentration in the recirculation mode. The experimental results obtained is validated by the simulation study. The power output of MFC in flow mode increased in the recirculation mode MFCs. enhanced by 14-fold compared to previous study due to low hydrodynamic boundary layer thickness 2 cm. High shear rate of 0.122/s in the hydrodynamic boundary layer of 2 cm caused the maximum voltage of 750 mV in MFC in dynamic mode, which was 14 times higher than previous reports. The charge transfer losses of anode decreased with the decreasing hydrodynamic boundary layer thicknesses. The charge transfer resistance of MFC in dynamic flow mode was 91 Ω, which was lesser than that of MFC in static mode. These findings are useful for the improvement in the performance of the continuous/recirculation flow mode MFCs. A good insight of the mechanisms involved are obtained and easy monitoring of the distribution of organics, electrons and protons is achieved. By implementing the findings, optimization of design can be achieved leading to higher current generation and cost-effective production.

Chapter-9

Concluding Remarks and Future Prospects

9.1 Concluding Remarks

MFCs undoubtedly have potential in terms of energy recovery with simultaneous wastewater treatment. In terms of commercial application, it can create its own niche as stand-alone power source and also in the direct treatment of wastewater. They can also treat wastewater of high (hospital wastewater) as well as low (domestic wastewater) strength, even at ambient temperatures, as demonstrated by this study. MFC configuration with its components have a direct impact on the cost for large scale applications where the electrode and membrane materials can increase considerably the capital cost while the MFC configuration can reduce the operational cost. The fabrication of biobased flexible PANi/PLA electrodes and the low-cost, biodegradable Cross-linked PVA and Chitosan membranes not only cuts down the capital cost drastically but the favourable antifouling property of the environmentally benign membranes ensures that the operational cost is minimalized. The MFCs harnessed electricity using mixed bacterial consortia from the wastewater devoid of any external catatyst or mediator which is of much significance from operation point of view. Molecular Dynamics simulation based on CHARMM force field has been used to investigate the mechanism of proton transport in crosslinked PVA fuel-cell membrane.The analysis of proton transport through the crosslinked PVA membrane for MFC application showed that vehicular mechanism is the preferred mode. Recirculation flow mode adopted in the current study will hinder the pH imbalances in the electrolytes

which could optimistically alter the bacterial metabolisms and thus leading to an improved reactor performance. Switching conventional materials with our novel materials in the MFC Configuration and incorporating flow conditions in MFCs will open up possibilities for its operation not only in lab scale but also pave new avenues for its integration in real industrial wastewater treatment plants. The balance between capital cost and operational costs is the key for sustainable wastewater treatment with electricity production. Therefore, further studies are needed to investigate the scale-up for large operation with the real wastewater in order to recover resource along with enhancing its power performance from treatment of such wastewater. Another important aspect that requires future investigation is an understanding of the relation between flow dynamics and multiple biofilm layers which will ensure optimal biofilm activity with reduction in the power overshoot in the system which is not desirable in long term operation.

9.2 Future Scope

MFCs represent a promising technology for renewable energy harvesting with simultaneous wastewater treatment. They will be useful as power sources for environmental sensors and environmental bioremediation. Microfabrication of the Microbial Fuel Cell to develop Mini biosensors to detect toxic heavy metals in wastewater is already in trend. Wearable devices can be fabricated using the flexible electrodes for electronic and biomedical application. Scale-up operation using the fabricated components assembled in the microbial fuel cells to treat various high strength wastewater can be used in the future integrating other systems such as anaerobic digestor, desalination unit. Incorporation of multiplier circuits to boost the voltage obtained using wastewater fed

MFCs is another promising aspect. Most important of all, to store the energy generated during the operation period of the MFC device, storage devices such as supercapacitors can be incorporated to harvest the energy generated for prolong use.

References

Adeniran, J. A., Huberts, R., De-Koker, J. J., Arotiba, O. A., Olorundare, O. F., Van-Zyl, E., & Du-Plessis, S. C. (2016). Energy generation from domestic wastewater using sandwich dual-chamber microbial fuel cell with mesh current collector cathode. International Journal of Environmental Science and Technology, 13(9), 2209–2218. https://doi.org/10.1007/s13762-016-1050-z

Aelterman, P., Rabaey, K., Clauwaert, P., & Verstraete, W. (2006). Microbial fuel cells for wastewater treatment. Water Science and Technology, 54(8), 9–15. https://doi.org/10.2166/wst.2006.702

Aelterman, P., Rabaey, K., Pham, H. T., Boon, N., & Verstraete, W. (2006). Continuous Electricity Generation at High Voltages and Currents Using Stacked Microbial Fuel Cells. Environmental Science & Technology, 40(10), 3388–3394. https://doi.org/10.1021/es0525511

Albarracin-Arias, J. A., Yu, C. P., Maeda, T., Valdivieso Quintero, W., & Sanchez-Torres, V. (2021). Microbial community dynamics and electricity generation in MFCs inoculated with POME sludges and pure electrogenic culture. International Journal of Hydrogen Energy. https://doi.org/10.1016/j.ijhydene.2021.08.218

Ali, A. K. M., Ali, M. E. A., Younes, A. A., Abo El fadl, M. M., & Farag, A. B. (2021). Proton exchange membrane based on graphene oxide/polysulfone hybrid nano-composite for simultaneous generation of electricity and wastewater treatment. Journal of Hazardous Materials. https://doi.org/10.1016/j.jhazmat.2021.126420

Anis, A., Banthia, A. K., & Bandyopadhyay, S. (2008). Synthesis & Characterization of PVA/STA Composite Polymer Electrolyte Membranes for Fuel Cell Application. Journal of Materials Engineering and Performance, 17(5), 772–779. https://doi.org/10.1007/s11665-008-9200-1

Arntsen, C., Savage, J., Tse, Y. L. S., & Voth, G. A. (2016). Simulation of Proton Transport in Proton Exchange Membranes with Reactive Molecular Dynamics. In Fuel Cells

(Vol. 16, Issue 6, pp. 695–703). John Wiley and Sons Ltd. https://doi.org/10.1002/fuce.201600024

Ayyaru, S., Letchoumanane, P., Dharmalingam, S., & Stanislaus, A. R. (2012). Performance of sulfonated polystyrene–ethylene–butylene–polystyrene membrane in microbial fuel cell for bioelectricity production. Journal of Power Sources, 217, 204–208. https://doi.org/10.1016/j.jpowsour.2012.05.053

Bahlakeh, G., Nikazar, M., Hafezi, M.-J., Dashtimoghadam, E., & Hasani-Sadrabadi, M. M. (2012). Molecular dynamics simulation study of proton diffusion in polymer electrolyte membranes based on sulfonated poly (ether ether ketone). International Journal of Hydrogen Energy, 37(13), 10256–10264. https://doi.org/10.1016/j.ijhydene.2012.03.004

Bermejo, J. S., & Ugarte, C. M. (2008). Influence of water content on structure and mobility of polyvinyl alcohol: A molecular dynamics simulation. *The Journal of chemical physics*, *129*(15), 154907. https://doi.org/10.1063/1.2994731

Bertini, F., Canetti, M., Patrucco, A., & Zoccola, M. (2013). Wool keratin-polypropylene composites: Properties and thermal degradation. Polymer Degradation and Stability. https://doi.org/10.1016/j.polymdegradstab.2013.02.011

Bhowmick, G. D., Noori, Md. T., Das, I., Neethu, B., Ghangrekar, M. M., & Mitra, A. (2018). Bismuth doped TiO2 as an excellent photocathode catalyst to enhance the performance of microbial fuel cell. International Journal of Hydrogen Energy, 43(15), 7501–7510. https://doi.org/10.1016/j.ijhydene.2018.02.188

Binsu, V. V., Nagarale, R. K., & Shahi, V. K. (2005). Phosphonic acid functionalized aminopropyl triethoxysilane–PVA composite material: organic–inorganic hybrid proton-exchange membranes in aqueous media. Journal of Materials Chemistry, 15(45), 4823. https://doi.org/10.1039/b511274e

Borole, A. P., Reguera, G., Ringeisen, B., Wang, Z.-W., Feng, Y., & Kim, B. H. (2011). Electroactive biofilms: Current status and future research needs. Energy & Environmental Science, 4(12), 4813. https://doi.org/10.1039/c1ee02511b

Celmer, D., Oleszkiewicz, J. A., & Cicek, N. (2008). Impact of shear force on the biofilm structure and performance of a membrane biofilm reactor for tertiary hydrogen-driven denitrification of municipal wastewater. Water Research, 42(12), 3057–3065. https://doi.org/10.1016/j.watres.2008.02.031

Chen, G., Wei, B., Luo, Y., Logan, B. E., & Hickner, M. A. (2012). Polymer Separators for High-Power, High-Efficiency Microbial Fuel Cells. ACS Applied Materials & Interfaces, 4(12), 6454–6457. https://doi.org/10.1021/am302301t

Chen, L., Zhang, H., Li, Z.-Z., He, Y.-L., & Tao, W.-Q. (2015). Experimental and Numerical Study on Thermal Conductivity of Proton Exchange Membrane. Journal of Nanoscience and Nanotechnology, 15(4), 3087–3091. https://doi.org/10.1166/jnn.2015.9633

Chen, X. F., Wang, X. S., Liao, K. T., Zeng, L. Z., Xing, L. D., Zhou, X. W., Zheng, X. W., & Li, W. S. (2015). Improved power output by incorporating polyvinyl alcohol into the anode of a microbial fuel cell. Journal of Materials Chemistry A, 3(38), 19402–19409. https://doi.org/10.1039/C5TA03318G

Chen, Y.-M., Wang, C.-T., & Yang, Y.-C. (2018). Effect of Wall Boundary Layer Thickness on Power Performance of a Recirculation Microbial Fuel Cell. Energies, 11(4), 1003. https://doi.org/10.3390/en11041003

Chi, H. Y., Chan, V., Li, C., Hsieh, J. H., Lin, P. H., Tsai, Y. H., & Chen, Y. (2020). Fabrication of polylactic acid/paclitaxel nano fibers by electrospinning for cancer therapeutics. BMC Chemistry, 14(1). https://doi.org/10.1186/s13065-020-00711-4

Choi, M.-J., Chae, K.-J., Ajayi, F. F., Kim, K.-Y., Yu, H.-W., Kim, C., & Kim, I. S. (2011). Effects of biofouling on ion transport through cation exchange membranes and microbial fuel cell performance. Bioresource Technology, 102(1), 298–303. https://doi.org/10.1016/j.biortech.2010.06.129

Cui, M.-H., Sangeetha, T., Gao, L., & Wang, A.-J. (2020). Hydrodynamics of up-flow hybrid anaerobic digestion reactors with built-in bioelectrochemical system. Journal of Hazardous Materials, 382, 121046. https://doi.org/10.1016/j.jhazmat.2019.121046

Daries Bella, R. S., Hirankumar, G., Navanietha Krishnaraj, R., & Prem Anand, D. (2016). Novel proton conducting polymer electrolyte and its application in microbial fuel cell. Materials Letters, 164, 551–553. https://doi.org/10.1016/j.matlet.2015.11.066

Das, B., Gaur, S. S., Katha, A. R., Wang, C. T., & Katiyar, V. (2021). Crosslinked poly(vinyl alcohol) membrane as separator for domestic wastewater fed dual chambered microbial fuel cells. International Journal of Hydrogen Energy. https://doi.org/10.1016/j.ijhydene.2020.11.213

Das, B., Gaur, S. S., Katha, A. R., Wang, C. T., & Katiyar, V. (2023). Hair hydrolysate functionalized cellulose nanocrystal based chitosan membrane to harness power from wastewater fed MFCs. International Journal of Hydrogen Energy, 48(25), 9451–9461. https://doi.org/10.1016/j.ijhydene.2022.12.054

Das, B., Soundararajan, N., Kashyap, S. P., Jang, J., Wang, C. T., Katha, A. R., & Katiyar, V. (2022). Bioaugmented polyaniline decorated polylactic acid nanofiber electrode by electrospinning technique for real wastewater-fed <scp>MFC</scp> application. International Journal of Energy Research, 46(3), 3588–3601. https://doi.org/10.1002/er.7407

Daud, S. M., Kim, B. H., Ghasemi, M., & Daud, W. R. W. (2015). Separators used in microbial electrochemical technologies: Current status and future prospects. Bioresource Technology, 195, 170–179. https://doi.org/10.1016/j.biortech.2015.06.105

Din, M. I., Nabi, A. G., Hussain, Z., Khalid, R., Iqbal, M., Arshad, M., Mujahid, A., & Hussain, T. (2021). Microbial fuel cells—A preferred technology to prevail energy crisis. In International Journal of Energy Research. https://doi.org/10.1002/er.6403

Dong, C., Zheng, W., Wang, L., Zhen, W., & Zhao, L. (2021). Insight into glass transition temperature and mechanical properties of PVA/TRIS functionalized graphene oxide composites by molecular dynamics simulation. Materials & Design, 206, 109770. https://doi.org/10.1016/j.matdes.2021.109770

ElMekawy, A., Hegab, H. M., Dominguez-Benetton, X., & Pant, D. (2013). Internal resistance of microfluidic microbial fuel cell: Challenges and potential opportunities. Bioresource Technology, 142, 672–682. https://doi.org/10.1016/j.biortech.2013.05.061

ElMekawy, A., Hegab, H. M., Losic, D., Saint, C. P., & Pant, D. (2017). Applications of graphene in microbial fuel cells: The gap between promise and reality. In Renewable and Sustainable Energy Reviews. https://doi.org/10.1016/j.rser.2016.10.044

Fan, Y., Hu, H., & Liu, H. (2007). Enhanced Coulombic efficiency and power density of air-cathode microbial fuel cells with an improved cell configuration. Journal of Power Sources, 171(2), 348–354. https://doi.org/10.1016/j.jpowsour.2007.06.220

Fangzhou, D., Zhenglong, L., Shaoqiang, Y., Beizhen, X., & Hong, L. (2011). Electricity generation directly using human feces wastewater for life support system. Acta Astronautica, 68(9–10), 1537–1547. https://doi.org/10.1016/j.actaastro.2009.12.013

Farber, P., Gräbel, J., Kroppen, N., Pötschke, L., Roos, D., Rosenbaum, M., Stegschuster, G., & Ueberholz, P. (2021). Electricity generation in a microbial fuel cell with textile carbon fibre anodes. Computers & Mathematics with Applications, 83, 4–23. https://doi.org/10.1016/j.camwa.2019.11.019

Feller, S. E., Zhang, Y., Pastor, R. W., & Brooks, B. R. (1995). Constant pressure molecular dynamics simulation: The Langevin piston method. The Journal of chemical physics, 103(11), 4613-4621.

Figueiredo, K. C. S., Alves, T. L. M., & Borges, C. P. (2009). Poly(vinyl alcohol) films crosslinked by glutaraldehyde under mild conditions. Journal of Applied Polymer Science, 111(6), 3074–3080. https://doi.org/10.1002/app.29263

Freier, E., Wolf, S., & Gerwert, K. (2011). Proton transfer via a transient linear water-molecule chain in a membrane protein. Proceedings of the National Academy of Sciences of the United States of America. https://doi.org/10.1073/pnas.1104735108

Gali, K. K., Soundararajan, N., Katiyar, V., & Sivaprakasam, S. (2021). Electrospun chitosan coated polylactic acid nanofiber: A novel immobilization matrix for α –

Amylase and its application in hydrolysis of cassava fibrous waste. Journal of Materials Research and Technology, 13, 686–699. https://doi.org/10.1016/j.jmrt.2021.05.001

Gaur, S. S., Dhar, P., Sonowal, A., Sharma, A., Kumar, A., & Katiyar, V. (2017). Thermo-mechanically stable sustainable polymer based solid electrolyte membranes for direct methanol fuel cell applications. Journal of Membrane Science. https://doi.org/10.1016/j.memsci.2016.12.030

Gaur, S. S., Dhar, P., Wani, K. M., Srivastava, M., Sakurai, S., Kumar, A., & Katiyar, V. (2021). Ion transfer channel network formed by flower and rod shape crystals of hair hydrolysate in poly(vinyl alcohol) matrix and its application as anion exchange membrane in fuel cells. Journal of Colloid and Interface Science. https://doi.org/10.1016/j.jcis.2020.12.012

Ghadge, A. N., & Ghangrekar, M. M. (2015). Development of low cost ceramic separator using mineral cation exchanger to enhance performance of microbial fuel cells. Electrochimica Acta, 166, 320–328. https://doi.org/10.1016/j.electacta.2015.03.105

Ghasemi, M., Daud, W. R. W., Hassan, S. H. A., Oh, S.-E., Ismail, M., Rahimnejad, M., & Jahim, J. M. (2013). Nano-structured carbon as electrode material in microbial fuel cells: A comprehensive review. Journal of Alloys and Compounds, 580, 245–255. https://doi.org/10.1016/j.jallcom.2013.05.094

Ghasemi, M., Wan Daud, W. R., Ismail, M., Rahimnejad, M., Ismail, A. F., Leong, J. X., Miskan, M., & Ben Liew, K. (2013). Effect of pre-treatment and biofouling of proton exchange membrane on microbial fuel cell performance. International Journal of Hydrogen Energy, 38(13), 5480–5484. https://doi.org/10.1016/j.ijhydene.2012.09.148

GOLCZAK, S., KANCIURZEWSKA, A., FAHLMAN, M., LANGER, K., & LANGER, J. (2008). Comparative XPS surface study of polyaniline thin films. Solid State Ionics, 179(39), 2234–2239. https://doi.org/10.1016/j.ssi.2008.08.004

Goy, R. C., De Britto, D., & Assis, O. B. G. (2009). A review of the antimicrobial activity of chitosan. In Polimeros. https://doi.org/10.1590/S0104-14282009000300013

Gunaseelan, K., Jadhav, D. A., Pant, D., & Gajalakshmi, S. (2022). Effectiveness of biophotovoltaics system modified with fuller-clay composite separators for chromium removal. Electrochimica Acta, 426, 140714. https://doi.org/10.1016/j.electacta.2022.140714

Gupta, A., Pal, A. K., Woo, E. M., & Katiyar, V. (2018). Effects of Amphiphilic Chitosan on Stereocomplexation and Properties of Poly(lactic acid) Nano-biocomposite. Scientific Reports, 8(1). https://doi.org/10.1038/s41598-018-22281-1

Hanna Rosli, N. A., Loh, K. S., Wong, W. Y., Mohamad Yunus, R., Khoon Lee, T., Ahmad, A., & Chong, S. T. (2020). Review of chitosan-based polymers as proton exchange membranes and roles of chitosan- supported ionic liquids. In International Journal of Molecular Sciences. https://doi.org/10.3390/ijms21020632

Holder, S. L., Lee, C. H., Popuri, S. R., & Zhuang, M. X. (2016). Enhanced surface functionality and microbial fuel cell performance of chitosan membranes through phosphorylation. Carbohydrate Polymers, 149, 251–262. https://doi.org/10.1016/j.carbpol.2016.04.118

Hong, Y., Call, D. F., Werner, C. M., & Logan, B. E. (2011). Adaptation to high current using low external resistances eliminates power overshoot in microbial fuel cells. Biosensors and Bioelectronics, 28(1), 71–76. https://doi.org/10.1016/j.bios.2011.06.045

Hou, Y., Li, K., Luo, H., Liu, G., Zhang, R., Qin, B., & Chen, S. (2014). Using crosslinked polyvinyl alcohol polymer membrane as a separator in the microbial fuel cell. Frontiers of Environmental Science & Engineering, 8(1), 137–143. https://doi.org/10.1007/s11783-013-0534-z

Hu, J., Zhang, Q., Lee, D.-J., & Ngo, H. H. (2018). Feasible use of microbial fuel cells for pollution treatment. Renewable Energy, 129, 824–829. https://doi.org/10.1016/j.renene.2017.02.001

Huang, J., & MacKerell, A. D. (2013). CHARMM36 all-atom additive protein force field: Validation based on comparison to NMR data. Journal of Computational Chemistry, 34(25), 2135–2145. https://doi.org/10.1002/jcc.23354

Humphrey, W., Dalke, A., & Schulten, K. (1996). VMD: Visual molecular dynamics. Journal of Molecular Graphics, 14(1), 33–38. https://doi.org/10.1016/0263-7855(96)00018-5

Ieropoulos, I., Winfield, J., & Greenman, J. (2010). Effects of flow-rate, inoculum and time on the internal resistance of microbial fuel cells. Bioresource Technology, 101(10), 3520–3525. https://doi.org/10.1016/j.biortech.2009.12.108

Ismail, H. K., Alesary, H. F., & Mohammed, M. Q. (2019). Synthesis and characterisation of polyaniline and/or MoO2/graphite composites from deep eutectic solvents via chemical polymerisation. Journal of Polymer Research, 26(3), 65. https://doi.org/10.1007/s10965-019-1732-6

Jafary, T., Daud, W. R. W., Ghasemi, M., Kim, B. H., Bakar, M. H. A., Jahim, J. M., Ismail, M., Satar, I., & Kamaruzzaman, M. A. (2017). Assessment of recirculation batch mode of operation in bioelectrochemical system; a way forward for cleaner production of energy and waste treatment. Journal of Cleaner Production, 142, 2544–2555. https://doi.org/10.1016/j.jclepro.2016.11.022

Jansen, J. C., Macchione, M., Tocci, E., De Lorenzo, L., Yampolskii, Y. P., Sanfirova, O., Shantarovich, V. P., Heuchel, M., Hofmann, D., & Drioli, E. (2009). Comparative Study of Different Probing Techniques for the Analysis of the Free Volume Distribution in Amorphous Glassy Perfluoropolymers. Macromolecules, 42(19), 7589–7604. https://doi.org/10.1021/ma901244d

Kang, M.-S., Kim, J. H., Won, J., Moon, S.-H., & Kang, Y. S. (2005). Highly charged proton exchange membranes prepared by using water soluble polymer blends for fuel cells. Journal of Membrane Science, 247(1–2), 127–135. https://doi.org/10.1016/j.memsci.2004.09.017

Kataky, K. P., Dalal, A., Biswas, G., & Wang, C.-T. (2020). Numerical simulation of three-dimensional microbial fuel cell. IOP Conference Series: Earth and Environmental Science, 463(1), 012062. https://doi.org/10.1088/1755-1315/463/1/012062

Katiyar, V., Gerds, N., Koch, C. B., Risbo, J., Hansen, H. C. B., & Plackett, D. (2010). Poly l-lactide-layered double hydroxide nanocomposites via in situ polymerization of l-lactide. Polymer Degradation and Stability, 95(12), 2563–2573. https://doi.org/10.1016/j.polymdegradstab.2010.07.031

Katuri, K. P., & Scott, K. (2010). Electricity generation from the treatment of wastewater with a hybrid up-flow microbial fuel cell. Biotechnology and Bioengineering, 107(1), 52–58. https://doi.org/10.1002/bit.22778

Kaur, D., Khaniya, U., Zhang, Y., & Gunner, M. R. (2021). Protein Motifs for Proton Transfers That Build the Transmembrane Proton Gradient. In Frontiers in Chemistry. https://doi.org/10.3389/fchem.2021.660954

Khalid, M., Momina, Imran, M., Rehman, M. F. ur, Braga, A. A. C., & Akram, M. S. (2021). Molecular engineering of indenoindene-3-ethylrodanine acceptors with A2-A1-D-A1-A2 architecture for promising fullerene-free organic solar cells. Scientific Reports, 11(1). https://doi.org/10.1038/s41598-021-99308-7

Kharazmi, A., Faraji, N., Mat Hussin, R., Saion, E., Yunus, W. M. M., & Behzad, K. (2015). Structural, optical, opto-thermal and thermal properties of ZnS–PVA nanofluids synthesized through a radiolytic approach. Beilstein Journal of Nanotechnology, 6, 529–536. https://doi.org/10.3762/bjnano.6.55

Kim, J., Kim, H., Kim, B., & Yu, J. (2014). Computational fluid dynamics analysis in microbial fuel cells with different anode configurations. Water Science and Technology, 69(7), 1447–1452. https://doi.org/10.2166/wst.2014.041

Kim, J. R., Premier, G. C., Hawkes, F. R., Rodríguez, J., Dinsdale, R. M., & Guwy, A. J. (2010). Modular tubular microbial fuel cells for energy recovery during sucrose wastewater treatment at low organic loading rate. Bioresource Technology, 101(4), 1190–1198. https://doi.org/10.1016/j.biortech.2009.09.023

Kim, S. H., Kwak, S.-Y., & Suzuki, T. (2005). Positron Annihilation Spectroscopic Evidence to Demonstrate the Flux-Enhancement Mechanism in Morphology-Controlled Thin-Film-Composite (TFC) Membrane. Environmental Science & Technology, 39(6), 1764–1770. https://doi.org/10.1021/es049453k

Kovalevsky, A. Y., Hanson, B. L., Mason, S. A., Yoshida, T., Fisher, S. Z., Mustyakimov, M., Forsyth, V. T., Blakeley, M. P., Keen, D. A., & Langan, P. (2011). Identification of the elusive hydronium ion exchanging roles with a proton in an enzyme at lower pH values. Angewandte Chemie - International Edition. https://doi.org/10.1002/anie.201101753

Kreuer, K. D., Paddison, S. J., Spohr, E., & Schuster, M. (2004). Transport in proton conductors for fuel-cell applications: Simulations, elementary reactions, and phenomenology. Chemical Reviews, 104(10), 4637–4678. https://doi.org/10.1021/cr020715f

Kristiansen, K. A., Potthast, A., & Christensen, B. E. (2010). Periodate oxidation of polysaccharides for modification of chemical and physical properties. Carbohydrate Research, 345(10), 1264–1271. https://doi.org/10.1016/j.carres.2010.02.011

Kulasekaran, P., Mahimai, B. M., & Deivanayagam, P. (2020). Novel cross-linked poly (vinyl alcohol)-based electrolyte membranes for fuel cell applications. RSC advances, 10(44), 26521-26527.

Kumari, A., Maurya, N. S., & Tiwari, B. (2020). Hospital wastewater treatment scenario around the globe. In Current Developments in Biotechnology and Bioengineering (pp. 549–570). Elsevier. https://doi.org/10.1016/B978-0-12-819722-6.00015-8

Lai, B., Tang, X., Li, H., Du, Z., Liu, X., & Zhang, Q. (2011). Power production enhancement with a polyaniline modified anode in microbial fuel cells. Biosensors and Bioelectronics, 28(1), 373–377. https://doi.org/10.1016/j.bios.2011.07.050

Leong, J. X., Daud, W. R. W., Ghasemi, M., Ahmad, A., Ismail, M., & Liew, K. Ben. (2015). Composite membrane containing graphene oxide in sulfonated polyether ether

ketone in microbial fuel cell applications. International Journal of Hydrogen Energy, 40(35), 11604–11614. https://doi.org/10.1016/j.ijhydene.2015.04.082

Li, M., Zhou, M., Tian, X., Tan, C., McDaniel, C. T., Hassett, D. J., & Gu, T. (2018). Microbial fuel cell (MFC) power performance improvement through enhanced microbial electrogenicity. In Biotechnology Advances. https://doi.org/10.1016/j.biotechadv.2018.04.010

Li, W.-W., Sheng, G.-P., Liu, X.-W., & Yu, H.-Q. (2011). Recent advances in the separators for microbial fuel cells. Bioresource Technology, 102(1), 244–252. https://doi.org/10.1016/j.biortech.2010.03.090

Li, X., Zeng, C., Lu, Y., Liu, G., Luo, H., & Zhang, R. (2019). Development of methanogens within cathodic biofilm in the single-chamber microbial electrolysis cell. Bioresource Technology. https://doi.org/10.1016/j.biortech.2018.12.002

Liu, H., Cheng, S., & Logan, B. E. (2005). Production of electricity from acetate or butyrate using a single-chamber microbial fuel cell. Environmental Science and Technology. https://doi.org/10.1021/es048927c

Liu, H., & Logan, B. E. (2004). Electricity Generation Using an Air-Cathode Single Chamber Microbial Fuel Cell in the Presence and Absence of a Proton Exchange Membrane. Environmental Science & Technology, 38(14), 4040–4046. https://doi.org/10.1021/es0499344

Liu, H., Ramnarayanan, R., & Logan, B. E. (2004). Production of Electricity during Wastewater Treatment Using a Single Chamber Microbial Fuel Cell. Environmental Science & Technology, 38(7), 2281–2285. https://doi.org/10.1021/es034923g

Liu, R., Zhang, S., Zhao, C., Yang, D., Cui, T., Liu, Y., & Min, Y. (2021). Regulated Surface Morphology of Polyaniline/Polylactic Acid Composite Nanofibers via Various Inorganic Acids Doping for Enhancing Biocompatibility in Tissue Engineering. Nanoscale Research Letters, 16(1). https://doi.org/10.1186/s11671-020-03457-z

Liu, Y., Su, J., Duan, F., Cui, X., Yan, W., & Jin, L. (2022). Molecular simulation of enhanced separation of humid air components using GO–PVA nanocomposite membranes under differential pressures. *Physical Chemistry Chemical Physics*, *24*(27), 16442-16452. DOI: 10.1039/D2CP01411D

Logan, B. E., Hamelers, B., Rozendal, R., Schröder, U., Keller, J., Freguia, S., Aelterman, P., Verstraete, W., & Rabaey, K. (2006). Microbial fuel cells: Methodology and technology. In Environmental Science and Technology (Vol. 40, Issue 17, pp. 5181–5192). https://doi.org/10.1021/es0605016

Logan, B. E., & Rabaey, K. (2012). Conversion of Wastes into Bioelectricity and Chemicals by Using Microbial Electrochemical Technologies. Science, 337(6095), 686–690. https://doi.org/10.1126/science.1217412

Logan BE. (2008). Microbial fuel cells. John Wiley & Sons.

Lu, Y., Armentrout, A. A., Li, J., Tekinalp, H. L., Nanda, J., & Ozcan, S. (2015). A cellulose nanocrystal-based composite electrolyte with superior dimensional stability for alkaline fuel cell membranes. Journal of Materials Chemistry A. https://doi.org/10.1039/c5ta02304a

Luo, J., Wu, C., Xu, T., & Wu, Y. (2011). Diffusion dialysis-concept, principle and applications. Journal of Membrane Science, 366(1–2), 1–16. https://doi.org/10.1016/j.memsci.2010.10.028

Ma, B., Qiao, X., Hou, X., & Yang, Y. (2016). Pure keratin membrane and fibers from chicken feather. International Journal of Biological Macromolecules. https://doi.org/10.1016/j.ijbiomac.2016.04.039

Magiera, A., Markowski, J., Menaszek, E., Pilch, J., & Blazewicz, S. (2017). PLA-Based Hybrid and Composite Electrospun Fibrous Scaffolds as Potential Materials for Tissue Engineering. Journal of Nanomaterials, 2017, 1–11. https://doi.org/10.1155/2017/9246802

Martyna, G. J., Klein, M. L., & Tuckerman, M. (1992). Nosé–Hoover chains: The canonical ensemble via continuous dynamics. The Journal of chemical physics, 97(4), 2635-2643.

Martínez, L., Andrade, R., Birgin, E. G., & Martínez, J. M. (2009). PACKMOL: A package for building initial configurations for molecular dynamics simulations. Journal of Computational Chemistry, 30(13), 2157–2164. https://doi.org/10.1002/jcc.21224

Mathuriya, A. S. (2016). Novel microbial fuel cell design to operate with different wastewaters simultaneously. Journal of Environmental Sciences, 42, 105–111. https://doi.org/10.1016/j.jes.2015.06.014

Mathuriya, A. S., & Pant, D. (2019). Assessment of expanded polystyrene as a separator in microbial fuel cell. Environmental Technology, 40(16), 2052–2061. https://doi.org/10.1080/09593330.2018.1435740

McCarty, P. L., Bae, J., & Kim, J. (2011). Domestic Wastewater Treatment as a Net Energy Producer–Can This be Achieved? Environmental Science & Technology, 45(17), 7100–7106. https://doi.org/10.1021/es2014264

Menazea, A. A., Mostafa, A. M., & Al-Ashkar, E. A. (2020). Effect of nanostructured metal oxides (CdO, Al2O3, Cu2O) embedded in PVA via Nd:YAG pulsed laser ablation on their optical and structural properties. Journal of Molecular Structure, 1203, 127374. https://doi.org/10.1016/j.molstruc.2019.127374

Menefee, E. (1977). Physical and chemical consequences of keratin crosslinking, with application to the determination of crosslink density. Advances in Experimental Medicine and Biology. https://doi.org/10.1007/978-1-4684-3282-4_19

Merkey, B. V., & Chopp, D. L. (2012). The Performance of a Microbial Fuel Cell Depends Strongly on Anode Geometry: A Multidimensional Modeling Study. Bulletin of Mathematical Biology, 74(4), 834–857. https://doi.org/10.1007/s11538-011-9690-0

Min, B., Cheng, S., & Logan, B. E. (2005). Electricity generation using membrane and salt bridge microbial fuel cells. Water Research, 39(9), 1675–1686. https://doi.org/10.1016/j.watres.2005.02.002

Mohan Bhasney, S., Kumar, A., & Katiyar, V. (2020). Microcrystalline cellulose, polylactic acid and polypropylene biocomposites and its morphological, mechanical, thermal and rheological properties. Composites Part B: Engineering, 184, 107717. https://doi.org/10.1016/j.compositesb.2019.107717

Mostafa, A. M., & Menazea, A. A. (2020). Polyvinyl Alcohol/Silver nanoparticles film prepared via pulsed laser ablation: An eco-friendly nano-catalyst for 4-nitrophenol degradation. Journal of Molecular Structure, 1212, 128125. https://doi.org/10.1016/j.molstruc.2020.128125

Mulchandani, N., Kimura, Y., & Katiyar, V. (2022). PREPARATION, STRUCTURE, AND PROPERTIES OF STEREOCOMPLEX-TYPE POLY(LACTIC ACID). In Poly(Lactic Acid) (pp. 73–86). Wiley. https://doi.org/10.1002/9781119767480.ch5

Narayanaswamy Venkatesan, P., & Dharmalingam, S. (2013). Characterization and performance study on chitosan-functionalized multi walled carbon nano tube as separator in microbial fuel cell. Journal of Membrane Science, 435, 92–98. https://doi.org/10.1016/j.memsci.2013.01.064

Neethu, B., Bhowmick, G. D., & Ghangrekar, M. M. (2019). A novel proton exchange membrane developed from clay and activated carbon derived from coconut shell for application in microbial fuel cell. Biochemical Engineering Journal, 148, 170–177. https://doi.org/10.1016/j.bej.2019.05.011

Ni, F., Wang, G. & Zhao, H. Molecular and condition parameters dependent diffusion coefficient of water in poly(vinyl alcohol): a molecular dynamics simulation study. Colloid Polym Sci 295, 859–868 (2017). https://doi.org/10.1007/s00396-017-4077-x

Obileke, K. C., Onyeaka, H., Meyer, E. L., & Nwokolo, N. (2021). Microbial fuel cells, a renewable energy technology for bio-electricity generation: A mini-review. In Electrochemistry Communications. https://doi.org/10.1016/j.elecom.2021.107003

Odella, E., Mora, S. J., Wadsworth, B. L., Huynh, M. T., Goings, J. J., Liddell, P. A., Groy, T. L., Gervaldo, M., Sereno, L. E., Gust, D., Moore, T. A., Moore, G. F., Hammes-Schiffer, S., & Moore, A. L. (2018). Controlling Proton-Coupled Electron Transfer in

Bioinspired Artificial Photosynthetic Relays. Journal of the American Chemical Society. https://doi.org/10.1021/jacs.8b09724

Odella, E., Wadsworth, B. L., Mora, S. J., Goings, J. J., Huynh, M. T., Gust, D., Moore, T. A., Moore, G. F., Hammes-Schiffer, S., & Moore, A. L. (2019). Proton-Coupled Electron Transfer Drives Long-Range Proton Translocation in Bioinspired Systems. Journal of the American Chemical Society. https://doi.org/10.1021/jacs.9b06978

Oh, S. T., Kim, J. R., Premier, G. C., Lee, T. H., Kim, C., & Sloan, W. T. (2010). Sustainable wastewater treatment: How might microbial fuel cells contribute. Biotechnology Advances, 28(6), 871–881. https://doi.org/10.1016/j.biotechadv.2010.07.008

Oh, S.-E., & Logan, B. E. (2007). Voltage reversal during microbial fuel cell stack operation. Journal of Power Sources, 167(1), 11–17. https://doi.org/10.1016/j.jpowsour.2007.02.016

Ohkubo, T., Kidena, K., Takimoto, N. et al. (2011). Molecular dynamics simulations of Nafion and sulfonated polyether sulfone membranes. I. Effect of hydration on aqueous phase structure. J Mol Model 17, 739–755. https://doi.org/10.1007/s00894-010-0767-8

Oliveira, V. B., Simões, M., Melo, L. F., & Pinto, A. M. F. R. (2013). Overview on the developments of microbial fuel cells. Biochemical Engineering Journal, 73, 53–64. https://doi.org/10.1016/j.bej.2013.01.012

Opoku, P. A., Jingyu, H., Yi, L., Guang, L., & Norgbey, E. (2022). Scaled-up multi-anode shared cathode microbial fuel cell for simultaneous treatment of multiple real wastewaters and power generation. Chemosphere, 299, 134401. https://doi.org/10.1016/j.chemosphere.2022.134401

Pal, A. K., & Katiyar, V. (2016). Nanoamphiphilic Chitosan Dispersed Poly(lactic acid) Bionanocomposite Films with Improved Thermal, Mechanical, and Gas Barrier Properties. Biomacromolecules, 17(8), 2603–2618. https://doi.org/10.1021/acs.biomac.6b00619

Pal, A. K., & Katiyar, V. (2017). Thermal degradation behaviour of nanoamphiphilic chitosan dispersed poly (lactic acid) bionanocomposite films. International Journal of Biological Macromolecules, 95, 1267–1279. https://doi.org/10.1016/j.ijbiomac.2016.11.024

Palmieri, S., Pierpaoli, M., Riderelli, L., Qi, S., & Ruello, M. L. (2020). Preparation and Characterization of an Electrospun PLA-Cyclodextrins Composite for Simultaneous High-Efficiency PM and VOC Removal. Journal of Composites Science, 4(2), 79. https://doi.org/10.3390/jcs4020079

Patel, D. K., Dutta, S. D., Ganguly, K., & Lim, K. T. (2021). Multifunctional bioactive chitosan/cellulose nanocrystal scaffolds eradicate bacterial growth and sustain drug delivery. International Journal of Biological Macromolecules, 170, 178–188. https://doi.org/10.1016/j.ijbiomac.2020.12.145

Peera, S. G., Maiyalagan, T., Liu, C., Ashmath, S., Lee, T. G., Jiang, Z., & Mao, S. (2021). A review on carbon and non-precious metal based cathode catalysts in microbial fuel cells. International Journal of Hydrogen Energy. https://doi.org/10.1016/j.ijhydene.2020.07.252

Peighambardoust, S. J., Rowshanzamir, S., & Amjadi, M. (2010). Review of the proton exchange membranes for fuel cell applications. International Journal of Hydrogen Energy, 35(17), 9349–9384. https://doi.org/10.1016/j.ijhydene.2010.05.017

Peng, X., Yu, H., Yu, H., & Wang, X. (2013). Lack of anodic capacitance causes power overshoot in microbial fuel cells. Bioresource Technology, 138, 353–358. https://doi.org/10.1016/j.biortech.2013.03.187

Pham, H. T., Boon, N., Aelterman, P., Clauwaert, P., De Schamphelaire, L., Van Oostveldt, P., Verbeken, K., Rabaey, K., & Verstraete, W. (2008). High shear enrichment improves the performance of the anodophilic microbial consortium in a microbial fuel cell. Microbial Biotechnology, 1(6), 487–496. https://doi.org/10.1111/j.1751-7915.2008.00049.x

Philips, J., Verbeeck, K., Rabaey, K., & Arends, J. B. A. (2016). Electron transfer mechanisms in biofilms. In Microbial Electrochemical and Fuel Cells (pp. 67–113). Elsevier. https://doi.org/10.1016/B978-1-78242-375-1.00003-4

Phillips, J. C., Hardy, D. J., Maia, J. D. C., Stone, J. E., Ribeiro, J. V., Bernardi, R. C., Buch, R., Fiorin, G., Hénin, J., Jiang, W., McGreevy, R., Melo, M. C. R., Radak, B. K., Skeel, R. D., Singharoy, A., Wang, Y., Roux, B., Aksimentiev, A., Luthey-Schulten, Z., … Tajkhorshid, E. (2020). Scalable molecular dynamics on CPU and GPU architectures with NAMD. The Journal of Chemical Physics, 153(4), 044130. https://doi.org/10.1063/5.0014475

Pinto, N. J., Ramos, I., Rojas, R., Wang, P.-C., & Johnson, A. T. (2008). Electric response of isolated electrospun polyaniline nanofibers to vapors of aliphatic alcohols. Sensors and Actuators B: Chemical, 129(2), 621–627. https://doi.org/10.1016/j.snb.2007.09.040

R, N. K., R, K., Berchmans, S., Chandran, S., & Pal, P. (2013). Functionalization of electrochemically deposited chitosan films with alginate and Prussian blue for enhanced performance of microbial fuel cells. Electrochimica Acta, 112, 465–472. https://doi.org/10.1016/j.electacta.2013.08.180

Rabaey, K., Clauwaert, P., Aelterman, P., & Verstraete, W. (2005). Tubular Microbial Fuel Cells for Efficient Electricity Generation. Environmental Science & Technology, 39(20), 8077–8082. https://doi.org/10.1021/es050986i

Rabaey, K., & Verstraete, W. (2005). Microbial fuel cells: novel biotechnology for energy generation. Trends in Biotechnology, 23(6), 291–298. https://doi.org/10.1016/j.tibtech.2005.04.008

Ren, H., Lee, H. S., & Chae, J. (2012). Miniaturizing microbial fuel cells for potential portable power sources: Promises and challenges. In Microfluidics and Nanofluidics (Vol. 13, Issue 3, pp. 353–381). https://doi.org/10.1007/s10404-012-0986-7

Ren, H., Torres, C. I., Parameswaran, P., Rittmann, B. E., & Chae, J. (2014). Improved current and power density with a micro-scale microbial fuel cell due to a small

characteristic length. Biosensors and Bioelectronics, 61, 587–592. https://doi.org/10.1016/j.bios.2014.05.037

Rozendal, R. A., Hamelers, H. V. M., Rabaey, K., Keller, J., & Buisman, C. J. N. (2008). Towards practical implementation of bioelectrochemical wastewater treatment. Trends in Biotechnology, 26(8), 450–459. https://doi.org/10.1016/j.tibtech.2008.04.008

Rudra, R., Kumar, V., & Kundu, P. P. (2015). Acid catalysed cross-linking of poly vinyl alcohol (PVA) by glutaraldehyde: effect of crosslink density on the characteristics of PVA membranes used in single chambered microbial fuel cells. RSC Advances, 5(101), 83436–83447. https://doi.org/10.1039/C5RA16068E

Rynkowska, Fatyeyeva, Marais, Kujawa, & Kujawski. (2019). Chemically and Thermally Crosslinked PVA-Based Membranes: Effect on Swelling and Transport Behavior. Polymers, 11(11), 1799. https://doi.org/10.3390/polym11111799

Ryu, J. H., Lee, H. L., Lee, Y. P., Kim, T. S., Kim, M. K., Anh, D. T. N., Tran, H. T., & Ahn, D. H. (2013). Simultaneous carbon and nitrogen removal from piggery wastewater using loop configuration microbial fuel cell. Process Biochemistry, 48(7), 1080–1085. https://doi.org/10.1016/j.procbio.2013.05.016

Sayed, E. T., Alawadhi, H., Elsaid, K., Olabi, A. G., Adel Almakrani, M., Bin Tamim, S. T., Alafranji, G. H. M., & Abdelkareem, M. A. (2020). A Carbon-Cloth Anode Electroplated with Iron Nanostructure for Microbial Fuel Cell Operated with Real Wastewater. Sustainability, 12(16), 6538. https://doi.org/10.3390/su12166538

Sengupta, S., & Lyulin, A. V. (2019). Molecular Modeling of Structure and Dynamics of Nafion Protonation States. The Journal of Physical Chemistry B, 123(31), 6882–6891. https://doi.org/10.1021/acs.jpcb.9b04534

Sevda, S., Dominguez-Benetton, X., Graichen, F. H. M., Vanbroekhoven, K., Wever, H. De, Sreekrishnan, T. R., & Pant, D. (2016). Shift to continuous operation of an air-cathode microbial fuel cell long-running in fed-batch mode boosts power generation.

International Journal of Green Energy, 13(1), 71–79. https://doi.org/10.1080/15435075.2014.909363

Shaari, N., & Kamarudin, S. K. (2015). Chitosan and alginate types of bio-membrane in fuel cell application: An overview. In Journal of Power Sources (Vol. 289, pp. 71–80). https://doi.org/10.1016/j.jpowsour.2015.04.027

Shakunthala, C., & Manoj, S. (2018). Energy harvesting from dairy and hospital wastewater using microbial fuel cell (MFC). Communications in Computer and Information Science, 801, 440–446. https://doi.org/10.1007/978-981-10-9059-2_39

Sharma, S., Gupta, A., Chik, S. M. S. T., Kee, C. G., Mistry, B. M., Kim, D. H., & Sharma, G. (2017). Characterization of keratin microparticles from feather biomass with potent antioxidant and anticancer activities. International Journal of Biological Macromolecules. https://doi.org/10.1016/j.ijbiomac.2017.06.015

Shen, Y., Wang, M., Chang, I. S., & Ng, H. Y. (2013). Effect of shear rate on the response of microbial fuel cell toxicity sensor to Cu(II). Bioresource Technology, 136, 707–710. https://doi.org/10.1016/j.biortech.2013.02.069

Srinophakun, P., Thanapimmetha, A., Plangsri, S., Vetchayakunchai, S., & Saisriyoot, M. (2017). Application of modified chitosan membrane for microbial fuel cell: Roles of proton carrier site and positive charge. Journal of Cleaner Production. https://doi.org/10.1016/j.jclepro.2016.06.153

Sun, L., Wang, J., Liang, J., & Li, G. (2020). Boric Acid Cross-linked 3D Polyvinyl Alcohol Gel Beads by NaOH-Titration Method as a Suitable Biomass Immobilization Matrix. Journal of Polymers and the Environment, 28(2), 532–541. https://doi.org/10.1007/s10924-019-01610-z

Supekar, S., Gamiz-Hernandez, A. P., & Kaila, V. R. I. (2016). A Protonated Water Cluster as a Transient Proton-Loading Site in Cytochrome c Oxidase. Angewandte Chemie - International Edition. https://doi.org/10.1002/anie.201603606

Tabassum, N., Islam, N., & Ahmed, S. (2021). Progress in microbial fuel cells for sustainable management of industrial effluents. In Process Biochemistry. https://doi.org/10.1016/j.procbio.2021.03.032

Tai, C. C., Chen, C. L., & Liu, C. W. (2017). Computer simulation to investigate proton transport and conductivity in perfluorosulfonate ionomeric membrane. International Journal of Hydrogen Energy, 42(7), 3981–3986. https://doi.org/10.1016/j.ijhydene.2016.11.047

Tender, L. M., Reimers, C. E., Stecher, H. A., Holmes, D. E., Bond, D. R., Lowy, D. A., Pilobello, K., Fertig, S. J., & Lovley, D. R. (2002). Harnessing microbially generated power on the seafloor. Nature Biotechnology, 20(8), 821–825. https://doi.org/10.1038/nbt716

Tiwari, B. R., Noori, Md. T., & Ghangrekar, M. M. (2016). A novel low cost polyvinyl alcohol-Nafion-borosilicate membrane separator for microbial fuel cell. Materials Chemistry and Physics, 182, 86–93. https://doi.org/10.1016/j.matchemphys.2016.07.008

Torres, C. I., Marcus, A. K., Lee, H. S., Parameswaran, P., Krajmalnik-Brown, R., & Rittmann, B. E. (2010). A kinetic perspective on extracellular electron transfer by anode-respiring bacteria. In FEMS Microbiology Reviews (Vol. 34, Issue 1, pp. 3–17). https://doi.org/10.1111/j.1574-6976.2009.00191.x

Tu, C., Silverman, D. N., Forsman, C., Jonsson, B. H., & Lindskog, S. (1989). Role of Histidine 64 in the Catalytic Mechanism of Human Carbonic Anhydrase II Studied with a Site-Specific Mutant. Biochemistry. https://doi.org/10.1021/bi00445a054

Tuckerman, M. E., Laasonen, K., Sprik, M., and Parrinello, M. (1994). Ab-initio simulations of water and water ions. J. Phys. Cond. Matter 6, A93–A100. doi: 10.1088/0953-8984/6/23A/010

Velenturf, A. P. M., & Purnell, P. (2017). Resource recovery from waste: Restoring the balance between resource scarcity and waste overload. Sustainability (Switzerland), 9(9). https://doi.org/10.3390/su9091603

Venkata Mohan, S., Velvizhi, G., Annie Modestra, J., & Srikanth, S. (2014). Microbial fuel cell: Critical factors regulating bio-catalyzed electrochemical process and recent advancements. Renewable and Sustainable Energy Reviews, 40, 779–797. https://doi.org/10.1016/j.rser.2014.07.109

Verma, P., Daverey, A., Kumar, A., & Arunachalam, K. (2021). Microbial Fuel Cell – A Sustainable Approach for Simultaneous Wastewater Treatment and Energy Recovery. Journal of Water Process Engineering, 40, 101768. https://doi.org/10.1016/j.jwpe.2020.101768

Villa, A. L. V., Aragão, M. R. S., dos Santos, E. P., Mazotto, A. M., Zingali, R. B., de Souza, E. P., & Vermelho, A. B. (2013). Feather keratin hydrolysates obtained from microbial keratinases: Effect on hair fiber. BMC Biotechnology. https://doi.org/10.1186/1472-6750-13-15

Vishnyakov, A., & Neimark, A. V. (2001). Molecular Dynamics Simulation of Microstructure and Molecular Mobilities in Swollen Nafion Membranes. The Journal of Physical Chemistry B, 105(39), 9586–9594. https://doi.org/10.1021/jp0102567

Wang, C., Lamb, R. A., & Pinto, L. H. (1995). Activation of the M2 ion channel of influenza virus: a role for the transmembrane domain histidine residue. Biophysical Journal. https://doi.org/10.1016/S0006-3495(95)80003-2

Wang, C.-T. (2014). Flow Control in Microbial Fuel Cells. In Technology and Application of Microbial Fuel Cells. InTech. https://doi.org/10.5772/58346

Wang, C.-T., Huang, Y.-S., Sangeetha, T., Chen, Y.-M., Chong, W.-T., Ong, H.-C., Zhao, F., & Yan, W.-M. (2018). Novel bufferless photosynthetic microbial fuel cell (PMFCs) for enhanced electrochemical performance. Bioresource Technology, 255, 83–87. https://doi.org/10.1016/j.biortech.2018.01.086

Wang, C.-T., Huang, Y.-S., Sangeetha, T., & Yan, W.-M. (2018). Assessment of recirculation batch mode operation in bufferless Bio-cathode microbial Fuel Cells (MFCs). Applied Energy, 209, 120–126. https://doi.org/10.1016/j.apenergy.2017.10.074

Wang, C.-T., Lee, Y.-C., Ou, Y.-T., Yang, Y.-C., Chong, W.-T., Sangeetha, T., & Yan, W.-M. (2017). Exposing effect of comb-type cathode electrode on the performance of sediment microbial fuel cells. Applied Energy, 204, 620–625. https://doi.org/10.1016/j.apenergy.2017.07.079

Wang, C.-T., Sangeetha, T., Yan, W.-M., Chong, W.-T., Saw, L.-H., Zhao, F., Chang, C.-T., & Wang, C.-H. (2019). Application of interface material and effects of oxygen gradient on the performance of single-chamber sediment microbial fuel cells (SSMFCs). Journal of Environmental Sciences, 75, 163–168. https://doi.org/10.1016/j.jes.2018.03.013

Winfield, J., Ieropoulos, I., Greenman, J., & Dennis, J. (2011). The overshoot phenomenon as a function of internal resistance in microbial fuel cells. Bioelectrochemistry, 81(1), 22–27. https://doi.org/10.1016/j.bioelechem.2011.01.001

Wong, C. Y., Wong, W. Y., Loh, K. S., Daud, W. R. W., Lim, K. L., Khalid, M., & Walvekar, R. (2020). Development of Poly(Vinyl Alcohol)-Based Polymers as Proton Exchange Membranes and Challenges in Fuel Cell Application: A Review. Polymer Reviews, 60(1), 171–202. https://doi.org/10.1080/15583724.2019.1641514

Wu, C., Wu, Y., Luo, J., Xu, T., & Fu, Y. (2010). Anion exchange hybrid membranes from PVA and multi-alkoxy silicon copolymer tailored for diffusion dialysis process. Journal of Membrane Science, 356(1–2), 96–104. https://doi.org/10.1016/j.memsci.2010.03.035

Wu, Y., Tepper, H. L., & Voth, G. A. (2006). Flexible simple point-charge water model with improved liquid-state properties. The Journal of Chemical Physics, 124(2), 024503. https://doi.org/10.1063/1.2136877

Wu, Y., Wu, C., Li, Y., Xu, T., & Fu, Y. (2010). PVA–silica anion-exchange hybrid membranes prepared through a copolymer crosslinking agent. Journal of Membrane Science, 350(1–2), 322–332. https://doi.org/10.1016/j.memsci.2010.01.007

Xu, J., Sheng, G.-P., Luo, H.-W., Li, W.-W., Wang, L.-F., & Yu, H.-Q. (2012). Fouling of proton exchange membrane (PEM) deteriorates the performance of microbial fuel cell. Water Research, 46(6), 1817–1824. https://doi.org/10.1016/j.watres.2011.12.060

Yaqoob, A. A., Ibrahim, M. N. M., & Guerrero-Barajas, C. (2021). Modern trend of anodes in microbial fuel cells (MFCs): An overview. Environmental Technology & Innovation, 23, 101579. https://doi.org/10.1016/j.eti.2021.101579

Yaqoob, A. A., Ibrahim, M. N. M., & Rodríguez-Couto, S. (2020). Development and modification of materials to build cost-effective anodes for microbial fuel cells (MFCs): An overview. Biochemical Engineering Journal, 164, 107779. https://doi.org/10.1016/j.bej.2020.107779

Yaqoob, A. A., Ibrahim, M. N. M., Umar, K., Parveen, T., Ahmad, A., Lokhat, D., & Setapar, S. H. M. (2021). A glimpse into the microbial fuel cells for wastewater treatment with energy generation. Desalination and water treatment, 214, 379–389. https://doi.org/10.5004/dwt.2021.26737

Yaqoob, A. A., Ibrahim, M. N. M., Yaakop, A. S., & Ahmad, A. (2021). Application of microbial fuel cells energized by oil palm trunk sap (OPTS) to remove the toxic metal from synthetic wastewater with generation of electricity. Applied Nanoscience (Switzerland), 11(6), 1949–1961. https://doi.org/10.1007/s13204-021-01885-6

Yaqoob, A. A., Khatoon, A., Mohd Setapar, S. H., Umar, K., Parveen, T., Mohamad Ibrahim, M. N., Ahmad, A., & Rafatullah, M. (2020). Outlook on the Role of Microbial Fuel Cells in Remediation of Environmental Pollutants with Electricity Generation. Catalysts, 10(8), 819. https://doi.org/10.3390/catal10080819

Yaqoob, A. A., Mohamad Ibrahim, M. N., Rafatullah, M., Chua, Y. S., Ahmad, A., & Umar, K. (2020). Recent Advances in Anodes for Microbial Fuel Cells: An Overview. Materials, 13(9), 2078. https://doi.org/10.3390/ma13092078

Yaqoob, A. A., Mohamad Ibrahim, M. N., Umar, K., Bhawani, S. A., Khan, A., Asiri, A. M., Khan, M. R., Azam, M., & AlAmmari, A. M. (2020). Cellulose Derived Graphene/Polyaniline Nanocomposite Anode for Energy Generation and

Bioremediation of Toxic Metals via Benthic Microbial Fuel Cells. Polymers, 13(1), 135. https://doi.org/10.3390/polym13010135

Ye, D., Yang, Y., Li, J., Zhu, X., Liao, Q., Deng, B., & Chen, R. (2013). Performance of a microfluidic microbial fuel cell based on graphite electrodes. International Journal of HydrogenEnergy,38(35),15710–15715. https://doi.org/10.1016/j.ijhydene.2013.05.034

Yellappa, M., Annie Modestra, J., Rami Reddy, Y. V., & Venkata Mohan, S. (2021). Functionalized conductive activated carbon-polyaniline composite anode for augmented energy recovery in microbial fuel cells. Bioresource Technology, 320, 124340. https://doi.org/10.1016/j.biortech.2020.124340

Yilmaz Atay, H. (2020). Antibacterial activity of chitosan-based systems. In Functional Chitosan: Drug Delivery and Biomedical Applications. https://doi.org/10.1007/978-981-15-0263-7_15

You, J., Preen, R. J., Bull, L., Greenman, J., & Ieropoulos, I. (2017). 3D printed components of microbial fuel cells: Towards monolithic microbial fuel cell fabrication using additive layer manufacturing. Sustainable Energy Technologies and Assessments, 19, 94–101. https://doi.org/10.1016/j.seta.2016.11.006

YOU, S. J., ZHAO, Q. L., JIANG, J. Q., ZHANG, J. N., & ZHAO, S. Q. (2006). Sustainable Approach for Leachate Treatment: Electricity Generation in Microbial Fuel Cell. Journal of Environmental Science and Health, Part A, 41(12), 2721–2734. https://doi.org/10.1080/10934520600966284

Yuan, Y., Zhou, S., Liu, Y., & Tang, J. (2013). Nanostructured Macroporous Bioanode Based on Polyaniline-Modified Natural Loofah Sponge for High-Performance Microbial Fuel Cells. Environmental Science & Technology, 47(24), 14525–14532. https://doi.org/10.1021/es404163g

Zhang, F., Cheng, S., Pant, D., Bogaert, G. Van, & Logan, B. E. (2009). Power generation using an activated carbon and metal mesh cathode in a microbial fuel cell.

Electrochemistry Communications, 11(11), 2177–2179. https://doi.org/10.1016/j.elecom.2009.09.024

Zhang, J., Li, Y., Li, J., Zhao, Z., Liu, X., Li, Z., Han, Y., Hu, J., & Chen, A. (2013). Isolation and characterization of biofunctional keratin particles extracted from wool wastes. Powder Technology. https://doi.org/10.1016/j.powtec.2013.05.037

Zhang, Q. G., Liu, Q. L., Chen, Y., & Chen, J. H. (2007). Dehydration of Isopropanol by Novel Poly(vinyl alcohol)−Silicone Hybrid Membranes. Industrial & Engineering Chemistry Research, 46(3), 913–920. https://doi.org/10.1021/ie0609719

Zhang, Q. G., Liu, Q. L., Jiang, Z. Y., & Chen, Y. (2007). Anti-trade-off in dehydration of ethanol by novel PVA/APTEOS hybrid membranes. Journal of Membrane Science, 287(2), 237–245. https://doi.org/10.1016/j.memsci.2006.10.041

Zhao, D., Yu, S., Sun, B., Gao, S., Guo, S., & Zhao, K. (2018). Biomedical applications of chitosan and its derivative nanoparticles. In Polymers (Vol. 10, Issue 4). https://doi.org/10.3390/polym10040462

Zhao, L., Li, J., Battaglia, F., & He, Z. (2016). Computational investigation of the flow field contribution to improve electricity generation in granular activated carbon-assisted microbial fuel cells. Journal of Power Sources, 333, 83–87. https://doi.org/10.1016/j.jpowsour.2016.09.113

Zhong, D., Liao, X., Liu, Y., Zhong, N., & Xu, Y. (2018). Enhanced electricity generation performance and dye wastewater degradation of microbial fuel cell by using a petaline NiO@ polyaniline-carbon felt anode. Bioresource Technology, 258, 125–134. https://doi.org/10.1016/j.biortech.2018.01.117

Zinadini, S., Zinatizadeh, A. A., Rahimi, M., Vatanpour, V., & Rahimi, Z. (2017). High power generation and COD removal in a microbial fuel cell operated by a novel sulfonated PES/PES blend proton exchange membrane. Energy, 125, 427–438. https://doi.org/10.1016/j.energy.2017.02.146

Research Outputs

Patent:

Vimal Katiyar, Bhanupriya Das and Anshuman Sharma, "Carbon Soot derived carbon nanoparticles decorated Polyaniline sponge 3D electrode for microbial fuel cells."(In process)

Publications from Thesis:

- Das, B., Gaur, S. S., Katha, A. R., Wang, C. T., & Katiyar, V. (2022). Hair hydrolysate functionalized cellulose nanocrystal-based chitosan membrane to harness power from wastewater fed MFCs. *International Journal of Hydrogen Energy*. https://doi.org/10.1016/j.ijhydene.2022.12.054 (I.F 7.139)

- Das, B., Soundararajan, N., Kashyap, S. P., Jang, J. H., Wang, C. T., Katha, A. R., & Katiyar, V. (2022). Bioaugmented polyaniline decorated polylactic acid nanofiber electrode by electrospinning technique for real wastewater-fed MFC application.

International Journal of Energy Research, *46*(3), 3588-3601. https://doi.org/10.1002/er.7407 (I.F 4.612)

- Das, B., Gaur, S. S., Katha, A. R., Wang, C. T., & Katiyar, V. (2021). Crosslinked poly (vinyl alcohol) membrane as separator for domestic wastewater fed dual chambered microbial fuel cells. *International Journal of Hydrogen Energy*, *46*(10), 7073-7086. https://doi.org/10.1016/j.ijhydene.2020.11.213 (I.F 7.139)

- Experimental and molecular dynamics simulation study on the effect of crosslinking in PVA separator for hospital wastewater fed MFC (Ready for submission).

- Proton Transport Mechanism in Crosslinked Poly (vinyl alcohol) Membrane for MFC Application. (Ready for submission).

- Experimental investigation and numerical modelling on flow dimensionless parameters for enhancing the performance of recirculation mode HoneyComb MFC (Ready for submission).

Awards/Recognition:

- Awarded with the **Best Oral Presentation in the DST-UKIERI supported Workshop cum Symposium-2020** on "**Bio-inspired Nanomaterials for Environmental Applications**" for the oral presentation held at IIT Guwahati during 12-13th Feb 2020.

- Awarded with **Best Paper Award** in **2019 Theory and Technique Taiwan Forum on Sustainable Environment-Academic Exchange and Job Fair (2019T&T TFOSE)** held at National Taiwan University, Taipei, Taiwan on April 2,2019.

Conference Presentations:

- Presented Oral Presentation in virtual mode on Polylactic acid based flexible electrode by electrospinning technique or real wastewater fed MFC application in **ACS Spring 2023,** March 26-30, 2023, Indianapolis, USA
- Presented Oral Presentation on Crosslinked PVA membrane as separator for real wastewater fed MFC in **International Conference on Polymers for Advanced Technology (APA2023)**, February 23-25, 2023, Goa, India
- Attended **International Conference on Biotechnology for Sustainable Bioresources and Bioeconomy (BSBB-2022)** at IIT Guwahati, India; December 7-11, 2022
- Attended International Hybrid mode **Taiwan India Exchange Workshop and Symposium**, (**ITEWS 2022**) IIT Guwahati, September 2022.
- Attended National level mega event **Northeast Research Conclave (NERC2022**) May 2022.

- Attended Web Conference on **"Trilateral Symposium on Bioinspired and Biobased Materials"** organized by Kyoto institute of Technology, Ca' Foscari University of Venice, Italy and Indian institute of Technology Guwahati, India on 5 March 2021
- Attended Web Conference on **Polymer Processing and Emerging Technologies** conducted by Polymer Processing Academy in association with IIT Alumni Centre, Bengaluru on Nov 5-7 2020.
- Presented oral presentation on "A microfluidic microbial fuel cell designed for simultaneous sensing of hexavalent chromium and powering nano-device" in **2019 International Conference on Smart Sensors**,Hsinchu, Taiwan on 3-4 June 2019.
- **Attended 4th International Conference on Alternative Fuels**, **Energy** and **Environment (ICAFEE): Future and Challenges**, 18-21 October 2019 at Feng Chia University Taichung, Taiwan.
- Presented Poster entitled "Bioderived ionic conductor-based Polyelectrolyte Membrane for Microbial Fuel Cells." in **International Conference on Sustainable Energy and Green Technology** held at Thailand during11-14 Dec 2019.
- Attended **GIAN Course on Biofuel Cell Technology** by Prof. Piet Lens at IIT Guwahati in April 2018
- Attended 2nd **Indo-Japan Bilateral symposium on future perspective of Bio-resource Utilization** "In North-Eat India" IJBS17 held on February 1-4, 2018 at Indian Institute of Technology, Guwahati, Assam, India.
- Attended Fourth Symposium on **Advances in Sustainable Polymers** (ASP-17) at Indian Institute of Technology, Guwahati, Assam, India. January 8–11, 2018.

INTERNATIONAL JOURNAL OF HYDROGEN ENERGY 46 (2021) 3073–3086

Available online at www.sciencedirect.com

ScienceDirect

journal homepage: www.elsevier.com/locate/he

Crosslinked poly(vinyl alcohol) membrane as separator for domestic wastewater fed dual chambered microbial fuel cells

Bhanupriya Das [a], Surendra Singh Gaur [a], Anki Reddy Katha [a], Chin-Tsan Wang [b,*], Vimal Katiyar [a,**]

[a] Department of Chemical Engineering, Indian Institute of Technology Guwahati, Assam, India
[b] Department of Mechanical and Electromechanical Engineering, National I-Lan University, I Lan, Taiwan

HIGHLIGHTS

- Catalyst-free PVA membrane synthesized by crosslinking with GA.
- Performance of Crosslinked PVA membrane and Nafion 117 were tested.
- Power performance enhanced by 3-fold using the complex substrate.
- Thermomechanical and antimicrobial property of the fabricated membrane studied.

ARTICLE INFO

Article history:
Received 15 October 2020
Received in revised form
21 November 2020
Accepted 23 November 2020
Available online 11 December 2020

Keywords:
Microbial fuel cells
Poly(vinyl alcohol)
Separator
Low-cost membrane
Renewable energy

ABSTRACT

The use of Nafion as a proton exchange membrane in microbial fuel cells (MFCs) is expensive with operational issues like biofouling and fuel crossover limiting the practical application of the device to harvest energy from wastewaters. In this connection, a facile route is adopted to fabricate a Nafion alternative membrane using poly(vinyl alcohol) (PVA) crosslinked with glutaraldehyde (GA) as a relatively low cost, effective membrane for MFCs. The crosslinking of the PVA membrane resulted in a reduction in hydroxyl groups and the formation of the acetal ring and ether linkage demonstrated by controlled water uptake and swelling ratio with enhanced thermo mechanical stability. The crosslinked membrane displayed higher power density than those typically reported for domestic wastewater fed MFCs, reaching a maximum of 158.28 mW/m^2 for the fabricated membrane. The PVA-GA membrane with antimicrobial activity, high power performance, and negligible fuel crossover shows its potential as a separator in future MFCs based on its performance and low cost of installation.

* Corresponding author.
** Corresponding author.
E-mail addresses: ctwang@ilau.edu.tw (C.-T. Wang), vkatiyar@iitg.ac.in (V. Katiyar).
https://doi.org/10.1016/j.ijhydene.2020.11.213
0360-3199/

Received: 2 July 2021 | Revised: 2 October 2021 | Accepted: 10 October 2021
DOI: 10.1002/er.7407

RESEARCH ARTICLE

INTERNATIONAL JOURNAL OF ENERGY RESEARCH WILEY

Bioaugmented polyaniline decorated polylactic acid nanofiber electrode by electrospinning technique for real wastewater-fed MFC application

Bhanupriya Das[1] | **Narendren Soundararajan**[1] | **Sourav Pratim Kashyap**[1] | **Jer-Huan Jang**[2,3] | **Chin Tsan Wang**[1,4] | **Anki Reddy Katha**[1] | **Vimal Katiyar**[1]

[1]Department of Chemical Engineering, Indian Institute of Technology Guwahati, Guwahati, India
[2]Department of Mechanical Engineering/Center of Reliability Engineering, Ming-Chi University of Technology, New Taipei, Taiwan
[3]Department of Mechanical Engineering, Chang Gung University, Taoyuan, Taiwan
[4]Department of Mechanical and Electromechanical Engineering, National I-Lan University, Yilan, Taiwan

Correspondence
Chin Tsan Wang, Department of Mechanical and Electromechanical Engineering, National I-Lan University, Yilan, Taiwan.
Email: ctwang@niu.edu.tw
Vimal Katiyar, Department of Chemical Engineering, Indian Institute of Technology Guwahati, Guwahati, Assam, India.
Email: vkatiyar@iitg.ac.in

Funding information
Taiwan MOST, Grant/Award Numbers: 106-2923-E-197-001-MY5, 107-2221-E-197-022-MY3, 108-2622-E-197-002-CC3, 108-2221-E-197-015-MY5

Summary

Bioaugmentation is considered a potential tool to boost the performance of microbial fuel cells (MFCs) by modifying electrodes with biopolymers. However, research on biopolymers in MFCs to treat real wastewater is very limited. Polylactic acid (PLA) is a biopolymer obtained from renewable feedstock, extensively being used in the form of nanofibers due to its biocompatible nature, while polyaniline (PANI) is a favorite candidate for electrode modification in MFC under its good electrical conductivity and stability. Interestingly, PANI-based degradable nanofibers are known to support cell adhesion and proliferation. The current work is, therefore, aimed at finding a new environmentally benign composite material using electrospun PLA nanofiber decorated with in situ polymerized PANI. The resultant PANI/PLA electrode was tested for its efficacy as anode with domestic wastewater-fed MFCs against conventional graphite felt. The flexible anode outperformed the flat graphite felt anode displaying a 92.32% decrement in charge transfer impedance and 8-fold increase in maximum power density with excellent cell adherence under which simultaneous COD removal of 91.7% was also achieved. The present study has successfully added a new dimension to the design of sustainable anode material to enhance microbial binding and achieve high power output, revealing the enormous potential of biopolymer-based MFCs in the future. By switching to the biopolymer flexible electrode that rivals its traditional polymers, the MFCs demonstrate promise to be a vital tool accessible in the remotest part of the world lacking electrical infrastructure for simultaneous clean water and electricity generation.

Highlights

- 8-fold increase in power density in real wastewater-fed MFCs using novel PANI/PLA anode.
- 91.7% COD removal from domestic wastewater using mediator-less MFCs.
- Pseudocapacitive nature displayed by the biopolymer-based anode.
- Enhanced bio-synergistic interaction between wastewater-borne microbial biofilm and bioaugmented anode.

INTERNATIONAL JOURNAL OF HYDROGEN ENERGY 48 (2023) 5451–5461

Available online at www.sciencedirect.com

ScienceDirect

journal homepage: www.elsevier.com/locate/he

Hair hydrolysate functionalized cellulose nanocrystal based chitosan membrane to harness power from wastewater fed MFCs

Bhanupriya Das [a], Surendra Singh Gaur [a], Anki Reddy Katha [b], Chin Tsan Wang [a,c,**], Vimal Katiyar [a,*]

[a] Department of Chemical Engineering, Indian Institute of Technology Guwahati, Assam, 781039, India
[b] Department of Chemical Engineering, Indian Institute of Technology Tirupati, Andhra Pradesh, 517619, India
[c] Department of Mechanical and Electromechanical Engineering, National I-Lan University, Yilan, Taiwan

HIGHLIGHTS

- Human hair waste for modification of chitosan membrane is demonstrated in MFC.
- Modified chitosan yields highest power density of 142.57 mW/m² from wastewater.
- Modified membrane treated domestic wastewater with 82% COD removal.
- Ion conductivity enhanced by four-fold, while swelling reduced by 40%.
- New low-cost membrane is less prone to biofouling compared to Nafion-117.

GRAPHICAL ABSTRACT

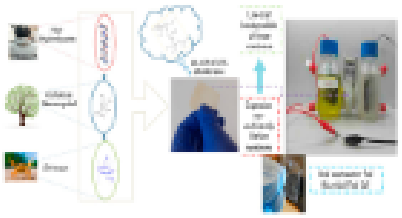

ARTICLE INFO

Article history:
Received 24 August 2022
Received in revised form
30 November 2022
Accepted 5 December 2022
Available online 28 December 2022

Keywords:
Microbial fuel cells
Chitosan

ABSTRACT

Chitosan (CS) is an environmentally benign polymer increasingly utilized to prepare low-cost proton exchange membranes (PEMs) for Microbial Fuel Cell (MFC) applications. In this work, hair hydrolysate functionalized CNCs have been utilized with CS matrix followed by cross-linking with epichlorohydrin to enhance the properties of neat chitosan for its application as Nafion-alternative membrane to harvest electricity from domestic wastewater fed MFC device for the first time. Characterizations reveals the structural interaction between the hair hydrolysate functionalized-CNC and chitosan matrix resulting in higher antibacterial property with a low percentage of water uptake (60%) and swelling (20%) and higher ion conductivity (1.04 mS/cm). Maximum power density of 142.57 mW/m² and maximum open circuit voltage of 703.58 mV is derived from real wastewater which is

* Corresponding author.
** Corresponding author.
E-mail addresses: ctwang@niu.edu.tw (C.T. Wang), vkatiyar@iitg.ac.in (V. Katiyar).
https://doi.org/10.1016/j.ijhydene.2022.12.054